Provisional Publication Schedule for 1969

In the interests of rapid publication it has been found necessary to schedule 5 volumes for appearance in 1969. Since monthly publication will be maintained, this implies that 2 of the volumes will each consist of three issues, while 3 of the volumes will each consist of only 2 issues. The following provisional schedule applies:

Vol. **44**, No. 1	January 1969	
Vol. **44**, No. 2	February 1969	(completing Vol. 44)
Vol. **45**, No. 1	March 1969	
Vol. **45**, No. 2	April 1969	
Vol. **45**, No. 3	May 1969	(completing Vol. 45)
Vol. **46**, No. 1	June 1969	
Vol. **46**, No. 2	July 1969	(completing Vol. 46)
Vol. **47**, No. 1	August 1969	
Vol. **47**, No. 2	September 1969	
Vol. **47**, No. 3	October 1969	(completing Vol. 47)
Vol. **48**, No. 1	November 1969	
Vol. **48**, No. 2	December 1969	(completing Vol. 48)

GENERAL INFORMATION

Languages

Papers will be published in English, French or German.

Submission of papers

Papers should be sent to:

PROF. PHILIP W. WEST,
Coates Chemical Laboratories,
College of Chemistry and Physics,
Louisiana State University,
Baton Rouge 3,
La. 70803 (U.S.A.)

or to:

DR. A. M. G. MACDONALD,
Department of Chemistry,
The University,
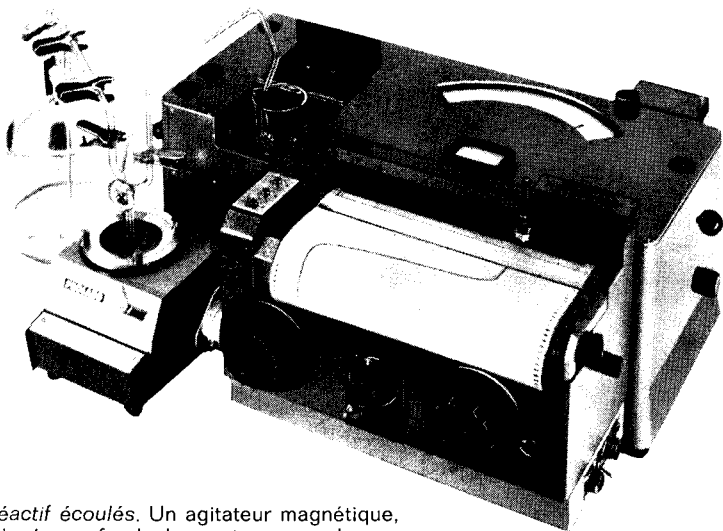P.O. Box 363
Birmingham 15 (Great Britain)

Reprints

Fifty reprints will be supplied free of charge. Additional reprints (minimum 100) can be ordered at quoted prices. They must be ordered on order forms which are sent together with the proofs.

THE ROLE OF IRON(III) HYDROXIDE AS A COLLECTOR OF MOLYBDENUM FROM SEA WATER

The behavior of iron(III) hydroxide was studied in order to clarify its role as a collector of the trace element molybdenum in sea water. Iron(III) hydroxide formed in sea water possesses a charge which is pH-dependent. At pH 4.0 the colloid has an apparent maximum positive-charge density and is able to adsorb molybdenum quantitatively as molybdate. Above pH 9 the charge is reversed and the iron(III) hydroxide no longer collects molybdate. Qualitative electrophoretic tests carried out in distilled water confirmed the positive and negative charge on the iron(III) hydroxide in acid and basic solution, respectively. At pH 10.0, calcium and magnesium salts coprecipitated molybdate in the presence or absence of iron(III) hydroxide. Procedures were worked out for the determination of molybdenum in sea water concentrated by iron(III) hydroxide at pH 4.0, and by calcium and magnesium salts at pH 10.0.

Y. S. KIM AND H. ZEITLIN,

CHELATE ENHANCEMENT OF THE SENSITIVITY FOR MAGNESIUM IN NEUTRON ACTIVATION ANALYSIS

A chelation technique is described in which the high sensitivity of neutron activation analysis for bromine is used to improve the activation sensitivity for magnesium. Magnesium is extracted with 5,7-dibromo-8-hydroxyquinoline in chloroform in the presence of 2,4,6-trimethylpyridine, the chelate is isolated by paper chromatography, and the amount of magnesium present is calculated from the bromine activity after activation. Experimental variables are discussed. The sensitivity limit for magnesium is *ca.* 0.1 μg.

J. B. SMATHERS, D. DUFFEY AND S. LAKSHMANAN,

EPITHERMAL NEUTRON ACTIVATION ANALYSIS FOR IODINE IN SMALL AQUEOUS SAMPLES

Selective activation by means of epithermal neutrons is discussed in the light of the WESTCOTT nomenclature. Expressions for the calculation of the "advantage" factor when epithermal activation is used, are given. The epithermal activation technique has been applied to the determination of iodine at the microgram level in aqueous solutions containing iodine and chlorine in the ratio of about 1:2000. Aqueous samples as small as 50 μl were irradiated while frozen.

D. BRUNE,

TREATISE ON ELECTROCHEMISTRY

Second, completely revised edition

by G. KORTÜM
Professor of Physical Chemistry, University of Tübingen, Germany

7 × 10″, xxii + 637 pages, 71 tables, 151 illust., 882 lit.refs., 1965, Dfl. 85.00, £ 10

Contents: 1. Definitions and fundamental laws. 2. Fundamental principles of thermodynamics. 3. The solvation of ions. 4. Weak and strong electrolytes. 5. Theory of ionic interaction. 6. Association and incomplete dissociation of strong electrolytes. 7. The results and applications of conductance measurements. 8. Electromotive forces. 9. Practical applications of potentiometric measurements. 10. Acids and bases. 11. Potential differences at phase boundaries. 12. Electrical polarization and the kinetics of electrode processes. 13. Applications of electrochemical processes. Appendix. Subject index.

OXIDATION AND COMBUSTION REVIEWS

edited by C. F. H. TIPPER,

Department of Inorganic, Physical and Industrial Chemistry, University of Liverpool, Great Britain

Volume 1

6 × 9″, viii + 344 pages, 29 tables, 45 illus., 815 lit.refs., 1965, Dfl. 40.00, 110s.

Contents: 1. Application of the theory of branched chain reactions in low temperature combustion. 2. Oxidation reactions induced by ionising radiation. 3. Gas phase photo-oxidation. 4 Oxidation reactions involving nitrogen dioxide. 5. Oxidative degradation high polymers. 6. The heterogeneous selective oxidation of hydrocarbons. Author and subject indexes.

Volume 2

6 × 9″, viii + 301 pages, 19 tables, 64 illus., 311 lit.refs., 1967, Dfl. 60.00, 150s.

Contents: 1. Thermal explosion theory. 2. Some fundamentals of combustion instability. 3. The use of adiabatic compression and mass spectrometry in the study of combustion. 4. Trapped radicals and combustion. Author and subject indexes.

Volume 3 and subsequent volumes are published as a review journal under the same title

ATMOSPHERIC OXIDATION AND ANTIOXIDANTS

by G. SCOTT,
Head of Works Research and Development Department, Dyestuffs Division, Imperial Chemical Industries Ltd., Grangemouth, Stirlingshire, Great Britain

7 × 10″, x + 528 pages, 172 tables, 174 illus., 1206 lit.refs., 1965, Dfl. 72.50, £ 8.10.0

Contents: 1. The historical development of antioxidants. 2. Peroxides. 3. Autoxidation. 4. Antioxidants: radical chain-breaking mechanisms. 5. Antioxidants: Preventive mechanisms. 6. Measurement of oxidative deterioration. 7. Oxidative deterioration of saturated oils and polymers. 8. Oxidation of olefinic oils, fats and polymers. 9. Degradation of vulcanised rubber. 10. Mechano-oxidation of polymers. Index.

A COMBINED ION-EXCHANGE SPECTROPHOTOMETRIC METHOD FOR THE DETERMINATION OF MOLYBDENUM AND TUNGSTEN IN SEA WATER

A combined ion-exchange spectrophotometric method has been developed for the determination of molybdenum and tungsten in sea water. The two elements are adsorbed quantitatively on Dowex 1-X8 (SCN-form) from sea water adjusted to 0.1 M in hydrochloric acid and 0.1 M in ammonium thiocyanate. Molybdenum also can be concentrated quantitatively on Dowex 1-X8 (Cl-form) from sea water acidified to 0.1 M in hydrochloric acid and containing < 6% hydrogen peroxide. In both concentration procedures, molybdenum and tungsten are easily eluted with 0.5 M sodium hydroxide–0.5 M sodium chloride solution. The adsorption and desorption steps provide selective concentration for molybdenum and tungsten, so that molybdenum can be determined spectrophotometrically with dithiol. Tungsten is separated from molybdenum by anion-exchange on DEAE (Cl-form), and can be determined similarly with dithiol. A sea-water sample collected from the Pacific Ocean, off the coast of Kominato, Chiba, gave values of 9.5 ± 0.1 μg Mo/l and 9.3 ± 0.2 μg Mo/l for the thiocyanate concentration and hydrogen peroxide concentration methods, respectively, with 1-l samples. Duplicate analyses of sea water from the same location as for molybdenum, gave values of 0.11$_5$ and 0.11$_6$ μg/l for tungsten, on a 20-l sample basis.

K. KAWABUCHI AND R. KURODA,

DETERMINATION OF SILICON IN ALUMINUM ALLOYS BY ATOMIC ABSORPTION SPECTROSCOPY

The determination of silicon in aluminum alloys after treatment with sodium hydroxide and hydrogen peroxide, can give excellent results if the standards used contain approximately the same amounts of aluminum and total solids as the sample solutions. Addition of organic solvents has little effect. Linear calibration graphs are obtained over the range 0–250 p.p.m. Si.

D. E. CAMPBELL,

DETERMINATION AND IDENTIFICATION OF AMINO ACIDS BY THERMOMETRIC TITRATION AND NMR SPECTROSCOPY

Thermometric titration coupled with NMR spectroscopy provides an elegant method of determination and identification of individual amino acids, and their binary mixtures. Experimental details and interpretation of thermometric and NMR spectroscopic data are presented.

B. SEN AND W. C. WU,

SPOT TESTS IN ORGANIC ANALYSIS

Seventh English Edition, completely revised and enlarged

by FRITZ FEIGL in collaboration with VINZENZ ANGER

6 x 9″, xxiii + 772 pages, 19 tables, over 2000 lit.refs., 1966, Dfl. 85.00, £10.0.0.

This 7th edition has involved complete revision and reorganisation of the subject in order to present a still clearer picture of the multitudinous applications open to organic spot test analysis. The amount of new work which is appearing has certainly necessitated expansion, but the author has kept this to a minimum by omitting the chapter on spot test techniques (which are covered in the companion volume *Spot Tests in Inorganic Analysis*) and by limiting the number of tables and structural formulae.
Comparison with the 6th edition reveals the following differences:

	Number in	
	6th Edn.	7th Edn.
Preliminary tests	32	45
Functional group tests	70	109
Individual compound tests	133	148
Detection of particular structures and types of compounds	0	74
Differentiation of isomers etc.	0	54
Applications in the testing of materials etc.	111	131

In total the book now gives in 561 sections information on more than 900 tests compared with 600 tests in 346 sections in the preceding edition.

An important feature is the inclusion of a large number of recently developed tests and comments which have not hitherto been published in any form.

It is the author's hope that this work will help to correct the widespread impression that physical instrumentation is always superior to chemical methods for solving analytical problems. Each of the chapters presents instances of problems for which no solutions by physical means have yet been developed, or for which the rapid spot tests are equal or superior to the expensive instrumental procedure.

CONTENTS: 1. Development, present state and prospects of organic spot test analysis. 2. Preliminary (exploratory) tests. 3. Detection of characteristic functional groups in organic compounds. 4. Detection of structures and certain types of organic compounds. 5. Identification of individual organic compounds. 6. Application of spot tests in the differentiation of isomers and homologous compounds. Determination of constitutions. 7. Application of spot reactions in the testing of materials, examinations of purity, characterization of pharmaceutical products, etc... Appendix: Individual compounds and products examined. Author index. Subject index.

FROM REVIEWS OF THE NEW EDITION

... As we have come to expect, Professor FEIGL has once more provided an outstanding service to the chemical community ...

Analytica Chimica Acta

... C'est pourquoi le livre du professeur FEIGL est extrêmement précieux pour le chimiste comme le montre la succession des éditions ...

Bulletin de la Société Chimique de France

... This volume, together with its companion on "Spot Tests in Inorganic Analysis" (5th ed., 1958), is a useful and authoritative source of information not only to analytical chemists but also to organic chemists, pharmaceutical chemists, and biochemists. Advanced students and research workers in analytical chemistry will find these two volumes stimulating and helpful ...

Analytical Chemistry

... As each successive edition of this book appeared, it was greeted with ever increasing praise. It is difficult, therefore, to find adequate superlatives to describe this new, completely revised edition ...
... The astonishing range of applications of the tests makes this book essential for every chemist concerned with organic compounds ...

Chemistry in Britain

A DISTRIBUTION STUDY OF THE ASSOCIATION OF 2,2-DIETHYLPROPANEDIOL-1,3 AND 2-ETHYLHEXANEDIOL-1,3 IN CHLOROFORM

The distribution of 2,2-diethylpropanediol-1,3 (DEPD) and 2-ethylhexanediol-1,3 (EHD) between chloroform and 0.5 M sodium chloride has been followed at 25° as a function of the diol concentration. The distribution data could be explained by assuming that the diol was monomeric in the aqueous layer but that, besides the monomer, a dimer and a polymer containing nine molecules were present in the chloroform layer. DEPD has a somewhat larger tendency to polymerize than EHD.

D. DYRSSEN, L. UPPSTRÖM AND M. ZANGEN,

A STUDY OF THE EXTRACTION OF BORIC ACID WITH 2,2-DIETHYLPROPANEDIOL-1,3 AND 2-ETHYLHEXANEDIOL-1,3 IN CHLOROFORM

The distribution of boric acid between chloroform and 0.5 M sodium chloride has been studied as a function of the concentration of 2,2-diethylpropanediol-1,3 (DEPD) and 2-ethylhexanediol-1,3 (EHD) between pH 2 and 12. EHD gives a higher distribution ratio for the same initial concentration in chloroform. The distribution data show that a 1:2 boric acid–diol complex in the chloroform phase is formed in two steps and that the equilibrium constant for the first step is considerably larger than that for the second. No complex between borate and the diols could be detected and the decrease in the distribution ratio above pH 8 is attributed to the formation of $B(OH)_4^-$. The possibility of finding more effective 1,3-diols is discussed.

D. DYRSSEN, L. UPPSTRÖM AND M. ZANGEN,

LIQUID ION-EXCHANGE ELECTRODES AS END-POINT DETECTORS IN COMPLEXIMETRIC TITRATIONS. DETERMINATION OF CALCIUM AND MAGNESIUM IN THE PRESENCE OF SODIUM

PART III. APPLICATION OF SIMPLE ION-EXCHANGE THEORY

For a given complexing titrant, the form of the potentiometric titration curves depends on the selectivity properties of the electrode and on the composition of the solution. These two factors can be combined into one term, the equilibrium composition of the liquid ion-exchanger, on the basis of simple ion-exchange theory. Data for EGTA titrations monitored with an Orion calcium-activity electrode are employed to illustrate how experimental observations over a wide range of solution compositions (pMg 1–4 and pCa 2–4) can be correlated by means of this parameter. Qualitative correlations are made on the basis of a three-coordinate plot of exchanger composition and equations are derived that allow a quantitative comparison of titration procedures to be made.

M. WHITFIELD AND J. LEYENDEKKERS,

AN IMPROVED METHOD OF COULOSTATIC TITRATIONS

The complexities of performing coulostatic titrations have been greatly reduced by using a special external sweep circuit which produces a horizontal sweep rate for the oscilloscope that varies with the square root of time. Since the potential decay at a large H.D.M.E. also varies with the square root of time and was applied to the vertical plates, linear decay curves were obtained. The slopes of the linear decay curves were plotted against volume of titrant. Lead and cadmium were titrated successfully in the concentration range of $4.4 \cdot 10^{-6}$–$4.7 \cdot 10^{-5}\,M$.

R. F. SYMPSON,

COULOMETRIC TITRATION OF BASES IN CONCENTRATED NEUTRAL SALT SOLUTIONS IN WATER AND NONAQUEOUS SOLVENTS

Weak bases were titrated with coulometrically generated hydrogen ions in aqueous 8 M sodium perchlorate solutions. Bases with ionization constants as low as $4 \cdot 10^{-12}$ were titrated in acetone containing 3 M lithium perchlorate. Enhancement of end-point breaks was obtained in both solvents in the presence of the concentrated salts. Methods of end-point detection were investigated.

G. D. CHRISTIAN,

AN AUTOMATED ION-EXCHANGE METHOD FOR THE DETERMINATION OF SODIUM MONOFLUOROPHOSPHATE IN DENTIFRICES

Sodium monofluorophosphate can be accurately analyzed in dental cream by an AutoAnalyzer method. The monofluorophosphate is separated from other phosphate species by gradient elution ion-exchange chromatography. The column effluent is fed to an Auto-Analyzer unit which continuously hydrolyzes the phosphates to orthophosphate and develops a color (molybdenum blue) proportional to the phosphate level. The method is useful for the analysis of large numbers of samples.

C. BENZ AND R. M. KELLEY,

Preliminary Announcement:

RADIOCHEMICAL AND RADIOANALYTICAL LETTERS

A **New** International Journal

Distributed to Subscribers by **Airmail**

Delay Between Receipt and Publication of Contributions
Reduced to **Eight Weeks**

Subject Coverage: Radiation Detection and Measurement - Radiochemical and
Radioanalytical Techniques - Radionuclide Production -
Separation Techniques - Syntheses of Labelled Compounds -
Nuclear Chemistry - Chemistry of Radioactive
Elements - Radio-Tracer and Radiation Chemistry - Activation
Analysis - Analysis by Radiation Absorption and Backscattering -
Isotope Dilution Analysis - Radioreagent Analysis and
Radiometric Titration - Instruments, Equipment and Controls

Editors: Dr. J. Tölgyessy, Bratislava and Dr. T. Braun, Budapest

Publishers: Elsevier Sequoia S.A., Lausanne, and Akadémiai Kiadó,
Budapest

Subscription rates: Vols 1 & 2, 1969 (400 pages in 6 to 9 issues per volume):
Swiss Francs 215.– (approx. US $ 50.00 or £ 21.10.0),
including airmail postage.

For further information and sample copies please apply to:

Elsevier Sequoia S.A.
P.O. Box 851
1001 Lausanne 1, Switzerland

435G

THE EXTRACTION OF LANTHANIDES AND ACTINIDES BY ALKYLPHOSPHINE OXIDES

PART IV. EXTRACTION OF THE TRIVALENT CATIONS BY TRI-n-BUTYL-PHOSPHINE OXIDE OR TRI-n-OCTYLPHOSPHINE OXIDE

(in French)

The extraction of trivalent lanthanides and actinides by trialkylphosphine oxides is based on the equilibrium

$$Me_a^{3+} + 3\,NO_{3a}^- + 3\,Alk_3PO_o \rightleftharpoons Me(NO_3)_3 \cdot 3\,Alk_3PO_o$$

At constant ionic strength (2 M sodium nitrate), the equilibrium constants for the complex formed between tri-n-octylphosphine oxide in n-octane and ^{241}Am or ^{244}Cm have been calculated; the values are respectively $(2.9 \pm 0.5) \cdot 10^7$ M^{-3} and $(1.7 \pm 0.15) \cdot 10^7$ M^{-3}. The distribution of lanthanides and actinides between 0.1 M tri-n-butylphosphine oxide in benzene and nitric acid solutions of different concentrations was examined and discussed.

J. GOFFART AND G. DUYCKAERTS,

SPECTROFLUORIMETRIC DETERMINATION OF EUROPIUM AND SAMARIUM AS THEIR 2-NAPHTHOYLTRIFLUOROACETONE–TRIOCTYLPHOSPHINE OXIDE COMPLEXES

The europium and samarium complexes with 2-naphthoyltrifluoroacetone (NTFA) can be used for the spectrofluorimetric determination of the two metals. Low concentrations of NTFA are needed, and trioctylphosphine oxide is used to enhance the extraction; the optimum pH range is 5.5–6.5. The fluorescence intensity is stable under irradiation for > 30 min. The detection limits are 0.1 p.p.b. Eu and 0.1 p.p.m. Sm. Few common ions interfere; iron(III) causes low results. Rare-earth ions, except samarium, in 50-fold amounts do not interfere with the determination of europium. Europium interferes with the determination of samarium, but a simultaneous determination is possible.

T. SHIGEMATSU, M. MATSUI AND R. WAKE,

THE DETERMINATION OF LIGHT ELEMENTS BY PROTON EXCITATION AND X-RAY SPECTROMETRY

Proton excitation is suggested for the X-ray spectrochemical analysis of light elements; a 200-kV proton source and a flat crystal X-ray spectrometer are used. Measurements of the X-ray spectra of B-Kα and C-Kα show that proton excitation is promising for analyses in the soft X-ray region. For boron in nickel base alloy and carbon in low alloy steel and white iron, the calibration curves obtained showed excellent linearity. The detection limits were 0.0014% for boron and 0.0090% for carbon for counting times of 1 min.

H. KAMADA, R. INOUE, M. TERASAWA, Y. GOHSHI, H. KAMEI AND I. FUJII,

COORDINATION CHEMISTRY REVIEWS

This international journal offers rapid publication of relatively short review articles in the field of coordination chemistry. The term "coordination chemistry" is interpreted broadly, but does not include "organometallic chemistry". In general the reviews published fall into the following categories:

—   surveys of developments in a particular area during the last few years
—   surveys and/or discussions of the results obtained with a particular technique during the last few years
—   general or philosophical discussions of some specific aspects of coordination chemistry

Articles dealing with the application of physical techniques are also included, as well as those on the theory or practice of the coordination chemistry of transition or non-transition metals. The main language of the journal is English, although reviews in French or German are also published.

THE DETERMINATION OF COBALT, COPPER, NICKEL AND IRON BY THIN-LAYER CHROMATOGRAPHY OF THEIR CHELATES WITH 1-(2-PYRIDYLAZO)-2-NAPHTHOL

The chelates of cobalt, copper, nickel and iron with PAN are extracted into chloroform, separated on Silufol thin-layer chromato-plates, and determined by means of scanning reflectance photometry *in situ*. The procedure was successfully applied to the trace analysis of various inorganic salts; the results agreed with those obtained by other methods. Experimental variables are discussed in detail.

A. GALÍK AND A. VINCOUROVÁ,

THE CHEMICAL SHIFT OF THE HYDROXYL PROTON OF BENZILDIOXIMES AND FURILDIOXIMES

The chemical shifts of the hydroxyl protons of benzil- and furildioxime isomers were measured in dimethyl sulfoxide or hexamethyl phosphorous triamide solvent. Each isomer gives a sharp signal at different fields and the signals are not affected by mixing of isomers, hence it is possible to determine and identify mixtures of the three isomers. The concentration and temperature dependences were investigated briefly.

M. TANAKA, T. SHONO AND K. SHINRA,

OXIDATION–REDUCTION REACTIONS IN FORMAMIDE MEDIA

Lead tetraformamide and trilead octaformamide have been isolated and, along with iodine and potassium dichromate, have been used as oxidising agents for the determination of Sn^{3+}, As^{3+}, Sb^{3+}, Ce^{3+}, Fe^{2+} and $S_2O_3^{2-}$ ions in formamide media. The course of these oxidation–reduction reactions can be followed potentiometrically. Visual titrations without indicator are possible when iodine in formamide is used as the titrant.

R. C. PAUL, K. S. SOOCH, O. C. VAIDYA AND S. P. NARULA,

INORGANIC ELECTRONIC SPECTROSCOPY

by A. B. P. LEVER, Associate Professor of Chemistry,
York University, Toronto, Canada

The first monograph in the series PHYSICAL INORGANIC CHEMISTRY,
edited by M. F. LAPPERT

Electronic spectroscopy has become, in recent years, a commonplace tool in inorganic research and development although few books dealing with the topic have appeared. Those books dealing with spectroscopy in general devote but a few pages to a discussion of the electronic spectra of inorganic compounds.

The aim of this book is (a) to provide the reader with a basic understanding of the methods and procedures involved in a study of the electronic spectra of inorganic compounds, (b) to discuss the information which may be derived from such study, with particular emphasis on stereochemistry and chemical bonding, and (c) to provide a reference text.

A beginning is made at a level which can be understood by an average student with a first degree, the first third of the book dealing with atomic theory, symmetry and group theory. In progressing further with the material presented, the reader can proceed from the construction of qualitative energy level diagrams and the assignment of transitions observed in the spectra of cubic molecules, to quantitative diagrams and the spectra of non-cubic molecules.

Having mastered this material the reader is shown how to derive useful information concerning stereochemistry and chemical bonding and even, qualitatively, such properties as effective nuclear charge and mean d-orbital radii. The spectra of the more common transition metal ions in their many oxidation states and stereochemistries are discussed in Chapter 9, which is a mine of information for the practising inorganic spectroscopist.

The book is unique in being the only reference work available which will bring the new graduate up to the level where he can read and usefully digest the original research papers in inorganic spectroscopy. Much of the material has not appeared in book form before and some of it has not appeared in print at all.

Contents: Preface. 1. Atomic structure. 2. Molecular symmetry. 3. Group theory. 4. Crystal field diagrams. 5. Term diagrams. 6. Selection rules, band intensities and dichroism. 7. Some theoretical aspects of electronic spectra. 8. Charge transfer spectra. 9. Crystal field spectra. Appendices. Indexes.

xii + 420 pages, 78 tables, 130 illus., 465 lit. refs., 1968, Dfl. 90.00, £11.10.0.

REAGENTS FOR THE SPECTROPHOTOMETRIC DETERMI-
NATION OF SULFHYDRYL GROUPS OVER A WIDE WAVE-
LENGTH RANGE

(Short Communication)

D. R. GRASSETTI AND J. F. MURRAY, JR,

EFFECTS OF BORATE ON ABSORBANCE OF
CARBOHYDRATES MIXED WITH THE PHENOL–SULFURIC
ACID REAGENT

(Short Communication)

R. D. DAFTARY AND Y. POMERANZ,

SPECTROPHOTOMETRIC DETERMINATION OF IRON IN
HIGH-PURITY YTTRIUM OXIDE WITH 1-(2-PYRIDYLAZO)-2-
NAPHTHOL

(Short Communication)

S. SHIBATA, K. GOTO AND R. NAKASHIMA,

HYDROUS MANGANESE DIOXIDE AS A SELECTIVE "COL-
LECTOR" FOR GALLIUM

PART I. THE QUANTITATIVE COPRECIPITATION OF GALLIUM

(Short Communication)

V. S. BISKUPSKY,

INTRODUCTION TO NUCLEAR CHEMISTRY

by D. J. CARSWELL

ix + 279 pages, 23 tables, 69 illus., 1967, Dfl. 32.50, 70s.

Contents: 1. The development of nuclear chemistry. 2. Fundamental particles and nuclear structure. 3. Nuclear reactions and radioactivity. 4. Properties of nuclear radiations. 5. The detection and measurement of nuclear radiation. 6. Nuclear instrumentation. 7. Radiation chemistry. 8. Isotope measurement and separation methods. 9. Charged particle accelerators, neutron sources, production and properties of the actinide elements. 10. Uses of isotopes. 11. Experimental nuclear chemistry (including 16 selected experiments). Index.

STATISTICAL THERMODYNAMICS

An Introduction to its Foundations

H. J. G. HAYMAN

ix + 256 pages, 14 illus., 1967, Dfl. 47.50, 110s.

Contents: Preface. Nomenclature. 1. An introductory survey. 2. Some simple partition functions. 3. The microcanonical assembly. 4. The second law of thermodynamics. 5. The canonical assembly. 6. The third law of thermodynamics. 7. Dilute gases. 8. The grand canoinical assembly. 9. Fermi-Dirac, Bose-Einstein and imperfect gases. 10. The partition function method applied to Fermi-Dirac, Bose-Einstein and photon gases. 11. Classical statistical thermodynamics. 12. The relationship between classical and quantum statistics.
Appendices: 1. The probability integral. 2. Stirling's formula for ln $n!$. 3. The method of variation of constants. 4. The dynamic equilibrium of a microcanonical assembly. 5. The adiabatic principle. 6. Liouville's theorem. Index.

THE STRUCTURE OF INORGANIC RADICALS

An Application of Electron Spin Resonance to the Study of Molecular Structure

by P. W. ATKINS and M. C. R. SYMONS

x + 280 pages, 57 tables, 74 illus., 357 lit. refs., 1967, Dfl. 60.00, £7.0.0.

Contents: 1. Introduction. 2. An introduction to electron spin resonance. 3. Formation and trapping of radicals. 4. Trapped and solvated electrons. 5. Atoms and monatomic ions. 6. Diatomic radicals. 7. Triatomic radicals. 8. Tetra-atomic radicals. 9. Penta-atomic radicals. 10. Summary and conclusions.
Appendices: 1. The language of group theory. 2. The spin Hamiltonian. 3. Calculation of g-values. 4. Determination of spin-density distribution and bond angles. 5. Analysis of electron spin resonance spectra. Index of data. Subject index.

FUNDAMENTALS OF METAL DEPOSITION

by E. RAUB and K. MÜLLER

viii + 265 pages, 10 tables, 138 illus., 245 lit. refs., 1967, Dfl. 60.00, £7.5.0.

Contents: 1. Chemical and electrochemical principles. 2. Electrode processes. 3. The cathodic discharge of ions. 4. The structure of electrolytic metal deposits. 5. Physical and chemical properties of electrolytic metal deposits. 6. Distribution of electrolytic metal deposits on the cathode. Index.

DETERMINATION OF GERMANIUM IN SYNTHETIC FIBERS BY SOLVENT EXTRACTION AND ATOMIC ABSORPTION SPECTROPHOTOMETRY

(Short Communication)

M. YANAGISAWA, M. SUZUKI AND T. TAKEUCHI,

SPECTROPHOTOMETRIC DETERMINATION OF THALLIUM(III) WITH THIOSALICYLAMIDE

(Short Communication)

S. C. SHOME AND M. MAZUMDAR,

ANALYTICAL APPLICATIONS OF THIO-, SELENO- AND TELLUROETHERS
PART I. DETECTION OF PALLADIUM

(Short Communication)

L. R. M. PITOMBO,

ห้องสมุด กรมวิทยาศาสตร์

Photoluminescence of Solutions

With Applications to Photochemistry and Analytical Chemistry

by C. A. Parker, Royal Naval Scientific Service, Head of Chemistry Division of the Admiralty Materials Laboratory, Holton Heath, Poole, Dorset, England

6 × 9″, xvi + 544 pages, 53 tables, 188 illus., 443 lit. refs., 1968, Dfl. 85.00, £11.10.0.

Contents: Basic principles, definitions and kinectics of fluorescence, phosphorescence and delayed fluorescence; polarisation; light scattering; monochromators; light sources; filters; photodetectors; actinometry; recording systems; inner filter effects; specimen compartments; correction of spectra; measurement of photoluminescence efficiency and lifetime; purity of materials; parameters of singlet and triplet states; equilibria in the excited state; excited dimers; solvent effects; fluorescence and phosphorescence analysis.

Comprehensive Analytical Chemistry

edited by C. L. Wilson, Professor of Inorganic and Analytical Chemistry, University of Belfast (Northern Ireland)
and D. W. Wilson, Head of the Chemistry Department, Sir John Cass College, London (England)

VOLUME IIB: Physical Separation Methods

6 × 9″, xvi + 445 pages, 30 tables, 116 illus., 897 lit.refs., 1968, Dfl. 70.00, £8.10.0.

Volume Two, Part B is devoted to physical separation methods. After an account of the theory and practise of liquid chromatography in columns, the volume continues with a lengthy treatment of gas chromatography.
The next chapter, on ion exchangers, is notable for the account it gives of analytical applications, while distillation (theory and technique) is the last topic to be treated in the present volume.

Contents: I. *Liquid Chromatography in Columns*. 1. Introduction. 2. Theory. 3. Apparatus and operation. II. *Gas Chromatography*. 1. Introduction and general principles. 2. Theoretical aspects. 3. Apparatus. 4. The partitioning phases. 5. Absorbents and gas-solid chromatography. 6. Gas-liquid chromatography. 7. Analytical methods. 8. Applications. III. *Ion Exchangers*. 1. Foreword. 2. Introduction. 3. The constitution of ion exchangers. 4. The mechanism of ion exchange. 5. Technique. 6. Analytical applications. Appendix 1: Ion-exchanger data. Appendix 2: Methods of testing ion exchangers. Appendix 3: Bibliography. IV. *Distillation*. 1. Introduction. 2. Theoretical background. 3. Experimental techniques.

Atomic–Absorption Spectroscopy

and Analysis by Atomic-Absorption Flame Photometry

by J. Ramírez-Muñoz, Principal Applications Chemist at Beckman Instruments Inc. and Scientific Research Collaborator of the C.S.I.C., Spain

6 × 9″, xii + 493 pages, 23 tables, 156 illus., 950 lit. refs., 1968, Dfl. 80.00, £9.15.0.

Contents: *Part I: Fundamentals*. 1. Origins of the method and nomenclature. 2. General principles and characteristics. 3. Absorption and emission. 4. The literature of atomic-absorption spectroscopy. 5. Theory. *Part II: Instrumental Systems*. 6. Instrumental systems. 7. Emission systems. 8. Absorption system. 9. Selection system. 10. Photometric system. 11. Instruments. *Part III: Range and Limitations of Atomic Absorption Methods*. 12. Determinable elements. Choice of lines. 13. Sensitivity. 14. Limitations in atomic absorption. *Part IV: Experimental Methods*. 15. Experimental process. 16. Standard solutions. 17. Preparation of the sample. 18. Experimental measurements and calibration. *Part V: Applications*. 19. Applications. Appendix. Bibliography.

ANALYTICA CHIMICA ACTA

Editors

PHILIP W. WEST *(Baton Rouge, La., U.S.A.)*

A. M. G. MACDONALD *(Birmingham, Great Britain)*

THE ROLE OF IRON(III) HYDROXIDE AS A COLLECTOR OF MOLYBDENUM FROM SEA WATER*

Y. S. KIM AND H. ZEITLIN
Department of Chemistry and Hawaii Institute of Geophysics, University of Hawaii, Honolulu 96822 (U.S.A.)
(Received February 6th, 1969)

Despite the fact that iron(III) hydroxide is one of the most commonly used and efficient collectors of trace metals in sea water, its role remains ambiguous and unclarified to a substantial degree. In brief discussions of its function, RILEY AND SKIRROW[1] and JOYNER et al.[2] subscribed to the view which appears to be generally accepted, *i.e.*, that iron(III) hydroxide behaves in sea water as a negatively charged colloid capable of scavenging numerous cationic species. These include Al, As, Be, Co, Ga, Ge, the lanthanons, Mo, Ni, Nb, Th, Sc, Se, U, V, W and Y[1]. The collection is usually carried out by adding iron(III) chloride solution to the sea water. The negatively charged iron(III) hydroxide sol which is formed, collects on its surface the cations in the sea water. The result is a coagulated coprecipitate enriched with trace metals that can easily be separated from their aqueous environment by filtration. The species of interest in the precipitate is then determined by an appropriate method.

During the course of a study which necessitated the use of iron(III) hydroxide in sea water as a trace metal collector, it became clear that the commonly accepted colloidal role for iron(III) hydroxide was an over-simplified one and did not explain satisfactorily the wide variety of elements collected. Specifically, it did not appear to be in accord with the known chemistry of several of the elements which are believed to exist in aqueous solution over a wide pH range as anionic species and, consequently, under those conditions, are not capable of being collected by a negatively charged colloid.

This paper is concerned with a study of the behavior and role of iron(III) hydroxide in sea water under a variety of controlled conditions. Molybdenum was selected as the model trace element since it has been established[3] that it exists in water as the molybdate anion (MoO_4^{2-}) above the pH of 1.0. In addition, it was hoped, through the establishment of optimum conditions, to work out the details of a procedure for the determination of molybdenum in sea water, comparable to that recently reported by KIM AND ZEITLIN[4].

The general procedure adopted was to add known amounts of molybdenum to filtered sea-water samples. After addition of iron(III) chloride solution, the pH of the sea-water samples was adjusted to cover a range of 4.0 to 10.0. The coprecipitates were collected by filtration and the molybdenum present in each case determined by

* Hawaii Institute of Geophysics Contribution No. 260.

the sensitive thiocyanate procedure of SANDELL[5]. The data expressed in absorbance units were compared with the absorbance of a standard regarded as 100% recovery, and the percent recoveries were calculated for each pH. The charge of the iron(III) hydroxide colloid formed in distilled water was determined qualitatively in an electrophoretic cell over a range of pH and the results were compared with the recovery data in order to elucidate the role of the collector. An analytical procedure for the determination of molybdenum in sea water was worked out and evaluated with and without the use of iron(III) hydroxide.

EXPERIMENTAL

Apparatus

Spectrophotometer, Beckman DU. Matched quartz cells of 1.0 cm path length.
pH meter, Beckman Zeromatic.
Filters, Millipore, HA-47 mm diameter.
Separatory funnels used for extraction were equipped with teflon stopcocks.

Reagents

All chemicals employed were of analytical grade; aqueous reagents were prepared in doubly distilled deionized water.

Standard molybdenum solution. Pure ammonium molybdate, $(NH_4)_2Mo_7O_{24}\cdot 4H_2O$, was used to prepare the standard solution as described previously[4]. Appropriate aliquots of the solution when added to filtered sea water furnished concentrations of molybdenum ranging from 0 to 6 $\mu g/500$ ml, not including that originally present in the sea water.

Effect of pH

The basic working procedure utilized clear, uncontaminated nearshore sea water filtered through a 0.45-μ millipore filter. The well-mixed pool of water upon which tests were conducted was analyzed for molybdenum content by the method described below and found to contain 6.0 $\mu g/500$ ml. To 500-ml samples were added 1 ml of 18 N sulfuric acid, 3.0 ml of 0.1 M iron(III) chloride, and 6.0 μg of molybdenum, thus providing samples containing a total of 12.0 μg molybdenum to be used in the pH studies. The samples in duplicate were adjusted with 6 M ammonia solution to pH 4.0, 5.5, 7.5, and 8.5, and 10.0 (± 0.1). Additional pairs of samples adjusted to each pH to which no molybdenum was added served as sea-water blanks. Each set of precipitates was collected on an 8-μ millipore filter and dissolved in 2–3 ml of concentrated hydrochloric acid. The solutions were evaporated to dryness on a low-temperature hot plate and allowed to cool. Hydrochloric acid (5 ml of 6 N) was added together with 3.0 ml of aqueous 10%(w/v) EDTA solution to complex the iron(III) to prevent interference with the thiocyanate method for molybdenum. The resulting solution was boiled for 1 min, and transferred upon cooling to a separatory funnel, and water was added to a volume of 40.0 ml. Then 1 ml of aqueous 40%(w/v) potassium thiocyanate solution and 1 ml of 40%(w/v) tin(II) chloride solution in 1.5 N hydrochloric acid were added and the solution was mixed thoroughly. Mixed organic solvent (5 ml, 1:1, chloroform:carbon tetrachloride) was added and the mixture shaken manually for 1 min in order to extract the molybdenum complex.

After separation, the bottom phase was drawn into a 1-cm cell and the absorbance measured at 470 nm against the blank (Table I).

In order to assess the effect of pH on the recovery of molybdenum, the absorbances measured were compared to the absorbance obtained from the analysis of replicate standards containing exactly 12.0 μg of molybdenum in which the precipitation step was omitted. For this purpose 3.0 ml of 0.1 M iron(III) chloride was evaporated to dryness in order to control the acidity. The residue was re-dissolved in 5.0 ml of 6 N hydrochloric acid and 3.0 ml of aqueous 10% EDTA solution were added. The solution was transferred to a separatory funnel and 12.0 μg of molybdenum was added together with water to a volume of 40.0 ml. The SANDELL procedure outlined above for molybdenum was carried out on a blank to which no molybdenum was added. In order to reconfirm the effectiveness of the coprecipitation of molybdenum with iron(III) hydroxide at the concentration of molybdenum originally present in the 500-ml sea-water sample (6.0 μg), and to test for a salt effect, the standard was analyzed and the absorbance was compared both with the absorbance from a 500-ml sample of 3.5% sodium chloride solution to which 12.0 μg of molybdenum had been added and with the absorbance from a 500-ml sea-water sample containing the collector to which 6.0 μg of molybdenum had been added and the pH adjusted to 4.0.

Determination of charge of iron(III) hydroxide colloid

The charge on the iron(III) hydroxide colloid was determined qualitatively in distilled water over a range of pH (4–10) in an electrophoretic cell composed basically of three cylindrical clear plexiglass compartments. A combined pH electrode was inserted in the central compartment while the two electrodes were placed in the outer compartments. The distance between the electrodes was about 16 cm. A solution of 0.01 M iron(III) chloride was poured into the cell, the pH was adjusted with 0.1 M ammonia, and the contents were stirred. In each of the runs, 500 V were applied for 10 min with a current of 5–15 mA which varied depending upon the pH of the solution. The directions of migration and charge were obtained through observation of the deposition of the iron(III) hydroxide suspension on rolled sections of filter paper in the cell located in the vicinity of the electrodes.

Determination of molybdenum. Method 1 (pH 4.0)

Since maximum recovery (see DISCUSSION OF RESULTS) of molybdenum from sea water was obtained by the iron(III) hydroxide collector at pH 4.0, this pH can be applied successfully for the determination of molybdenum. To duplicate samples of 500 ml of sea water were added 2.0, 4.0, and 6.0 μg of molybdenum. One pair of samples receiving no molybdenum was included as sea-water blanks. Sulfuric acid (1 ml of 18 N) and 3.0 ml of 0.1 M iron(III) chloride were added to each sample. The pH was adjusted to 4.0 with ammonia. The coprecipitate was allowed to settle for 2 h, and collected on an 8-μ millipore filter, and the molybdenum determined according to the basic working procedure described above. A straight line in conformity with Beer's law was obtained when absorbance was plotted *versus* molybdenum concentration. When the absorbance obtained from the sea-water blank was subtracted, the line passed through the origin. The absorbance obtained by the analysis of sea water to which no molybdenum was added was practically identical with the

absorbance from a sea-water sample containing 6.0 μg of molybdenum (Fig. 1, curves A, A'). This demonstrates that the concentration of molybdenum in sea water is 6.0 μg/500 ml.

Determination of molybdenum. Method 2 (pH 10.0)

An identical procedure was carried out on duplicate filtered sea-water samples which were adjusted to pH 10.0 with ammonia, but the addition of iron(III) chloride was omitted. The absorbance plotted *versus* molybdenum concentration yielded a straight line which passed through the origin when the absorbance from the sea-water blank was subtracted (Fig. 2).
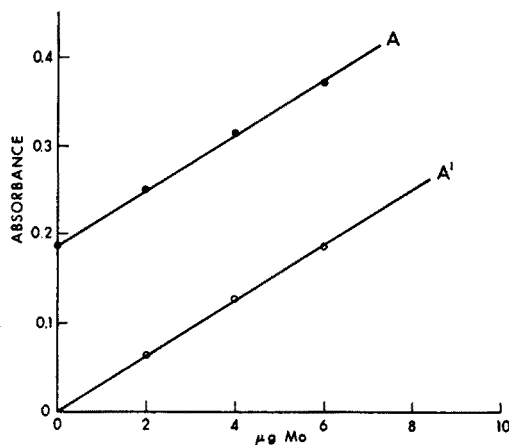
Fig. 1. Calibration curve for molybdenum precipitated by iron(III) hydroxide at pH 4.0 ($\pm$0.1). A' = A — 0.187.
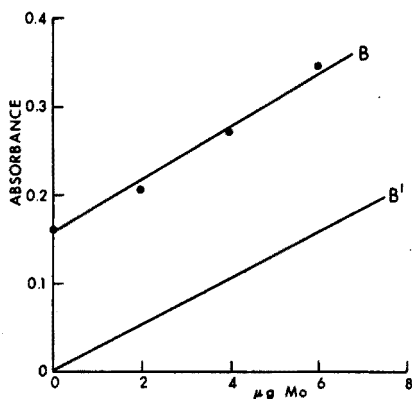
Fig. 2. Calibration curve for molybdenum precipitated by calcium and magnesium salts at pH 10.0 ($\pm$0.1). B' = B — 0.160.

DISCUSSION OF RESULTS

Effect of pH and determination of charge

The rust-brown iron(III) hydroxide precipitate starts to form at pH 2.2, and, according to CHARLOT[6], precipitation is complete at 3.5, although at pH *ca.* 10 con-

TABLE I

RECOVERY DATA FOR MOLYBDENUM IN SEA WATER

(6 μg Mo added to 500 ml of sea water)

pH ($\pm$0.1)	Absorbance (mean of duplicates)	Recovery (%)
4.0	0.372	96.5
5.5	0.344	89.4
7.5	0.236	61.4
8.5	0.090	23.4
10.0	0.340	88.5

siderable quantities of calcium and magnesium salts are deposited from sea water. Table I shows the striking dependence of recovery of molybdenum upon pH, as measured by the absorbance of the thiocyanate complex. The yield of molybdenum was optimal at pH 4.0, decreasing significantly with increasing pH to a minimum at 8.5 where a small but still detectable amount of molybdenum was noted. Beyond pH 9, the bulky white precipitates of calcium and magnesium salts were superimposed upon the iron(III) hydroxide and interfered with the assessment of iron(III) hydroxide as a collector of molybdenum. A high recovery was also obtained at pH 10.0, but it is believed that the collection of molybdenum by iron(III) hydroxide would be expected to decrease above pH 8.5. In order to confirm this view and to evaluate quantitatively the effect of iron(III) hydroxide in the absence of calcium and magnesium salts, iron(III) chloride solution was added to duplicate 500-ml samples of 3.5% sodium chloride solution containing 12.0 μg of molybdenum, the pH was adjusted to 9.5, and the precipitate was collected and analyzed for molybdenum. The absorbance obtained was zero, indicating that no molybdenum was collected by iron(III) hydroxide under these conditions. Consequently, the high recovery of molybdenum obtained in sea water at the pH of 10.0 (Table I) was attributed entirely to occlusion or coprecipitation by the calcium and magnesium salts deposited at this pH. This conclusion was verified by carrying out tests on 500-ml samples of sea water enriched with 12 μg of molybdenum, which were adjusted to pH 10.0 but to which no iron(III) chloride was added. The absorbance (average) obtained was identical with that for sea water containing 12 μg of molybdenum treated with iron(III) chloride.

Quantitative data expressed in percent recovery of molybdenum are given in Table I in order to evaluate the effectiveness of the coprecipitation of molybdenum with iron(III) hydroxide as a function of pH. The coprecipitation was virtually complete (96.5%) at pH 4.0. In order to account for the major portion of molybdenum that remained unprecipitated at pH 8.5, iron(III) chloride was added to the filtrate, the pH readjusted to pH 4.0, and the second precipitate collected and analyzed for molybdenum. Practically all of the molybdenum not present in the first precipitate was detected in the second. At pH 10.0, 88.5% of the molybdenum was brought down by the calcium and magnesium salts. The relatively high recoveries of molybdenum obtained at pH 4.0 and 10.0 suggested their feasibility for the determination of molybdenum (see below).

The observations and results are best explained on the basis of a colloidal iron(III) hydroxide model in sea water; this model was suggested earlier by HARVEY[7] who showed that iron(III) hydroxide is negatively charged in alkaline solution and positive in acid. ISHIBASHI AND FUJINAGA[8], in related work concerning the collection of molybdenum in artificial sea water through the introduction of solid iron(III) hydroxide, demonstrated that the most effective recovery of molybdenum took place in the 3–4 pH range. The charge on the colloid was not considered. The present work, which is in general agreement with the above, shows conclusively that the iron(III) hydroxide upon its formation in an aqueous medium possesses a charge which is pH-dependent. At pH 4.0 the colloid apparently has maximum positive-charge density on its surface, and thus is able to adsorb quantitatively the negatively charged molybdate anions and presumably other anionic species. An increase in pH is accompanied by a decrease in the positive-charge density, resulting in a decreased recovery of molybdenum. At pH 8.5 the positive-charge density is relatively low and

the recovery of molybdenum is consequently low. Above this pH and presumably beyond the isoelectric point—not determined in sea water because of experimental difficulties—the charge on the iron(III) hydroxide is reversed and presumably the colloid is able to collect cations. At pH 10.0, the negatively charged iron(III) hydroxide is not capable of collecting an anionic species such as molybdate ion, which is completely unaffected.

A second condition, however, besides that of charge, may be necessary for the quantitative collection of a trace species such as molybdenum. The PANETH–FAJANS–HAHN rule[9] may also apply in this situation. The collector should contain an ion which forms a compound of low solubility with the counter ion adsorbed. This requirement is met in the case of iron(III) hydroxide at a low pH since iron(III) molybdate is relatively insoluble. Aluminum hydroxide behaves like iron(III) hydroxide in that at pH 5.5 it forms a positively charged colloid in sea water and should adsorb molybdenum effectively. Actually, the recovery of molybdate at pH 5.5 is only 7.8%, a result best explained by the solubility of aluminum molybdate.

Attempts made to determine the charge of the iron(III) hydroxide colloid in sea water by electrophoresis were inconclusive and were abandoned because of the high ionic strength of the sea water, the difficulty in maintaining pH control due to electrolysis, and the rapid flocculation of the colloid in the sea water. Qualitative tests on the charge were carried out in distilled water which were in fairly good agreement with the findings of HARVEY and with the present recovery data and conclusions. At pH 4.0, the bulk of the iron(III) hydroxide precipitate was deposited on the filter paper located at the negative electrode, confirming the positive charge on the colloid. A similar result was obtained at pH 6 and pH 7.5, but to a lesser degree. At pH 9–10, however, the iron(III) hydroxide suspension migrated to the positive electrode, demonstrating a reversal of charge.

The results point to the conclusion that in order for iron(III) hydroxide to collect cations in sea water, the pH of the water should be on the basic side (>9). Since the charge of the iron(III) hydroxide is pH-dependent, it is suggested, whenever this collector is employed for preconcentration purposes, that the optimum pH be determined and clearly specified.

Determination of molybdenum. Method 1 (pH 4.0)

As mentioned in the EXPERIMENTAL section, iron(III) hydroxide can be used successfully for the determination of molybdenum in sea water by adjusting the pH of the water sample to 4.0 and completing the analysis by the procedures outlined. Iron(III), which is the principal interfering species since it reacts readily with thiocyanate, is easily masked with EDTA. The determination is simple to carry out and the standard calibration curve reproducible (Fig. 1, curve A). The accuracy and precision are similar to those of the method reported recently by KIM AND ZEITLIN[4], which involved formation of molybdenum oxinate and coprecipitation with aluminum sulfate and tannic acid at pH 4.0.

Determination of molybdenum. Method 2 (pH 10.0)

If desired, pH 10.0 can be employed in place of 4.0 for the determination of molybdenum in sea water; iron(III) is then not necessary or desirable. A working curve can be obtained by the standard addition method (Fig. 2, curve B). The re-

covery of molybdenum, however, is less than at pH 4.0 (Table I), and the linearity of the working curve is less pronounced than that at pH 4.0. These disadvantages, together with the bulky nature of the calcium and magnesium precipitates containing the molybdenum, suggest that Method 1 is preferable.

SUMMARY

The behavior of iron(III) hydroxide was studied in order to clarify its role as a collector of the trace element molybdenum in sea water. Iron(III) hydroxide formed in sea water possesses a charge which is pH-dependent. At pH 4.0 the colloid has an apparent maximum positive-charge density and is able to adsorb molybdenum quantitatively as molybdate. Above pH 9 the charge is reversed and the iron(III) hydroxide no longer collects molybdate. Qualitative electrophoretic tests carried out in distilled water confirmed the positive and negative charge on the iron(III) hydroxide in acid and basic solution, respectively. At pH 10.0, calcium and magnesium salts coprecipitated molybdate in the presence or absence of iron(III) hydroxide. Procedures were worked out for the determination of molybdenum in sea water concentrated by iron(III) hydroxide at pH 4.0, and by calcium and magnesium salts at pH 10.0.

RÉSUMÉ

On examine le comportement de l'hydroxyde de fer(III), comme collecteur du molybdène dans l'eau de mer. Cet hydroxyde formé dans l'eau de mer possède une charge dépendant du pH. A pH 4.0, le colloïde présente un maximum de densité de charge positive et peut adsorber quantitativement le molybdène sous forme de molybdate. Au dessus du pH 9, la charge est inversée et l'hydroxyde de fer(III) n'est plus capable de collecter le molybdate. Des tests par électrophorèse qualitative, effectués dans l'eau distillée confirment la charge positive et négative sur l'hydroxyde de fer(III), respectivement en milieu acide et basique. Au pH 10, il y a coprécipitation des sels de calcium et de magnésium en présence ou en l'absence d'hydroxyde de fer(III). Des méthodes ont été mises au point pour le dosage du molybdène dans l'eau de mer, concentré par hydroxyde de fer(III) à pH 4.0 et par calcium et magnésium à pH 10.0.

ZUSAMMENFASSUNG

Das Verhalten von Eisen(III)-hydroxid wurde untersucht, um seine Rolle als Sammler für das Spurenelement Molybdän in Seewasser aufzuklären. In Seewasser gebildetes Eisen(III)-hydroxid besitzt eine vom pH-Wert abhängige Ladung. Beim pH 4 hat das Kolloid offenbar eine maximale positive Ladungsdichte und ist imstande, das Molybdän quantitativ als Molybdat zu adsorbieren. Oberhalb pH 9 besitzt das Eisen(III)-hydroxid eine umgekehrte Ladung und ist nicht länger fähig, Molybdat zu adsorbieren. Qualitative, elektrophoretische Prüfungen in destilliertem Wasser bestätigen die positive und negative Ladung des Eisen(III)-hydroxids in saurer bzw. basischer Lösung. Beim pH 10 wird das Molybdat in Anwesenheit oder Abhängigkeit von Eisen(III)-hydroxid durch Calcium- und Magnesiumsalze mit-

gefällt. Es werden Verfahren angegeben zur Bestimmung von Molybdän im See-
wasser nach Konzentrierung durch Mitfällung durch Eisen(III)-hydroxid beim pH 4
und durch Calcium- und Magnesiumsalze beim pH 10.

REFERENCES

1 J. P. RILEY AND G. SKIRROW, *Chemical Oceanography*, Vol. I, Academic Press, London and
  New York, 1965, p. 327.
2 T. JOYNER, M. L. HEALY, D. CHAKRAVARTI AND T. KOYANAGI, *Environ. Sci. Tech.*, 1 (1967) 417.
3 A. K. BABKO AND B. I. NABIVANETS, *Zh. Neorgan. Khim.*, 2 (1957) 2096.
4 Y. S. KIM AND H. ZEITLIN, *Limnol. Oceanog.*, 13 (1968) 434.
5 E. B. SANDELL, *Colorimetric Determination of Traces of Metals*, Interscience, New York, 1959,
  p. 644.
6 G. CHARLOT, *Qualitative Inorganic Analysis*, John Wiley, New York, 1954, p. 162.
7 H. W. HARVEY, *J. Marine Biol. Assoc. U.K.*, 22 (1937) 222.
8 M. ISHIBASHI AND T. FUJINAGA, *J. Chem. Soc. Japan*, 79 (1958) 1496.
9 H. A. LAITINEN, *Chemical Analysis*, McGraw-Hill, 1960, p. 167.

CHELATE ENHANCEMENT OF THE SENSITIVITY FOR MAGNESIUM IN NEUTRON ACTIVATION ANALYSIS

JAMES B. SMATHERS
Nuclear Engineering Department, Texas A. and M. University, College Station, Texas 77843 (U.S.A.)
DICK DUFFEY AND SITMARA LAKSHMANAN
University of Maryland, College Park, Md. (U.S.A.)
(Received January 10th, 1969)

Of the many trace metal analysis techniques available neutron activation analysis is one of the more recently developed, and consequently has not been refined to yield the optimum sensitivities possible in many cases. This paper presents a method which was developed to increase the sensitivity for magnesium. It is based on the suggestion by YUROW[1] that bromine-containing derivatives of standard chelating agents might be utilized to increase the sensitivity of detection of elements such as iron, calcium or magnesium. The magnesium in the sample is chelated by the bromine-containing derivative, the chelate isolated by paper chromatography, the sample irradiated, and the amount of magnesium present inferred from the ^{82}Br activity.

The neutron activation methods presently used depend on the thermal neutron reaction ^{26}Mg (n, γ) ^{27}Mg, and are reported[2] to yield a sensitivity of 0.5 μg of magnesium with a 10^{12} n/cm²/sec flux, which was confirmed in the present work. Another neutron activation method for magnesium is commonly employed in threshold detector flux analysis[3]. The reaction ^{24}Mg (n, p) ^{24}Na has a 6.3-MeV threshold energy, and an effective cross-section of 0.144 barns. However, the low flux levels of reactors for energies above the 6.3-MeV threshold preclude the use of this method for determination of magnesium in the microgram range, though it may be feasible for use with 14-MeV neutron generators. In the latter case, however, the neutron flux intensity obtainable at the present time is not great enough to achieve the 0.5-μg sensitivity.

Chelate formation

The optimum chelating agent for the method will contain multiple atoms of an element which possesses a large neutron cross-section, and a half-life long enough to permit reasonable handling of the sample after activation. The method presented below utilizes the chelating agent, 5,7-dibromo-8-hydroxyquinoline (bromoxine), bromine having the desired neutron activation characteristics; magnesium forms a 1:2 chelate with bromoxine, as is well known.

Bromoxine is very soluble in chloroform and acetone, and varies from soluble to insoluble in carbon tetrachloride, methanol, butanol, isopropanol, ethanol, and benzene. Chloroform was therefore selected as the organic phase solvent.

Throughout the development of the method, the isotopic tracer ^{28}Mg was used

extensively to verify the separations and efficiency values. In the following sections, this method of determining the parameter under discussion is to be assumed, unless stated otherwise.

Preliminary work indicated that the magnesium chelate would only form above pH 9, hence it was necessary to add another complexing agent while the solution was acidic, to prevent the formation and precipitation of magnesium hydroxide in the basic solution. Ammonium tartrate and ammonium oxalate were examined, and the extraction efficiency of the magnesium–bromoxine chelate was found to be independent of the choice of intermediate complexing agent. Ammonium oxalate was subsequently selected for use, because it also aided in the separation of magnesium from calcium-containing samples (see below).

Initial studies at pH 10.5 indicated incomplete extraction of magnesium. A survey to find an extraction enhancing agent which would increase the extraction percentage to 95% or greater yielded three agents, pyridine, butanol, and 2,4,6-trimethylpyridine. The results (Table I) suggest that all three agents are equally successful. Butanol was rejected as the chelate was more soluble in the other extraction solutions, and pyridine was rejected because of its miscibility with water. Thus, 2,4,6-trimethylpyridine was selected as the extraction enhancing agent.

TABLE I

EFFICIENCY OF EXTRACTION ENHANCEMENT ADDITIVES

Additive	Percentage extracted per extraction					
	Extraction	1	2	3	4	5
Chloroform (blank)		63	14	11	6	5
Butanol		92	7	1	—	—
Pyridine		96	3	1	—	—
2,4,6-Trimethylpyridine		95	3	1	—	—
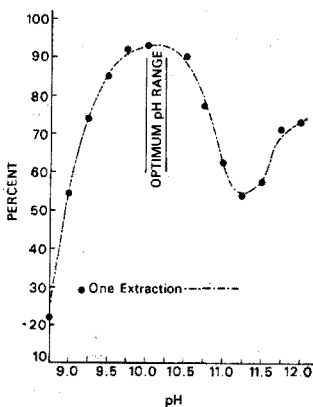
Fig. 1. Percentage extraction of magnesium–bromooxinate vs. pH of aqueous phase.

The relationship between the quantity of enhancing agent added and the percentage of magnesium extracted was evaluated; 1 ml of enhancing agent per 10 ml of extraction solution was found to be adequate, and increasing the amount had no beneficial effect.

The efficiency of extraction *vs.* pH was measured (Fig. 1); the aqueous sample was treated with 1 ml of saturated ammonium oxalate solution, adjusted to the required pH value, and extracted with 10 ml of a 95:5 mixture of 0.1% bromoxine in chloroform, and 2,4,6-trimethylpyridine. The optimum pH value for a single extraction was found to be 10.0–10.2.

Extraction conditions having been optimized, the sensitivity limitations and linearity of the extraction method were then determined. The data obtained showed excellent linearity over the range 1 μg Mg (*ca.* 500 counts/min) to 1000 μg Mg (*ca.* $10^{5.5}$ counts/min). Below 1 μg of magnesium, linearity was maintained but precision was poor. The sensitivity was limited by poor counting statistics due to the low specific activity of the ^{28}Mg tracer.

The 1:4 magnesium–bromine ratio in the chelate was verified by Job's spectrophotometric transmission method; the absorbances of extraction solutions of varying molar ratios of magnesium and bromoxine were measured at 392 nm and the peak absorbance occurred at a magnesium–bromoxine ratio of 1:2.

Chromatographic separation

For the amount of magnesium present to be inferred from the ^{82}Br activity which results from thermal neutron irradiation of the chelate, the excess of bromoxine must be separated from the magnesium–bromoxine chelate. Paper chromatography was chosen for this separation, and some 28 solvent systems were evaluated for their ability to elute the two compounds. However, no single eluent for the two substances could be found, and it proved necessary to develop the strips first in a solvent to move the excess of bromoxine, and then in a second solvent to move the chelate from any residue present at the origin.

The loading characteristics of the solvent systems for moving the excess bromooxine were determined by assaying the ^{82}Br activity resulting from neutron irradiation of 1-in strip segments after an 8-in development of a 25 μl spot of 0.1% bromooxine in chloroform. A second series of strips was developed until the solvent front had reached the top of the strip (18 in) to determine if any residue in excess of the 0.3% counting statistics detection limit, was left at the origin. Both xylene and carbon tetrachloride were found to give acceptable results. Neither xylene or carbon tetrachloride solvent systems moved the chelate spot from the origin and because xylene gave a faster development, it was selected for use.

TABLE II

MOVEMENT OF CHELATE SPOT TAGGED WITH ^{28}Mg BY SOLVENT SYSTEMS[a]

Position of 1-in strip increment	% of initial spot			
	Pyridine + NH$_4$OH	Acetone + NH$_4$OH	2,4,6-Trimethyl-pyridine + water	Ethyleneglycol monoethyl ether
1	1	—	—	—
2 (Origin)	—	4	18	35
3	—	2	28	17
4	2	3	21	15
5	2	32	12	31
6	95	59	22	2

[a] Because of a low count rate, the counting statistics for this determination gave a standard deviation of ±3%.

The solvent systems evaluated for the development of the magnesium–bromoxine chelate and the results are listed in Table II; the ammoniacal pyridine system was obviously the most suitable.

Autoradiographs of the induced [82]Br activity indicated that the chelate spot was splitting into three separate spots during some of the developments with pyridine. One spot ran at the solvent front, one at the R_F value given in Fig. 2, and the third halfway between the two. Various possible causes were studied, and the following were found not to be the cause: amount of ammonium oxalate added to the extraction vessel, pH of the extraction solution, amount of shaking for extraction, drying time of the spot, impurities in the bromoxine or other contaminating elements, amount of 2,4,6-trimethylpyridine added for extraction, concentration of magnesium in the aqueous phase or concentration of bromoxine in the chloroform phase.

When radioautographs indicated identical triple spots for the magnesium–8-hydroxyquinoline chelate, the effect was attributed to the hygroscopic nature of magnesium chelates of the oxine family. STARY[4] has reported that the magnesium–oxine chelate adds water and forms an insoluble compound $Mg(Ox)_2 \cdot 2H_2O$.

Solution of the problem proved simple. If a fresh 1:1 (v/v) pyridine–concentrated ammonia solution is used for each chromatogram, the three spots run as one at the solvent front. The 4:1 bromine:magnesium ratio of this combined spot was confirmed by means of neutron activation analysis. The cause of the triple spotting is not known with certainty, but the remedy is simple and acceptable.

Contaminating elements

As the method was developed for analysis of magnesium in biological samples, the problem of interferences from other elements had to be considered. The contaminating elements most likely to pose problems were iron, calcium, sodium, chlorine, phosphorus, and potassium. Of these six, sodium, chlorine, potassium, and phosphorus were eliminated as they did not complex with bromoxine, and remained in the aqueous phase during extraction.

Iron was eliminated by prior extraction with 2-thenoyltrifluoroacetone[5,6]. Because of the higher pH values used (pH 5 and 7) CHENG's procedure[5] for the extraction of iron was utilized. Calcium was also removed in the extraction of iron; moreover, the calcium–oxalate complex is insoluble at pH 10, and this further hinders the formation of a calcium–bromoxine chelate.
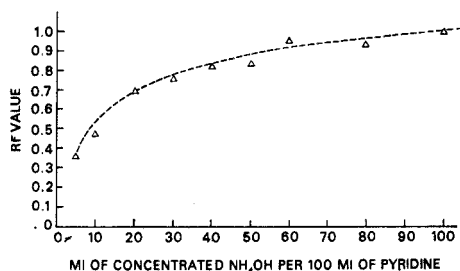
Fig. 2. R_F Value of third region *vs.* solvent composition.
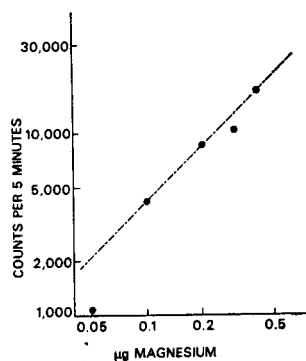
Fig. 3. Linearity of method *vs.* quantity of magnesium present in sample.

Based on an extensive tabulation of $pH_{\frac{1}{2}}$ values for metal ion chelates published by STARY[7], it would seem that if an extraction with bromoxine at pH 7 is performed after the above, then only barium(II), mercury(II), and strontium(II) would remain and might form chelates with bromoxine at pH 10, and so interfere. However, since none of the three ions are present to any significant extent relative to magnesium in normal biological specimens, the purification procedure was not elaborated to guarantee their removal.

The chromatographic separation and procedures for the removal of contaminating elements having been developed, it remained to verify that the linearity of the solvent extraction step had not been lost in the additional steps. Figure 3 illustrates the range and reproducibility possible, determined by means of the induced [82]Br activity.

GENERAL PROCEDURE

For the biological samples analyzed in this work, a nitric acid digestion procedure was used to obtain the sample in solution. The digested sample was then transferred quantitatively to a separatory funnel and 1 ml of saturated ammonium oxalate solution was added.

After the pH had been adjusted to 5 with ammonium hydroxide, an initial series of extractions were performed to remove possible interfering elements; after extraction with 0.5 M thenoyltrifluoroacetone solution[5], the pH of the aqueous solution was adjusted to 7, and a further extraction with 0.1 M bromooxine was carried out.

Then the pH was raised to 10 by addition of ammonia solution, and magnesium was extracted with 10 ml of extraction solution (5% 2,4,6-trimethylpyridine and 95% 0.1% bromooxine in chloroform). The volume of extraction solution may be varied depending on the expected amount of magnesium.

Aliquots (100 μl each) of the extraction solution were spotted on the chromatographic strip and the excess of chelating agent was separated from the magnesium–bromooxine chelate by development with xylene saturated with water. The excess of bromooxine moved at the solvent front to the top of the strip. The strip was then dried and developed with a freshly prepared 1:1 (v/v) mixture of pyridine and concentrated ammonia solution to move the chelate about 3 cm from the origin.

The chelate spot was then excised from the strip, sealed in an irradiation vial, and irradiated in the reactor at a thermal neutron flux of 10^{12} n cm^{-2} sec^{-1}. Standards of bromine salts were spotted on equal sized segments of chromatographic paper, sealed in vials, and irradiated simultaneously with the chelate samples. The samples were subsequently counted with a NaI (Tl) spectrometer system and the [82]Br activity of the chelate samples was determined by comparison to the known bromine standards. Since a known ratio exists between the bromine and magnesium in the chelate, the amount of magnesium in the sample was easily calculated.

APPLICATION TO BIOLOGICAL SPECIMENS

To demonstrate the applicability of the method to the determination of magnesium in biological specimens, a diluted sample of canine serum was analyzed

for magnesium content. For confirmation of the amount of magnesium present, an aliquot of the pooled sample was also analyzed for magnesium by atomic absorption spectrophotometry. The results of 12.7 μg/ml and 12.2 μg/ml, respectively, are in acceptable agreement, and tend to confirm the assumptions made about the removal of possible contaminating elements.

The method developed increases the neutron activation sensitivity for magnesium by a factor of five. In addition, it allows the determination of magnesium in matrices which would otherwise preclude analysis. The method also possesses the feature of replacing the time constraint imposed by the 9.5-min half-life of magnesium-27 with the flexibility associated with the 36-h half-life of bromine-82.

SUMMARY

A chelation technique is described in which the high sensitivity of neutron activation analysis for bromine is used to improve the activation sensitivity for magnesium. Magnesium is extracted with 5,7-dibromo-8-hydroxyquinoline in chloroform in the presence of 2,4,6-trimethylpyridine, the chelate is isolated by paper chromatography, and the amount of magnesium present is calculated from the bromine activity after activation. Experimental variables are discussed. The sensitivity limit for magnesium is *ca.* 0.1 μg.

RÉSUMÉ

Une technique par "chélation" est décrite; on utilise la grande sensibilité de l'analyse du brome par activation au moyen de neutrons pour augmenter la sensibilité d'activation du magnésium. Le magnésium est extrait avec la dibromo-5,7-hydroxy-8-quinoléine dans le chloroforme, en présence de triméthyl-2,4,6-pyridine. Le chélate formé est isolé par chromatographie sur papier; la teneur en magnésium est calculée à partir de l'activité du brome après activation. Divers facteurs expérimentaux sont discutés. La limite de sensibilité du magnésium est d'environ 0.1 μg.

ZUSAMMENFASSUNG

Es wird eine Technik beschrieben, bei der die Komplexbildung verwendet wird, um die hochempfindliche Neutronenaktivierungsanalyse für Brom zu nutzen und dadurch die Aktivierungsempfindlichkeit für Magnesium zu verbessern. Das Magnesium wird mit 5,7-Dibromo-8-hydroxychinolin in Chloroform in Gegenwart von 2,4,6-Trimethyl-pyridin extrahiert und das Chelat papierchromatographisch isoliert. Der Gehalt des Magnesiums wird dann aus der Brom-Aktivität nach der Aktivierung berechnet. Der Einfluss unterschiedlicher Versuchsbedingungen wird diskutiert. Die Nachweisgrenze für das Magnesium beträgt etwa 0.1 μg.

REFERENCES

1 H. W. YUROW, *Determination of Vanadium and Cobalt in Plants by Neutron Activation Analysis of Paper Chromatograms*, Ph.D. Thesis, Pennsylvania State University, 1960.
2 H. P. YULE, *Anal. Chem.*, 37 (1965) 129.

3 D. T. KILMINSTER, J. C. SACCENTI, J. H. MCNEILLY AND R. F. BENCK, *NDL-TR-57*, U. S. Army
   Nuclear Defense Laboratory, Edgewood Arsenal, Maryland, Dec. 1963.
4 J. STARY, *Anal. Chim. Acta*, 28 (1963) 132.
5 F. C. CHENG, D. DUFFEY AND S. LAKSHMANAN, Spectrophotometric and Derivative Activation
   Analysis of Iron(II), and Iron(III), *152 National Meeting Am. Chem. Soc., New York, 1966*.
6 F. L. MOORE, W. D. FAIRMAN, J. G. GANCHOFF AND J. G. SURAK, *Anal. Chem.*, 31 (1959) 1148.
7 J. STARY, *The Solvent Extraction of Metal Chelates*, MacMillan Co., New York, 1964.

EPITHERMAL NEUTRON ACTIVATION ANALYSIS FOR IODINE IN SMALL AQUEOUS SAMPLES

D. BRUNE

AB Atomenergi, Studsvik (Sweden)

(Received February 20th, 1969)

Neutron activation by means of epithermal neutrons has been achieved by several investigators[1-5]. This form of selective activation is simply carried out by absorption of the thermal neutrons in a suitable material, *e.g.* cadmium. The activity formed for a nuclide which possesses resonances in the epithermal part of the spectrum can thus be enhanced by comparison with that of a nuclide possessing smaller resonances.

The advantage of epithermal neutron activation compared with thermal neutron activation (with an epithermal contribution) can be measured quantitatively by means of the cadmium ratio, R_{Cd}.

Consider a nuclide which is to be determined (designated D) and an interfering nuclide (designated d); the enhancement in activity can be expressed simply as the ratio of their two cadmium ratios[2]:

$$F = \frac{(R_{Cd})_d}{(R_{Cd})_D} \tag{1}$$

The factor F may be described as the "advantage" factor. Generally, this "advantage" factor can be calculated from a knowledge of such parameters as thermal and epithermal neutron cross-sections, the epithermal index, the neutron temperature, and the cadmium cut-off energy. Compilations of thermal and epithermal cross-section data have recently been given by GOLDMAN *et al.*[6] and by DRAKE[7], respectively.

According to the WESTCOTT formulation[8], the total and the epithermal activation rates, C_{tot} and C_{epi}* respectively, are obtained from the following expressions[2]:

$$C_{tot} = nv_0 \left(g\sigma_0 + \frac{2}{\sqrt{\pi}} r \sqrt{\frac{T}{T_0}} I\right) \tag{2}$$

$$C_{epi} = nv_0 \frac{2}{\sqrt{\pi}} r \sqrt{\frac{T}{T_0}} (0.44\,\sigma_0 + I) \tag{3}$$

where n denotes the total unperturbed neutron density, v_0 is the neutron velocity at the energy $E_0 = 0.0253$ eV, g is a correction factor[8], r is the epithermal index, T is the neutron temperature of the Maxwellian distribution (T_0 the temperature corresponding to E_0), and I is the resonance integral ($1/v$ contribution excluded).

---

* C_{epi} corresponds to an effective cadmium cut-off energy of 0.5 eV.

Moreover,

$$R_{Cd} = \frac{C_{tot}}{C_{epi}} \tag{4}$$

and by substitution of (2) and (3) in (1), an expression for the "advantage" factor can be obtained.

In practice, however, an approximate knowledge of the F factor is sufficient for deciding whether a thermal or an epithermal activation should be preferred.

By approximating $g*$ and

$$\frac{2}{\sqrt{\pi}}\sqrt{\frac{T}{T_0}} **$$

each to unity, the following simplified expression for F is obtained:

$$F \approx \left[\frac{\sigma_0 + rI}{r(0.4\,\sigma_0 + I)}\right]_d \times \left[\frac{r(0.4\,\sigma_0 + I)}{\sigma_0 + rI}\right]_D \tag{5}$$

In a heavy water-moderated reactor, the epithermal index, r, is in the region of 0.04–0.06, whereas this index can reach 0.07–0.15 in a light water-moderated reactor.

As regards epithermal activation, the ratio of the activity of the nuclide to be determined to that of the interfering nuclide is independent of the epithermal index. According to eqn. (3) this ratio is given by:

$$\frac{(C_{epi})_D}{(C_{epi})_d} = \frac{(0.44\,\sigma_0 + I)_D}{(0.44\,\sigma_0 + I)_d} \tag{6}$$

In this connection therefore, the r value is only of importance as regards the absolute epithermal activity level. If the r value is not known for the irradiation position used, this value can be derived from cadmium ratio measurements of gold (thin gold foils or a lead gold alloy) by means of eqns. (2) and (3).

If all measurements are referred to the cadmium ratio for gold, the cadmium ratios for various other nuclides can be calculated from the following expression, which is deduced from eqns. (2) and (3):

$$R_{Cd} = 1 + \frac{\sigma_0}{\sigma_0^{Au}} \cdot \frac{0.44\,\sigma_0^{Au} + I^{Au}}{0.44\,\sigma_0 + I}(R_{Cd}^{Au}-1) \tag{7}$$

This formula is in agreement with those derived by alternative approaches[9,10].

APPLICATIONS OF EPITHERMAL NEUTRON ACTIVATION ANALYSIS

Some practical examples of epithermal neutron activation analysis which have been carried out are mentioned in Table I.

In the present work, the determination of iodine was studied in detail. The determination of iodine at the microgram level is of interest in the analysis of various pharmaceutical plasma solutions. Since such samples contain 0.9% sodium chloride, the induced iodine-128 activity suffers mainly by interference from chlorine-38 and to a smaller extent from sodium-24.

* The value of g for most nuclides[8] is close to 1.
** In heavy water-moderated reactors, T is often around 50°.

TABLE I

PRACTICAL APPLICATIONS OF EPITHERMAL NEUTRON ACTIVATION ANALYSIS

Nuclide		Material studied	"Advantage" factor	Ref.
Nuclide measured	Interfering nuclide			
^{56}Mn	^{38}Cl (^{24}Na)	Biological sample	6.5	1
^{99}Mo (^{99m}Tc)	^{59}Fe	Steel	15	2
^{98}Au	^{24}Na	Biological sample	6	4
^{80}Br	^{38}Cl (^{24}Na)	Sea water	17	5
^{239}U	^{56}Mn (^{24}Na)	Mineral	19	11
^{128}I	^{38}Cl (^{24}Na)	Pharma-ceutical	11	This work

Resonance parameters for chlorine-37 and iodine-127 in the (n,γ) reaction[7,12] suggest that the performance of an epithermal activation would be favourable for an enhancement of the iodine-128 activity. The "advantage" factor as measured, amounted to 11.

Samples as small as 50 μl were employed in order to decrease the sample volume so that not only would the simultaneous irradiation of several samples in the cadmium container be possible, but also flux distortion effects could be avoided. The activation procedure was accomplished by irradiating the aqueous droplets in a frozen condition.

EXPERIMENTAL

Aqueous samples of 50 μl containing 450 μg of sodium chloride and iodine in the range 0.2–50 μg, relevant to certain pharmaceutical plasma solutions, were frozen solid on pure aluminium foils. The foils were folded and transferred to the cadmium container which was cooled in liquid nitrogen before being placed inside the aluminium container. During the irradiation the cadmium container was cooled with dry ice (see Fig. 1).

The irradiation was performed for 3 min at a central position in the reactor R1. The epithermal index, r, in this position amounted to 0.048 and the thermal flux to $2.7 \cdot 10^{12}$ n cm^{-2} sec^{-1}.

After the irradiation the ice samples were quickly removed from the aluminium foils.

The iodine-128 produced was measured by γ-spectrometry. About 10 samples could be irradiated simultaneously.

RESULTS AND DISCUSSION

The technique of epithermal neutron activation analysis applied to 50-μl portions of aqueous samples, i.e. single water drops irradiated while frozen, made it possible to determine iodine in the concentration range 0.2–50 μg with a precision bet-
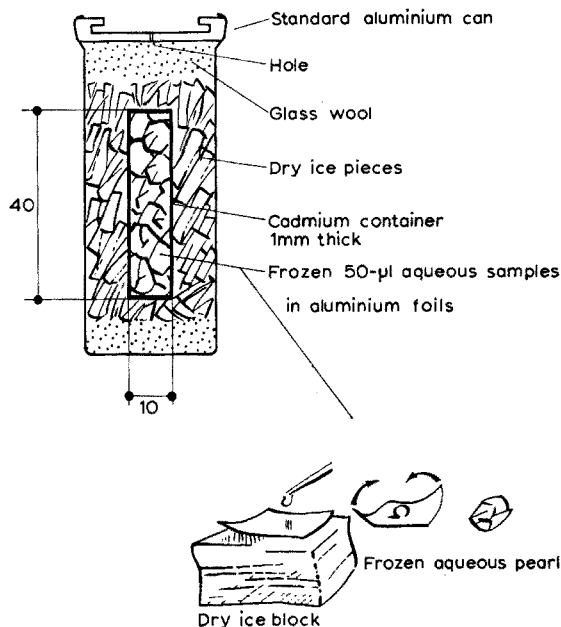
Fig. 1. Arrangement of frozen aqueous samples in cadmium covers cooled with dry ice.

ter than 10% by simple instrumental methods. These samples contained 0.9% sodium chloride; accordingly, iodine was measured in the presence of chlorine at a ratio of 1:2000.

During freezing of the small aqueous samples, some escape of iodine might be expected on account of segregation effects. This effect was not observed, however, as demonstrated by the ^{131}I freezing studies.

The technique described above for the low-temperature irradiation of small aqueous samples may find various applications in the analysis of biological tissues, enzyme solutions and certain pharmaceutical products.

The author is grateful to Dr. ERIK JOHANSSON for valuable discussions.

SUMMARY

Selective activation by means of epithermal neutrons is discussed in the light of the WESTCOTT nomenclature. Expressions for the calculation of the "advantage" factor when epithermal activation is used, are given. The epithermal activation technique has been applied to the determination of iodine at the microgram level in aqueous solutions containing iodine and chlorine in the ratio of about 1:2000. Aqueous samples as small as 50 μl were irradiated while frozen.

RÉSUMÉ

On examine l'activation sélective au moyen de neutrons épithermiques, selon

la nomenclature de WESTCOTT. On donne des expressions pour le calcul du facteur d'"avantage" obtenu avec l'activation épithermique. Cette technique d'activation épithermique a été appliquée au dosage de microquantités d'iode en solutions aqueuses, renfermant iode et chlore dans le rapport 1:2000. On a pu irradier de petits échantillons allant jusqu'à 50 μl, à l'état congelé.

ZUSAMMENFASSUNG

Die selektive Aktivierung mit epithermischen Neutronen wird in Hinblick auf die WESTCOTT-Nomenklatur diskutiert. Ausdrücke zur Berechnung des Nutzfaktors bei der Verwendung epithermischer Aktivierung werden angegeben. Die epithermische Aktivierungstechnik wird zur Bestimmung von Jod im Mikrogrammbereich in wässrigen Lösungen angewendet, die Jod und Chlor im Verhältnis von etwa 1:2000 enthalten. Wässrige Proben von 50 μl werden im gefrorenen Zustand bestrahlt.

REFERENCES

1 D. C. BORG, R. E. SEGEL, P. KIENLE AND L. CAMPBELL, Intern. J. Appl. Radiation Isotopes, 11 (1961) 10.
2 D. BRUNE AND K. JIRLOW, Nukleonik, 6 (1964) 242.
3 R. MALVANO, Eur-2076e, 1965.
4 M. RAKOVIČ AND Z. PROUZA, Isotopenpraxis, 4 (1968) 11.
5 H. W. NASS, Intern. Conf. on Modern Trends in Activation Analysis, Gaithersburg, U.S.A., Oct. 7–11, 1968.
6 D. T. GOLDMAN, P. ALINE, G. E. SAN JOSE AND R. SHER, Internal report FFX-105, AB Atomenergi, Studsvik, 1968.
7 M. K. DRAKE, Nucleonics, 24 (1966) 8, 108.
8 C. H. WESTCOTT, AECL-1101, 1960.
9 R. L. MACKLIN AND H. S. POMERANCE, Proc. Intern. Conf. Peaceful Uses At. Energy, Geneva, 1955, Vol. 5, U.N., New York, 1956, p. 96.
10 O. T. HÖGDAHL, Proc. Conf. Radiochemical Methods of Analysis, Vienna, 19–23 Oct. 1964, I.A.E.A., Vienna, 1965, p. 23.
11 E. STEINNES AND D. BRUNE, to be published.
12 R. B. TATTERSALL, H. ROSE, S. K. PATTENDEN AND D. JOWITT, J. Nucl. Energy, Pt. A, 12 (1960) 32.

A COMBINED ION-EXCHANGE SPECTROPHOTOMETRIC METHOD FOR THE DETERMINATION OF MOLYBDENUM AND TUNGSTEN IN SEA WATER

KAZUAKI KAWABUCHI* AND ROKURO KURODA

Laboratory for Analytical Chemistry, Faculty of Engineering, University of Chiba, Yayoi-cho, Chiba (Japan)

(Received January 20th, 1969)

Since the concentrations of molybdenum and tungsten in sea water are too low to allow direct determination, it is necessary to concentrate both elements before their determination. For molybdenum, coprecipitation[1-7], cocrystallization[8], solvent extraction[9], and ion-exchange[10,11] with chelating ion-exchange resins have been used for concentration, the subsequent determination being accomplished spectrophotometrically in most cases.

For the determination of tungsten, coprecipitation with iron(III) hydroxide and manganese dioxide have been used, respectively, by ISHIBASHI et al.[1,12] and by CHAN AND RILEY[13]. Since the carrier or cocrystallizing agent has generally to be removed before molybdenum or tungsten can be determined spectrophotometrically, the procedures are tedious and time-consuming. The use of chelating ion-exchange resins appears to provide one of the best techniques for analytical concentration of molybdenum and tungsten before their determination. Thus, RILEY AND TAYLOR[11] have accomplished the determination of molybdenum in sea water in this way.

Since molybdenum and tungsten behave similarly in all the concentration techniques above, and molybdenum interferes seriously in most sensitive photometric methods for tungsten, it is of primary importance to separate the two elements, present at an approximate ratio of Mo:W = 100:1 in sea water, for the determination of tungsten. However, there are still lacking satisfactory separation methods for tungsten in μg amounts from other elements including molybdenum. In connection with the development of the procedure for tungsten in sea water, ISHIBASHI et al.[1] have used precipitation of molybdenum as sulfide for removal of the bulk of molybdenum. SANDELL[14] has suggested the use of antimony(V) sulfide as a carrier for molybdenum sulfide. These methods do not afford quantitative results according to CHAN AND RILEY[13]. These authors separated molybdenum by extraction of its dithiol complex from 2.4 N hydrochloric acid containing citric acid, leaving tungsten in the aqueous phase. Destruction of citric acid was necessary to determine tungsten photometrically with dithiol.

In this work it has been found that molybdenum can be quantitatively concentrated on a conventional strong-base anion-exchange resin from an acidified seawater sample which contains either thiocyanate or hydrogen peroxide. Tungsten also

---

* Present address: Laboratory of Science Education, Faculty of Education, Ehime University, Bunkyo-cho, Matsuyama, Japan.

can successfully be concentrated on the anion-exchange resin from sea-water samples adjusted to 0.1 M in ammonium thiocyanate and 0.1 M in hydrochloric acid. A new analytical separation of molybdenum and tungsten is also developed to achieve the separation of tungsten at microgram levels from a large quantity of molybdenum.

EXPERIMENTAL

Reagents and apparatus

Stock solutions. Molybdenum(VI): An appropriate amount of ammonium molybdate was dissolved in water to give *ca.* 10 mg Mo/ml. The solution was standardized against EDTA.

Tungsten(VI): An appropriate amount of sodium tungstate was dissolved in water to give *ca.* 10 mg W/ml. The solution was standardized gravimetrically.

Ion-exchange resin. A strong-base anion-exchange resin, Dowex 1-X8, SCN- and Cl-form, 100–200 mesh in particle size, was used.

Cellulose exchanger. DEAE (diethylaminoethylcellulose; Serva; Gallard-Schlesinger Chemical Manufacturing Corp.) in a chloride form was used.

These exchangers were stored in a desiccator over a saturated potassium bromide solution.

Columns. For the resin column, 10 g of the resin was slurried with water and poured into a conventional glass column, int. diam. 2.5 cm, pulled to a tip and plugged with glass wool at the outlet. The resulting bed was usually 3.5 cm long. The top of the resin bed was covered with a thin glass wool layer. For the DEAE column, 1 g of dried DEAE was slurried with water and poured into a glass column, int. diam. 1.5 cm, also pulled to a tip and plugged with glass wool at the outlet. The resulting bed was usually 2.8 cm high. A filter paper disk of the same diameter was placed on to the layer of packed glass wool. The column was further placed in a conventional glass jacket column through which temperature-regulated water (50°) was passed.

Before use, the resin and DEAE columns were washed with several column volumes of 0.1 M hydrochloric acid–0.1 M ammonium thiocyanate and of buffer solution pH 3.2 (a mixture of 0.1 M acetic acid and 0.1 M sodium acetate), respectively.

Adsorption of molybdenum(VI) and tungsten(VI)

The distribution coefficient, K_d, for molybdenum(VI) and tungsten(VI) on Dowex 1-X8 (SCN-form) as a function of concentration of ammonium thiocyanate was determined by a batch equilibrium method, the concentration of hydrochloric acid being kept constant at 0.1 M. Portions of dried resin (1 g each) were weighed and placed in conical flasks with glass stoppers, to which 41-ml portions of sea water were added, which was previously adjusted to 0.1 M in hydrochloric acid and contained varying amounts of ammonium thiocyanate, and 1.03 mg of molybdenum(VI) or 1.04 mg of tungsten(VI). After mechanical shaking for 20 h at room temperature, the two phases were separated by filtration. An aliquot of the filtrate was analyzed for the respective element colorimetrically. The K_d value then was calculated by the following formula:

$$K_d = \frac{\text{amount of ion in resin phase/g of resin}}{\text{amount of ion in solution phase/ml of solution}}$$

The K_d values for molybdenum(VI) and tungsten(VI) on DEAE as a function

of pH were determined by the batch method in 0.50 M chloride solution. Portions of DEAE (0.5 g each) were equilibrated with 41 ml of 0.50 M chloride solutions of varying pH values at 25° for 20 h. Equilibrium pH values were recorded. The added amount of molybdenum(VI) or tungsten(VI) and the computation of K_d were the same as used in the thiocyanate system above.

Procedure

Molybdenum. A 1-l sample acidified to 0.1 M with respect to hydrochloric acid is percolated through a 0.45-μ millipore filter, the filtrate being adjusted to 0.1 M in ammonium thiocyanate. The resulting solution is passed down the resin (SCN-form) column at a flow rate of 4–5 ml per min. The column is then washed with about 100 ml of 1 M sulfuric acid. Molybdenum is stripped by elution with 60 ml of 0.5 M sodium hydroxide–0.5 M sodium chloride solution and determined spectrophotometrically.

Alternatively, to 1 l of the membrane-filtered water, which is 0.1 M in hydrochloric acid, 250 ml of 30% hydrogen peroxide is added. The peroxide solution then is passed through the resin (Cl-form) column at a flow rate of about 5 ml per min. After the column has been washed with 50 ml of 0.5 M sodium chloride solution, molybdenum is stripped by elution with 60 ml of 0.5 M sodium hydroxide–0.5 M sodium chloride solution, and determined spectrophotometrically.

Tungsten. A 10-l of the membrane-filtered water sample, which is 0.1 M in hydrochloric acid, is adjusted to 0.1 M in ammonium thiocyanate and passed down the resin (SCN-form) column at a flow rate of 5 ml per min. With another column, an additional 10-l aliquot of the same sample solution is treated similarly. After each column has been washed with 100 ml of 1 M sulfuric acid, tungsten is stripped along with molybdenum with 0.5 M sodium hydroxide–0.5 M sodium chloride solution. The first 25-ml fraction of the effluent can be discarded, and the subsequent 30-ml fraction is collected. The combined effluent is then neutralized with 6 M hydrochloric acid. After 12 ml of 1 M acetic acid has been added, the solution is adjusted to pH 3.2 by dropwise addition of 1 M sodium acetate solution. After dilution to 120 ml with deionized water, the buffered solution is loaded onto the top of the DEAE column regulated to 50°. The first 80-ml fraction of the effluent from the loaded solution can be discarded and the subsequent 40-ml fraction is collected and reserved for the determination of molybdenum, if needed. The column is then washed with 100 ml of 0.5 M sodium chloride solution adjusted to pH 4.2 (prepared by dissolving sodium chloride in a mixture of 0.1 M acetic acid and 0.1 M sodium acetate solutions). The effluent is combined with the early 40-ml fraction obtained previously and used for the determination of molybdenum.

Tungsten is removed from the column by elution with about 20 ml of 0.1 M sodium hydroxide–0.1 M sodium chloride solution. Eluted tungsten is usually contaminated by a residual amount of molybdenum running to *ca.* 1 μg, so that the separation may be repeated again to ensure complete removal of molybdenum, on a second small column containing 0.5 g of DEAE.

Photometric determination of molybdenum and tungsten. The procedure used was essentially the same as that developed by ALLEN AND HAMILTON[15], except that the insoluble dithiol complexes of molybdenum and tungsten were extracted into *n*-butyl acetate instead of petroleum ether.

RESULTS AND DISCUSSION

Adsorption on Dowex 1 ion-exchange resin

K_d values for molybdenum(VI) and tungsten(VI) in thiocyanate media on Dowex 1-X8 are tabulated in Table I as a function of the thiocyanate concentration. The K_d values for molybdenum agree well with those on Dowex 1 in ammonium thiocyanate media, which are kept at 0.5 M in hydrochloric acid[16]. Over the wide range of thiocyanate concentration, the K_d values are sufficiently high to adsorb molybdenum and tungsten from sea water on the resin. Fortunately, the elements adsorbed can easily be stripped quantitatively from the column by elution with 0.5 M sodium hydroxide–0.5 M sodium chloride solution.

TABLE I

DISTRIBUTION COEFFICIENTS FOR Mo(VI) AND W(VI) AS A FUNCTION OF THE THIOCYANATE CONCENTRATION

NH_4SCN (M)	0.03	0.10	0.30	1.00	3.00
K_d Mo(VI)	$9 \cdot 10^3$	$1 \cdot 10^5$	$> 10^5$	$> 10^5$	$> 10^5$
W(VI)	$3 \cdot 10^3$	$1 \cdot 10^4$	$2 \cdot 10^4$	$4 \cdot 10^4$	$6 \cdot 10^4$

TABLE II

DETERMINATION OF MOLYBDENUM IN SEA WATER[a]

Thiocyanate method (R-SCN resin)				Peroxide method (R-Cl resin)			
Run	Added (μg)	Found (μg)	Mo content in original sample ($\mu g/l$)	Run	Added (μg)	Found (μg)	Mo content in original sample ($\mu g/l$)
1	0.0	9.2	9.2	1	0.0	9.6	9.6
2	0.0	9.6	9.6	2	0.0	9.9	9.9
3	0.0	9.7	9.7	3	5.2	14.6	9.4
4	0.0	9.5	9.5	4	10.3	19.3	9.0
5	5.2	14.3	9.1	5	10.3	19.7	9.4
6	5.2	14.8	9.6	6	15.5	24.1	8.6
7	10.3	19.9	9.6				
8	10.3	19.9	9.6				
			Av. 9.5 ± 0.1				Av. 9.3 ± 0.2

[a] Collected at 4 km off the coast of Kominato, Chiba, on October 27th, 1967.

Because of the comparatively high content of molybdenum (*ca.* 10 $\mu g/l$) in sea water, the use of 1 l of sea water is sufficient to permit the subsequent quantitative determination of molybdenum with dithiol. Repeated determinations of molybdenum in a sea-water sample are given in Table II, run 1 through 4 (thiocyanate method). To evaluate the accuracy of the method, a known amount of molybdenum was added to the sample water and the overall recovery was obtained. The results, also quoted in Table II, run 5 through 8, indicate satisfactory recoveries. The errors given indicate the standard deviation based on all determinations including the addition tests. Another two determinations on the sea-water sample collected from Tokyo Bay, off the coast of Inage, gave 7.7 μg Mo/l and 7.7 μg Mo/l, respectively.

To justify the thiocyanate concentration method, an alternative method was

developed; this permits the effective concentration of molybdenum by quantitative adsorption on Dowex 1, in a chloride form, from sea water adjusted to 0.1 M in hydrochloric acid and 6% in hydrogen peroxide. The adsorbed molybdenum can be removed very easily by elution with 0.5 M sodium hydroxide–0.5 M sodium chloride solution. With 1-1 portions of the same sample as used in the thiocyanate method, analyses were repeated for molybdenum with or without addition of known amounts of molybdenum. The results of these determinations are also quoted in Table II for comparison. The precision indicated is the standard deviation based on all determinations including addition tests. There is no significant difference between the averages for molybdenum in the original samples (9.5 and 9.3 μg/l) obtained by the thiocyanate and peroxide methods. Although in the present procedure the sea water was adjusted to 6% in hydrogen peroxide, further work showed that quantitative uptake of molybdenum is quite feasible from sea water adjusted to as little as 0.3% in hydrogen peroxide and 0.1 M in hydrochloric acid.

Uptake of molybdenum from thiocyanate media on Dowex 1 and subsequent elution with sodium hydroxide–sodium chloride provides a selective removal of molybdenum from many other elements. When sea water adjusted to 0.1 M ammonium thiocyanate–0.1 M hydrochloric acid is passed down the Dowex 1 (R-SCN form) column, alkali metals, alkaline earths, tellurium(IV), selenium(IV), arsenic(III), manganese, thorium, rare earths, nickel, etc. are not adsorbed to any great extent, while molybdenum(VI), tungsten(VI), tin(IV), antimony(III), bismuth(III), copper-(II), mercury(II), platinum metals, etc. show strong adsorption on the resin[17]. However, antimony(III) and bismuth(III) can be effectively removed from the column by elution with 1 M sulfuric acid[18-20]. A small quantity of copper(II), mercury(II) and platinum metals cannot be stripped from the column by elution with 0.5 M sodium hydroxide–0.5 M sodium chloride solution. Tin(IV) behaves very much like molybdenum and tungsten, so that tin in sea water may quantitatively be enriched in the eluted fraction of molybdenum and tungsten. If molybdenum is to be determined spectrophotometrically with dithiol, however, tin does not interfere; the tin–dithiol complex is not extracted by the n-butyl acetate used. As little as 0.1 μg of tungsten taken up from 1 l of a sea-water sample also does not interfere with the photometric determination of molybdenum at any significant level. Similarly, the concentration of molybdenum from sea water containing hydrogen peroxide and subsequent elution with 0.5 M sodium hydroxide–0.5 M sodium chloride provides a highly selective enrichment method for molybdenum. It will not generally be necessary to purify the concentrate, particularly if molybdenum is to be determined spectrophotometrically with dithiol. The adsorption of tungsten on Dowex 1 is not sufficient to permit the concentration of tungsten from a sea-water sample containing peroxide and hydrochloric acid.

The molybdenum contents of sea water obtained here, are reasonably consistent with recently reported colorimetric results, which range from 9 to 13 μg Mo/l.

In order to check the adsorption behavior of tungsten in thiocyanate media, 83.2 μg of tungsten was added to 10 l of sea water, which contained 7.7 μg Mo/l, and the thiocyanate sea-water solution was passed down the column as in the procedure given. After molybdenum and tungsten had been eluted with 0.5 M sodium hydroxide–0.5 M sodium chloride solution, the two elements were determined simultaneously with dithiol by measuring two absorbances at 670 and 630 nm[21]. Because of the two

elements being present in this sample in a similar amount, the simultaneous determination is quite feasible without appreciable loss of precision. The recoveries were 76.3 μg Mo and 84.0 μg W, thus, as far as about a 100 μg amount of tungsten is concerned, the recovery is satisfactory. In actual sea-water samples the ratio of molybdenum to tungsten is approximately 100:1 and the amount of tungsten concerned is only 1–2 μg on the basis of a 20-l sample, so that it is of primary importance to separate the two elements and to recover the microgram amounts of tungsten.

Separation on DEAE columns

The new separation method developed here involves the use of DEAE, on which the difference in distribution coefficients between molybdenum(VI) and tungsten(VI) is great enough in chloride media to permit quantitative separations. The equilibrium K_d values are given in Table III as a function of pH. As can be seen,

TABLE III

DISTRIBUTION COEFFICIENTS OF Mo(VI) AND W(VI) ON DEAE IN A CHLORIDE FORM AS A FUNCTION OF pH [a]

pH	2.05	2.84	3.42	4.39	5.36	6.10
Mo(VI)	162	347	327	47	21	14
W(VI)	$7.6 \cdot 10^3$	$2.5 \cdot 10^4$	$2.3 \cdot 10^4$	$2.9 \cdot 10^3$	82	7.6

[a] Equilibrium pH is recorded. Buffer solution of pH 2.05 consisted of a mixture of 0.5 M sodium chloride and 0.5 M hydrochloric acid. Other solutions were prepared by mixing acetic acid, sodium acetate and sodium chloride solutions to give desired buffer solutions of 0.5 M in sodium chloride and 0.1 M in total acetate. All measurements were made at 25.0 ± 0.1°.

the K_d values for the two elements increase with increasing pH, reaching a maximum at about pH 3, and then drop sharply with further increase of pH. Attempts to perform the separation at pH 4.2 at room temperature led to appreciable tailing of molybdenum, probably because of the rather high K_d value for molybdenum at that pH value. By raising the elution temperature to 50°, the tailing of molybdenum could be eliminated almost completely. When about 200 μg of molybdenum concentrated from as much as 20 l of sea water is eluted, however, a minute amount of molybdenum, usually 1–2 μg, remains on the DEAE column, being stripped along with tungsten by elution with 0.1 M sodium hydroxide–0.1 M sodium chloride solution. This residual amount of molybdenum can easily be removed from tungsten by repeating the procedure with a small column containing 0.5 g of DEAE.

In order to obtain a general idea about the overall recovery of tungsten from sea water, addition tests were carried out with a 20-l portion of the sea water which contained about 0.07 μg W/20 l. With an added amount of 8.3 μg W, an overall recovery of 77% was obtained. Similar recoveries of 76 and 78% on the basis of two 2-l portions of the same water sample with the added amount of 10.4 μg W were also obtained. Therefore, the results obtained in the photometric analysis should be multiplied by a factor of 1.3 to correct for these losses of tungsten.

Two determinations were conducted on 20-l aliquots of a sample of surface water from the Pacific Ocean, 4 km off the coast of Kominato, Chiba, Japan, collected on February 17th, 1968. Identical results of 0.11₅ and 0.11₆ μg W/l were obtained,

which are in excellent agreement with the average concentration of 0.12 μg W/l reported by ISHIBASHI *et al.*[1] for Pacific Ocean water from off the coast of Japan. The values also agree well with the average tungsten content of 0.116 μg/l reported by CHAN AND RILEY[13] for Irish Sea water.

Storage of samples

The sample waters for molybdenum and tungsten were acidified to 0.1 M in hydrochloric acid immediately after collection and filtered through the 0.45-μ membrane filter shortly before the column concentration. During the storage time of over one month there was no evidence that molybdenum had become precipitated or adsorbed on the wall of a polyethylene container. However, the sea-water sample which contained 0.115 μg W/l, showed only 0.003₅ μg W/l after one month had elapsed. The membrane filter used shortly before the column concentration contained 0.052 μg W per liter of the solution. Therefore, about 0.07 μg W per liter of the solution is thought to have deposited on the wall of the polyethylene container (20-l capacity). It is recommended that sea-water samples acidified with hydrochloric acid should be analyzed for tungsten as rapidly as possible to avoid loss of tungsten, presumably by hydrolytic precipitation. CHAN AND RILEY[13] stated that in an experiment in which the water sample was acidified to 0.1 N with respect to hydrochloric acid before storage in a polyethylene bottle, no loss of tungsten occurred after two weeks.

SUMMARY

A combined ion-exchange spectrophotometric method has been developed for the determination of molybdenum and tungsten in sea water. The two elements are adsorbed quantitatively on Dowex 1-X8 (SCN-form) from sea water adjusted to 0.1 M in hydrochloric acid and 0.1 M in ammonium thiocyanate. Molybdenum also can be concentrated quantitatively on Dowex 1-X8 (Cl-form) from sea water acidified to 0.1 M in hydrochloric acid and containing < 6% hydrogen peroxide. In both concentration procedures, molybdenum and tungsten are easily eluted with 0.5 M sodium hydroxide–0.5 M sodium chloride solution. The adsorption and desorption steps provide selective concentration for molybdenum and tungsten, so that molybdenum can be determined spectrophotometrically with dithiol. Tungsten is separated from molybdenum by anion-exchange on DEAE (Cl-form), and can be determined similarly with dithiol. A sea-water sample collected from the Pacific Ocean, off the coast of Kominato, Chiba, gave values of 9.5±0.1 μg Mo/l and 9.3±0.2 μg Mo/l for the thiocyanate concentration and hydrogen peroxide concentration methods, respectively, with 1-l samples. Duplicate analyses of sea water from the same location as for molybdenum, gave values of 0.11₅ and 0.11₆ μg/l for tungsten, on a 20-l sample basis.

RÉSUMÉ

Une méthode combinée spectrophotométrie–échange d'ions est proposée pour le dosage du molybdène et du tungstène dans l'eau de mer. Ces deux éléments sont adsorbés quantitativement sur Dowex 1-X8 (forme SCN) — milieu HCl 0.1 M et thiocyanate d'ammonium 0.1 M. Le molybdène peut également être concentré

quantitativement sur Dowex 1-X8 (forme Cl) d'eau de mer acidifiée par acide chlorhydrique 0.1 M et renfermant moins de 6% d'eau oxygénée. Dans les deux procédés, le molybdène et le tungstène sont facilement élués avec hydroxyde de sodium 0.5 M–chlorure de sodium 0.5 M. Le molybdène est dosé spectrophotométriquement à l'aide de dithiol. Le tungstène est séparé d'avec le molybdène par échangeur d'anions sur DEAE (forme Cl) et est dosé de la même façon par le dithiol. Une échantillon d'eau de mer a fourni les valeurs de 9.5 ± 0.1 $\mu g/l$ Mo et 9.3 ± 0.2 $\mu g/l$ Mo, respectivement par les méthodes de concentration au thiocyanate et au peroxyde d'hydrogène, pour des échantillons d'un litre. On a trouvé 0.11_5 et 0.11_6 $\mu g/l$ de tungstène dans les mêmes eaux avec des échantillons de 20 litres.

ZUSAMMENFASSUNG

Eine kombinierte ionenaustauscher–spektralphotometrische Methode wurde zur Bestimmung von Molybdän und Wolfram in Seewasser entwickelt. Die 2 Elemente werden quantitativ an einen Kationenaustauscher aus 0.1 M Salzsäure und 0.1 M Ammoniumthiocyanat haltiger Lösung adsorbiert. Zur Adsorption von Molybdän kann auch Wasserstoffperoxid zugegeben werden. Die Elution erfolgt mit 0.5 M Natriumhydroxid–0.5 M Natriumchlorid-Lösung. In der so angereicherten Lösung wird Molybdän spektralphotometrisch mit Dithiol bestimmt. Wolfram wird vom Molybdän mit einem Anionenaustauscher getrennt, und kann auf ähnliche Weise mit Dithiol bestimmt werden. Seewasser aus dem Pazifischen Ozean von der Küste von Kominato, Chiba, enthielt etwa 9.5 μg Mo pro l und 0.11 $\mu g/l$ Wolfram.

REFERENCES

1 M. ISHIBASHI, T. SHIGEMATSU AND Y. NAKAGAWA, Bull. Inst. Chem. Res. Kyoto Univ., 32 (1954) 199.
2 M. ISHIBASHI, T. FUJINAGA AND T. KUWAMOTO, J. Chem. Soc. Japan, Pure Chem. Sect. (Nippon Kagaku Zasshi), 79 (1958) 1496.
3 K. SUGAWARA, M. TANAKA AND S. OKABE, Bull. Chem. Soc. Japan, 32 (1959) 221.
4 K. SUGAWARA, K. TERADA, S. NAKAMORI, N. NAKAMORI AND S. OKABE, J. Earth Sci. Nagoya Univ., 10 (1962) 34.
5 K. M. CHAN AND J. P. RILEY, Anal. Chim. Acta, 36 (1966) 220.
6 S. OKABE AND Y. TOYOTA, J. Chem. Soc. Japan, Pure Chem. Sect. (Nippon Kagaku Zasshi), 88 (1967) 863.
7 S. OKABE AND T. MORINAGA, J. Chem. Soc. Japan, Pure Chem. Sect. (Nippon Kagaku Zasshi), 89 (1968) 284.
8 H. V. WEISS AND M. G. LAI, Talanta, 8 (1961) 72.
9 T. K. ZHAVORONKINA, Morsk Gidrofiz Inst. Akad. Nauk SSSR, 19 (1960) 38; C.A., 55 (1961) 17359c.
10 J. P. RILEY AND D. TAYLOR, Anal. Chim. Acta, 40 (1968) 479.
11 J. P. RILEY AND D. TAYLOR, Anal. Chim. Acta, 41 (1968) 175.
12 M. ISHIBASHI, T. FUJINAGA, T. KUWAMOTO, M. KOYAMA AND S. SUGIBAYASHI, J. Chem. Soc. Japan, Pure Chem. Sect. (Nippon Kagaku Zasshi), 81 (1960) 392.
13 K. M. CHAN AND J. P. RILEY, Anal. Chim. Acta, 39 (1967) 103.
14 E. B. SANDELL, Ind. Eng. Chem., Anal. Ed., 18 (1946) 163.
15 S. H. ALLEN AND M. B. HAMILTON, Anal. Chim. Acta, 7 (1952) 483.
16 H. HAMAGUCHI, K. KAWABUCHI AND R. KURODA, Anal. Chem., 36 (1964) 1654.
17 K. KAWABUCHI, H. HAMAGUCHI AND R. KURODA, J. Chromatog., 17 (1965) 567.
18 K. KAWABUCHI, Japan Analyst (Bunseki Kagaku), 14 (1965) 52.
19 K. KAWABUCHI, J. Chem. Soc. Japan, Pure Chem. Sect. (Nippon Kagaku Zasshi), 87 (1966) 262.
20 K. KAWABUCHI, M. KAYA AND Y. OUCHI, Japan Analyst (Bunseki Kagaku), 15 (1966) 543.
21 P. G. JEFFERY, Analyst, 81 (1956) 104.

DETERMINATION OF SILICON IN ALUMINUM ALLOYS BY ATOMIC ABSORPTION SPECTROSCOPY

D. E. CAMPBELL

Metallurgical Research Laboratories, Reynolds Metals Company, Richmond, Va. 23218 (U.S.A.)
(Received February 6th, 1969)

BOWMAN AND WILLIS[1] have determined silicon in bauxite by atomic absorption spectroscopy after a borate–carbonate fusion technique for dissolution of the samples, and DELGADO AND MANNING[2] have determined silicon in cements. Determinations of silicon in organic matrices[3] and silicates[4] have also been described. In this paper, investigations on the determination of silicon in aluminum alloys by atomic absorption spectroscopy are discussed. Only major alloying amounts (>5%) have been investigated.

The determination of silicon is of interest in the analysis of all aluminum alloys. Depending on the alloy involved, it will be found in concentrations ranging from a few p.p.m. up to nearly 20%. Direct-reading emission spectrometers are generally used for production control in the aluminum industry. However, chemical determinations must be made periodically to check on the repeatability and general accuracy of the direct readers, especially for high concentration levels.

EXPERIMENTAL

Instrumentation

All work was carried out with a Jarrell-Ash maximum-versatility atomic absorption spectrophotometer. Initial work was done with the Jarrell-Ash laminar flow burner, but most of the work described in this paper was done with the Techtron AB-40 burner (5-cm slot) with a nitrous oxide–acetylene flame in a single-pass system. The light source was a Westinghouse single-element silicon hollow-cathode lamp, No. 45-479. The detector was an R-106 photomultiplier, coupled with an a.c. amplifier and a 10-mV recorder.

Absorption measurements were made for moderately luminous flames. The acetylene pressure was adjusted to give the maximum "red feather" without the flame becoming luminous. With this type of flame, carbon deposits were kept to a minimum.

Reagents

A stock solution of silicon was prepared by dissolving 5 g of reagent-grade sodium silicate ($Na_2SiO_3 \cdot 9H_2O$) in 25 ml of deionized water. This was then diluted to 100 ml with deionized water. Various other concentrations were made by diluting aliquots of the stock solution.

Procedure

Weigh a 0.500-g sample of drillings and transfer to a stainless steel or nickel beaker. Dissolve in 10 ml of 20% sodium hydroxide solution in the covered beaker, and then rinse the sides of the beaker and the lid with a few ml of hot water. Add 2–3 ml of 30% hydrogen peroxide, cover the beaker and evaporate the solution to a syrupy consistency. After the silicon has reacted, dilute the samples with hot water to dissolve the pasty residue and pour into a 400-ml beaker containing 10 ml of concentrated nitric acid. Wash the beaker with a stream of hot water, and add about 25 ml of 1:1 hydrochloric acid. Transfer the washings quantitatively to a glass beaker, cool, and transfer to 100-ml volumetric flasks.

Standard preparation

Transfer 5 aliquots of the stock sodium silicate solution, to encompass the range 50–250 p.p.m. of silicon, to 100-ml volumetric flasks and dilute to volume with deionized water. Sodium silicate stock solutions were standardized gravimetrically.

Monochromator slit width

Calibration curves were drawn for slit widths of 400, 300, 200, 100 and 50 μ (Fig. 1). Since the curves drawn for the 300- and 400-μ slits were nearly identical to that for 200-μ slit, they are not included in Fig. 1.
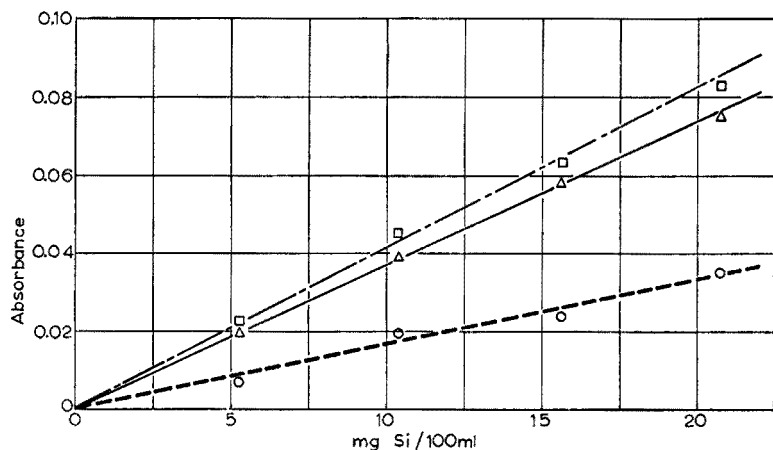
Fig. 1. Effect of slit width on absorption of Si. ($\square$) 50μ slit; (O) 200 μ slit; ($\triangle$) 100 μ slit.

Burner height

Three different burner settings were used, corresponding to heights of the center of the light beam above the burner top of 6, 9 and 13 mm. Moving the burner so that the light beam center was below 6 mm resulted in blockage of the light beam. A plot of absorbance *vs.* concentration for these three positions is shown in Fig. 2.

Fuel–oxidant ratio

Three different flame compositions were examined; lean, moderately luminous, and luminous. A lean flame is defined as one which has a distinct reddish cone about
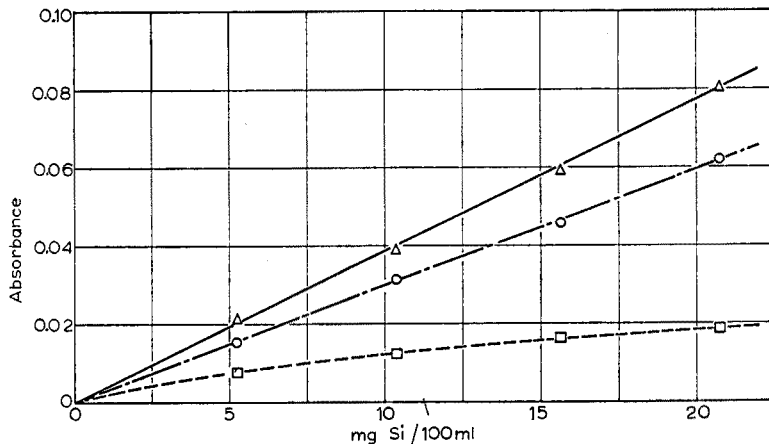
Fig. 2. Effect of vertical height of burner on absorption of Si. Vertical position: (□) 13 mm; (○) 9 mm; (△) 6 mm.
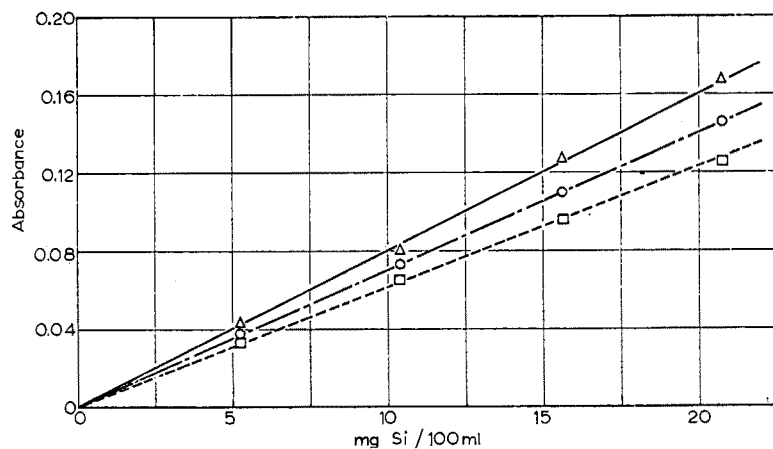
Fig. 3. Effect of flame composition on absorbance. (○– ——–) luminous; (△ ———–) moderately luminous; (□– – – –) lean.

0.5 inch above the base of the burner head. A moderately luminous flame does not have a distinctive reddish cone present, but reddish streaks can be seen dispersed throughout the flame. A strongly luminous flame is totally white in appearance. A graph of absorbance *vs.* concentration is given for these conditions in Fig. 3.

Influence of aluminum

Samples containing 1200 p.p.m. of aluminum were analyzed against standards that contained only 700 p.p.m. of aluminum; poor agreement was obtained (Table I). When these samples were analyzed against standards that more closely approximated the aluminum concentration of the samples (1200 p.p.m.), a considerable improvement in agreement with wet chemical values was achieved (Table I).

Influence of organic solvents

The presence of certain organic solvents influences the absorption sensitivity of many elements. Experiments with methanol, ethanol, isopropanol, and acetone, were conducted in order to determine the extent of the enhancement of silicon absorption. Table II shows that ethanol gave slightly higher absorption readings with increases in solvent concentration. Methanol behaved similarly with the exception of

TABLE I

COMPARATIVE ANALYSES OF SAMPLES AGAINST MATCHED AND UNMATCHED STANDARDS

(Samples contained 1200 p.p.m. of Al)

Sample no.	p.p.m. Al in standards	% Si a.a.	% Si wet	% Relative error
1	700	7.57	6.92	9.4
2	700	9.21	8.50	8.4
3	700	9.59	8.89	3.4
1	1200	6.92	6.92	0.0
2	1200	8.50	8.50	0.0
3	1200	8.72	8.89	1.9

TABLE II

INFLUENCE OF ORGANIC SOLVENTS ON % Si ABSORPTION[a]

Solvent	% Solvent[b] (v/v)	% Absorption
H_2O	--	8.9
Methanol	10	9.0
	30	8.3
	50	10.0
	70	10.6
Ethanol	10	10.9
	30	12.4
	50	13.6
	70	13.8
Isopropanol	10	14.5
	30	11.9
	50	10.0
	70	8.4
Acetone	10	9.0
	30	8.6
	50	5.5
	70	3.0

[a] All solutions contained 136 p.p.m. Si.
[b] 100 ml dilutions.

the 30% solution. Isopropanol and acetone gave lower absorption readings with increases in concentration. Acetone solutions appeared to swamp the flame. With the exception of the acetone solutions, most of the absorption readings were greater than the absorption readings of the aqueous sample. However, care must be exercised in the

use of organic solvents in the type of solutions required for silicon. Side reactions, possibly between the organic material and nitric acid, have been observed, and the reaction products make the solutions useless.

DISCUSSION AND RESULTS

With the Jarrell-Ash laminar flow burner which was used initially, sensitivity was quite low. Much better sensitivity was achieved with the Techtron burner assembly, possibly because of more efficient atomization. With this burner, the range of standards used was 50–250 p.p.m. of silicon, and good linearity was found in this range.

The initial work with silicon gave results that were 2–3% lower than the chemical values, probably because the total salt concentrations of samples and standards were not closely matched. This interference was probably caused by excessive energy consumption in the dissociation of sodium salts; this energy would otherwise be available for dissociating silicon salts. Two 400-p.p.m. silicon standards were prepared, one with the addition of 10 ml of 20% sodium hydroxide, and another without this addition; the former standard gave an absorption value about 1.5% lower than the latter. Accordingly, it was considered necessary to match the total salt content between samples and standards as closely as possible (see Table III).

TABLE III

INFLUENCE OF TOTAL SALT CONCENTRATION ON SILICON ABSORPTION

Sample no.	% Si a.a.[a]	% Si a.a.[b]	% Si wet
1	9.28	11.15	11.07
2	9.52	11.55	11.64

[a] Total salt concentration different in samples and standards.
[b] Total salt concentration matched in samples and standards.

TABLE IV

DETERMINATION OF SILICON IN ALLOYS

Sample no.[a]	% Si a.a.	% Si wet	% Relative error	Sample no.[e]	% Si a.a.	% Si wet	% Relative error
1	12.93	13.10	1.3	6	11.15	11.07	0.7
2	13.76	13.79	0.2	7	11.55	11.64	0.8
3	13.20	13.40	1.5	8	13.23	13.41	1.3
4	18.35	18.28	0.4	9	10.99	11.07	0.7
5	14.12	14.05	0.5	10	11.66	11.64	0.2
87–a[b]	6.30[c]	6.24	0.9[d]	11	12.30	12.18	1.0
				12	17.59	17.50	0.5
				13	17.47	17.50	0.2
				14	17.67	17.80	0.7

[a] Samples 1–5 were analyzed in duplicate; total solids content was ca. 1.7% (w/w).
[b] Certificate value 6.24% Si.
[c] Mean of 7 determinations.
[d] Average % error.
[e] Samples 6–14 had a total solids content of 0.5% (w/w).

Six samples were prepared in duplicate and analyzed (Table IV); five of these samples were experimental hypereutectic Si–Al alloys and the other sample was N.B.S. 87-a, a Si–Al binary, which was the only certified sample available to evaluate the accuracy of the method.

In sample analyses, flame gaps often appeared near the end of a series, and their appearance coincided with a decrease in agreement between chemical and atomic absorption results. The gaps were probably caused by salt accumulation in the burner slot, since the total solids content of the samples was about 1.7% (w/w). New standards and samples were prepared with a 0.5% total solids content; aspiration of these samples did not result in any noticeable gaps, and the agreement between atomic absorption and chemical values improved. BOWMAN AND WILLIS[1] have also reported burner blockage with 2% solid content working with bauxite. Several additional samples of various alloy types have since been analyzed with the reduced salt content without any noticeable gaps in the flame (Table IV).

SUMMARY

The determination of silicon in aluminum alloys after treatment with sodium hydroxide and hydrogen peroxide, can give excellent results if the standards used contain approximately the same amounts of aluminum and total solids as the sample solutions. Addition of organic solvents has little effect. Linear calibration graphs are obtained over the range 0–250 p.p.m. Si.

RÉSUMÉ

On décrit une méthode de dosage du silicium dans les alliages d'aluminium par spectroscopie par absorption atomique. On obtient de bons résultats par traitement des échantillons avec hydroxyde de sodium et peroxyde d'hydrogène, à condition que les étalons utilisés renferment approximativement les mêmes teneurs en aluminium et solides que les solutions à analyser. L'addition de solvants organiques n'a que peu d'effet. Des graphiques d'étalonnage linéaires sont obtenus de 0 à 250 p.p.m. de silicium.

ZUSAMMENFASSUNG

Die Bestimmung von Silicium in Aluminiumlegierungen nach Behandlung mit Natriumhydroxid und Wasserstoffperoxid kann ausgezeichnete Resultate ergeben, wenn Vergleichsproben auch in bezug auf den Aluminiumgehalt näherungsweise die gleiche Zusammensetzungen besitzen. Die Zugabe organischer Lösungsmittel hat nur einen geringen Einfluss. Im Bereich von 0–250 p.p.m. Si ergeben sich lineare Eichkurven.

REFERENCES

1 J. A. BOWMAN AND J. B. WILLIS, *Anal. Chem.*, 39 (1967) 1210.
2 L. DELGADO AND D. C. MANNING, *Analyst*, 92 (1967) 553.
3 C. M. PARALUSZ, Johnson and Johnson, New Brunswick, N. J., presented at *the 20th Conference on Analytical Chemistry and Applied Spectroscopy, Cleveland, Ohio, March, 1968*.
4 B. BERNAS, National Academy of Sciences, Greenbelt, Md., presented at *the 20th Conference on Analytical Chemistry and Applied Spectroscopy, Cleveland, Ohio, March, 1968*.

DETERMINATION AND IDENTIFICATION OF AMINO ACIDS BY THERMOMETRIC TITRATION AND NMR SPECTROSCOPY

BUDDHADEV SEN AND WILLIAM C. WU*

Coates Chemical Laboratories, Louisiana State University, Baton Rouge, La. 70803 (U.S.A.)

(Received February 6th, 1969)

At present the different amino acids are determined by a variety of chemical, biological and physicochemical methods[1-4]. Thermometric titration techniques offer a method of determination which is uniformly applicable to all the amino acids provided that a few reaction conditions are fulfilled. Excellent reviews on the theory and the methodology of thermometric titrations are available[5-7]. Most conventional titration methods are fundamentally free energy methods, whereas the thermometric titrations are controlled by free energy and entropy which are essentially independent of each other. Consequently an unfavorable free energy term may be compensated by a favorable entropy term. The feasibility of the thermometric titrations for analytical determinations as well as their precision and accuracy depend on three variables: they are (a) equilibrium constant of the reaction, (b) reaction enthalpy and (c) the concentration of the reactants. The equilibrium constant of the reaction must exceed a certain minimum value in order to achieve suitable accuracy. Beyond the minimum free energy requirement, the precision and the accuracy of thermometric titrations are solely determined by the reaction enthalpies and the concentration of the reactants.

Nuclear magnetic resonance (NMR) spectra of most of the important amino acids have been studied quite exhaustively[8-11]. However, these studies are primarily concerned with investigating the physicochemical properties and structural features of the amino acids. It was considered worthwhile to investigate the possible analytical application of NMR spectroscopy for the identification of the amino acids. The experimental results are discussed in a later section of this paper.

EXPERIMENTAL

All titrations were performed by means of an Aminco Titra-Thermo-Mat provided with a motor-driven buret which delivers the titrant at a fixed rate of 600 μl/min. The titrations curves were recorded by means of a Minneapolic-Honeywell Electronik 17 recorder. Chart speed was calibrated in terms of volume of the titrant added, and the ordinate was calibrated in terms of calories. Calibration of the ordinate is not necessary unless computation of reaction enthalpy is contemplated.

The concentration of sodium hydroxide solution was varied depending upon the concentration of the acid, in order to obtain a convenient abscissa of the titration

---

* Present address: Corning Glass Company, Corning, New York. Abstracted in part from Ph.D. Dissertation.

curve in a relatively short time so that the adiabatic condition is maintained. Amino acids (Nutritional Biochemical Corporation) were used without further purification.

The ordinate of the chart paper was calibrated in calories by means of the heating element in the titrator whose resistance (R) was known. The heater was powered by a d.c. source whose voltage (V) could be measured precisely. The heater was immersed in 25 ml of water and was turned on for a precisely recorded time (t), and the calorie input was calculated using the relation, calories $= V^2 t / R4.18$. Response of the temperature-sensing device (thermistor) and the recorder was directly proportional to the change in temperature. The entire titration assembly was placed inside the adiabatic tower. The calibration plots, calories *vs.* recorder output (cm) were straight lines passing through origin. The recorder chart was driven by a synchronous motor, adjustable to $\frac{1}{2}$, 1, 2, and 4 in/min. A calibration in ml of titrant per inch of chart traveled was obtained by comparing the chart speed with the volume of titrant delivered per unit time.

Titration procedure

In each titration, 25 ml of amino acid solution was pipetted into the polyethylene beaker. The stirrer, thermistor, bridge, and the recorder were turned on, and appropriate instrument sensitivity chosen. The recorder was standardized, and the bridge was brought to balance. After an equilibration period of *ca.* 10 min, the bridge was rebalanced, and a fairly level base line was obtained. The drive motor of the buret was turned on, the titration curve was recorded, and the titrator was turned off. The buret was then refilled for the next titration. All titrations were performed in the concentration range of the acid between 10^{-2} M and 10^{-4} M, and the duration of the titration was less than 2 min. This minimized any heat loss. The titrant concentration was varied so as not to exceed a titrant volume of 3 ml for neutralization. Titrant volume was usually kept at about 1 ml.

All NMR spectra were taken with a Varian Associates HA60 high-resolution spectrometer. Samples were examined in a spinning cylindrical pyrex glass tube of 5 mm outside diameter. Tertiary butanol was used as the internal standard. The instrument was first aligned by fixing a chemical shift of $\delta = 1.28$ for *t*-butanol.

Treatment of experimental data

(*a*) *Analytical.* Figure 1 represents a typical thermometric titration curve of a diprotic acid (glutamic acid). Computation of amino acid content is straightforward.

(*b*) *Thermodynamic.* The specific heats of the various solutions used in this study were assumed to be equal and constant. The observed reaction enthalpy, ΔH_r, is the sum of the heat of neutralization, ΔH_n, and the heat of ionization, ΔH_i. Under the experimental conditions employed, it is quite reasonable to assume that ΔH_n and ΔH_i are respectively equal to ΔH_n^0 and ΔH_i^0. One may then write

$$\Delta H_r = \Delta H_i^0 + \Delta H_n^0$$

$$\Delta H_i = \frac{\Delta H_r - \Delta H_n^0}{1 - \varkappa}$$

in which $\varkappa$ denotes the fraction of the acid ionized. In the case of amino acids, ioniza-

tion constants being very small, $(1 - x) \simeq 1$, the above equation reduces to

$$\Delta H_i{}^0 = \Delta H_r - \Delta H^0 \tag{1}$$

in which $\Delta H^0 =$ standard heat of ionization and $\Delta H_n{}^0 =$ standard heat of formation of water (-13.5 kcal. mole^{-1} at $25°$).
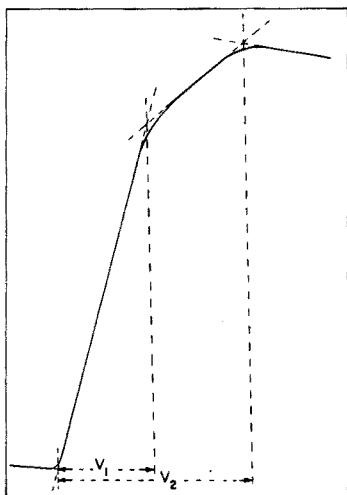
Fig. 1. Thermometric titration curve of 25 ml of $1.056 \cdot 10^{-2}$ M glutamic acid, HOOCCH$_2$CH$_2$-CH(NH$_2$)COOH, by NaOH. V$_1$ $\equiv$ first hydronium ion; V$_2$ $\equiv$ first plus second hydronium ion.

Both the total and the individual heats of ionization of diprotic acids may be calculated when two end-points are distinguishable on the titration curve.

Entropies of ionization were calculated using the relation

$$\Delta S_i{}^0 = \frac{\Delta H_i{}^0 - \Delta F_i{}^0}{T} \tag{2}$$

in which $\Delta F_i{}^0 = RT \ln K_i$.

The values of thermodynamic ionization constants, K_i, were taken from the literature[12].

RESULTS AND DISCUSSION

Selected analytical and thermodynamic data are summarized in Tables I–VI. The amino acids may be classified into three groups: (I) neutral amino acids, which contain one carboxyl group and an amino group attached to the α-carbon atom; (II) acidic amino acids, which contain two carboxyl groups and one amino group attached to the α-carbon atom; (III) basic amino acids, which contain one carboxyl group and two or more amino groups. The titration curves for all monoprotic (neutral) amino acids are similar in shape, i.e., there is one break at the start of the titration and another at the end-point and a uniform slope in between. The titration curve of a mixture of two neutral acids also has the same shape as that of a single acid, as is

TABLE I

TYPICAL ANALYTICAL RESULTS FOR A NEUTRAL AMINO ACID, l-α-ALANINE

True concentration (M)	True weight (mg)	Weight found (mg)	No. of analyses	% Error	Absolute error (mg)	Precision
$3.766 \cdot 10^{-2}$	83.90	84.14	3	+ 0.28	+0.24	0.15
$9.825 \cdot 10^{-3}$	21.89	22.72	3	+ 3.7	+0.83	0.08
$4.646 \cdot 10^{-3}$	10.35	11.64	4	+12.5	+1.29	0.16

TABLE II

TYPICAL ANALYTICAL RESULTS FOR AN ACIDIC AMINO ACID, l-α-GLUTAMIC ACID

True concentration (M)	True weight (mg)	Weight found (mg)	No. of analyses	% Error	Absolute error (mg)	Precision
$1.056 \cdot 10^{-2}$	38.84	40.36	4	+ 3.9	+1.52	0.05
$5.527 \cdot 10^{-3}$	20.33	20.44	4	+ 0.5	+0.11	0.13
$1.382 \cdot 10^{-3}$	5.08	5.25	3	+ 3.3	+0.17	0.04
$1.106 \cdot 10^{-3}$	4.07	4.12	4	+ 1.4	+0.05	0.01
$8.295 \cdot 10^{-4}$	3.05	3.35	4	+ 9.8	+0.30	0.11
$5.527 \cdot 10^{-4}$	2.03	3.61	4	+52.0	+1.58	0.11

TABLE III

TYPICAL ANALYTICAL RESULTS FOR A BASIC AMINO ACID, l-α-HISTIDINE·HCl·H$_2$O

True concentration (M)	True weight (mg)	Weight found (mg)	No. of analyses	% Error	Absolute error (mg)	Precision
$1.857 \cdot 10^{-2}$	97.34	96.38	3	0.98	−0.96	0.01
$9.285 \cdot 10^{-3}$	48.67	48.49	3	0.37	−0.18	0.05
$4.643 \cdot 10^{-3}$	24.34	24.70	3	1.49	+0.36	0.13
$9.285 \cdot 10^{-4}$	4.87	4.56	2	6.34	−0.31	0.11

TABLE IV

ANALYTICAL RESULTS FOR MIXTURES OF AMINO ACIDS dl-α-ALANINE AND l-ASPARTIC ACID

Component A			Component B		
Weight of dl-alanine (mg)	Weight found (mg)	% Error	Weight of aspartic acid (mg)	Weight found (mg)	% Error
71.69	70.33	− 1.9	22.51	22.38	−0.7
30.20	30.62	+ 1.3	25.85	25.16	−2.3
21.14	22.17	+ 4.8	25.85	25.24	−2.4
12.08	13.37	+10.6	25.85	25.24	−2.4
12.08	12.98	+ 7.4	12.93	12.51	−3.2
0	0	0	38.78	38.78	0

TABLE V

ANALYTICAL RESULTS FOR MIXTURES OF AMINO ACIDS: GLUTAMIC ACID WITH ARGININE HYDROCHLORIDE

Component A			Component B		
Weight of glutamic acid (mg)	Weight found (mg)	% Error	Weight of arginine HCl (mg)	Weight found (mg)	% Error
15.35	14.72	−4.1	36.73	39.50	+7.5
15.35	15.45	+0.6	55.09	58.90	+8.7
30.70	29.81	−2.9	36.73	37.39	+4.5
30.70	29.44	−4.1	18.36	18.54	+0.9
30.70	30.02	−2.3	0	0	0

TABLE VI

THERMODYNAMIC DATA OF NEUTRAL AMINO ACIDS AT 25 ± 2°

Acid	$pK(NH_3^+)$ [a]	ΔH_1 [b] (kcal/mole)	ΔF_1 [c] (kcal/mole)	ΔS_1 [d] (eu)
Glycine	9.60	9.9	13.0	−11
Alanine	9.69	10.7	13.1	− 8.3
Valine	9.62	10.5	13.0	− 9.6
Leucine	9.60	10.6	13.0	− 8.2
Isoleucine	9.62	10.2	13.0	− 9.6
Phenylalanine	9.13	9.9	12.4	− 8.3
Proline	10.60	10.7	14.4	−12
Hydroxyproline	9.60	8.5	13.1	−15
Serine	9.15	9.1	12.4	−11
Threonine	9.12	9.2	12.4	−11
Methionine	9.12	9.9	12.5	− 8.6
Tryptophan	9.39	10.4	12.6	− 7.5

[a] Dissociation constant K_1 for the process $NH_3^+RCOO^- \rightleftarrows NH_2RCOO^- + H^+$, taken from GREENSTEIN AND WINITZ[12].
[b] Computed from experimental data using eqn. (1).
[c] Calculated from pK_1 value.
[d] Calculated from eqn. (2).

expected from their ionization constants ($pK(NH_3^+) \sim 9$–10). Therefore, it is not possible to determine the components of such a mixture.

The diprotic acids showed two distinct equivalence points with a steeper slope between the start and the first end-point than between the first and the second end-points. A mixture of a diprotic acid and a monoprotic acid could be easily titrated. The first end-point in the titration curve corresponded to the neutralization of the first ionizable hydronium ion of the diprotic acid, whereas the second end-point corresponded to the neutralization of the second hydronium ion of the diprotic acid and the monoprotic acid. The basic amino acids are most easily titrated as their hydrochlorides. A mixture of the hydrochloride of a basic amino acid and an acidic or neutral amino acid can be easily titrated.

The precision of the titrations in terms of standard deviations was acceptable at all concentrations used in this investigation. It will be noted that the precision of the titrations rarely varied more than two-fold while the concentration of the acid was changed twenty times (cf. Tables I–V). Absolute errors were, however, higher at

higher dilutions, especially for the neutral amino acids, probably because the heat exchange caused by extraneous factors was no longer negligible at high dilution and under the experimental conditions. Figure 2 shows that the accuracy of the titration depended both on the type of the acid and the concentration. For neutral amino acids, the titrations became less reliable at concentrations less than $6 \cdot 10^{-3}$ M, whereas diprotic (acidic) and basic (after conversion to hydrochloride) amino acids yielded excellent results even at concentrations of 10^{-4} M.
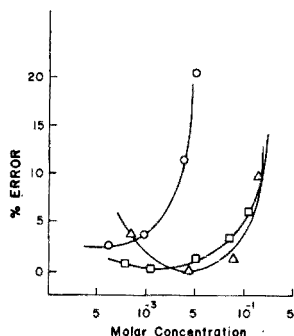

Fig. 2. Plot of percent error *vs.* concentration of amino acid. (○) Alanine, (□) histidine hydrochloride dihydrate, (△) glutamic acid.
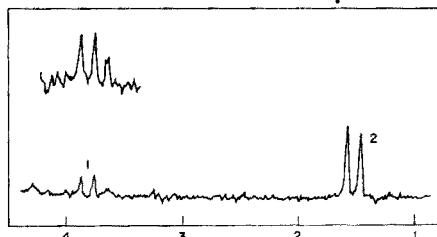
Fig. 3. NMR spectrum of alanine, $CH_3CH(NH_2)COOH$, in water. Inset: α-proton after multiple scan. (1) α-proton; (2) methyl proton.

The results of the attempts to titrate the conjugate bases of the amino acids with copper(II) ion were not encouraging, despite the fact that excellent curves were obtained. The position of the end-point was dependent on a number of factors, such as the pH of the solution, the concentration of the reactants, and the temperature. Therefore, the stoichiometry involved was variable and was unsuitable for analytical titrimetry.

Thermodynamics. While it was not the purpose of this investigation to study the thermodynamics of amino acids, it was found that thermometric titration frequently surpassed in elegance and simplicity many other methods of evaluating heats of ionization. The method is rapid and simple, and has the advantage of corresponding to virtually isothermal conditions, being averaged over a temperature range of 0.1° or less. The observed values of ΔH_1^0 indicated that ionization proceeded[12] via the amino group, $O_2^-RNH_3^+ \rightleftarrows O_2^-RNH_2 + H^+$. The results are summarized in Table VI.

NMR studies

With the exception of glycine, alanine, proline, and hydroxyproline, the solubility of the other fundamental amino acids in water is far below 10%. NMR spectra of the aqueous solutions were ill-defined even after multiple scanning. The CH quadruplet of even alanine with 16.7% solubility became distinct only after multiple scanning (*cf.* Fig. 3). The use of D_2O would, of course, yield a much superior spectrum. The solutions of the amino acids for spectral studies were prepared in a solution 0.25 M with respect to sodium carbonate and bicarbonate in order to enhance

the solubility of the amino acids. The spectra of such solutions were superior to those in unbuffered solutions (cf. Figs. 4 and 5). Carboxyl and amino proton peaks were not observed in any of the spectra owing to rapid exchange with solvent proton. This was, in fact, an added advantage. Assignment of peaks to structural groups of amino acids was based on the predicted splitting, the intensities of absorption peaks, and published data[8-11].
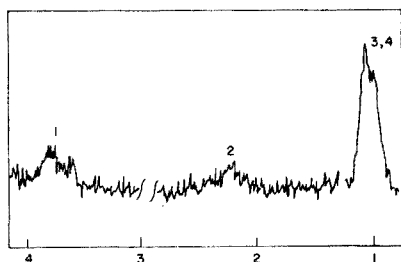

Fig. 4. NMR spectrum of valine, $(CH_3)_2CHCH(NH_2)COOH$, in water. (1) α-proton; (2) methylene proton; (3,4) methyl proton.
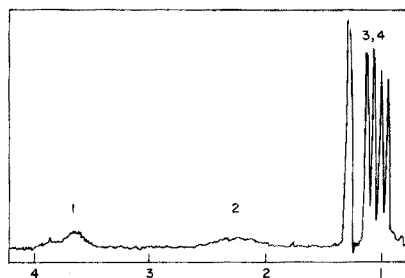
Fig. 5. NMR spectrum of valine, $(CH_3)_2CHCH(NH_2)COOH$, in 0.25 M Na_2CO_3 and $NaHCO_3$. (1) α-proton; (2) methylene proton; (3,4) methyl proton.

The chemical shifts of the different protons follow the general rule, i.e., the greater the shielding around the proton, the lower the chemical shift. Hence, the α-CH group which is relatively unshielded appeared at a lower field than the groups removed from α-carbon. Of these latter groups, the shifts are influenced by the substituents directly attached to them. The relative positions of the absorption peaks for each amino acid are given in Table VII.

TABLE VII

POSITIONS OF THE CHARACTERISTIC NMR PEAKS OF SOME AMINO ACIDS
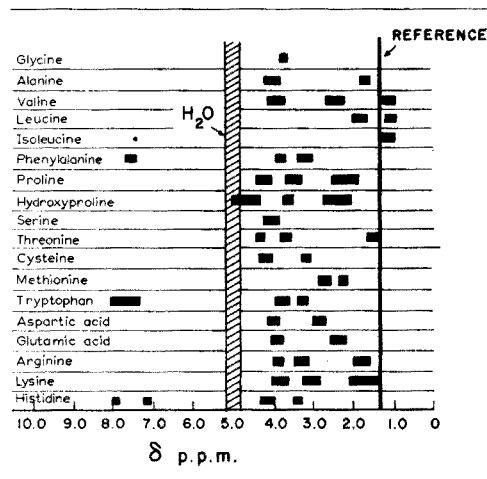
The terminal methyl groups of valine, leucine and isoleucine are most shielded, and appeared in the vicinity of 1 p.p.m. The methyl peak of leucine is a doublet, whereas that of isoleucine has a multiplet structure. Besides, leucine has an extra low broad band extending between 1.6 and 1.8 p.p.m. The methyl groups of alanine and threonine are relatively less shielded, the former being next to an α-carbon (doublet $\sim$1.5 p.p.m.) and the latter being in close proximity to the hydroxyl group (doublet $\sim$1.5 p.p.m.). Following the decreasing order of shielding is the S-methyl of methionine ($\sim$2.2 p.p.m.).

The protons of unsaturated and nearly unsaturated rings are expected to give peaks at relatively low field, and accordingly, phenylalanine, tryptophan and histidine gave peaks in the region 7–8.5 p.p.m. The aromatic proton peaks in the three cases are quite distinctive. Histidine shows two characteristic peaks at 7.2 p.p.m. and 7.9 p.p.m. which are highly suitable for identification. For some inexplicable reason, tyrosine did not show any peak.

In serine, $HOCH_2CH(NH_2)COOH$, the α-hydrogen plus methylene hydrogens absorb together at 3.8–4.1 p.p.m. Methionine, $CH_3SCH_2CH(NH_2)COOH$, is distinguished by a very narrow prominent peak at 2.2 p.p.m. which is attributed to the terminal methyl group. This methyl peak is unique among all those occurring in the natural amino acids in that there are no neighboring protons to split it. Cystine, $[-SCH_2CH(NH_2)COOH]_2$, in accordance with its structure, shows two multiplet peaks (CH_2 doublet at $\sim$3.1; CH triplet at $\sim$4).

In general, it is possible to relate the chemical shifts to the order of effectiveness of different substituent atoms in deshielding a given group by the order of the electro-negativities of the substituent atoms $(O > N > S)$, and by their proximity to the
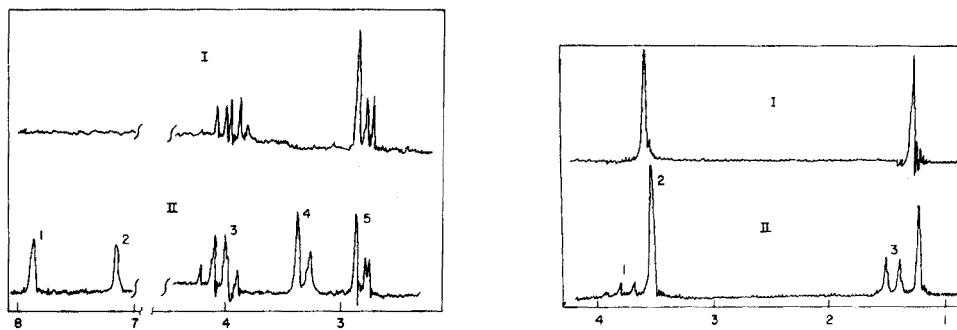
Fig. 6. NMR spectra of (I) aspartic acid, $HOOCCH_2CH(NH_2)COOH$, and mixture of (II) aspartic acid and histidine
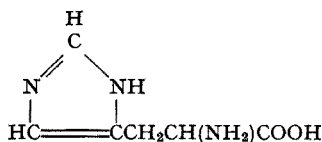
(1,2) histidine ring proton; (3) α-proton of histidine and aspartic acid; (4) methylene proton of histidine; (5) methylene proton of aspartic acid.

Fig. 7. NMR spectra of (I) glycine, $CH_2(NH_2)COOH$, and mixture of (II) glycine and alanine, $CH_3CH(NH_2)COOH$. (1) α-proton of alanine; (2) α-proton of glycine; (3) methyl proton of alanine.
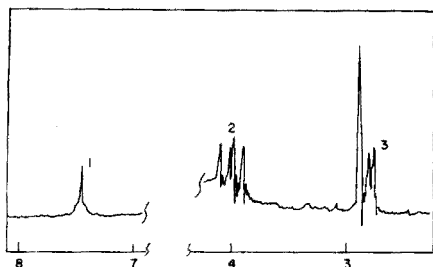
Fig. 8. NMR spectrum of a mixture of aspartic acid, $HOOCCH_2CH(NH_2)COOH$, and phenyl-alanine, $\bigcirc$-$CH_2CH(NH_2)COOH$. (1) Ring proton of phenylalanine; (2) α-proton of aspartic acid; (3) methylene proton of aspartic acid.
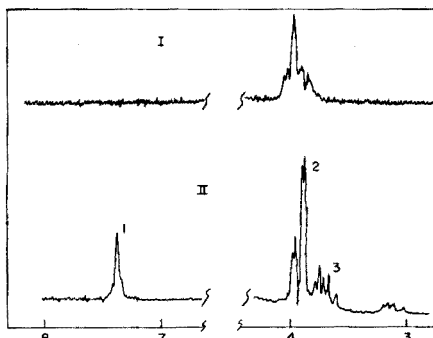
Fig. 9. NMR spectra of (I) serine, $HOCH_2CH(NH_2)COOH$, and mixture of (II) serine and phenyl-alanine, $\bigcirc$-$CH_2CH(NH_2)COOH$. (1) Ring proton of phenylalanine; (2) α and methylene protons of serine; (3) α and methylene protons of serine; (3) α and methylene protons of phenyl-alanine.
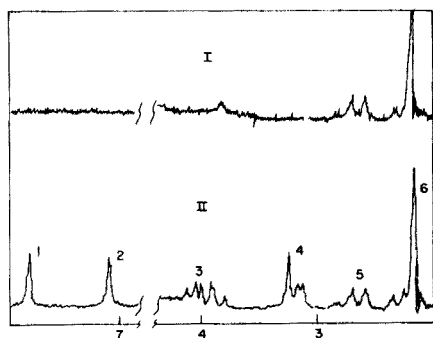
Fig. 10. NMR spectra of (I) methionine, $CH_3SCH_2CH_2CH(NH_2)COOH$, and mixture of (II) methionine and histidine
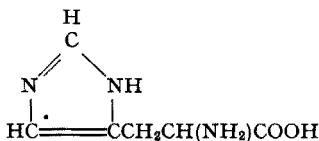
(1,2) ring proton of histidine; (3) α-proton of histidine; (4) methylene proton of histidine; (5) S-methylene proton of methionine; (6) methyl proton of methionine.

Fig. 11. NMR spectra of (I) lysine, $H_2N(CH_2)_4CH(NH_2)COOH$, and mixture of (II) lysine and histidine
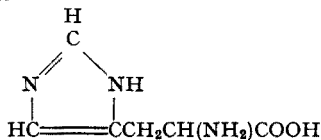
(1,2) ring proton of histidine; (3) α-proton of histidine; (4) α-proton of lysine; (5) methylene proton of histidine; (6) N-methylene proton of lysine; (7) other methylene protons of lysine.

observed protons. When the chemical shifts of the various protons are summarized, four different regions may be established as follows:

Type of proton	δ (p.p.m.)	Example
Aliphatic	0.5–2.0	Terminal –CH_3 groups of leucine, isoleucine, valine
Aliphatic and β-substituted	0.9–4.5	–CH_3 group in alanine, isoleucine; –CH_2– in glutamic acid
Aliphatic and α-substituted	2.0–5.0	α-CH group in all amino acids
Aromatic and hetero-aromatic	7.0–8.5	Phenylalanine, histidine, tryptophan

A closer study of Table VII reveals that each amino acid, being structurally different apart from their common carboxyl and amino groups, has a unique NMR spectrum. In a binary mixture of amino acids, if there are no chemical interactions between the acids and the solvent, the intensity of absorption is simply additive if both acids have peaks located in the same position. With the characteristic absorption peak of each compound, it is, therefore, possible to identify the components in a binary mixture, and in several cases in ternary mixtures. NMR spectra for a few such mixtures are shown in Figs. 3–11. The component acids in the mixtures may be identified by matching the peaks with Table VII or the spectra of the individual acids.

SUMMARY

Thermometric titration coupled with NMR spectroscopy provides an elegant method of determination and identification of individual amino acids, and their binary mixtures. Experimental details and interpretation of thermometric and NMR spectroscopic data are presented.

RÉSUMÉ

Le titrage thermométrique, combiné à la spectroscopie NMR constitue une méthode élégante pour le dosage et l'identification d'acides aminés individuels ou dans des mélanges binaires. Des détails expérimentaux sont donnés ainsi que l'interprétation des valeurs obtenues.

ZUSAMMENFASSUNG

Die thermometrische Titration verknüpft mit der NMR-Spektroskopie ist eine elegante Methode zur Bestimmung und Identifizierung individueller Aminosäuren und ihrer binären Mischungen. Experimentelle Einzelheiten und die Interpretation der thermometrischen und NMR-Spektroskopie-Daten werden angegeben.

REFERENCES

1 R. J. BLOCK AND D. BOLLENG, *The Determination of Amino Acids*, Burgess, Minnesota, 1948.
2 R. J. BLOCK AND K. W. WEISS, *Amino Acid Handbook*, Charles C. Thomas, Illinois, 1955.
3 D. M. GREENBERG, *Amino Acids and Proteins*, Charles C. Thomas, Illinois, 1951.
4 S. BLACKBURN, *Methods of Biochemical Analysis*, Vol. XIII, Ch. I, Interscience, New York, 1965.
5 J. JORDAN, Thermochemical Titrations, *Record Chem. Progr.*, 19 (1958) 193.
6 J. JORDAN, Thermometric Titrator, *J. Chem. Educ.*, 40 (1963) A5.
7 W. W. WENDTLAND, *Thermal Methods of Analysis*, Ch. 9, Interscience, New York, 1964.
8 F. A. BOVEY AND G. V. D. TIERS, *J. Am. Chem. Soc.*, 52 (1959) 863.
9 O. JARDETZKY AND C. D. JARDETZKY, *J. Biol. Chem.*, 233 (1958) 383.
10 M. TAKEDA AND O. JARDETZKY, *J. Chem. Phys.*, 26 (1957) 1346.
11 VARIAN ASSOCIATES, *High Resolution NMR Spectra Catalog*, Vols. 1 and 2, California, 1963.
12 J. P. GREENSTEIN AND M. WINITZ, *Chemistry of Amino Acids*, Vol. I, John Wiley, New York, 1961.

A DISTRIBUTION STUDY OF THE ASSOCIATION OF 2,2-DIETHYLPROPANEDIOL-1,3 AND 2-ETHYLHEXANEDIOL-1,3 IN CHLOROFORM

D. DYRSSEN AND L. UPPSTRÖM

Department of Analytical Chemistry, University of Gothenburg, P.O. Box, S-402 20 Göteborg 5 (Sweden)

M. ZANGEN

Soreq Nuclear Research Center, Yavne (Israel)

(Received February 10th, 1969)

In connection with an investigation of the extraction of boric acid in sea water by chloroform in the presence of 1,3-diols it became necessary to examine the state of association of the diols in the chloroform layer. Most earlier studies on the hydrogen bonding of diols[1-6] have been concerned with the strength of the intramolecular hydrogen bond, whose presence is indicated by the infrared spectra[2-6] of dilute solutions of the diols (< 0.005 M) in carbon tetrachloride. Studies on the undiluted diols[7-9] show, however, that intermolecular association takes place, but the degree of association obtained by combination of viscosity and vapour pressure measurements[9] seems to give much too low a value for the association number. The effect of structure on the association of polyhydroxy compounds has been discussed by BENNETT, EGLINTON AND KOVAC[10]. In his study of boric acid chelates GEORGE[11] made measurements on the distribution of diethylpropanediol (DEPD) and ethylhexanediol (EHD) but observed no concentration dependence of the distribution caused by association of the diols in the chloroform phase.

EXPERIMENTAL

Reagents

2,2-Diethylpropanediol-1,3 (DEPD; J. T. Baker Chemical Co, Phillipsburg, U.S.A.) was recrystallized from benzene (m.p. 63.5–64.5°). 2-Ethylhexanediol-1,3 (EHD; Kebo AB, Stockholm, Sweden) was redistilled at 239.5–240.5°. The p.a. chloroform (Merck A.G., Darmstadt, West Germany) was washed twice with redistilled water and then once with 0.5 M sodium chloride (p.a.). Aliquots of the solutions of the diols in chloroform (0.003–1 M) were subjected to thin-layer evaporation of the chloroform, and water was removed at reduced pressure in a desiccator. The remaining diol was weighed and the results were found to be consistent with the calculated original concentration of the diol.

Distribution measurements

Solutions containing different concentrations of the diols in chloroform (0.0018–1 M) were equilibrated with known volumes of 0.5 M sodium chloride for

5 min. The organic layer was separated and evaporated as above, the amount of diol dissolved in the aqueous phase being obtained from the difference in weight. The ratio of organic/aqueous volumes was adjusted so that the fraction of the diol in the aqueous phase was always large enough for an accurate determination. The following values were obtained for the distribution ratios, D, at the molar concentrations of diols in the aqueous phase given in parenthesis. DEPD: 1.04 (0.0050), 1.03 (0.00135), 1.23 (0.0225), 1.25 (0.0435), 1.51 (0.0666), 1.72 (0.0875), 1.93 (0.1056), 2.84 (0.1320), 4.45 (0.1442) and 5.42 (0.1600). EHD: 4.91 (0.0003), 5.00 (0.0012), 5.35 (0.0027), 5.15 (0.0033), 6.50 (0.0065), 7.00 (0.0089), 6.10 (0.0097), 7.40 (0.0120), 7.55 (0.0168), 8.60 (0.0210), 9.52 (0.0224), 9.44 (0.0227), 12.65 (0.0289), 14.80 (0.0330), 17.30 (0.0331) and 22.25 (0.0375).   .

RESULTS AND TREATMENT OF DISTRIBUTION DATA

The distribution data given above were plotted as D against the concentration of the diol in the aqueous phase, [A]. By extrapolation the following values were obtained for the distribution constant of the monomer,

$$K_e = [A]_{org}/[A].$$

DEPD: $K_e = 1.0$; EHD: $K_e = 5.0$.
The distribution curves showed an increase of D with [A] (or $[A]_{org}$) which may be explained by the formation of dimeric and polymeric species according to

$$D = ([A]_{org} + 2[A_2]_{org} + \ldots + n[A_n]_{org})/[A]$$

or if $[A]_{org} = K_e[A]$ and $[A_n]_{org} = K_n[A]^n_{org}$ are introduced

$$D/K_e = 1 + 2K_2(K_e[A]) + \ldots + nK_n(K_e[A])^{n-1}$$

The data were then plotted as $\log D/K_e$ against $\log K_e[A]$ ($= \log [A]_{org}$) as shown in Fig. 1. It is obvious from this Fig. that there is a considerable deviation from the

Fig. 1. Distribution data for 2,2-diethylpropanediol-1,3 (crosses) and 2-ethylhexanediol-1,3 (filled circles) between chloroform and 0.5 M sodium chloride plotted as $\log D/K_e$ against the logarithm of the concentration of the diol monomer in the chloroform phase, ($\log K_e[A]$), thus permitting a direct comparison of the two diols. The curves are calculated from the equation $\log (D/K_e) = \log\{1 + 2K_2(K_e[A]) + 9K_9(K_e[A])^8\}$ with the constants given in the text. The dashed curve is calculated neglecting the last term for the polymeric species.

dashed curve based on the assumption that only dimers are formed besides the monomers, *i.e.* $\log D/K_e = \log\{1 + 2K_2(K_e[A])\}$.

Thus a species with $n > 2$ must be formed at higher concentrations. It is also obvious that the tendency for this formation is more pronounced with DEPD than with EHD.

Curve-fitting the data for $\log K_e[A] < -1$ with the normalised curve $Y = \log(1 + v)$; $X = \log v$ gave $\log K_2 = 0.56$ for both diols. In order to estimate n and K_n the data for $\log K_e[A] > -0.9$ were plotted as $\log Q = \log\{D/K_e - 1 - 2K_2(K_e[A])\}$ against $\log (K_e[A])$. The data in these plots (not shown) could be fitted to straight lines with slope 8. This treatment of the extraction data is very similar to the graphical method suggested by ROSSOTTI AND ROSSOTTI[12]. Since these straight lines are explained by the equation

$$\log Q = (n-1) \log (K_e[A]) + \log nK_n$$

it follows that $n - 1 = 8$ and values can be obtained for $\log K_9$. This indicates that only one polymeric species with $n = 9$ is formed at higher diol concentrations, but too much emphasis should not be placed on the values of either n or K_n. It is probable that there is, in fact, a mixture of several polymers, but the presence of one other species in addition to the monomer and the dimer is sufficient to explain our distribution data. The curves in Fig. 1 have been drawn with the following equation

$$\log(D/K_e) = \log\{1 + 2K_2(K_e[A]) + 9K_9(K_e[A])^8\}$$

and the following values of the constants:

DEPD: $\log K_e = 0.00$, $\log K_2 = 0.56$, $\log K_9 = 6.01$

EHD: $\log K_e = 0.70$, $\log K_2 = 0.56$, $\log K_9 = 5.27$

Figure 2 shows that curves based on these constants also fit the distribution data when D/K_e is plotted against $K_e[A]$.

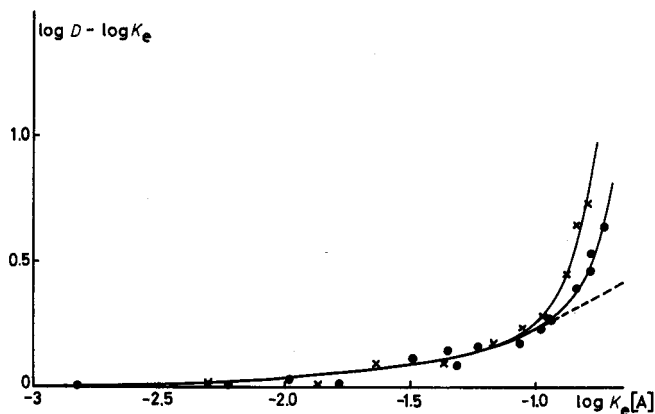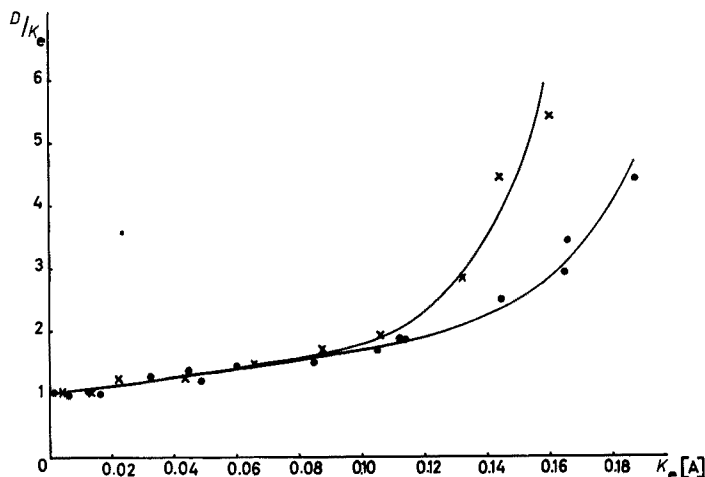Fig. 2. The linear relationships of the distributions of 2,2-diethylpropanediol-1,3 (crosses) and 2-ethylhexanediol-1,3 (filled circles) between chloroform and 0.5 M sodium chloride. The curves are calculated from the equation $D/K_e = 1 + 2K_2(K_e[A]) + 9K_9(K_e[A])^8$ with the constants given in text. *Cf.* Fig. 1.

The difference in log K_e can be explained by the fact that EHD contains one more CH_2 group than DEPD. The difference in log K_9 can probably be explained by the structural difference between the two 1,3-diols.

It should be emphasized that the expression given above for log (D/K_e) containing the constants K_2 and K_9 does not explain the results obtained with more concentrated solutions. Thus for an initial concentration of 1.044 M EHD in chloroform the values $[A] = 0.046$ and $D = 21.7$ were obtained.

SUMMARY

The distribution of 2,2-diethylpropanediol-1,3 (DEPD) and 2-ethylhexanediol-1,3 (EHD) between chloroform and 0.5 M sodium chloride has been followed at 25° as a function of the diol concentration. The distribution data could be explained by assuming that the diol was monomeric in the aqueous layer but that, besides the monomer, a dimer and a polymer containing nine molecules were present in the chloroform layer. DEPD has a somewhat larger tendency to polymerize than EHD.

RÉSUMÉ

Le partage du diéthyl-2,2-propanediol-1,3 (DEPD) et de l'éthyl-2-hexanediol-1,3 (EHD) entre chloroforme et chlorure de sodium 0.5 M a été suivi à 25°, en fonction de la concentration en diol. Les valeurs obtenues pourraient s'expliquer en supposant que le diol est monomère dans la couche aqueuse, tandis que dans la couche chloroforme on aurait en plus du monomère, un dimère et un polymère renfermant neuf molécules. DEPD a plus tendance à se polymériser que EHD.

ZUSAMMENFASSUNG

Die Verteilung von 2,2-Diäthylpropandiol-1,3 (DEPD) und 2-Äthylhexandiol-1,3 (EHD) zwischen Chloroform und 0.5 M Natriumchlorid ist bei 25° eine Funktion der Diol-Konzentration. Die Verteilungskoeffizienten konnten erklärt werden unter der Annahme, dass das Diol in der wässrigen Phase monomer vorliegt, aber dass ausser dem monomeren ein dimeres und ein polymeres, welches neun Moleküle enthält, in der Chloroformschicht anwesend sind. DEPD besitzt eine etwas grössere Tendenz zu polymerisieren als EHD.

REFERENCES

1 G. C. PIMENTEL AND A. L. McCLELLAN, The Hydrogen Bond, W. H. Freeman, San Francisco–London, 1959.
2 L. P. KUHN, J. Am. Chem. Soc., 74 (1952) 2492; 80 (1958) 5950.
3 A. B. FOSTER, A. H. HAINES AND M. STACEY, Tetrahedron, 16 (1961) 177.
4 H. BUC, Ann. Chim. (Paris), 13 (1963) 409, 431.
5 C. QUIVORON AND J. NEEL, J. Chim. Phys., 63 (1966) 1210.

6 V. I. MALYSHEV AND V. N. MURZIN, *Izv. Akad. Nauk SSSR, Ser. Fiz.*, 22 (1958) 1107.
7 C. MORIAMEZ, *J. Chim. Phys.*, 61 (1964) 298.
8 T. YONEZAWA, H. SAITÔ, S. MATSUOKA AND K. FUKUI, *Bull. Chem. Soc. Japan*, 38 (1965) 1431.
9 L. H. THOMAS AND R. MEATYARD, *J. Chem. Soc.*, (A) (1966) 92.
10 W. S. BENNETT, G. EGLINTON AND S. KOVAC, *Nature*, 214 (1967) 776.
11 R. S. GEORGE, *Thesis*, Northwestern University, 1962, p. 102.
12 F. J. C. ROSSOTTI AND H. ROSSOTTI, *J. Phys. Chem.*, 65 (1961) 926.

A STUDY OF THE EXTRACTION OF BORIC ACID WITH 2,2-DIETHYLPROPANEDIOL-1,3 AND 2-ETHYLHEXANEDIOL-1,3 IN CHLOROFORM

D. DYRSSEN AND L. UPPSTRÖM

Department of Analytical Chemistry, University of Gothenburg, P.O. Box, S-402 20 Göteborg 5 (Sweden)

M. ZANGEN

Soreq Nuclear Research Center, Yavne (Israel)

(Received February 10th, 1969)

Boron can be extracted with the aid of polyhydroxy compounds (organic polyols) in two main ways: from alkaline solutions as an ion-pair (borate didiol ester, $B(O_2R)_2^- M^+$, or polyborate ester) or from acid solutions as the boric acid ($B(OH)_3$-$((HO)_2R)_x$ associate or ester). The former process has been used in the large-scale recovery of boron from brines[1-3] while the latter has been used in the chemical analysis of boron to enrich and separate boron from elements which interfere with its determination[4,5]. AGAZZI[5] has shown that boron can be determined in the organic layer by flame photometry, but a much lower sensitivity is obtained than in the curcumin method suggested by UPPSTRÖM[6]. In the present work the amount of boron in the organic layer has therefore been determined by the latter method, after evaporation of the organic solvent (chloroform).

Isoamyl alcohol[7-11] and tributyl phosphate[12] have also been used for the extraction of boric acid, but these reagents are less effective than the 1,3-diols.

In order to simplify the search for reagents with suitable chelating groups and a sufficiently large hydrocarbon residue, we decided to investigate thoroughly the equilibria involved in the solvent extraction of boric acid. The behaviour of two diols in a two-phase system, chloroform–0.5 M sodium chloride, was therefore studied separately[13].

EXPERIMENTAL

Reagents

2,2-Diethylpropanediol-1,3 (DEPD; J. T. Baker Chemical Co, Phillipsburg, U.S.A.) and 2-ethylhexanediol-1,3 (EHD; Kebo AB, Stockholm, Sweden) were purified as in the previous work[13].

Chloroform (p.a.) was washed twice with redistilled water and then once with 0.5 M sodium chloride. Boric acid (p.a.) was purchased from Merck A.G., Darmstadt, West Germany.

Distribution measurements

Solutions were prepared which contained different concentrations of the diols

in chloroform. The ionic strength of the aqueous phase was held at 0.5 M with sodium chloride in all experiments, either hydrochloric acid or sodium hydroxide being added in order to vary the pH between 2 and 12. The aqueous phase contained boric acid in concentrations varying from 0.0005 to 0.01 M. The aqueous and organic phases were equilibrated for 5 min, this length of time having been shown by previous experiments to be sufficient for equilibrium to be attained. After separation of the phases by centrifugation, the boron content of both phases was determined by the modified curcumin method[6]. Samples from the organic phase were evaporated, 1 ml of water was added and the samples were then treated in the same way as those from the aqueous phase. All experiments were carried out at $25 \pm 1°$.

RESULTS AND DISCUSSION

Extraction at pH 2

The results for the extraction at pH 2 as a function of the diol concentration are given in Tables I and II. Figures 1 and 2 show that EHD is more effective than DEPD for the extraction of boric acid at the same initial concentration of diol in chloroform. In order to obtain a high value of D or E ($=100D/(1+D)$) at equal phase

TABLE I

DISTRIBUTION OF BORIC ACID BETWEEN CHLOROFORM AND 0.01 M HCl + 0.49 M NaCl FOR DIFFERENT CONCENTRATIONS OF 2,2-DIETHYLPROPANEDIOL-1,3 (DEPD)

Initial molar concn. of DEPD in org. phase	Equil. concn. of DEPD in aq. phase[a]	Distribution ratio of $B(OH)_3$ at different initial molar concns. of $B(OH)_3$ in aq. phase			
		0.01	0.005	0.002	0 (extra-pol.)
1.0	0.158	23.2	24.0	18.62	25.7
0.3	0.102	5.07	7.63	7.18	8.5
0.1	0.044	0.96	1.24	1.38	1.5
0.03	0.015	0.178	0.294	0.171	0.28
0.01	0.0049	0.0489	0.0363	0.0551	0.056

[a] The amount of DEPD bound to boric acid is neglected.

TABLE II

DISTRIBUTION OF BORIC ACID BETWEEN CHLOROFORM AND 0.01 M HCl + 0.49 M NaCl FOR DIFFERENT CONCENTRATIONS OF 2-ETHYLHEXANEDIOL-1,3 (EHD)

Initial concn. of diol in org. phase	Equil. concn. of diol in aq. phase[a]	Distribution ratio of $B(OH)_3$ at different initial molar concns. in aq. phase					
		0.01	0.005	0.002	0.001	0.0005	0 (ex-trapol.)
1.0	0.046	57.4	59.4	62.0	51.6	(42.9)	62.5
0.3	0.0259	19.2	19.9	22.7	17.5	17.4	20.4
0.1	0.0123	4.43	4.94	5.16	5.16	5.42	5.3
0.03	0.0046	0.796	0.893	0.985	0.886	0.957	0.96
0.01	0.0018	0.199	0.250	0.279	0.276	0.269	0.282
0.003	0.0005	0.0571	0.0625	0.0675	0.0724	(0.0842)	0.072

[a] The amount of EHD bound to boric acid is neglected.

volumes, it is necessary to use 1 M EHD in chloroform (ca. 15%, v/v). According to AGAZZI[5] the distribution ratio decreases somewhat at higher concentrations of the diol. The increases in the distribution ratios for the diols and for boric acid are compared in Figures 2 and 3. The increase in the distribution ratio, D, can be explained by the formation of complexes between boric acid and the diol in the chloroform phase. If the diol is denoted by A then D can be expressed as

$$D = \frac{\sum_{0}^{n}[B(OH)_3A_n]_{org}}{[B(OH)_3]}$$
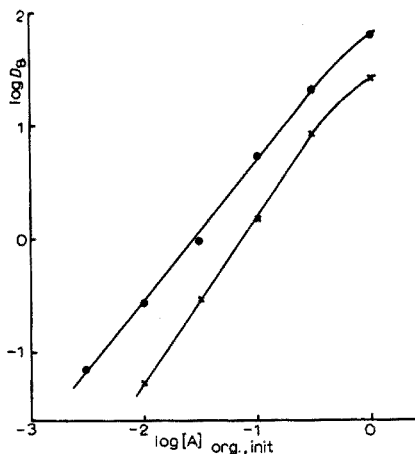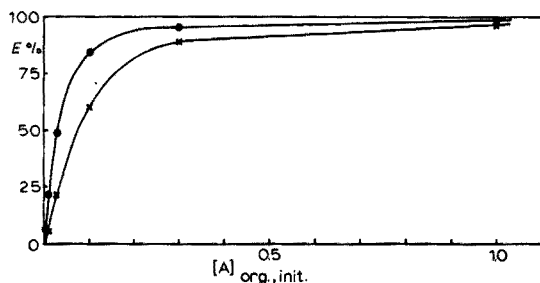
Fig. 1. Percentage extraction of boric acid ($E = 100D/(1 + D)$) with chloroform as a function of the initial concentration of DEPD and EHD in the chloroform phase. The aqueous phase contained 0.01 M HCl $+ 0.49$ M NaCl. ($\times$) DEPD; ($\bullet$) EHD.

Fig. 2. Logarithmic distribution ratio of boric acid between chloroform and 0.01 M HCl $+ 0.49$ M NaCl as a function of the logarithm of the initial concentration of DEPD and EHD in the chloroform phase. ($\times$) DEPD; ($\bullet$) EHD.
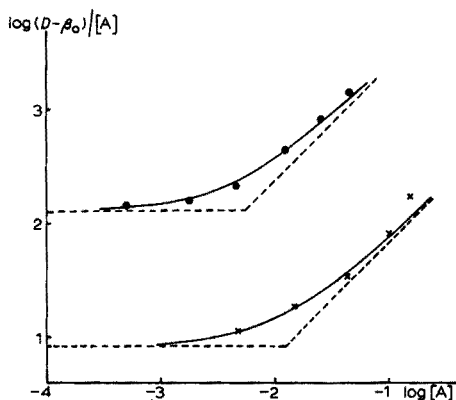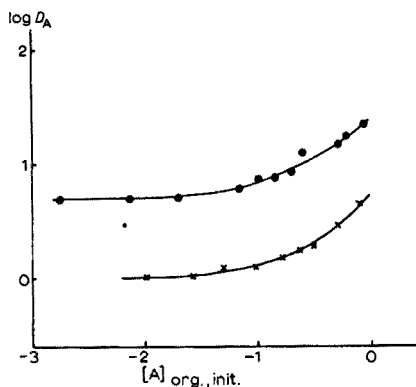
Fig. 3. Logarithmic distribution ratio of DEPD and EHD between chloroform and 0.5 M NaCl in the absence of boric acid as a function of the logarithm of the initial concentration of the diols in the chloroform phase. ($\times$) DEPD; ($\bullet$) EHD.

Fig. 4. Distribution of boric acid between chloroform and 0.01 M HCl $+ 0.49$ M NaCl. The data are plotted as log $(D - \beta_0)/[A]$ as a function of log $[A]$, where $[A]$ is the equilibrium molar concentration of the diol in the aqueous phase. ($\times$) DEPD; ($\bullet$) EHD. The normalized curve $Y = \log (1 + v)$; $X = \log v$ is fitted to the data. The constants derived are given in the text.

Introducing the constant β_n for the equilibria

$$B(OH)_3 \text{ (aq)} + n A \text{ (aq)} \rightleftharpoons B(OH)_3 A_n \text{ (org)}$$
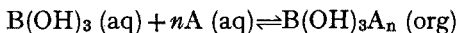
where the distribution constant for boric acid between chloroform and 0.5 M sodium chloride in the absence of diol ($n = 0$) is β_0. The value of β_0 obtained was $4.07 \cdot 10^{-5}$, which is considerably lower than the value of 0.015 reported by GEORGE[4]. The distribution ratio can be expressed in terms of the constants β_n

$$D = \beta_0 + \beta_1[A] + \beta_2[A]^2 + \ldots + \beta_n[A]^n$$

where [A] is the equilibrium concentration of the diol in the aqueous phase.

In order to be able to neglect the amount of diol bound to boric acid the distribution ratios given in Tables I and II were extrapolated to zero boric acid concentration. [A] could be calculated from the investigation of the diol distribution reported in a previous paper[13].

A plot of $Y = \log (D - \beta_0)/[A]$ against $\log [A]$ is shown in Fig. 4. Since the data fit the normalized curve $Y = \log (1 + v)$; $X = \log v$, only species with one or two diol molecules per boric acid are formed in the organic layer. The best fits yield the following equilibrium constants:

DEPD: $\log \beta_1 = 0.92$ and $\log \beta_2 = 2.82$

EHD: $\log \beta_1 = 2.10$ and $\log \beta_2 = 4.36$

With $\log \beta_0 = -4.39$ and $\log K_e = 0.00$ and 0.70 for DEPD and EHD, respectively[13] the constants for the equilibria between boric acid and the diols in the chloroform phase could be calculated:

$$B(OH)_3 + A \rightleftharpoons B(OH)_3 A; \; K_1$$

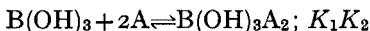$$B(OH)_3 A + A \rightleftharpoons B(OH)_3 A_2; \; K_2$$

$$B(OH)_3 + 2A \rightleftharpoons B(OH)_3 A_2; \; K_1 K_2$$
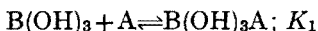
These constants are related to β_1 and β_2 in the following way:

$$K_1 = \beta_1/\beta_0 K_e$$

$$K_1 K_2 = \beta_2/\beta_0 K_e^2$$

The values obtained for the two diols are:

DEPD: $\log K_e = 0.00$; $\log K_1 = 5.31$; $\log K_1 K_2 = 7.21$; $\log K_2 = 1.90$.

EHD: $\log K_e = 0.70$; $\log K_1 = 5.79$; $\log K_1 K_2 = 7.35$; $\log K_2 = 1.56$.

The values of K_1 and K_2 for the equilibria in the organic layer are thus very similar for the two diols. Since DEPD contains two substituted ethyl groups in position 2 between the 1- and 3-hydroxy groups while EHD has only one substituted ethyl group, it might be expected that EHD ought to be less hindered in its reaction with boric acid. That K_1 is considerably larger than K_2 can just as well be explained by the fact that boric acid forms esters with the elimination of two and three water molecules as it retains its planar configuration forming a 1:1 $B(OH)_3$–diol chelate with two "double" hydrogen bonds ($2+2$ hydroxy groups involved) and a 1:2 $B(OH)_3$–didiol complex in which the second diol is bound by only one "double" hydrogen bond. These complexes will be investigated further by means of NMR. According to KÖSTER[14] some boric acid diol esters are stable in water.

Extraction with other 1,3-diols

If the hydrocarbon residue of a 1,3-diol is increased to C_9 (C_7 in DEPD and C_8 in EHD), K_e would be expected to increase to 20–25. This would lead to an increase in $[A]_{org}$ for a given initial concentration of the diol in the chloroform phase from 50% for DEPD and 83% for EHD to 95–96% (neglecting polymerisation effects). Apart from this effect, the distribution ratio

$$D = \beta_0(1 + K_1[A]_{org} + K_1K_2[A]^2_{org})$$

should not, however, be changed to any great extent. Substitution of both hydrogen atoms at the 2 position might give a slightly lower value of K_1. It is thus probably more profitable to search for compounds with chelating groups other than hydroxyl.

The effect of pH

Figures 5 and 6 show that the distribution decreases above pH 8 for a constant diol concentration and constant ionic strength. Since the boric acid concentration was kept as low as 0.001 M in order to avoid the formation of polyborates[15], the

Fig. 5. Distribution of boric acid between chloroform and mixtures of 0.5 M HCl, NaCl and NaOH. The circles represent data for an initial concentration of 1 M DEPD in chloroform and the triangles data for 0.1 M DEPD. The normalized curve $Y = -\log(1 + v)$; $X = \log v$ is fitted to the data. The equilibrium constants are given in the text.
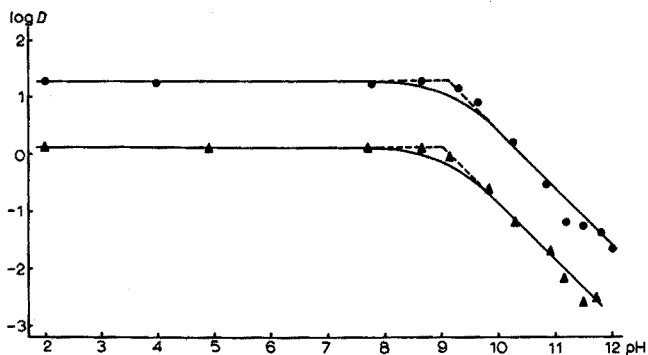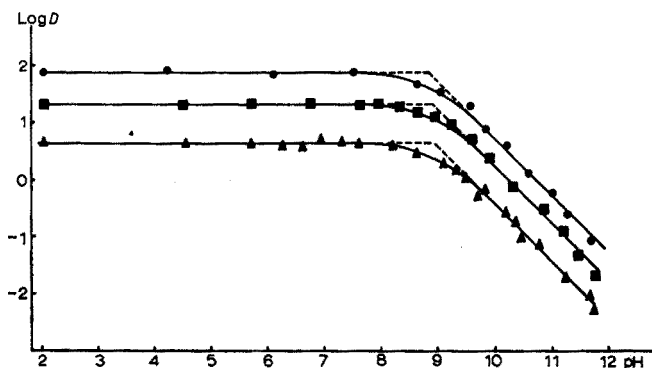

Fig. 6. Distribution of boric acid between chloroform and mixtures of 0.5 M HCl, NaCl and NaOH. The circles represent data for an initial concentration of 1 M EHD, the squares for 0.3 M and the triangles for 0.1 M EHD. The normalized curve $Y = -\log(1 + v)$; $X = \log v$ is fitted to the data. The equilibrium constants are given in the text.

decrease in log D with pH can only be explained by the fact that complexes with the two 1,3-diols in the aqueous phase can be neglected and that no sodium salt of diol esters with $B(OH)_4^-$ is extracted into chloroform. Thus the distribution ratio is given by

$$D = \frac{[B(OH)_3]_{org} + [B(OH)_3A]_{org} + [B(OH)_3A_2]_{org}}{[B(OH)_3] + [B(OH)_4^-]}$$

or if β_n (defined above) and $K_a = [H^+][B(OH)_4^-]/[B(OH)_3]$ are introduced

$$D = (\beta_0 + \beta_1[A] + \beta_2[A]^2)/(1 + K_a/[H^+])$$

At constant $[A]$ one obtains

$$\log D = -\log (1 + K_a/[H^+]) + \text{constant}.$$

This curve, which is of the normalized type $Y = -\log (1 + v)$; $X = \log v$, fits the data in Figs. 5 and 6. The asymptotes to the curve intersect at pH = 8.9–9.0, a reasonable value for an ionic strength of 0.5 M. If borate–diol complexes had been formed in the aqueous layer a considerably lower value of pK_a would have been obtained. This effect is well-known from the titration of boric acid with mannitol.

SUMMARY

The distribution of boric acid between chloroform and 0.5 M sodium chloride has been studied as a function of the concentration of 2,2-diethylpropanediol-1,3 (DEPD) and 2-ethylhexanediol-1,3 (EHD) between pH 2 and 12. EHD gives a higher distribution ratio for the same initial concentration in chloroform. The distribution data show that a 1:2 boric acid–diol complex in the chloroform phase is formed in two steps and that the equilibrium constant for the first step is considerably larger than that for the second. No complex between borate and the diols could be detected and the decrease in the distribution ratio above pH 8 is attributed to the formation of $B(OH)_4^-$. The possibility of finding more effective 1,3-diols is discussed.

RÉSUMÉ

Le partage de l'acide borique entre chloroforme et chlorure de sodium 0.5 M a été examiné en fonction de la concentration de diéthyl-2,2-propanediol-1,3 (DEPD) et de l'éthyl-2-hexanediol-1,3 (EHD) entre pH 2 et 12. EHD présente un coefficient de partage plus élevé pour une même concentration initiale dans le chloroforme. Les valeurs obtenues montrent qu'un mélange acide borique–complexe diol (1:2) se forme dans la phase chloroforme en deux étapes; la constante d'équilibre pour le premier stade est considérablement plus élevée que celle du second. On n'a pu déceler aucun complexe entre borate et diols; la diminution du coefficient de partage en dessus du pH 8 est attribuée à la formation de $B(OH)_4^-$. On examine la possibilité de trouver des 1,3-diols plus efficaces.

ZUSAMMENFASSUNG

Die Verteilung von Borsäure zwischen Chloroform und 0.5 M Natriumchlorid wurde in Abhängigkeit von der Konzentration des 2,2-Diäthylpropandiol-1,3 (DEPD) und 2-Äthylhexandiol-1,3 (EHD) zwischen pH 2 und 12 untersucht. EHD ergibt einen höheren Verteilungskoeffizienten bei gleicher Anfangskonzentration in Chloroform. Die Verteilungskoeffizienten zeigen, dass ein 1:2 Borsäure–Diol-Komplex in der Chloroformphase in 2 Schritten gebildet wird und dass die Gleichgewichtskonstante für den ersten Schritt beträchtlich grösser ist als die für den zweiten. Zwischen dem Borat und den Diolen konnte kein Komplex nachgewiesen werden. Die Abnahme des Verteilungskoeffizienten oberhalb pH 8 wird der Bildung von $B(OH)_4^-$ zugeschrieben. Die Möglichkeit effektivere 1,3-Diole aufzufinden, wird diskutiert.

REFERENCES

1 R. K. KLOPFENSTEIN AND D. S. ARNOLD, *J. Metals*, 18 (1966) 1195.
2 D. E. GARRETT, *U.S. Patent No. 2,969,275*, 1961.
3 D. E. GARRETT, F. J. WECK, A. J. MARSH AND H. R. FOSTER, JR., *U.S. Patent No. 3,111,383*, 1963.
4 R. S. GEORGE, *Investigation of the Nature of Chelates Formed by Boric Acid in Aqueous Solution*, Thesis, Northwestern University, 1962.
5 E. J. AGAZZI, *Anal. Chem.*, 39 (1967) 233.
6 L. UPPSTRÖM, *Anal. Chim. Acta*, 43 (1968) 475.
7 S. NAKAMURA AND K. SUZUKI, *Japan Patent 174, 696*, 1947.
8 E. E. VINOGRADOV, *Zh. Neorgan. Khim.*, 7 (1961) 2813.
9 V. I. YASHKISHEV AND E. E. VINOGRADOV, *Zh. Strukt. Khim.*, 3 (1962) 213.
10 E. E. VINOGRADOV, *Zh. Strukt. Khim.*, 3 (1962) 468.
11 V. I. YASHKISHEV, *Zh. Strukt. Khim.*, 7 (1966) 103.
12 S. S. KOROVIN, V. G. YURKIN AND A. P. MIRONENKO, *Zh. Neorgan. Khim.*, 11 (1966) 1910.
13 D. DYRSSEN, L. UPPSTRÖM AND M. ZANGEN, *Anal. Chim. Acta*, 46 (1969) 49.
14 R. KÖSTER, *Organische Derivate der Borsäuren*, Houben-Weyl, Bd VI/2, 1963, p. 221–222.
15 N. INGRI, *Acta Chem. Scand.*, 16 (1962) 439.

LIQUID ION-EXCHANGE ELECTRODES AS END-POINT DETECTORS IN COMPLEXIMETRIC TITRATIONS. DETERMINATION OF CALCIUM AND MAGNESIUM IN THE PRESENCE OF SODIUM

PART III. APPLICATION OF SIMPLE ION-EXCHANGE THEORY

M. WHITFIELD AND J. V. LEYENDEKKERS

Division of Fisheries and Oceanography, CSIRO, P. O. Box 21, Cronulla, Sydney, N.S.W. 2230 (Australia)

In Part I of this study[1], theoretical equations were derived and used to predict the effects of changing solution composition on the form of potentiometric titration curves. The experimental data discussed in Part II indicated the feasibility of this approach[2]. The theoretical equations were developed on the assumption that equilibrium boundary processes were predominant in controlling the electrode potential. On this basis, the potential of the Orion calcium-activity electrode was related to the solution composition by an equation of the form[3],

$$E = E' + S \log (a_{Ca} + K_{CaMg}a_{Mg} + K_{CaNa}a_{Na}^2) \tag{1}$$

where the electrode response to the ions has been expressed relative to the calcium ion. In general, K_{AB} is the selectivity coefficient of the electrode for ion B relative to ion A. The product of the selectivity coefficient and the activity of an ion indicates the extent to which that ion contributes to the cell potential. For convenience, this product may be termed the "effective activity", denoted by A. Thus, for the calcium activity electrode,

$$A_{Ca} = a_{Ca} \tag{2}$$

$$A_{Mg} = K_{CaMg}a_{Mg} \tag{2b}$$

$$A_{Na} = K_{CaNa}a_{Na}^2 \tag{2c}$$

The coefficient K_{AB} is related to the ion-exchange constant for the ions A and B ($_1K_{AB}$) and the relative mobility of the two ions (μ_B/μ_A) by[4]

$$K_{AB} = (\mu_B/\mu_A)_1 K_{AB} \tag{3}$$

Since the counter-ions diffuse freely within a liquid ion-exchanger[5], $\mu_B/\mu_A \sim 1$ and the selectivity coefficient is equated to the ion exchange constant $_1K_{AB}$. This is in direct contrast with the situation in glass electrodes where the selectivity is usually *controlled* by the relative mobilities of the selected ions in the hydrated surface layer[3,4].

For a given complexone, the form of the titration curve depends on the solution composition and on the values of the selectivity coefficients used in eqn. (1). Simple ion-exchange theory can be used to relate both of these factors to a single parameter, the composition of the liquid ion-exchanger. This parameter should be useful for comparing the performance of a number of electrodes with different selectivity characteristics or for evaluating the behaviour of a given electrode over a wide

range of solution compositions. To illustrate the method, regular solution ion-exchange theory is used to calculate the equilibrium composition of the exchanger at the beginning of a series of EGTA titrations of calcium–magnesium–sodium mixtures monitored with the Orion calcium-activity electrode[2]. The titration results are analysed on this basis.

COMPOSITION OF ION-EXCHANGER

If two ions (e.g. calcium(II) and magnesium(II)) are competing for sites in an ion-exchanger then the composition of the exchanger may be related to the composition of the solution by[6],

$$a_{Ca}/a_{Mg} = {}_1K_{CaMg}(N_{CaX_2}/N_{MgX_2}) \cdot \exp\left[(-W_{CaMg}/RT)(N_{CaX_2} - N_{MgX_2})\right] \qquad (4)$$

where a_M represents the activity of the ion M in the aqueous phase and N_{MX_2} the mole fraction of sites occupied by that ion in the exchanger; W_{CaMg} is a constant for the given pair of ions; and ${}_1K_{CaMg}$ is the equilibrium ion-exchange constant of the resin for magnesium(II) relative to calcium(II). Equation (4) can be expressed simply as

$$a_{Ca}/a_{Mg} = K'_{CaMg}(N_{CaX_2})/(N_{MgX_2}) \qquad (5a)$$

where $K'_{CaMg} = {}_1K_{CaMg} \cdot \exp\left[(-W_{CaMg}/RT)(N_{CaX_2} - N_{MgX_2})\right]$ and is termed the "corrected selectivity coefficient"[7].

By definition, K'_{CaMg} is a function of ion-exchanger composition. However, since no experimental data are available to allow for this variation, the corrected selectivity coefficients will be treated as constants. For liquid ion-exchange electrodes, these terms can be equated to the corresponding selectivity coefficients in eqn. (1).

When the two competing ions have different valencies (e.g. Ca^{2+} and Na^+ or Mg^{2+} and Na^+), the corresponding equation has the form

$$a_{Ca}/a_{Na}^2 = K'_{CaNa}(N_{CaX_2})/(N_{Na_2X_2}) \qquad (5b)$$

When three ions such as calcium(II), magnesium(II) and sodium(I) are all competing for the ion-exchange sites, the equations may be combined to give,

$$a_{Ca}^2/a_{Mg}a_{Na}^2 = K'_{CaMg}K'_{CaNa}(N_{CaX_2}^2)/(N_{MgX_2} \cdot N_{Na_2X_2}) \qquad (6a)$$

$$a_{Mg}^2/a_{Ca}a_{Na}^2 = K'_{MgCa}K'_{MgNa}(N_{MgX_2}^2)/(N_{CaX_2} \cdot N_{Na_2X_2}) \qquad (6b)$$

$$a_{Na}^4/a_{Ca}a_{Mg} = K'_{NaCa}K'_{NaMg}(N_{Na_2X_2}^2)/(N_{MgX_2} \cdot N_{CaX_2}) \qquad (6c)$$

if regular solution theory is obeyed.

Combining this set of equations with set 2, explicit equations can be obtained for the mole fraction of sites occupied by each component in the exchanger in terms of solution composition.

$$N_{CaX_2} = A_{Ca}/x \qquad (7a)$$

$$N_{MgX_2} = A_{Mg}/x \qquad (7b)$$

$$N_{Na_2X_2} = A_{Na}/x \qquad (7c)$$

where $x = A_{Ca} + A_{Mg} + A_{Na}$ \qquad (8)

Ammonium ions will also compete for exchange sites. However, because of lack of

data on the ammonium-ion coefficients we have only considered solutions 0.5 M in sodium (Table attached to Fig. 1) for which the ammonium-ion interference can be neglected. The initial composition of the ion-exchanger of the electrode when immersed in a given solution was calculated from eqns. (7a), (7b), (7c) with the values for the selectivity and activity coefficients given previously[1]. The results are plotted in Fig. 1 where each corner of the triangle represents an exchanger containing only one cation species. Despite the wide range of solution compositions the points are quite evenly distributed on the diagram.

In EGTA titrations, calcium is removed selectively by the reagent while the sodium-to-magnesium ratio remains effectively constant. Therefore, the composition of the ion-exchanger for an equilibrium titration will follow one of a series of lines radiating from the high calcium corner (Fig. 1). The exact position of the line will depend on the sodium-to-magnesium ratio in the solution. The various compositions
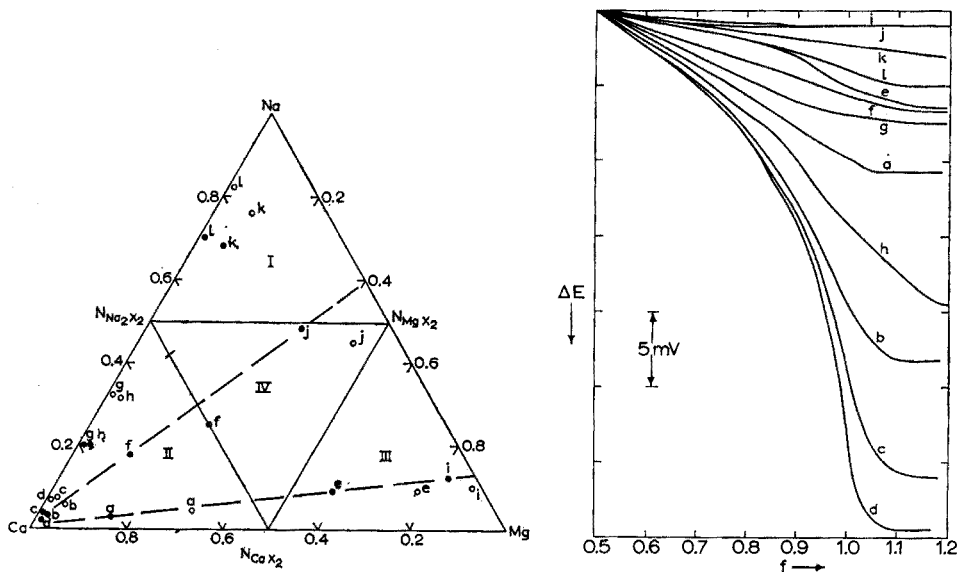
Fig. 1. Equilibrium composition of the ion-exchanger in the Orion calcium-activity electrode at the start of a titration (from eqns. (7a), (7b) and (7c)). (●) $K'_{CaMg} = 0.014$; $K'_{CaNa} = 0.0005$ (used in this work). (○) $K'_{CaMg} = 0.04$; $K'_{CaNa} = 0.001$ (ref. 10). (— — —) course of equilibrium EGTA titrations. Areas designated by Roman numerals are discussed in the text.

Composition of mixed electrolyte solutions

pCa\pMg	1	2	3	4
2		a	b	c	d
3		e	f	g	h[a]
4		i	j	k	l

[a] No value for overall potential drop available for this composition.
[Na+]=0.5 M throughout. pM = $-\log_{10}$ [M]. Square brackets indicate the initial concentrations of ions in the solution.

Fig. 2. Practical curves for EGTA titrations using a calcium-ion electrode. f is the ratio of the volume of titrant added to the equivalent volume. Solution compositions are given in the legend to Fig. 1. Order predicted from Fig. 1 (increasing potential drop): i, j, k, l, e, f, g, h, a, b, c, d.

of the ion-exchanger may be considered as intermediate stages in the equilibrium titration of a solution high in calcium. For example, compositions e and i appear as intermediate stages in the titration of solution a (see legend to Fig. 1). As the distance from the high calcium corner increases, the starting point of each successive titration will be further down the equilibrium titration curve. In consequence, the overall potential drop accompanying the titration should decrease as N_{CaX_2} decreases. For example, the overall potential drop should decrease in the order a, e, i for solutions containing 10^{-3} M magnesium (Fig. 1). If the sections of the practical titration curves near the end-point are arranged in order of increasing potential drop (Fig. 2, $cf.$ Fig. 1) the sequence corresponds almost exactly with that of increasing N_{CaX_2}; only curve h is out of sequence.

RELATIONSHIP BETWEEN EXCHANGER COMPOSITION AND POTENTIAL DROP

EGTA titrations

This relationship can be put on a quatitative basis by combining the ion-exchange equations with the relationship between cell potential and solution composition. At the beginning of a titration, the cell potential (E_1) can be obtained by combining eqns. (1) and (8)

$$E_1 = E' + S \log x \tag{9}$$

After the end-point, when a_{Ca} is very small, the cell potential (E_0) is given by,

$$E_0 = E' + S \log(A_{Mg} + A_{Na}) \tag{10}$$

Since a considerable amount of sodium chloride is present throughout, the ionic strength of the solution will remain effectively constant throughout the titration, and this should minimize variations in E' and the activity coefficient ratios. Assuming that these terms remain constant throughout the titration, the overall potential drop is given by,

$$\Delta E = E_1 - E_0 = S \log [x/(A_{Mg} + A_{Na})] \tag{11}$$

Combining eqns. (7b), (7c) and (11) gives

$$\Delta E = -S \log (1 - N_{CaX_2}) \tag{12}$$

since $N_{CaX_2} + N_{MgX_2} + N_{Na_2X_2} = 1$.
The term $(1 - N_{CaX_2})^{-1}$ is proportional to the distance of the point representing a particular resin composition from the sodium–magnesium line in Fig. 1. This distance is measured along the line joining the point to the pure calcium corner.

If dilution effects are significant, eqn. (11) can be corrected for changes in concentration to give,

$$\Delta E = -S \log(\bar{V}^2 N_{Na_2X_2} + \bar{V} N_{MgX_2}) \tag{13}$$

where $\bar{V} = V_1/(V_1 + V_0)$. V_1 and V_0 represent the initial and final volumes of the solution respectively. This form of the equation will be used in the subsequent discussion although the titration data fit eqn. (12) quite well because dilution effects were small. When ΔE is plotted against $-\log(\bar{V}^2 N_{Na_2X_2} + \bar{V} N_{MgX_2})$, the data points group about two straight lines passing through the origin (Fig. 3). For the ion-exchan-

gers with compositions in the high sodium corner (area I, Fig. 1) the data points fall on a line with a slope of 36.mV (line I, Fig. 3). This slope is greater than the theoretical value for divalent ions (29.6 mV at 25°), which indicates that the sodium ions may be making a significant contribution to the charge transfer process. This observation might explain the enhancement of electrode performance when sodium is added to mixtures containing divalent cations as noted by KING AND MUKHERJI[8]. The rest of the data points lie on a line with a slope of 20.8 mV (line II, Fig. 3).
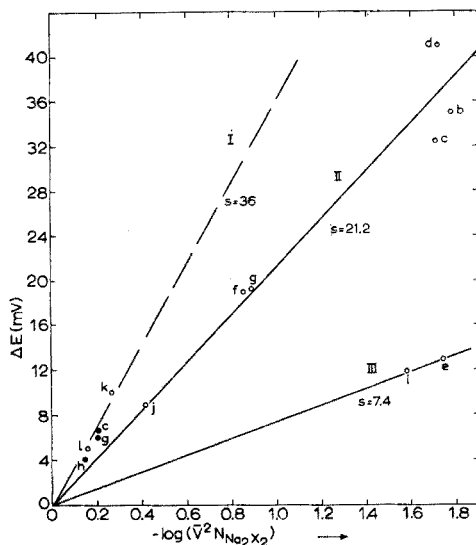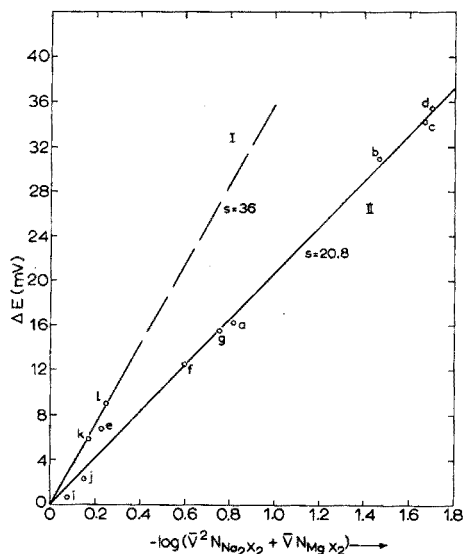

Fig. 3. Relationship between the overall potential drop accompanying the titration and the initial composition of the ion-exchanger, for EGTA titrations according to eqn. (13). Roman numerals correspond to areas marked in Fig. 1 and solution compositions are given in the legend to Fig. 1.

Fig. 4. Relationship between the overall potential drop accompanying the titration and the initial composition of the ion-exchanger for DCTA titrations according to eqn. (15a). (O) Calcium-activity electrode; $K'_{CaMg} = 0.014$; $K'_{CaNa} = 0.0005$. (●) Divalent-ion electrode; $K'_{CaNa} = 0.12$; $K'_{CaMg} = 1.0$. Other designations as in Fig. 1. No value for the overall potential drop is available for solution a.

For a given set of coefficient values, the value of S observed will depend on the experimental procedure used. As the end-point is approached interfering ions will begin to dominate the electrode response and diffusion-migration processes will become significant. The electrode potential will become time-dependent[5] and 10–20 min must elapse after each addition of titrant before complete equilibrium is restored[9]. In consequence the ΔE value will depend on the timing of successive additions of titrant in the vicinity of the end-point. If the titration is used as a practical analytical method the titrant must be added quite rapidly. In the titrations discussed here[2] each reading was taken within 30 sec of the addition of the titrant and the average duration of each titration was about 20 min. This might explain the relatively low S values obtained from Fig. 3.

RECHNITZ AND LIN[10] have recently determined the selectivity ratios K_{CaNa} and K_{CaMg} for the Orion calcium-activity electrode at pH 9.5 and ionic strength 0.01 M

(using tetraethylammonium borate solutions). They give the values as 0.001 and 0.04 respectively. Resin compositions calculated from these values (plotted in Fig. 1) do not give such a coherent pattern when plotted in the form shown in Fig. 3. Some recent investigations in this laboratory indicate that the value of 0.014 is more appropriate at ionic strengths around 0.5 M.

DCTA titrations

An analogous treatment can be used for DCTA titrations. The cell equation after the end-point is given by:

$$E_0 = E' + S \log A_{Na} \tag{14}$$

Combining eqns. (9) and (14) gives the overall potential drop as,

$$\Delta E = S \log(x/A_{Na})$$

Therefore, from eqn. (7a),

$$\Delta E = -S \log N_{Na_2X_2} \tag{15}$$

which, allowing for dilution, becomes

$$\Delta E = -S \log(V^2 N_{Na_2X_2}) \tag{15a}$$

where V is defined in eqn. (13).

In this instance the application of the simple eqn. (15) is restricted by the effects of dilution on the activity of the sodium ions and by the influence of ammonium-ion activity on the overall potential drop. When ΔE values for the DCTA titrations are plotted against $-\log(V^2 N_{Na_2X_2})$, the data fall into three groups (Fig. 4). The first two groups correspond to those observed for EGTA titrations (compare lines I and II in Figs. 3 and 4). As might be expected, the scatter about line II is greater in Fig. 4 than in Fig 3. The data points for ion-exchanger compositions lying in the high magnesium corner of the composition diagram (area III, Fig. 1) lie on a third line with a slope of 7 mV. Solution i in Fig. 3 would also fall on a line of this slope. The shallow slope reflects the combination of low effective activity and high concentration of divalent ions in these solutions. This line should not be observed in titrations with the divalent ion electrode which has an equal selectivity for calcium and magnesium.

APPLICATION TO OTHER ELECTRODES

The equilibrium compositions of the ion-exchangers for two divalent-ion electrodes are shown in Fig. 5. Most points lie in the high sodium corner of the diagram reflecting the high selectivity of these electrodes for sodium ions. DCTA titrations of solutions with composition points within the areas II and III should be feasible, although only solutions a, e and i could be expected to give good titrations if monitored with an electrode with $K_{CaMg} = 1.0$, $K_{CaNa} = 0.012$. The ΔE values for each composition can be read off from curves I and II in Figs. 3 and 4, assuming that the selectivity coefficients used to draw up Fig. 5 are applicable to the titration conditions. As an example, ΔE values for DCTA titrations of solutions C, g and h, with an electrode with $K'_{CaNa} = 0.12$, have been plotted in Fig. 4. As expected from Fig. 6 the points lie close to line I.
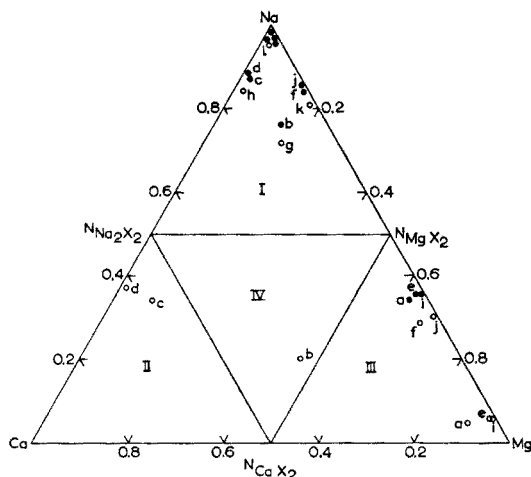
Fig. 5. Equilibrium composition of ion-exchanger in divalent-ion electrode for solution compositions listed in the legend to Fig. 1. (o) K'_{CaNa} = 0.012; K'_{CaMg} = 1.0. (●) K'_{CaNa} = 0.12[a]; K'_{CaMg} = 1.0.

[a] The points for compositions g, h, k and l for this exchanger lie very close to the pure high sodium corner and have not been labelled individually.

CONCLUSIONS

In general, the best titration curves are obtained with the calcium electrode if the initial ion-exchanger composition, as defined in this paper, lies within the high calcium corner of the composition diagram (area II, Fig. 1). By using figures analogous to Figs. 1 and 3 it should be possible to estimate the potential drop that could be expected experimentally for electrodes with any selectivity characteristics, monitoring a wide range of solutions.

Essentially, the method involves the comparison of effective ion activities in complex solutions expressed in terms of the mole fractions of exchanger sites occupied by individual ions. This procedure illustrates clearly the link between eqn. (1) and the simple ion-exchange theory. Although the composition of the ion-exchanger obtained in this way may bear little relationship to the true composition, this will not affect the applicability of the technique since the concept has been introduced mainly for descriptive purposes. The success of this approach depends on the availability of the appropriate values for the corrected selectivity coefficients. In this study these coefficients have been treated as constants for a given pair of ions competing for sites in a particular exchanger. While this may be valid at constant ionic strength, there is evidence[7,11] to suggest that these coefficients are functions of the solution composition. A detailed study of these variations will enable the simple technique outlined here to be applied with greater confidence over a wider range of solution compositions.

SUMMARY

For a given complexing titrant, the form of the potentiometric titration curves depends on the selectivity properties of the electrode and on the composition of the solution. These two factors can be combined into one term, the equilibrium composi-

tion of the liquid ion-exchanger, on the basis of simple ion-exchange theory. Data for EGTA titrations monitored with an Orion calcium-activity electrode are employed to illustrate how experimental observations over a wide range of solution compositions (pMg 1–4 and pCa 2–4) can be correlated by means of this parameter. Qualitative correlations are made on the basis of a three-coordinate plot of exchanger composition and equations are derived that allow a quantitative comparison of titration procedures to be made.

RÉSUMÉ

Pour un complexe donné, la forme de la courbe de titrage potentiométrique dépend des propriétés sélectives de l'électrode ainsi que de la composition de la solution. Ces deux facteurs peuvent être combinés en un seul: la composition d'équilibre de l'échangeur d'ions liquide, en se basant sur la théorie du simple échange d'ions. On utilise les valeurs relatives aux titrages EGTA, contrôlées au moyen d'une électrode activité-calcium Orion, pour illustrer la manière dont les observations expérimentales (pMg 1 à 4 et pCa 2 à 4) peuvent être interprétées au moyen de ce paramètre. On établit des corrélations qualitatives de la composition de la résine à l'aide d'un graphique, à trois dimensions; les équations qui en dérivent permettent une comparaison quantitative des procédés de titrage.

ZUSAMMENFASSUNG

Für ein gegebenes Komplexon hängt der Verlauf der Titrationskurve von den Selektivitätseigenschaften der Elektrode und von der Zusammensetzung der Lösung ab. Auf Grund der einfachen Ionenaustauschtheorie können diese zwei Faktoren in einem einzigen Ausdruck, der Gleichgewichtszusammensetzung des flüssigen ionenaustauschenden Harzes, zusammengefasst werden. Daten für mit einer Orion Kalzium Aktivitäts-elektrode überwachte EGTA Titrationen werden angeführt um zu zeigen wie Versuchsbeobachtungen über einen weiten Bereich von Lösungszusammensetzungen (pMg 1–4 und pCa 2–4) mit Hilfe dieses Parameters in Korrelation zueinander gebracht werden können. Qualitative Korrelationswerte werden auf Grund eines Dreikoordinaten Diagrammes der Harzzusammensetzung erhalten und Gleichungen werden abgeleitet die den quantitativen Vergleich von Titrationsmethoden ermöglichen.

REFERENCES

1 M. WHITFIELD AND J. V. LEYENDEKKERS, Anal. Chim. Acta, 45 (1969) 383.
2 M. WHITFIELD, J. V. LEYENDEKKERS AND J. KERR, Anal. Chim. Acta, 45 (1969) 399.
3 A. H. TRUESDELL AND C. L. CHRIST, in G. EISENMAN, Glass Electrodes for Hydrogen and Other Cations, Marcel Dekker, New York, 1967, Chapter 11.
4 G. EISENMAN, in G. EISENMAN, Glass Electrodes for Hydrogen and Other Cations, Marcel Dekker, New York, 1967, Chapter 3.
5 G. EISENMAN, Anal. Chem., 40 (1968) 310.
6 R. M. GARRELS AND C. L. CHRIST, in Solutions, Minerals and Equilibria, Harper & Row, New York, 1965, Chapter 8.
7 D. REICHENBERG, in J. A. MARINSKY, Ion-exchange, Vol. I, Edward Arnold, London, 1966, Chapter 7.
8 J. A. KING AND A. K. MUKHERJI, Naturwiss., 53 (1966) 702.
9 J. W. ROSS, Science, 156 (1967) 1378.
10 G. A. RECHNITZ AND Z. F. LIN, Anal. Chem., 40 (1968) 696.
11 E. W. MOORE AND J. W. ROSS, Science, 148 (1965) 71.

AN IMPROVED METHOD OF COULOSTATIC TITRATIONS

R. F. SYMPSON

Clippinger Laboratories, Department of Chemistry, Ohio University, Athens, Ohio 45701 (U.S.A.)
(Received February 3rd, 1969)

The coulostatic technique was proposed as an analytical method several years ago, but it is not a practical analytical tool at present [1,2]. The method has several inherent disadvantages. It is a potential relaxation technique in which the electrode potential decays with the one-half power of time under conditions of semi-infinite linear diffusion or conditions that approximate semi-infinite linear diffusion. The value of $\Delta E/\Delta t^{\frac{1}{2}}$ is proportional to the concentration of the electroactive species. The potential–time curve that appears on the oscilloscope screen is photographed. It is then necessary to plot an E *vs.* $t^{\frac{1}{2}}$ curve from this E *vs.* t curve, which is a tedious and time-consuming step. In order to relate the value of $\Delta E/\Delta t^{\frac{1}{2}}$ to concentration it is necessary to know the diffusion coefficient of the electroactive species in the medium used and the value of the double-layer capacitance per unit area which actually varies with potential but is assumed to be virtually constant over a limited potential range. These quantities can be determined experimentally with a solution of known concentration of the electroactive species, or a calibration curve can be constructed by measuring $\Delta E/\Delta t^{\frac{1}{2}}$ for a series of standard solutions of the electroactive species. In comparing $\Delta E/\Delta t^{\frac{1}{2}}$ slopes of unknown solutions with a working curve, it is necessary to keep constant any variables that affect the diffusion coefficient such as temperature and viscosity of the medium. Trace levels of electroactive impurities will also introduce errors.

In the present work the method was used to follow the course of a titration. This eliminates the need for precise temperature control and exact electrode reproducibility from one experiment to the next, and it gives greater accuracy while retaining the sensitivity of the coulostatic technique. A previous report[3] gave the equation for the coulostatic relaxation at a dropping mercury electrode (D.M.E.) and presented results of coulostatic titrations with a D.M.E. The changing area of the D.M.E. caused the equation to be sufficiently complex that it was convenient to use a computer to obtain the slopes of the E *vs.* F (t) curves at various points during the course of the titration. Although the analytical results were reasonably good for the concentration range employed, the titration procedure was too involved for the method to be practical.

In order to simplify the procedure a hanging drop mercury electrode (H.D.-M.E.) was employed that was sufficiently large that conditions of semi-infinite linear diffusion were approximated. Under these conditions the relaxation obeys the equation

$$E_t - E_0 = -2nFCD^{\frac{1}{2}}t^{\frac{1}{2}}/(\pi^{\frac{1}{2}}c_{\mathrm{dl}})$$

where c_{dl} is the double-layer capacitance per unit area and E_0 is the potential of the

H.D.M.E. at the beginning of the relaxation. By using a horizontal sweep voltage that varies with the square root of time instead of the internal saw tooth signal, a linear E vs. $t^{\frac{1}{2}}$ trace can be produced directly on the screen of the oscilloscope. These linear traces can be photographed at different stages of the titration, and the slopes can be measured and plotted against volume of titrant. This technique eliminates the necessity of plotting E vs. $t^{\frac{1}{2}}$ curves from the E vs. t curves normally photographed. To simplify the technique further the vertical deflection of the trace from some arbitrary point can be observed visually at constant time at various points during the titration. Vertical deflections are proportional to the slopes of the E vs. $t^{\frac{1}{2}}$ curves and can be plotted against volume of titrant.

EXPERIMENTAL

Apparatus
        The coulostat has been described previously[2,3]. O'DOM AND MURRAY[4,5] have described a simple circuit which produces a voltage proportional to the square root of time. Their circuit was modified only by substituting a Heath EUW 19A operational amplifier manifold for the Philbrick Model K7-A10 manifold, a Bourns Model 4100A-1-010 (10 V) Quadratron for the Douglas Type P, Model E Quadraton, and inserting switch S_2 shown in Fig. 1. A diagram of the apparatus is shown in Fig. 1.

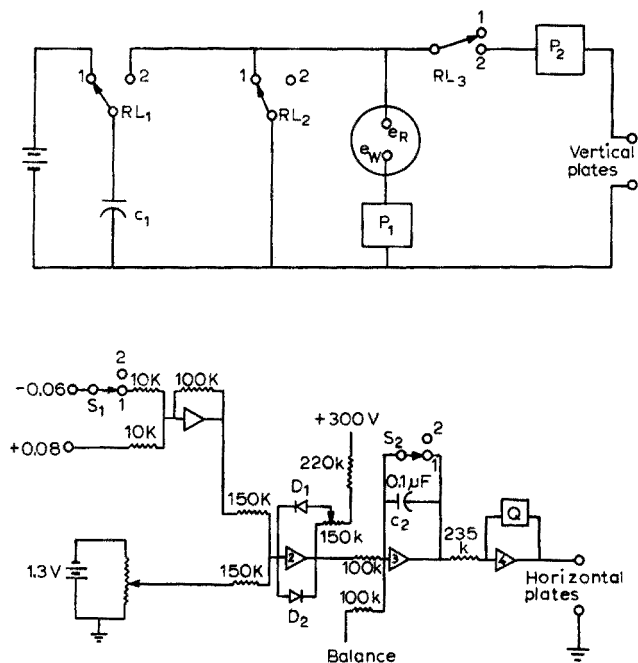Fig. 1. Coulostat and external sweep circuit. P_1 and P_2: potentiometers. Q: Bourns Model 4100A-1-010 Quadratron. D_1 and D_2: 1N485A.

S_1, S_2, and the activating switch for relays 1, 2, and 3 are all connected to a 3-ganged rotary switch. Details of the functioning of the coulostat and $\sqrt{E}$ generator are given in the original papers. At the beginning of an experiment, switches 1 and 2 and relays

1, 2, and 3 are in the positions shown in Fig. 1. By means of the rotary switch, switches 1 and 2 are opened simultaneously, and the relays in the coulostat are switched from position 1 to 2. Capacitor 1 discharges across the working electrode, e_w, and the reference electrode, e_R. The voltage between the working electrode and reference electrode is applied to the vertical plates of the oscilloscope. When switches S1 and S2 open, the output of amplifier 3 is a ramp voltage. The square root of this ramp voltage is taken by amplifier 4, and the output of amplifier 4 is applied to the horizontal plates of the oscilloscope.

Reagents

All chemicals used were reagent grade. A stock solution of ethylenediaminetetraacetic acid (EDTA) was standardized against freshly ignited zinc oxide by potentiometric titration with a mercury indicator electrode[6,7]. An aliquot of this solution was diluted to give a solution of concentration appropriate for the titrations. Stock solutions of cadmium and lead were standardized by potentiometric titration with the standard EDTA using the mercury indicator electrode[6,7]. All solutions were prepared with double distilled water, the second distillation being from alkaline permanganate. Solutions were de-aerated with Matheson prepurified nitrogen.

Titration conditions

Titrations of lead and cadmium with standard EDTA were performed in a supporting electrolyte of 0.06 *M* acetate buffer of pH 5.3. The volume of solution titrated was about 120 ml. A 5-ml buret was used. The titration cell was a Sargent S-29314 electrolysis cell. Titrations were followed by applying either cathodic or anodic pulses to the working electrode. In the former case a charge pulse was applied which caused the potential of the H.D.M.E. to shift cathodically to a value such that the surface concentration of reducible metal ion was reduced to zero. The potential was followed as it decayed to more positive values, owing to consumption of charge by metal ions diffusing to the electrode surface and being reduced. In the case of anodic pulses, a charge pulse was applied that caused the potential to shift to a value positive enough that mercury oxidized in the presence of EDTA. The surface concentration of EDTA was reduced to zero, and the potential decay was governed by the rate of diffusion of EDTA to the electrode surface. Charge pulses were obtained from a 0.00967 μF capacitor, c_1, charged to a voltage of 65–72 V. For the titrations with cathodic pulses, the initial potentials applied to the H.D.M.E. were –0.500 and –0.375 V *vs.* saturated calomel electrode for cadmium and lead titrations respectively. For all titrations with anodic pulses, the initial potential applied to the H.D.M.E. was –0.100V *vs.* saturated calomel electrode. For the cathodic-pulse titrations the H.D.-M.E. consisted of four mercury drops collected from a dropping mercury capillary. A fresh four drops were used for each relaxation. For the anodic-pulse titrations the H.D.M.E. consisted of two mercury drops. In either case the size of the H.D.M.E. was large enough that diffusion conditions approximated those of semi-infinite linear diffusion.

The sweep rate was adjusted so that the full scale horizontal sweep required 1–2 sec for titrations in which the oscilloscope trace was photographed. The sweep rate was not calibrated because it is necessary that it be constant only during the course of a titration but not necessarily reproducible from one titration to the next.

For the titrations in which the vertical deflection was observed visually at a constant time, the sweep rate was adjusted so it reached the horizontal midscale at about 1 sec. This was done because it is easier to read vertical deflections at the horizontal midpoint where grid graduations are in 0.2-cm units instead of 1-cm units. The square root of time base was checked periodically by applying the voltage to the vertical plates while sweeping horizontally with the internal sweep signal.

The bias voltage on potentiometer 2 was adjusted so the initial point of the trace on the oscilloscope screen was approximately at the zero point of the oscilloscope. In most of the titrations the traces were photographed and slopes of the straight-line portions measured and plotted against volume of titrant. In some of the titrations the vertical deflection at the horizontal midpoint was observed visually and plotted against volume of titrant.

RESULTS AND DISCUSSION

A series of anodic-pulse titrations of lead and cadmium were performed. These titrations gave consistently high results for the metal. As in the previous work[3], it was found that the high results were due to a significant blank observed when supporting electrolyte alone was titrated. In the present work an average end-point of 0.58 ml was obtained when 120 ml of 0.01 M acetic acid–0.05 M sodium acetate was titrated. The results of a series of titrations corrected for the blank are given in Table I.

TABLE I

COULOSTATIC TITRATIONS WITH ANODIC PULSES

$\mu moles$ taken	$\mu moles$ found	$\mu moles$ taken	$\mu moles$ found
Lead		Cadmium	
1.07	1.07	1.01	0.956
1.61	1.55	2.54	2.55, 2.54, 2.53, 2.41, 2.50, 2.54, 2.63, 2.53, 2.54, 2.50, 2.53
2.68	2.57, 2.65, 2.55	5.07	5.07

The cause of the blank correction remains undetermined. It would appear to be due to some impurity that will form a complex with EDTA at pH 5.3. The impurity is not reducible at ordinary potentials and forms an EDTA complex less stable than EDTA complexes of cadmium or lead, because no blank correction is found when cathodic pulses are applied and relaxation from uncomplexed metal occurs. In the previous work, ordinary distilled water was used, and the impurity was assumed to be present in the water. In this work doubly distilled water was used to prepare all solutions. After the magnitude of the blank correction had been discovered, attempts were made to eliminate the blank by further purification of the supporting electrolyte. A 0.1 M acetic acid–0.5 M sodium acetate buffer was electrolyzed for 1 h at a current of 0.2 A with a mercury pool cathode and an isolated anode. A portion of this electrolyzed solution was diluted ten-fold with triply distilled water. A 115-ml portion of this 0.01 M acetic acid–0.05 M sodium acetate buffer was titrated with $4.98 \cdot 10^{-4}$ M EDTA, and a blank of 0.39 ml was obtained.

The results of a series of titrations of lead and cadmium followed by application of cathodic pulses to the H.D.M.E. are summarized in Table II.

In the titrations represented in Tables I and II the oscilloscope traces were photographed, and the slopes of the straight lines were measured. If the sweep rate is constant and the potential excursion is the same each time, the slope of the trace should be proportional to the vertical deflection from the zero point of the scope at a

TABLE II

COULOSTATIC TITRATIONS WITH CATHODIC PULSES

$\mu moles$ taken	$\mu moles$ found	$\mu moles$ taken	$\mu moles$ found
Lead		Cadmium	
0.537	0.539, 0.538, 0.541	0.507	0.513, 0.513, 0.508
1.07	1.08, 1.16, 1.11	1.01	1.04, 1.00, 1.07,
1.61	1.61, 1.65, 1.63	1.52	1.52, 1.50, 1.59
2.68	2.51, 2.49, 2.69	2.54	2.53, 2.55, 2.53, 2.51, 2.49
5.37	5.30, 5.41	5.07	5.03

constant time after the beginning of the relaxation. A number of titrations were performed in which the vertical deflection was observed visually at the midpoint of the horizontal range following the cathodic pulse. These vertical deflections were plotted against volume of titrant. A series of 7 titrations of 1.60 μmoles of lead in 115–120 ml of buffer yielded results varying from 1.55 to 1.73 μmoles and an average of 1.63. The results of a series of 5 titrations of 1.52 μmoles of cadmium in 115–120 ml of acetate buffer ranged from 1.50 to 1.56 μmoles with an average value of 1.54 μmoles. When the vertical deflections are observed visually, the method is about as convenient and rapid as amperometric titrations with a dropping mercury electrode.

SUMMARY

The complexities of performing coulostatic titrations have been greatly reduced by using a special external sweep circuit which produces a horizontal sweep rate for the oscilloscope that varies with the square root of time. Since the potential decay at a large H.D.M.E. also varies with the square root of time and was applied to the vertical plates, linear decay curves were obtained. The slopes of the linear decay curves were plotted against volume of titrant. Lead and cadmium were titrated successfully in the concentration range of $4.4 \cdot 10^{-6}$–$4.7 \cdot 10^{-5}$ M.

RÉSUMÉ

La complexité des titrages coulostatiques a été grandement réduite en utilisant un circuit de balayage externe spécial qui produit une vitesse de balayage de l'oscilloscope, variant avec la racine carrée du temps. La chute de potentiel à l'électrode à goutte de mercure pendant variant également avec la racine carrée du temps, on obtient des courbes de chute linéaires. Le plomb et le cadmium ont été titrés ainsi avec succès en concentrations allant de $4.4 \cdot 10^{-6}$ à $4.7 \cdot 10^{-5}$ M.

ZUSAMMENFASSUNG

   Die Schwierigkeiten bei coulostatischen Titrationen werden stark reduziert durch Verwendung einer besonderen äusseren Schaltung, welche horizontale sweep-Raten im Oscilloskop erzeugen, die mit der Wunzel der Zeit variieren. Da der Potentialabfall bei grossem H.D.M.E. auf die gleiche Weise variiert, werden lineare Abfallkurven erhalten. Der Verlauf dieser linearen Kurven wurde gegen die verbrauchten ml aufgetragen. Blei und Cadmium wurden erfolgreich im Konzentrationsbereich von $4.4 \cdot 10^{-6}$–$4.7 \cdot 10^{-5}$ M titriert.

REFERENCES

1 P. DELAHAY, *Anal. Chem.*, 34 (1962) 1267.
2 P. DELAHAY AND Y. IDE, *Anal. Chem.*, 34 (1962) 1580.
3 R. W. SORENSEN AND R. F. SYMPSON, *Anal. Chem.*, 39 (1967) 1238.
4 R. W. MURRAY, *Anal. Chem.*, 35 (1963) 1784.
5 G. W. O'DOM AND R. W. MURRAY, *Anal. Chem.*, 39 (1967) 51.
6 C. N. REILLEY AND R. W. SCHMID, *Anal. Chem.*, 30 (1958) 947.
7 C. N. REILLEY, R. W. SCHMID AND D. W. LAMSON, *Anal. Chem.*, 30 (1958) 953.

COULOMETRIC TITRATION OF BASES IN CONCENTRATED NEUTRAL SALT SOLUTIONS IN WATER AND NON-AQUEOUS SOLVENTS

GARY D. CHRISTIAN

Department of Chemistry, University of Kentucky, Lexington, Ky. 40506 (U.S.A.)

Coulometric acid–base titrations have been performed in aqueous solutions[1-4] but the range of compounds which can be titrated is limited for very weak acids or bases because of the small change in pH at the end-point. The acidity or basicity of weak acids or bases can be markedly enhanced in nonaqueous solvents and extensive information is available for nonaqueous volumetric titrations. Very little work has been performed on coulometric titrations in nonaqueous solvents. STREULI *et al.*[5-6] and MATHERS AND ANSON[7] have titrated bases while CRISLER AND CONLAN[8], STREULI *et al.*[9], and GAINER[10] have titrated acids in nonaqueous solvents.

CRITCHFIELD AND JOHNSON[11] reported that weak bases in strong aqueous solutions of neutral salts can be titrated in much the same manner as in nonaqueous solvents. While bases with ionization constants less than 10^{-9} are too weak to be titrated in water, titrations in concentrated salt solutions are applicable to bases with ionization constants as low as 10^{-12}. This is apparently due to an increase in the activity of the hydrogen ion in these solutions. This is supported by further work[12] in which comparative pH and acidity function (H_0) data indicate that the decrease in pH of acids by neutral salts is accompanied by corresponding increase in acidity of the solution. Salts with the highest positive heat of solution produce the greatest change in pH. KILPATRICK *et al.*[13] have investigated the dissociation constants of benzoic acid, acetic acid and glycolic acid in salt solutions while ROSENTHAL AND DWYER[14] have considered the factors which affect the efficiency of the salt effect. PAUL AND LONG[15] have reviewed H_0 and related indicator acidity functions, including the effect of neutral salts on H_0.

The present paper reports a study of coulometric acidimetric titrations in concentrated salt solutions. Aqueous and nonaqueous solvents were employed. Enhancement of end-point breaks in nonaqueous solvents was obtained and micro-equivalent quantities of bases with K_1 values as small as $4 \cdot 10^{-12}$ were titrated. An added advantage of coulometric titrations is that the concentrated salt solutions are not diluted by addition of titrant. Methods of end-point detection were studied.

EXPERIMENTAL

Reagent-grade chemicals were used when available. Ethylenediamine was distilled before use. All base solutions were standardized volumetrically. Coulometric titrations were performed with a Chris-Feld Microcoulometric Quantalyzer, with a

generating current of 9.65 mA. The titration cell contained 1-cm² platinum foil generating electrodes. The cathode was separated from the test solution via a salt bridge (3% agar-agar, 1 M potassium nitrate) which was placed in an aqueous solution of 1 M potassium nitrate. The pH indicating electrodes were a glass-SCE pair unless otherwise stated. pH measurements were made with a Corning pH meter, Model 7. Solutions were deaerated with nitrogen before titration. The nitrogen was scrubbed by bubbling through a train consisting of 0.1 N hydrochloric acid, 0.1 N potassium hydroxide, and the solvent used for the titration. In many cases, electrode response was sluggish, and several minutes were required after each addition of titrant before stable readings were reached. Usually readings were taken 1–3 min after addition of titrant. For titrations in nonaqueous solvents, the solvent contained 1% of water as a source of hydrogen ions; anhydrous salts were used in these solvents.

RESULTS AND DISCUSSION

The use of a fiber junction SCE did not appear to introduce appreciable chloride impurities for the duration of the titrations. Concentrated solutions of lithium iodide and other halide salts have been shown to provide large enhancement of acidity in volumetric titrations[12,14,15]. Unfortunately, these cannot be used for coulometric titrations because the halide ions are oxidized at the anode in preference to the oxidation of water. Attempts were made to add an electrolyte which would react with the product ($e.g.$, I_3^-) to produce an equivalent amount of hydrogen ion. An example was addition of a dilute solution of sulfite, approximately equivalent to the amount of sample to be titrated:

$$H_2O + I_3^- + SO_3^{2-} \rightarrow 3\ I^- + SO_4^{2-} + 2\ H^+$$
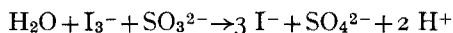
However, the buffering capacity of the sulfite/bisulfite system was sufficiently great to prevent good end-point breaks. Several other systems were also considered but they all exhibited buffering capacities.

It has been demonstrated that the salts of sulfuric acid actually inhibit the titration break of aniline. The salts must, therefore, be derived[12] from an acid having an ionization constant greater than 10^{-2}. For the above reasons, concentrated solutions of perchlorate salts were chosen as possible electrolytes in coulometric titrations. The pH of equal concentrations of hydrochloric acid ($ca.$ 0.01 N) in water and in the presence of the salts was measured and the results were as follows: H_2O, 2.16; 3 M $LiClO_4$, 0.80; 8 M $NaClO_4$, −0.5. The volumetric titration of 0.1 meq of ammonia in 6 M sodium perchlorate demonstrated an enhancement in the end-point break of about 1.5 pH units. Volumetric titrations of 0.1 meq of aniline in 40 ml of solution with 0.02 N hydrochloric acid showed a pH change at the end-point of 0.5, 1.4, and 1.5 in 3 M lithium perchlorate, 8 M sodium iodide, and 8 M sodium perchlorate, respectively. Thus, sodium perchlorate compares favorably with sodium iodide for the enhancement of acidity. Readings in aqueous lithium perchlorate solutions were unstable and this salt could not be used satisfactorily for titrations in water.

Coulometric titrations of different bases are summarized in Table I. In all coulometric titrations, the solution was pretitrated by adding the base to be titrated and then titrating to an end-point break. The sample was then added. Aniline under-

went a color change in the vicinity of the end-point, turning from colorless to pink or violet. The color remained upon addition of more aniline to make the solution alkaline. Apparently, some of the aniline was oxidized directly at the generating anode. Results were, however, nearly stoichiometric, and the direct electrolysis did not detract significantly from the accuracy. This color change near the end-point was similar to a color change observed for histidine when it was oxidized with coulometrically generated hypobromite[16]. Only one end-point break was obtained with ethylene-diamine, corresponding to titration of both amine groups.

TABLE I

COULOMETRIC TITRATIONS OF BASES IN AQUEOUS SALT SOLUTIONS

Electrolyte	Base	μeq taken	μeq found
6 M NaClO$_4$	NaOH	16.23	16.15
	NH$_3$	68.2	69.0
		68.2	69.2
		12.35	12.50
8 M NaClO$_4$	Aniline	62.4	61.4
	Ethylenediamine	38.2	38.4
		38.2	38.4

It was considered probable that addition of concentrated salts to nonaqueous solvents would further enhance the end-point breaks in these solvents. An initial titration of aniline in acetonitrile containing 0.1 M lithium perchlorate was attempted, but results were very low. Lithium perchlorate was the salt chosen for nonaqueous studies because of its higher solubility. It has a high solubility in acetone and this neutral solvent was investigated for coulometric titrations. Volumetric titration of 0.1 meq of aniline in 40 ml of acetone containing 3 M lithium perchlorate as above for aqueous solutions exhibited a pH change of 2.7 at the end-point compared to 1.4 in 8 M aqueous sodium perchlorate. Coulometric titrations of bases in this system are summarized in Table II. Results tended to be somewhat high, particularly for *m*-

TABLE II

COULOMETRIC TITRATIONS OF BASES IN ACETONE CONTAINING 3 M LITHIUM PERCHLORATE AND 1% WATER

Base	μeq taken	μeq found
NaOH	16.23	16.50
Aniline	20.8	20.8
Ethylenediamine	38.2	38.9
m-Nitroaniline	20.1	23.5
		23.5

nitroaniline. This would indicate that generating efficiency is about 99%, and in the case of *m*-nitroaniline, there may have been some direct electrolysis at the anode which was not stoichiometric with respect to consuming hydrogen ions. Aniline did not undergo the color change found in aqueous solution. No end-point break could be obtained for this base in acetone containing only 0.1 M lithium perchlorate. Ethylene-

diamine again exhibited one end-point break, equivalent to the titration of two amine groups. The ionization constant of m-nitroaniline is only $4 \cdot 10^{-12}$, which demonstrates the utility of the present method for titrating microequivalent quantities of weak bases. An added advantage of the combined organic solvent–concentrated salt system is that organic bases, such as aniline, have a higher solubility than in the aqueous system.

Because of the sluggishness of the glass electrode response in some of the solutions, especially the nonaqueous ones, other means of end-point detection were investigated. SVOBODA[17] has employed constant-current potentiometry with two platinum electrodes for nonaqueous titrations of organic bases. A peak-shaped titration curve is obtained, if an acidic (noncarboxylic) solvent is used. SVOBODA used a 1:1 mixture of m-cresol and acetonitrile. In the present study, no end-point break could be found in the coulometric titration of microequivalent amounts of bases (sodium hydroxide and aniline) in either the above mixture or in acetone (each containing 3 M lithium perchlorate). DOLEZAL AND STULIK[18] have used platinum and carbon indicating electrodes for potentiometric acid–base titrations in aqueous solutions. The equilibrium potential was given by the redox system consisting of the cathodic reduction of dissolved oxygen and the anodic oxidation of water, which is dependent on the pH. Adsorbable ions (*e.g.*, chloride) decreased the potential break and oxidizing anions (permanganate, chromate, bromate) increased the break. A platinum indicating electrode was investigated for use in the present studies. Coulometric titrations were tested for sodium hydroxide in 0.1 M potassium sulfate, sodium hydroxide in acetone containing 3 M lithium perchlorate, and aniline in acetone containing 3 M lithium perchlorate. Titration curves for the first case were drawn out, even in the presence of added potassium permanganate. In the other cases, results were high; deaeration gave improved stability and larger potential breaks, but results were still significantly high. STREULI *et al.*[19] have reported that poor results were obtained when a platinum indicating electrode was substituted for a glass electrode in the coulometric titration of organic acids in acetone.

SUMMARY

Weak bases were titrated with coulometrically generated hydrogen ions in aqueous 8 M sodium perchlorate solutions. Bases with ionization constants as low as $4 \cdot 10^{-12}$ were titrated in acetone containing 3 M lithium perchlorate. Enhancement of end-point breaks was obtained in both solvents in the presence of the concentrated salts. Methods of end-point detection were investigated.

RÉSUMÉ

On décrit une méthode pour le titrage de bases faibles par les ions hydrogène coulométriquement formés, en solutions aqueuses perchlorate de sodium 8 M. Les bases à constante d'ionisation jusqu'à $4 \cdot 10^{-12}$ sont titrées dans l'acétone renfermant perchlorate de lithium 3 M. Les points finals sont mieux marqués, dans les deux

solvants, en présence de sels concentrés. On examine des méthodes de détection du point final.

ZUSAMMENFASSUNG

Schwache Basen wurden mit coulometrisch erzeugten Wasserstoffionen in wässrigen 8 M Natriumperchloratlösungen titriert. Basen mit Ionisationskonstanten von weniger als $4 \cdot 10^{-12}$ wurden in acetonhaltigem 3 M Lithiumperchlorat titriert. Eine Verstärkung des Endpunktes wurde in beiden Lösungsmitteln in Gegenwart von konzentrierten Salzen erhalten. Methoden zur Endpunktsanzeige wurden untersucht.

REFERENCES

1 J. K. TAYLOR AND S. W. SMITH, *J. Res. Natl. Bur. Std.*, 63A (1959) 153.
2 L. SZEBELLEDY AND Z. SOMOGYI, *Z. Anal. Chem.*, 112 (1935) 395.
3 J. J. LINGANE AND L. A. SMALL, *Anal. Chem.*, 21 (1949) 1119.
4 E. L. ECKFELDT AND E. W. SHAFFER, JR., *Anal. Chem.*, 37 (1965) 1534.
5 C. A. STREULI, *Anal. Chem.*, 29 (1956) 139.
6 R. B. HANSELMAN AND C. A. STREULI, *Anal. Chem.*, 29 (1956) 916.
7 W. A. MATHERS, JR. AND F. C. ANSON, *Anal. Chem.*, 33 (1961) 132, 1634.
8 R. O. CRISLER AND R. D. CONLAN, *J. Am. Oil Chemists' Soc.*, 39 (1962) 470.
9 C. A. STREULI, J. J. CINCOTTA, D. L. MARICLE AND K. K. MEAD, *Anal. Chem.*, 36 (1964) 1371.
10 F. G. GAINER, *U. S. At. Energy Comm.*, 1967, IS-T-159.
11 F. E. CRITCHFIELD AND J. B. JOHNSON, *Anal. Chem.*, 30 (1958) 1247.
12 F. E. CRITCHFIELD AND J. B. JOHNSON, *Anal. Chem.*, 31 (1959) 570.
13 M. KILPATRICK, *J. Am. Chem. Soc.*, 75 (1953) 584, 587; M. KILPATRICK AND R. D. EANES, 75 (1953) 586.
14 D. ROSENTHAL AND J. S. DWYER, *Anal. Chem.*, 35 (1963) 161.
15 M. A. PAUL AND F. A. LONG, *Chem. Rev.*, 57 (1957) 1.
16 G. D. CHRISTIAN, unpublished work.
17 G. R. SVOBODA, *Anal. Chem.*, 33 (1968) 1638.
18 J. DOLEZAL AND K. STULIK, *J. Electroanal. Chem. and Interfacial Electrochem.*, 17 (1968) 87.

AN AUTOMATED ION-EXCHANGE METHOD FOR THE DETERMINATION OF SODIUM MONOFLUOROPHOSPHATE IN DENTIFRICES

C. BENZ AND R. M. KELLEY

Colgate–Palmolive Research Center, Piscataway, N.J. 08854 (U.S.A.)

(Received December 2nd, 1968)

The usual method for the determination of fluoride in dental cream involves ashing of the sample with calcium oxide followed by a steam distillation procedure[1]. For dentifrices formulated with either tin(II) fluoride or sodium fluoride as the sole fluorine donor, the total fluoride level obtained may be factored to either entity.

Incorporation of sodium monofluorophosphate (Na_2PO_3F) in a dentifrice formulation has been shown to result in a significant reduction in dental caries when the dentifrice was used in a clinical test[2]. In addition, sodium monofluorophosphate has been shown to result in caries reduction in animal experiments[3,4] and with topical application in children[5].

In the development of a dental cream formulated with 0.76% sodium mono-fluorophosphate as the sole fluorine donor, the need arose for an improved analytical method for the specific determination of monofluorophosphate in order to monitor its stability under various conditions.

In the early development of an approach, a method was evolved which depended on the quantitative precipitation of silver monofluorophosphate under controlled conditions followed by a distillation of the fluoride in the usual manner[6,7]. Investigations were initiated for a more convenient method, particularly for handling a large volume of samples. This resulted in the development of the AutoAnalyzer procedure described below.

EXPERIMENTAL

Reagents

Deionized water was used for all preparations.

Sulfuric acid 6 N. To a 2-l volumetric flask containing about 1,500 ml of water add, very carefully, 333 ml of concentrated C.P. sulfuric acid. Cool to room temperature, make to volume with water and mix well.

Ammonium molybdate. In a 2-l volumetric flask containing 1,500 ml of water dissolve 30 g of $(NH_4)_6Mo_7O_{24} \cdot 4H_2O$ and add 200 ml of concentrated C.P. sulfuric acid. Cool to room temperature, make to volume with water and mix well.

Hydrazine sulfate. In a 2-l volumetric flask containing water, dissolve 2 g of hydrazine sulfate. Make up to volume with water and mix well.

Stock buffer solution (pH 5.0). Weigh 70.0 g of potassium acetate and 18.0 g

of glacial acetic acid and dilute to 1 l with water. Adjust the pH to 5.0 with 2%
acetic acid or potassium hydroxide as necessary.

Potassium chloride (0.15 M). Weigh 22.5 g of potassium chloride, add 50 ml
of stock buffer solution and dilute to 2 l with water.

Potassium chloride (0.25 M). Weigh 37.5 g of potassium chloride, add 50 ml
of stock buffer solution and dilute to 2 l with water.

Standard P₂O₅ solutions

Standard P_2O_5 solutions

(a) P_2O_5 *stock solution (1000 mg P_2O_5/1000 ml)*. Dry some potassium dihydrogen
phosphate (Baker's Analyzed Reagent, Crystal, 99.0% purity minimum) in an oven
at 105° for 1–2 h. Accurately weigh 1.9180 g (if 100.0% pure) to the nearest 0.1 mg
and carefully transfer it to a 1-l volumetric flask. Dilute to volume with water after
the salt is dissolved, and mix well.

(b) 75.00 mg P_2O_5/500 ml—Standard. Accurately pipet 75.00 ml of the stock
solution into a 500-ml volumetric flask. Dilute to volume with water and mix well.

Ion-exchange resin

Ion-exchange resin

Dowex 1-X8, 100–200 mesh. Soak the resin in 2.0 N hydrochloric acid over-
night. Decant, wash a few times with water and 0.25 M potassium chloride, and
store in water.

Apparatus

Apparatus

The analytical system consists of the following modules:

Ion-exchange column, 8 mm in diam., 15 cm resin bed, 12–13 cm head space.
The resin is equilibrated by washing with 20 ml of 0.25 M potassium chloride before
the first analysis.

Technicon AutoAnalyzer, consisting of: (a) Proportioning pump. (b) Heating
bath 95°±0 1° with one 40-ft., 2-mm in diam. glass coil for hydrolysis. (c) Dialyzer at
38°±0 1° with standard membrane. (d) Heating bath with one 40-ft., 2-mm in diam.
glass coil maintained at 95°±0.1° for color development. (e) Colorimeter with 15-mm
tubular flow cell and equipped with 660 nm filters. (f) Recorder with absorbance
paper, chart speed 2.54 cm/200 sec.

Procedure

Procedure

The Technicon AutoAnalyzer flow system and the ion-exchange arrangement
are shown in Fig. 1. A representative sample of toothpaste containing 6–7 mg of
fluoride is slurried in water with a magnetic stirrer. Quantitatively transfer the
sample to a 100-ml volumetric flask, dilute to volume and mix well. Centrifuge a
portion of the sample in screw-cap tubes. During the centrifugation period, introduce
a 5.0-ml aliquot of the 75.00-mg P_2O_5 standard into the column, wash down with
2–3 ml of 0.25 M potassium chloride and elute from the resin with a total of about
15 ml of the same solution. When this first operation is finished, add to the column
a 5.0-ml aliquot of the clear supernatant liquid from the centrifuged sample. At the
same time start pumping the 0.25 M potassium chloride solution and when the
liquid level in the column is about 2 cm above the resin, close reservoir A. The
volume of 0.15 M potassium chloride in reservoir A depends on the instrument and
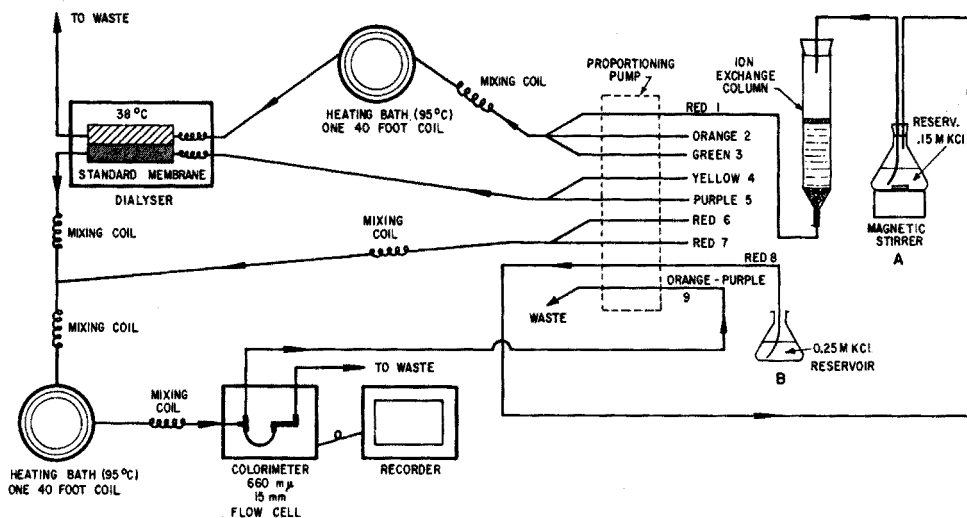the ion-exchange resin packing and may vary from 60 ml to 100 ml; it is adjusted

Fig. 1. Flow diagram for the automated determination of monofluorophosphate. Red 1, sample; orange 2, air; green 3, 6 N H_2SO_4; yellow 4, air; purple 5, distilled water; red 6, hydrazine sulfate; red 7, NH_4 molybdate; red 8, eluant; orange-purple 9, de-bubble.

according to the chromatographic separation obtained between monofluorophosphate and pyrophosphate. Wash the sample down the column with 2–3 ml of 0.15 M potassium chloride and, after the addition of another 5 ml of this solution, connect the top of the column to reservoir A. The addition of 0.25 M chloride solution is made at the same rate as the solution from reservoir A is withdrawn, permitting a uniform increase in salt concentration. The monofluorophosphate is eluted from the resin and separated from organic interferences and other phosphate species by the automatic gradient elution system; it is introduced into the flow system, mixed with sulfuric acid and, after hydrolysis through the first heated glass coil, it is dialyzed through the standard membrane. The dialyzable portion is picked up by water and added to the mixed hydrazine and molybdate reagents. The color reaction is developed in the second glass coil of the heating bath, and the sample stream is continuously fed to the colorimeter flow cell. The absorbance is measured at 660 nm and monitored on the strip chart of the recorder. When the apex of the MFP peak appears on the chart, the column is disconnected and the stand-by column connected to the sample line of the manifold. A second sample, prepared at the proper time, can be analyzed following the procedure described above and beginning with addition of the 75 mg of P_2O_5 standard. The first column is regenerated by washing with 10 ml of 2 N hydrochloric acid followed by 10 ml of 0.25 M potassium chloride.

Measurement of the area of individual peaks has been described by LUNDGREN AND LOEB[8]. The concentration of monofluorophosphate as fluoride is calculated as follows:

$$\frac{B \times 0.75 \times 2.03 \times 20 \times 100}{A \times S \times 7.58} = \% \text{ sodium monofluorophosphate as F}$$

where: A = area of standard in absorbance/mm; B = area of sample in absorbance/mm; S = weight of original sample in mg (Step 3); 0.75 = mg P_2O_5 in aliquot of standard

P_2O_5; 2.03 = factor to convert P_2O_5 to monofluorophosphate; 20 = aliquoting factor; 7.58 = factor to convert sodium monofluorophosphate to fluoride.

RESULTS AND DISCUSSION

The feasibility of the separation of monofluorophosphate from other phosphate entities present in dental cream by ion exchange was demonstrated in earlier work[9,10].

These approaches involved separation of the phosphate species by gradient elution column chromatography. The eluate fractions were analyzed for phosphorus by standard colorimetric methods. Because of the fact that these approaches were time-consuming, consideration was given to the use of an AutoAnalyzer for the automation of the method.

In order to determine the optimum conditions for operation, complete chromatograms were obtained with the following samples:

(a) sodium monofluorophosphate, commercial grade;

(b) a dentifrice formulated with 0.76% commercial sodium monofluorophosphate;

(c) a dentifrice of the same formulation as in (b) but containing no sodium monofluorophosphate; and

(d) a detergent formulated with commercial sodium tripolyphosphate. The individual peaks obtained in each case and their identifications are shown in Table I.

TABLE I

SEPARATION OF PHOSPHATES FROM DENTAL CREAM

Sample ＼ Peak	Unknown	Ortho-phosphate	Mono-fluoro-phosphate	Pyro-phosphate	Tripoly-phosphate
Sodium monofluorophosphate	Absent	Present	Present	Present	Present
Dental cream	Present	Present	Present	Present	Present
Dental cream blank	Present	Present	Absent	Present	Present
Detergent	Absent	Present	Absent	Present	Present

In performing these experiments buffered water was used (in reservoir A) and the column was subjected to a gradient elution increase with 0.5 M potassium chloride in reservoir B.

Application of the formula: $C_t = C_1 (1 - e^{-rt/v})$

(where C_t = concentration at time t; C_1 = concentration of the solution being fed (reservoir B); r = pumping rate in ml/min; v = volume of liquid in the reservoir A; t = time in min)

yielded the following eluant concentrations for the main species in the system:

Orthophosphate: 0.085 M potassium chloride

Monofluorophosphate: 0.194 M potassium chloride

Pyrophosphate: 0.218 M potassium chloride

This experiment clearly indicated that there were no interferences with the method and that a very slow elution system would have to be used so as to allow a clear separation between the monofluorophosphate and pyrophosphate peaks. Further experimentation resulted in the selection and adoption of a 15–17-cm, 8-mm in diam.

resin bed column, 75–85 ml of 0.15 M potassium chloride in reservoir A and 0.25 M potassium chloride in reservoir B (see Fig. 1).

Typical chromatograms for application of the method to a dentifrice formulated with 0.76% sodium monofluorophosphate and to the commercial sodium monofluorophosphate alone are shown in Figs. 2 and 3. The commercial monofluorophosphate, although consisting of a high level of the monofluorophosphate specie, does contain small amounts of ortho- and pyrophosphates. In addition, small amounts of tripoly- and trimetaphosphates are usually found.
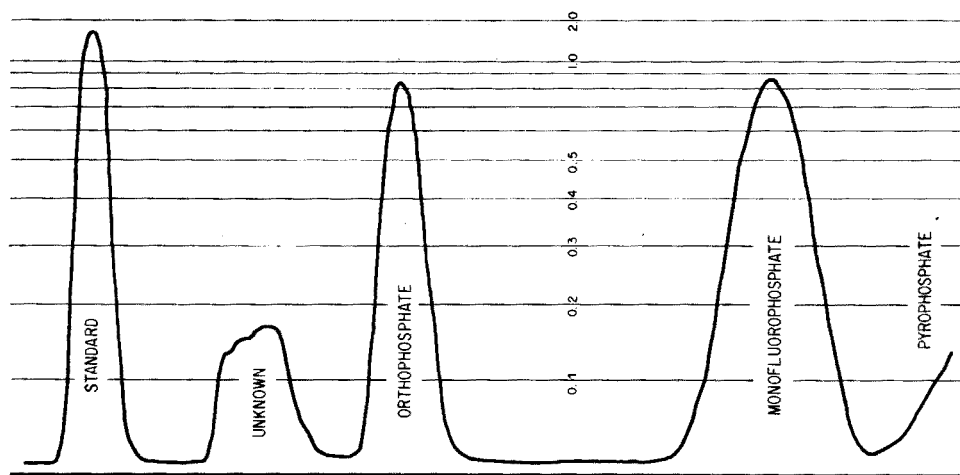
Fig. 2. Application of method to dentifrice.
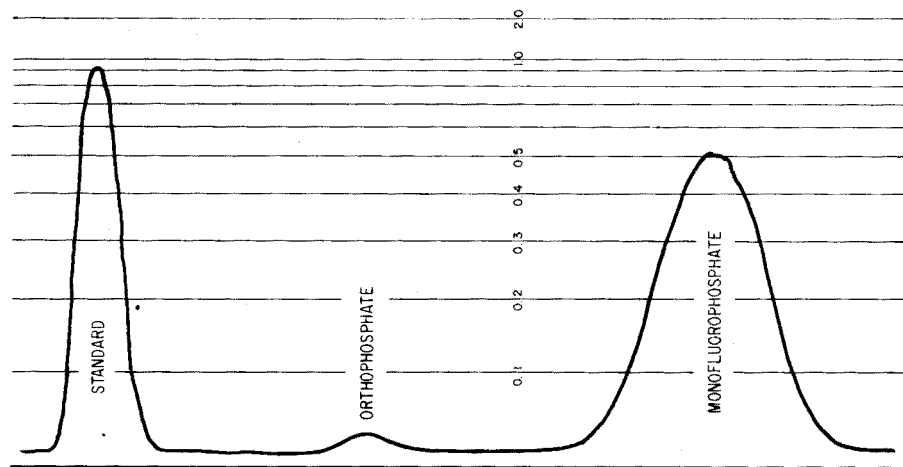
Fig. 3. Application of method to commercial sodium monofluorophosphate.

The basic approach of measurement and calculations of results differs considerably from that used in calculating phosphate species in previously published work[8,11]. In the individual phosphates analysis, the ratio of peak areas is calculated on a relative basis whereas for the monofluorophosphate determination the calculated peak area

is related, on an absolute basis, to the peak area of a known concentration of ortho-phosphate which is eluted through the column just ahead of the sample. The advantage of this "external standard" practice is reflected in both the accuracy and precision of the method but it also slows down the analysis time considerably. Approximately 20% of the 70 min required for the complete analysis are taken up by the introduction of the standard ahead of the sample.

Attempts to shorten the analysis time have been successful only to the detri-ment of the precision of the method. Speeding up the system by means of a reduction in sample weight and/or column size results in considerable sharpening of the peaks. However, since measurements of absolute areas are involved, very small differences in measurement represent large errors in calculations. For this reason, some speed was sacrificed in order to obtain a more accurate and precise method.

A large number of samples were analyzed by both the proposed method and the previously developed procedure based upon silver precipitation and distillation. Results calculated as fluoride equivalent to monofluorophosphate which are shown in Table II were analyzed by the paired differences method. Calculation of the

TABLE II

COMPARISON OF AUTOMATED AND PRECIPITATION METHODS

Sample number	% Sodium monofluorophosphate as F		Sample number	% Sodium monofluorophosphate as F	
	AutoAnalyzer	Precipitation method		AutoAnalyzer	Precipitation method
1	0.079	0.080	17	0.090	0.095
2	0.094	0.088	18	0.087	0.090
3	0.079	0.082	19	0.090	0.094
4	0.082	0.080	20	0.092	0.095
5	0.077	0.072	21	0.074	0.080
6	0.071	0.075	22	0.088	0.084
7	0.073	0.076	23	0.095	0.088
8	0.091	0.096	24	0.080	0.076
9	0.094	0.100	25	0.090	0.084
10	0.073	0.078	26	0.088	0.082
11	0.073	0.079	27	0.085	0.091
12	0.090	0.090	28	0.079	0.083
13	0.094	0.102	29	0.078	0.079
14	0.096	0.094			
15	0.095	0.098			
16	0.099	0.098			

TABLE III

PRECISION ANALYSIS OF METHOD

Dentifrice sample no.	No. of determinations	Mean % F[a]	$s^{b} \cdot 10^{-3}$	Coeff. of variation
1	8	0.095	2.6	2.7
2	6	0.089	2.7	3.0
3	12	0.093	2.8	3.0
4	12	0.090	3.1	3.4
5	14	0.094	3.5	3.7

[a] Equivalent to sodium monofluorophosphate.
[b] Standard deviation.

paired differences yielded a "Student" t test of 0.638, less than the table value of t_{025} (29 D.F) $= 2.045$. There is therefore no significant difference between the two methods at the 95% confidence level.

The precision of the method was tested by performing replicate analyses of five different dentifrices. The data (Table III) were subjected to statistical analysis and the calculated coefficient of variation was found to fall within the limits of 2.7 to 3.7 indicating the procedure to be acceptable for routine analysis.

In addition, the precision of the method was tested by two analysts who followed the described procedure independently. The results (Table IV) were subjected to an analysis of variance (ANOVA) and no significant difference between results obtained by the two analysts, on different days, was observed.

TABLE IV

PRECISION OF METHOD BETWEEN ANALYSTS

Analyst	No. of determinations	Mean % F[a]	Standard deviation $\cdot 10^{-3}$
A	6	0.090	4.3
B	6	0.091	1.7

[a] Equivalent to sodium monofluorophosphate.

TABLE V

ANALYSIS OF COMMERCIAL SODIUM MONOFLUOROPHOSPHATE

% F[a] (proposed method)	% F[a] (silver method)
12.3	12.4
12.4	

[a] Equivalent to Na_2PO_3F.

The method was also checked for the analysis of commercial sodium monofluorophosphate (Table V). The results obtained were within specifications and checked values obtained by the silver precipitation method. The theoretical fluoride content of sodium monofluorophosphate is 13.20% indicating that the above commercial sample is of 93.1% purity. This is typical of commercial samples, the balance consisting of other phosphates, plus residual sodium fluoride.

SUMMARY

Sodium monofluorophosphate can be accurately analyzed in dental cream by an AutoAnalyzer method. The monofluorophosphate is separated from other phosphate species by gradient elution ion-exchange chromatography. The column effluent is fed to an AutoAnalyzer unit which continuously hydrolyzes the phosphates to orthophosphate and develops a color (molybdenum blue) proportional to the phosphate level. The method is useful for the analysis of large numbers of samples.

RÉSUMÉ

Le monofluorophosphate de sodium dans les dentifrices peut être analysé avec précision et reproductibilité par la méthode décrite utilisant l'AutoAnalyzer. Le monofluorophosphate est separé des autres phosphates par chromatographie sur résine échangeuse d'ions avec l'aide d'un système d'élution gradient. L'effluent de la colonne est introduit dans un AutoAnalyzer qui hydrolyse les phosphates en ortho-phosphate, puis développe une couleur (le bleu de molybdène) qui est proportionnelle à la concentration en phosphate. La méthode a été prouvé efficace pour l'analyse d'un grand nombre d'échantillons.

ZUSAMMENFASSUNG

Natriummonofluorophosphat kann mit einem Autoanalyzer in Zahnpasta genau analysiert werden. Das Monofluorophosphat wird von anderen Phosphaten durch Ionenaustauscherchromatographie abgetrennt. Das Eluat wird in einen Autoanalyzer gegeben, welcher es kontinuierlich zu Orthophosphat hydrolysiert und eine Farbe (Molybdänblau) entwickelt, welche proportional dem Phosphatgehalt ist. Die Methode eignet sich für die Analyse einer grossen Zahl von Proben.

REFERENCES

1 H. WILLARD AND O. WINTER, *Ind. Eng. Chem., Anal. Ed.*, 5 (1933) 7.
2 S. B. FINN AND H. C. JAMISON, *J. Dent. Child.*, 30 (1963) 17.
3 K. L. SHOURIE, J. W. HEIN AND H. C. HODGE, *J. Dental Res.*, 29 (1950) 529.
4 I. ZIPKIN AND F. J. McCLURE, *Am. Public Health Report, Washington, D.C.*, 66 (1951) 1623.
5 R. R. HAWES, S. SANNES AND F. BRUDEVOLD, *J. Dental Res.*, 33 (1954) 661.
6 L. V. DEVONSHIRE, *Ph. D. Thesis*, University of Oklahoma, 1954.
7 J. C. MOORE AND R. M. KELLEY, unpublished report, Colgate–Palmolive Co., 1963.
8 D. P. LUNDGREN AND N. P. LOEB, *Anal. Chem.*, 33 (1961) 366.
9 B. ROTOLO, unpublished report, Colgate–Palmolive Co., 1963.
10 A. KENT, D. LEFFERTS AND S. BABULAK, unpublished report, Colgate–Palmolive Co., 1961.
11 C. BENZ AND L. M. PAIXAO, *Technicon Symposia*, 1 (1967).

L'EXTRACTION DES LANTHANIDES ET DES ACTINIDES PAR LES OXYDES D'ALKYLPHOSPHINE

TOME IV. L'EXTRACTION DES CATIONS TRIVALENTS PAR LES OXYDES DE TRI-*n*-BUTYLPHOSPHINE ET DE TRI-*n*-OCTYLPHOSPHINE*

J. GOFFART** ET G. DUYCKAERTS

Laboratoire de Chimie Analytique et Nucléaire, Université de Liège, Sart Tilman (Belgique)

(Reçu le 10 mars, 1969)

L'extraction des lanthanides et des actinides trivalents par le phosphate de tri-*n*-butyle, $(C_4H_9O)_3PO$, a fait l'objet d'un nombre considérable de publications: néanmoins, tous les résultats expérimentaux n'ont pu être interprétés. Certaines réactions responsables du passage des cations en phase organique sont encore ignorées.

Dans ces conditions, il nous a semblé que, dans le cadre de l'étude des mécanismes fondamentaux de l'extraction liquide–liquide, les phénomènes seraient peut-être plus simples avec les oxydes d'alkylphosphine (R_3PO) qui ne possèdent pas de fonction ester. A cet effet, nous exposons dans cette publication les résultats des travaux que nous avons effectués avec les oxydes de tri-*n*-butylphosphine, $(C_4H_9)_3PO$ ou TBPO, et de tri-*n*-octylphosphine, $(C_8H_{17})_3PO$ ou TOPO.

Dans une première série de publications[1-4], nous avons exposé nos résultats concernant les complexes formés, lors de l'extraction, entre quelques composés organophosphorés neutres, d'une part, et l'acide nitrique[1-3] et/ou l'eau[4], d'autre part. La connaissance de ces réactions est indispensable à l'interprétation quantitative de l'extraction des métaux.

PARTIE EXPÉRIMENTALE

Réactifs

La synthèse et la purification des composés organophosphorés utilisés dans ce travail sont décrites dans la littérature[1,2].

Les réactifs employés sont tous de qualité "pour analyse". Le benzène a été recristallisé. La fraction du *n*-octane distillant entre 125 et 126° a été utilisée. La pureté des radioisotopes[4] a été vérifiée, suivant les cas, par mesure de la décroissance ou par spectrométrie-α ou -γ selon la nature du rayonnement émis.

Mode opératoire

Toutes les expériences de distribution ont été effectuées dans des tubes à extraction thermostatisés à 25°.

Bien qu'une agitation de 3 minutes soit suffisante pour atteindre l'équilibre de distribution, la durée d'équilibration a été la plupart du temps plus longue.

La séparation totale des deux phases est obtenue par centrifugation, puis trois parties aliquotes de chacune des phases sont prélevées pour la mesure de l'activité. Dans le cas des émetteurs-γ, les échantillons sont placés dans des tubes calibrés et l'activité est mesurée au moyen d'un cristal scintillant à puits.

Pour les émetteurs-β, les prélèvements sont placés sur des coupelles concaves; le liquide est évaporé sous lampe infrarouge et l'activité du résidu est mesurée au moyen d'un tube Geiger.

La mesure de l'activité, dans les deux phases, en ^{244}Cm et en ^{250,252}Cf est effectuée soit au moyen d'un compteur à flux gazeux, soit par scintillation liquide[5,6]. Cette dernière méthode a été employée notamment dans les expériences d'extraction effectuées en présence de nitrate sodique.

Quelques complexes solides formés entre des nitrates de lanthanide et l'oxyde de triméthylphosphine, $(CH_3)_3PO$ ou TMPO, ont été préparés par la méthode suivante: une solution alcoolique de nitrate de lanthanide est versée dans un large excès de TMPO. La solution est concentrée à température ambiante par balayage de la surface du liquide au moyen d'un courant d'azote. Le précipité formé est séparé, puis trituré avec du benzène pour dissoudre un éventuel excès de TMPO. Le complexe est ensuite redissous dans du méthanol anhydre et reprécipité par évaporation lente du solvant en atmosphère sèche. La teneur en phosphore du précipité est déterminée par gravimétrie[7] ou par colorimétrie[8]. La fonction PO a été titrée par la méthode de Wimer[9] légèrement modifiée[4]. La teneur en métal a été déterminée par titrage compleximétrique[10].

RÉSULTATS EXPÉRIMENTAUX

Nous avons mesuré la distribution de ^{241}Am entre une phase aqueuse contenant

TABLEAU I

DISTRIBUTION DE ^{241}Am ENTRE TOPO ET $NaNO_3$ 2 M + HNO_3 10^{-2} N

n-Octane			Cyclohexane		Benzène	
$C_0^1(TOPO)\cdot 10^3$ (M)	D(Am)[a]	D(Cm)	$C_0^1(TOPO)\cdot 10^3$ (M)	D(Am)	$C_0^1(TOPO)\cdot 10^3$ (M)	D(Am)
1.25	0.003		2.4	0.018	2.32	0.00084
1.88	0.0065	0.004	4.8	0.144	4.65	0.039
2.50	0.020	0.012	9.6	1.1	6.97	0.118
3.75	0.079	0.044	14.5	3.5	9.29	0.26
5.00	0.18	0.095	18.9	8.3	19.6	1.9
6.25	0.29	0.154	23.2	14.9	27.9	6.1
7.50	0.44	0.34	27.8	22.3		
12.5	2.2	1.3				
25.0	4.2					
	4.4					
37.5	10.3	4.8				
50.0	12.3					
62.5	16.0					
75.0	17.5	7.3				

[a] D = coefficient de partage.

du nitrate sodique 2 M et de l'acide nitrique $10^{-2}N$ et une solution organique de concentration variable en TOPO dans les diluants suivants: le n-octane, le benzène et le cyclohexane (Tableau I). Les résultats de l'extraction du ^{244}Cm par le TOPO en solution dans le n-octane figurent également dans le Tableau I.

Nous avons également déterminé la distribution de l'yttrium, des lanthanides et de quelques actinides trivalents avec l'oxyde de tri-n-butylphosphine, TBPO, 0.1 M dans le benzène en fonction de la concentration en acide nitrique (Figs. 1 à 3).
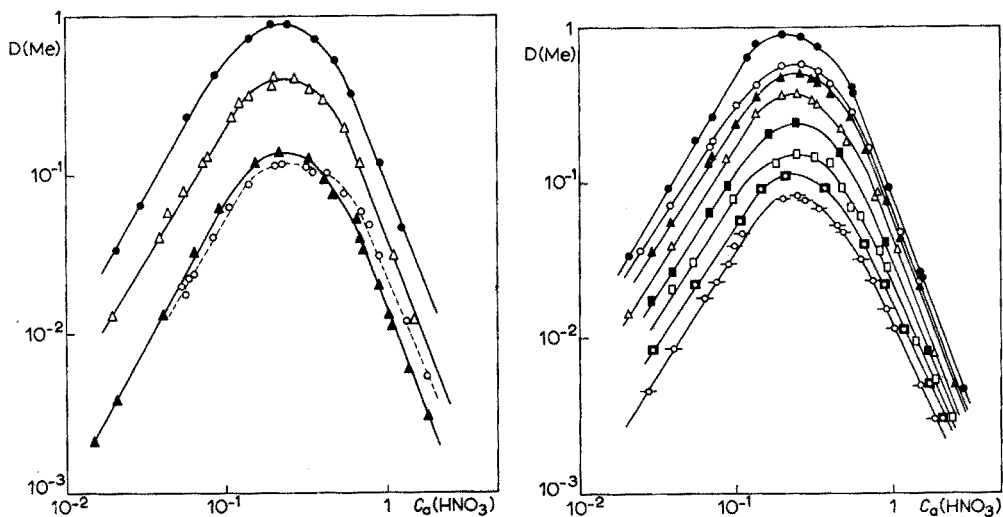
Fig. 1. Influence de la concentration en acide nitrique en phase aqueuse sur le coefficient de partage des lanthanides et de l'yttrium. C_0^t (TBPO) = 0.1 M dans le benzène. (--- ○) Yttrium; (●) prométhium; (△) cérium; (▲) lanthane.

Fig. 2. Influence de la concentration en acide nitrique en phase aqueuse sur le coefficient de partage des lanthanides. C_0^t (TBPO) = 0.1 M dans le benzène. (●) Europium; (○) gadolinium; (▲) terbium; (△) holmium; (■) erbium; (□) thulium; (◘) ytterbium; (−○−) lutétium.
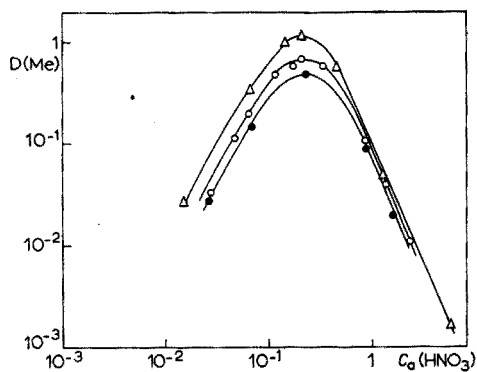
Fig. 3. Influence de la concentration en acide nitrique en phase aqueuse sur le coefficient de partage des actinides. C_0^t (TBPO) = 0.1 M dans le benzène. (○) Américium; (●) curium; (△) californium.

INTERPRÉTATION ET DISCUSSION DES RÉSULTATS

Expériences à force ionique constante

Pour connaître la stoechiométrie du ou des complexes formés dans la phase organique entre les lanthanides ou les actinides trivalents et les oxydes d'alkylphosphine, nous avons d'abord mesuré, en fonction de la concentration en TOPO dans le *n*-octane, la distribution de ^{241}Am entre cette phase organique et une phase aqueuse de force ionique pratiquement constante ($NaNO_3$ 2 M + HNO_3 $10^{-2}N$).

Le choix du système a été dicté par le fait que TOPO est très peu soluble dans la phase aqueuse[2] et BAES[11] a déterminé son activité thermodynamique dans le *n*-octane.

Dans l'hypothèse de l'équilibre de distribution suivant:

$$Me_a^{3+} + 3 NO_{3_a}^- + n \, TOPO_o \rightleftharpoons Me(NO_3)_3 \cdot n \, TOPO_o \qquad (1)$$
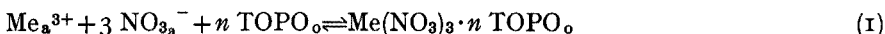
la loi d'action des masses permet d'écrire à concentration en anion pratiquement constante:

$$\frac{[Me(NO_3)_3 \cdot n \, TOPO]_o \, \gamma_2}{[Me^{3+}]_a \, [TOPO]_o^n \, \gamma_1} = K'(Me) \qquad (2)$$

γ_1 et γ_2 sont respectivement les coefficients d'activité du réactif basique libre et du complexe en phase organique; $[TOPO]_o$ représente la concentration du TOPO libre dans le *n*-octane; il nous est possible, en effet, de calculer cette concentration grâce à nos mesures antérieures de distribution d'eau[4] et d'acide nitrique[2].

Etant donné que le coefficient de partage du métal est, par définition,

$$D(Me) = \frac{[Me(NO_3)_3 \cdot n \, TOPO]_o}{[Me^{3+}]_a} \qquad (3)$$

la relation (2) peut se mettre sous la forme suivante en admettant les coefficients d'activité constants et en les faisant rentrer dans la constante d'équilibre,

$$\log K''(Me) = \log D(Me) - n \log [TOPO]_o \qquad (4)$$

Dans les Figs. 4 et 5, nous avons porté $\log D(Me)$ en fonction de $\log [TOPO]_o$ pour deux actinides trivalents. Nous observons que la pente calculée pour les concentrations en réactif basique inférieures à $6 \cdot 10^{-3}$ M est de 3.0. Dès lors, on peut proposer, pour le complexe formé, la formule: $Me(NO_3)_3 \cdot 3 \, TOPO$.

Ce résultat est semblable à celui obtenu pour les complexes entre les nitrates de lanthanide et le TBP[12] ou l'oxyde de triphénylphosphine[13].

En tenant compte de l'hydratation du réactif basique[4] et de la formation de $TOPO \cdot HNO_3$ en phase organique[2], on peut mettre l'équation (2) sous la forme suivante:

$$K''(Me) = \frac{D(Me)(1 - \mathscr{K}''(H_2O)[H_2O]_o)^3}{[C_o^1(TOPO) - C_o(HNO_3)]^3} \qquad (5)$$

où $\mathscr{K}''(H_2O)$ vaut[4] 467 M^{-1} et $[H_2O]_o = 3 \cdot 10^{-3}$ M est la concentration de saturation dans le *n*-octane en équilibre avec nitrate sodique 2 M. La différence $C_o^1(TOPO) - C_o(HNO_3)$ est tirée des résultats obtenus antérieurement[2].

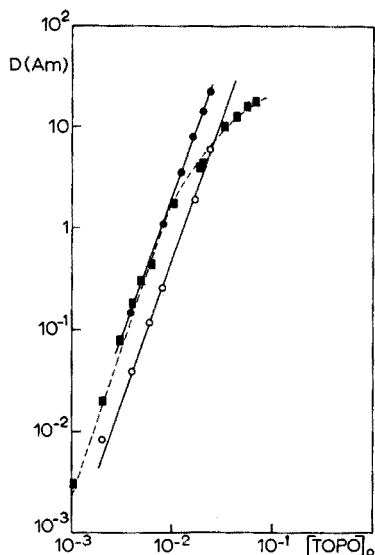Fig. 4. Détermination graphique de la structure du complexe $Am(NO_3)_3 \cdot n$ TOPO. Force ionique de la phase aqueuse: 2 M en $NaNO_3$. (o) TOPO dans le benzène; (■) TOPO dans le n-octane; (●) TOPO dans le cyclohexane.
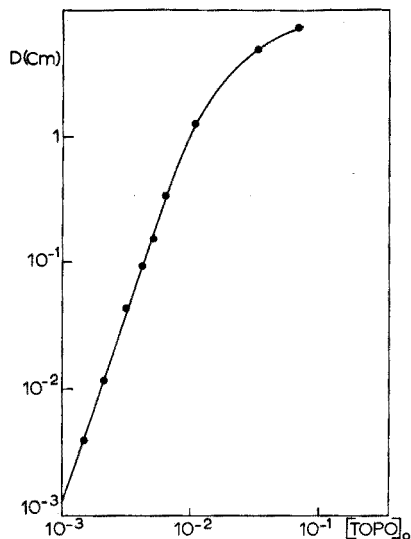
Fig. 5. Détermination graphique de la structure du complexe $Cm(NO_3)_3 \cdot n$ TOPO. Force ionique de la phase aqueuse: 2 M en $NaNO_3$. (●) TOPO dans le n-octane.

Les constantes d'équilibre obtenues dans ces conditions sont les suivantes:

$$K''(Am) = (2.9 \pm 0.5) \cdot 10^7 \ M^{-3}$$

$$K''(Cm) = (1.7 \pm 0.15) \cdot 10^7 \ M^{-3}$$

Pour les concentrations en TOPO supérieures à $6 \cdot 10^{-3} \ M$, la correction d'activité[11] que nous pouvons appliquer à la courbe correspondant au n-octane en introduisant les valeurs de γ_1 dans l'équation (2) n'est pas suffisante pour rendre compte de l'écart existant entre la droite extrapolée et les valeurs expérimentales; il faut donc admettre que d'autres réactions interviennent à partir de là.

Comme le montre la Fig. 4, on obtient également des droites dans le cas des solutions de TOPO dans le cyclohexane et dans le benzène. Le fait que les pentes ne valent pas exactement 3, mais respectivement 2.8 et 2.7 indique sans doute que le complexe a toujours une stoechiométrie 1:3, mais que le rapport des coefficients d'activité n'est pas constant dans ces deux diluants.

La stoechiométrie 1:3 est également celle qui résulte de l'analyse des complexes solides formés entre quelques nitrates de lanthanide et l'oxyde de triméthylphosphine (Tableau II).

Expériences à force ionique variable

Les Figs. 1, 2 et 3 présentent les courbes de distribution de l'yttrium, des lanthanides et de trois actinides entre le TBPO 0.1 M dans le benzène et une solution aqueuse de concentration variable en l'acide nitrique. Il est assez aisé d'interpréter l'allure générale de ces courbes de distribution; l'augmentation de $D(Me)$ lorsque la

TABLEAU II

ANALYSE DES COMPLEXES SOLIDES DE NITRATES DE LANTHANIDES AVEC L'OXYDE DE TRIMÉTHYL-PHOSPHINE

Complexes	% Me_{th}	% Me_{exp}	% P_{th}	% P_{th}	Titrage par quantité pesée (mg)	$HClO_4$ quant. trouvée exp. (mg)
$Y(NO_3)_3 \cdot 3TMPO$	16.13	15.9	16.86	16.8	24.5	24.4
				17.0[a]		
$La(NO_3)_3 \cdot 3TMPO$	23.11	23.2	15.46	15.6	30	31
$Pr(NO_3)_3 \cdot 3TMPO$	23.36	23.3	15.41	15.5	31	30.8
				15.5[a]		
$Sm(NO_3)_3 \cdot 3TMPO$	24.54	24.5	15.17	15.5	24.5	24.4
$Er(NO_3)_3 \cdot 3TMPO$	26.57	26.2	14.76	15.1	30.3	30
				14.8[a]	27	26.8

[a] Fournis par la méthode calorimétrique.

concentration en acide nitrique croît s'explique clairement sur la base de la loi d'action des masses (équation (1)); toutefois, très rapidement, nous assistons à une réaction compétitive, à savoir, la formation de TBPO·HNO₃, qui diminue la concentration en TBPO libre. Aux concentrations en acide où cette dernière réaction l'emporte, nous assistons à une diminution de $D(Me)$.

L'interprétation plus quantitative de ces courbes nous paraît difficile actuellement étant donné que la force ionique de la phase aqueuse varie avec la concentration en acide nitrique et que nous ne sommes pas à même de calculer l'activité en Me^{3+}.

Il est intéressant de signaler que contrairement à ce qui se passe avec le TBP, nous n'obtenons jamais de remontée du coefficient de partage aux concentrations élevées en l'acide nitrique, même pour des solutions de TBPO M.

La variation du coefficient de partage en fonction du nombre atomique du métal extrait, telle qu'elle se présente dans la Fig. 6 pour différentes acidités de la
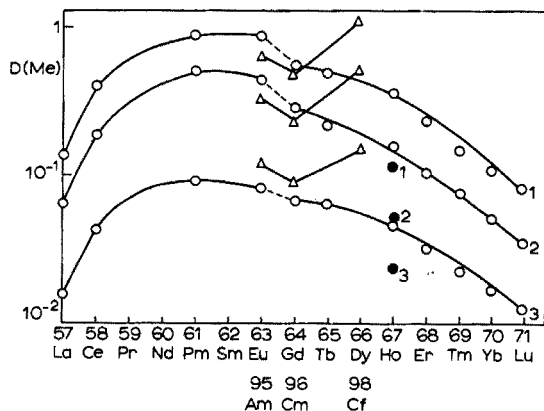
Fig. 6. Evolution du coefficient de partage de l'yttrium, des lanthanides et des actinides en fonction du nombre atomique. C_0^1 (TBPO) = 0.1 M dans le benzène. (○) Lanthanides; (△) actinides; (●) yttrium. (1) 0.25 N HNO₃; (2) 0.10 N HNO₃; (3) 1.0 N HNO₃.

phase aqueuse, mérite une attention particulière. Pourquoi cette variation en cloche plutôt qu'une évolution monotone avec Z? On peut, dans l'examen de cette question, envisager deux étapes dans l'extraction des métaux, d'abord la déshydratation des cations et, ensuite, la formation du complexe $Me(NO_3)_3 \cdot 3$ TBPO. Il semble, en effet, d'après les travaux de la littérature[12,13] que le complexe existant dans la phase organique est anhydre; les résultats que nous avons obtenus avec le TMPO (Tableau II) confirment ces conclusions.

Si l'on examine d'abord la variation d'énergie libre correspondant à la seconde étape, c'est-à-dire, la formation du complexe, on serait peut-être tenté d'admettre que ce terme varie de façon monotone avec Z; en effet, si l'on examine les spectres infrarouges des complexes solides[14] (Tableau III), on constate une variation monotone de la fréquence de vibration du groupement $P=O$ avec le nombre atomique; elle augmente régulièrement en passant du lanthane au lutécium. Cette observation concorde d'ailleurs avec celle rapportée par FERRARO[12] pour les complexes avec le TBP et par COUSINS[13] pour les mêmes complexes avec l'oxyde de triphénylphosphine. Il semble donc y avoir un affaiblissement progressif et régulier de la liaison $P=O \ldots Me$ au fur et à mesure que Z croît.

TABLEAU III

Substances étudiées	Fréquence (cm⁻¹) de la bande de vibration P=O	Δν (cm⁻¹)
TMPO	1178	—
La(NO₃)₃·3TMPO	1132	−46
Pr(NO₃)₃·3TMPO	1133	−45
Sm(NO₃)₃·3TMPO	1136	−42
Er(NO₃)₃·3TMPO	1144	−34
Y(NO₃)₃·3TMPO	1144	−34

Dans ces conditions, on est tenté d'attribuer l'allure de la courbe en cloche essentiellement à l'étape de déshydratation du cation, mais il est bien difficile, à l'heure actuelle, d'avancer des données précises sur la variation de cette énergie libre de déshydratation, d'autant plus que les ions nitrates peuvent également y jouer un certain rôle[15,16]. Il faut encore ajouter qu'il est possible qu'il y ait dans le complexe en phase organique une variation du nombre de coordination en passant du lanthane au lutécium, les ions nitrates peuvent être coordonnés à l'ion central par un ou deux oxygènes suivant la terre rare considérée. La position de l'yttrium mérite également d'être signalée: alors qu'on lui attribue, en général, des propriétés voisines de celles du holmium on observe, dans nos expériences d'extraction, un comportement beaucoup plus proche de celui de l'ytterbium ou du thulium. Cette situation varie d'ailleurs avec l'acidité[17] et tend à se rapprocher de celle correspondant à son rayon ionique cristallographique au fur et à mesure que l'acidité augmente.

RÉSUMÉ

L'extraction des lanthanides et des actinides trivalents par les oxydes d'alkyl-phosphine repose essentiellement sur l'équilibre suivant:

$$Me_a^{3+} + 3\ NO_{3_a}^- + 3\ Alk_3PO_o \rightleftharpoons Me(NO_3)_3 \cdot 3\ Alk_3PO_o$$

A force ionique constante (nitrate sodique 2 M), les constantes d'équilibre de cette réaction pour le complexe formé entre l'oxyde de tri-n-octylphosphine en solution dans le n-octane et, soit ^{241}Am, soit ^{244}Cm ont été déterminées. Elles valent respective-ment $(2.9 \pm 0.5) \cdot 10^7\ M^{-3}$ et $(1.7 \pm 0.15) \cdot 10^7\ M^{-3}$. Les courbes de distribution des lanthanides et des actinides entre l'oxyde de tri-n-butylphosphine 0.1 M dans le benzène et une solution aqueuse d'acide nitrique de concentration variable ont été déterminées et sont discutées.

SUMMARY

The extraction of trivalent lanthanides and actinides by trialkylphosphine oxides is based on the equilibrium

$$Me_a^{3+} + 3\ NO_{3_a}^- + 3\ Alk_3PO_o \rightleftharpoons Me(NO_3)_3 \cdot 3\ Alk_3PO_o$$

At constant ionic strength (sodium nitrate 2 M), the equilibrium constants for the complex formed between tri-n-octylphosphine oxide in n-octane and ^{241}Am or ^{244}Cm have been calculated; the values are respectively $(2.9 \pm 0.5) \cdot 10^7\ M^{-3}$ and $(1.7 \pm 0.15) \cdot 10^7\ M^{-3}$. The distribution of lanthanides and actinides between 0.1 M tri-n-butylphosphine oxide in benzene and nitric acid solutions of different con-centrations was examined and discussed.

ZUSAMMENFASSUNG

Die Extraktion der dreiwertigen Lanthaniden und Aktiniden durch Alkyl-phosphinoxide beruht hauptsächlich auf folgendem Gleichgewicht:

$$Me_a^{3+} + 3\ NO_{3_a}^- + 3\ Alk_3PO_o \rightleftharpoons Me(NO_3)_3 \cdot 3\ Alk_3PO_o$$

Die Gleichgewichtskonstanten dieser Reaktion wurden bei konstanter Ionenstärke (NaNO$_3$ 2 M) für die Komplexe des Tri-n-oktylphosphinoxides (in n-Oktan) und ^{241}Am bzw. ^{244}Cm bestimmt. Ihr Wert beträgt $(2.9 \pm 0.5) \cdot 10^7\ M^{-3}$ bzw. $(1.7 \pm 0.15) \cdot 10^7\ M^{-3}$. Die Verteilungskurven der Lanthaniden und Aktiniden zwischen einer 0.1 molaren Tri-n-butylphosphinoxidlösung in Benzol und wässrigen Salpetersäure-lösungen verschiedener Konzentrationen wurden bestimmt und erörtert.

BIBLIOGRAPHIE

1 J. GOFFART ET G. DUYCKAERTS, Anal. Chim. Acta, 36 (1966) 499.
2 J. GOFFART ET G. DUYCKAERTS, Anal. Chim. Acta, 38 (1967) 529.
3 J. GOFFART ET G. DUYCKAERTS, Anal. Chim. Acta, 39 (1967) 57.
4 J. GOFFART, Thèse de Doctorat en Sciences Chimiques, Université de Liège, 1968.
5 PH. DREZE, Thèse annexe—Doctorat en Sciences Chimiques, Université de Liège, 1966.
6 K. JOON, P. A. DEURLOO ET I. A. HUNDERE, Rapport du "Kjeller Research Establishment", Novembre 1965.

7 D. W. ARCHER, R. B. HESLOP ET R. KIRBY, *Anal. Chim. Acta*, 30 (1964) 450.
8 L. WINAND, *J. Chromatog.*, 7 (1962) 400.
9 D. C. WIMER, *Anal. Chem.*, 34 (1962) 873.
10 J. S. FRITZ ET B. B. GARRALDA, *Anal. Chem.*, 36 (1964) 737.
11 C. F. BAES, *J. Phys. Chem.*, 66 (1962) 1929.
12 J. R. FERRARO, C. CRISTALLINI ET I. FOX, *J. Inorg. & Nucl. Chem.*, 29 (1967) 139.
13 D. R. COUSINS ET F. A. HART, *J. Inorg. & Nucl. Chem.*, 29 (1967) 1745.
14 C. VERHEIRSTRAETEN, *Thèse de Licence en Sciences Chimiques*, Université de Liège, 1964.
15 G. R. CHOPPIN ET W. F. STRAZYK, *Inorg. Chem.*, 4 (1965) 1250.
16 D. F. PEPPARD, G. W. MASON ET I. HUCHER, *J. Inorg. & Nucl. Chem.*, 24 (1962) 881.
17 E. HESFORD, E. E. JACKSON ET H. A. C. MACKAY, *J. Inorg. & Nucl. Chem.*, 9 (1959) 279.

SPECTROFLUORIMETRIC DETERMINATION OF EUROPIUM AND SAMARIUM AS THEIR 2-NAPHTHOYLTRIFLUOROACETONE–TRIOCTYLPHOSPHINE OXIDE COMPLEXES

TSUNENOBU SHIGEMATSU, MASAKAZU MATSUI AND RYOUSUKE WAKE

Institute for Chemical Research, Kyoto University, Uji, Kyoto (Japan)

It is well known that some tervalent rare-earth chelates with β-diketones fluoresce under ultraviolet light[1-4], and the phenomenon has been used for the determination of trace amounts of rare earths[5-8]. Methods for the determination of europium and samarium with thenoyltrifluoroacetone (TTA) and trioctylphosphine oxide as synergetic agent have been described[6], the detection limits being *ca.* 5 p.p.b. Eu and 1 p.p.m. Sm. Benzoyltrifluoroacetone has also been used for the determination of europium[8]. In the present paper, the use of 2-naphthoyltrifluoroacetone for the spectrofluorimetric determination of europium and samarium is discussed.

2-Naphthoyltrifluoroacetone has various advantages: quantitative extraction is readily achieved at pH *ca.* 6 in the presence of trioctylphosphine oxide, as in the case of TTA[6], and replacement of the phenyl group[6,8] by the naphthyl group leads to an intensification of fluorescence[4], and thus an improvement in sensitivity; the detection limits are 0.01 p.p.b. of europium and 0.1 p.p.m. of samarium in the proposed method.

EXPERIMENTAL

Apparatus

Spectrofluorimetric measurements were made with a Hitachi Spectrophotometer, model EPU-2A, and a fluorescence attachment, model L-3, with 1-cm silica cells; the light source for excitation was a mercury lamp with a cut-filter. A Hitachi-Horiba glass electrode pH meter, model M-3, was used for the pH measurements. Radioactivity was measured with a NaI(Tl) well-type scintillation counter (1.75 × 2-in crystal), coupled to a Metro Electric Digital Scaler, model MP-6A.

Reagents and chemicals

Stock solutions of europium and samarium chloride were prepared by dissolving the 99.9% and 99.99% pure oxides (Shin-Etsu Chem. Ind. Co., Ltd.) in dilute hydrochloric acid; standard solutions were prepared by suitable dilution.

2-Naphthoyltrifluoroacetone (NTFA) was synthesized from 2-acetonaphthone and trifluoroacetic acid[9,10]. The crude product was purified by recrystallizing twice from ethanol–water mixture.

Rhodamine B (reagent-grade) was dissolved in water and used as an internal standard for fluorescence measurements.

Trioctylphosphine oxide (TOPO; Tokyo Kasei Kogyo Co., Ltd.) was used without further purification. All the other reagents were reagent-grade materials, and redistilled water was used throughout.

Procedure

Transfer a hydrochloric acid solution containing europium ($1 \cdot 10^{-3}$–50 μg) or/and samarium (1–50 μg) to a 30-ml beaker. Add 1 ml of 1.0 M sodium acetate, adjust the pH to 5.5–6.5, transfer the solution to a glass-stoppered centrifuge tube, and dilute to 10 ml. Add 10 ml of benzene solution containing 10^{-4} or $5 \cdot 10^{-5}$ M NTFA (see p. 101) and 10^{-2} M of TOPO to the aqueous solution, and shake for about 30 min. Transfer the organic layer to a 1-cm silica cell, and measure the fluorescence at 565 nm for samarium and 615 nm for europium, using the rhodamine B solution (0.3 and 0.03 μg/ml) as a standard.

RESULTS AND DISCUSSION

Fluorescence spectra

The uncorrected fluorescence spectra of the europium and samarium complexes extracted into benzene are shown in Figs. 1 and 2. The europium–NTFA–TOPO complex shows only one sharp emission maximum at 615 nm. The samarium complex shows three emission maxima at 645, 598 and 565 nm, but, only the maximum at 565 nm is suitable for the determination of samarium in the presence of europium, because the fluorescence intensity of europium is about a hundred times stronger than that of samarium.
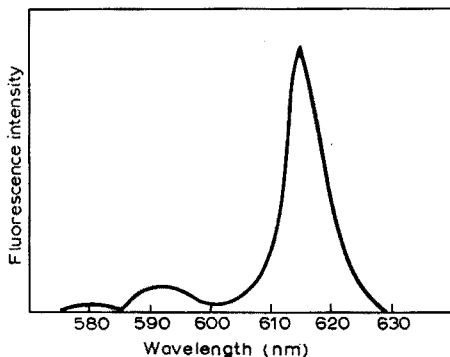
Fig. 1. Fluorescence spectrum of europium (1 p.p.m.).
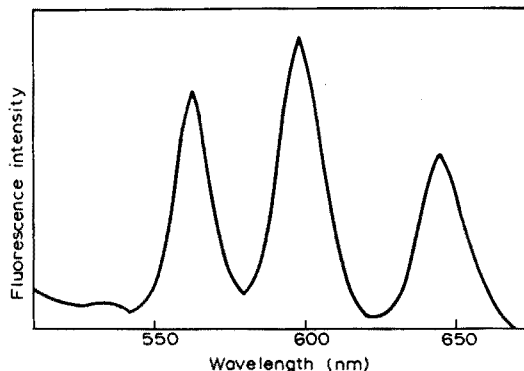
Fig. 2. Fluorescence spectrum of samarium (5 p.p.m.).

Effect of pH

The effect of pH on the fluorescence intensity, or on the extractability, of the europium and samarium chelates, was investigated. The intensity rose steeply over the pH range 3.5–5 and reached a plateau in the pH range 5.5–7.0. The extraction

behavior of europium was also observed by means of [152,154]Eu, and similar results were obtained. The optimum pH range for the extraction and determination of europium and samarium is 5.5–7.0.

Effect of the reagent concentration

A study of the effect of the concentration of NTFA showed that the fluorescence intensity decreased rapidly with an increase in the concentration of NTFA. With high concentrations of NTFA, *e.g.* 10^{-4} M, only the surface of the sample towards the irradiated light emitted, probably because of absorption of the irradiating light by the reagent, which has a strong absorption band in the ultraviolet region, rather than because of quenching of the fluorescence. Thus, the lower the concentration of NTFA, the more sensitive the fluorimetry of the rare-earth elements. However, when the concentration of NTFA was too low, the extraction of the elements became incomplete even in the presence of 10^{-2} M TOPO. Then, the concentration of NTFA was carefully maintained at $5 \cdot 10^{-5}$ M for up to 1 μg of europium and at $1 \cdot 10^{-4}$ M for 1–50 μg of europium and samarium.

The extraction recovery was again checked on samples containing 50 μg of europium by the [152,154]Eu tracer method, and it was confirmed that more than 99.0% of europium was extracted above pH 5.0, with $1 \cdot 10^{-4}$ M NTFA and $1 \cdot 10^{-2}$ M TOPO in benzene.

Effect of temperature

The effect of temperature was studied in the range 10–50°; changes in temperature up to 30° had very little influence on the fluorescence intensity.

Effect of the irradiation time

The stability of the fluorescence against prolonged irradiation was examined. Although the fluorescence was intensified very gradually by continuous irradiation, the change seemed to be negligible for at least 30 min.
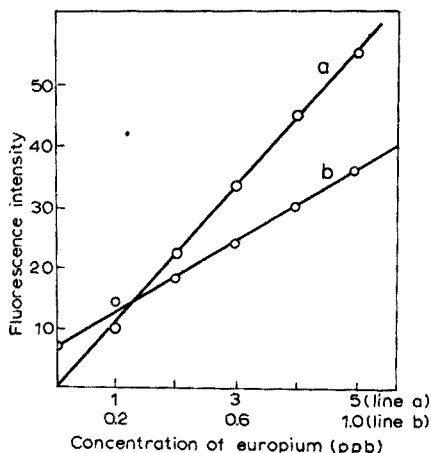
Fig. 3. Calibration curves for europium. (a) 0–5 p.p.b. Eu; (b) 0.2–1.0 p.p.b. Eu

Calibration curves

Figure 3 shows the calibration curves obtained for the determination of europium in different ranges; excellent linearity and precision were achieved. For samarium excellent linearity was obtained in the range 0.1–5 p.p.m.

Influence of foreign ions

The influence of diverse cations on the determination of europium is summarized in Tables I (rare-earth elements) and II. Fifty-fold amounts of the other rare-earth ions, except samarium, do not interfere with the determination of europium; large amounts of samarium give a positive error because of the fluorescence of samarium itself. Iron(III) causes a negative error, but 100-fold amounts of common cations can be tolerated, and common anions such as chloride, perchlorate, nitrate and sulfate in the concentrations of 0.1 M do not interfere.

TABLE I

EFFECT OF TERVALENT RARE-EARTH IONS ON THE DETERMINATION OF EUROPIUM

(0.100 μg Eu and 5.0 μg of other rare earth present in 10 ml)

Ion	Eu found ($\mu g/10\ ml$)	Ion	Eu found ($\mu g/10\ ml$)	Ion	Eu found ($\mu g/10\ ml$)
La	0.100	Gd	0.104	Er	0.102
Ce	0.109	Tb	0.109	Tm	0.109
Pr	0.107	Dy	0.102	Tb	0.100
Nd	0.108	Ho	0.102	Lu	0.102
Sm	0.180				

TABLE II

EFFECT OF DIVERSE IONS

(0.1 μg Eu/10 ml)

Ion	added ($\mu g/10\ ml$)	Eu found ($\mu g/10\ ml$)	Ion	added ($\mu g/10\ ml$)	Eu found ($\mu g/10\ ml$)
Rb+	1000	0.102	Ni²+	10	0.104
Cs+	1000	0.102	Cu²+	10	0.091
Mg²+	100	0.107	Zn²+	10	0.093
Ca²+	1000	0.103	Al³+	25	0.132
Sr²+	1000	0.107	Sb³+	25	0.096
Ba²+	50	0.100	Pb²+	25	0.100
Cr³+	10	0.095	Bi³+	50	0.102
Mn²+	25	0.115	Cd²+	10	0.100
Fe³+	5	0.058	Hf⁴+	5	0.093
Co²+	10	0.118			

Determination of europium in mixtures of rare-earth metals

Sample solutions containing all rare-earth metal ions in the composition of Clarke numbers were synthesized and europium was determined. The results (Table III) indicate that the proposed method can be successfully applied.

Simultaneous determination of samarium and europium

Because the fluorescence of europium is over a hundred times more intense

than that of samarium, samarium in up to 10-fold amounts does not affect the determination of europium; in the reverse case, interference is apparent even when both metal ions are present in almost the same concentration. Accordingly, europium and samarium were determined simultaneously at 565 nm, and then europium was determined separately. The results obtained on various mixtures of known composition (Table IV) show that the technique is adequate, although somewhat high values are obtained for samarium.

TABLE III

ANALYSIS OF SYNTHESIZED SOLUTION

Synthesized sample solution R.E. added (p.p.m.)	Eu	
	Present (p.p.m.)	Found (p.p.m.)
La 0.18, Ce 0.45, Pr 0.05, Nd 0.22, Sm 0.06	0.010	0.011
Gd 0.06, Tb 0.008, Dy 0.04, Ho 0.01, Er 0.02	0.020	0.022
Tm 0.002, Yb 0.025, Lu 0.007		

TABLE IV

SIMULTANEOUS DETERMINATION OF Eu^{3+} AND Sm^{3+}

Present (p.p.m.)		Found (p.p.m.)	
Eu^{3+}	Sm^{3+}	Eu^{3+}	Sm^{3+}
0.20	0.20	0.19	0.23
0.20	0.40	0.21	0.44
0.20	0.60	0.20	0.65
0.20	0.80	0.18	0.84
0.20	1.00	0.20	1.05
0.10	0.50	0.10	0.58
0.20	0.50	0.20	0.57
0.30	0.50	0.31	0.55
0.40	0.50	0.38	0.58

SUMMARY

The europium and samarium complexes with 2-naphthoyltrifluoroacetone (NTFA) can be used for the spectrofluorimetric determination of the two metals. Low concentrations of NTFA are needed, and trioctylphosphine oxide is used to enhance the extraction; the optimum pH range is 5.5–6.5. The fluorescence intensity is stable under irradiation for > 30 min. The detection limits are 0.1 p.p.b. Eu and 0.1 p.p.m. Sm. Few common ions interfere; iron(III) causes low results. Rare-earth ions, except samarium, in 50-fold amounts do not interfere with the determination of europium. Europium interferes with the determination of samarium, but a simultaneous determination is possible.

RÉSUMÉ

Les complexes d'europium et de samarium avec la 2-naphtoyltrifluoacétone

(NTFA) peuvent être utilisés pour le dosage spectrofluorimétrique de ces deux métaux. De faibles concentrations de NTFA sont nécessaires; le trioctylphosphine oxyde permet de faciliter l'extraction—pH optima de 5.5 à 6.5. L'intensité de fluorescence est stable sous irradiation, pendant plus de 30 minutes. Les limites de détection sont 0.1 p.p.b. Eu et 0.1 p.p.m. Sm. Peu d'ions gênent; le fer(III) donne des résultats abaissés. Les ions des terres rares, excepté le samarium, ne gênent pas, même pas en quantités de 50 fois en surplus. L'europium gêne le dosage du samarium, mais le dosage simultané est possible.

ZUSAMMENFASSUNG

Die Komplexe des Europiums und des Samariums mit 2-Naphthoyltrifluoro-aceton (NTFA) können für die spektralfluorimetrische Bestimmung dieser 2 Metalle verwendet werden. Geringe Konzentrationen von NTFA sind erforderlich, und Trioctylphosphinoxid wird zur Förderung der Extraktion verwendet; der optimale pH-Bereich liegt zwischen 5.5 und 6.5. Die Fluoreszenzintensität ist für eine Bestrahlungszeit von mehr als 30 Minuten stabil. Die Nachweisgrenzen betragen 0.1 p.p.b. Eu und 0.1 p.p.m. Sm. Nur wenige der üblichen Ionen stören; Eisen(III) verursacht niedrigere Ergebnisse. Der fünfzigfache Gehalt anderer Seltener Erdionen ausser Samarium stören die Bestimmung des Europiums nicht. Europium stört die Bestimmung des Samariums, aber eine gleichzeitige Bestimmung ist möglich.

REFERENCES

1 G. A. CROSBY, R. E. WHAN AND R. M. ALIRE, J. Chem. Phys., 34 (1961) 743.
2 G. A. CROSBY, R. E. WHAN AND J. J. FREEMAN, J. Phys. Chem., 66 (1962) 2493.
3 J. J. FREEMAN AND G. A. CROSBY, J. Phys. Chem., 67 (1963) 2717.
4 N. FILIPESCU, W. F. SAGER AND F. A. SERAFIM, J. Phys. Chem., 68 (1964) 3324.
5 L. I. KONONENKO, N. S. POLUEKTOV AND M. P. NIKONOVA, Zavodsk. Lab., 30 (1964) 779.
6 R. E. BALLARD AND J W. EDWARDS, Proc. S.A C. Conference, Nottingham, 1965, Heffer, Cambridge, 1966, p. 328.
7 E. C. STANLEY, B. I. KINNEBERG AND L. P. VARGA, Anal. Chem., 38 (1966) 1363.
8 T. SHIGEMATSU, M. MATSUI AND T. SUMIDA, Bull. Inst. Chem. Res., Kyoto Univ., 46 (1968) 248.
9 J. T. ADAMS AND C. R. HAUSER, J. Am. Chem. Soc., 66 (1944) 1220.
10 J. C. REID AND M. CALVIN, J. Am. Chem. Soc., 72 (1950) 2948.

THE DETERMINATION OF LIGHT ELEMENTS BY PROTON EXCITATION AND X-RAY SPECTROMETRY

H. KAMADA AND R. INOUE

University of Tokyo, Tokyo

M. TERASAWA, Y. GOHSHI, H. KAMEI AND I. FUJII

Central Research Laboratory, Tokyo Shibaura Electric Co., Ltd., Kawasaki (Japan)

(Received December 26th, 1968)

Various techniques have been studied in order to extend the X-ray spectro-chemical method to the determination of elements lighter than sodium. Fluorescence methods and electron excitation methods have been investigated by many workers[1-3]. The electron excitation method, especially in EPMA, established the feasibility of determining light elements by X-ray spectroscopy with fairly good sensitivity, but the method has the disadvantage that bremsstrahlung causes high backgrounds. A proton excitation method, as suggested by STERK[4], is promising for the analysis of light elements. In the characteristic production of X-rays by proton bombardment, incident protons are hardly deflected by the target material, so that the intensity of bremsstrahlung X-rays is extremely low. Thus the proton excitation method can improve the peak-to-background ratio in X-ray spectrochemical analysis by primary X-rays. The efficiency of X-ray production by protons is not very high at wavelengths below 10 Å, but it increases rapidly with the wavelength of the excited X-ray line and becomes similar to, or larger than, that of electron excitation in the soft X-ray region. Moreover, the matrix effect is small because the X-rays are generated only at the target surface. The application of this method of X-ray spectrochemical analysis has been investigated and this paper presents the preliminary results of some analytical studies for boron and carbon.

EXPERIMENTAL

Apparatus

The proton beams are accelerated by a Toshiba 200-kV d.c. accelerator, and led to the target through a deflecting magnet. Figure 1 is a schematic diagram of the apparatus used. The proton beam of 5-mm diameter hits the target perpendicularly. The take-off angle of emitted X-rays is 55°. Dispersion is accomplished with a flat crystal of lead stearate soap film consisting of 100 layers and with Soller slits. The detector is a gas-flow proportional counter with a 1.3-μ thick stretched polypropylene film window, supported by 50%-transmission nickel mesh. A gas mixture of 25% argon and 75% methane is used.

Methods

Standard samples of nickel base alloy and stainless steel for boron analysis, and low alloy steel and white iron for carbon analysis were used in constructing calibration curves. A sample was abrased to a mirror-like surface finish. X-Ray counts were normalized by the total number of incident protons on the target by means of a current integrator. Target contamination by the deposition of carbonaceous materials under the proton bombardment was made negligible with a Vacion pump (125 l/sec) and a cold plate near the target. The pressure during operation was $2 \cdot 10^{-6}$ mm Hg in the sample chamber.
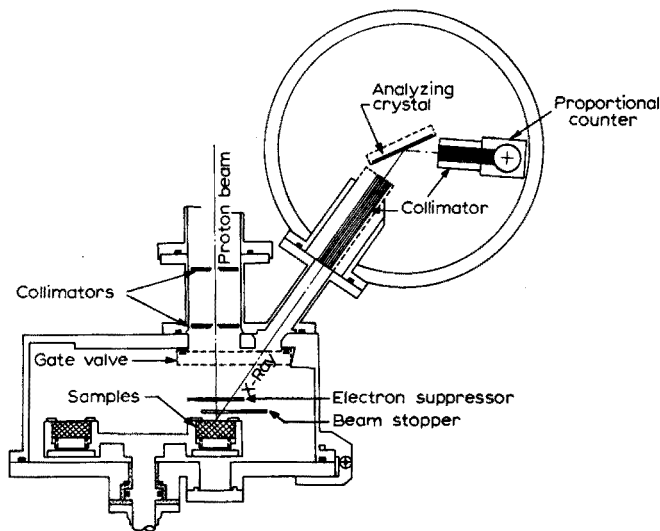
Fig. 1. Schematic diagram of apparatus used for X-ray analysis by proton excitation.
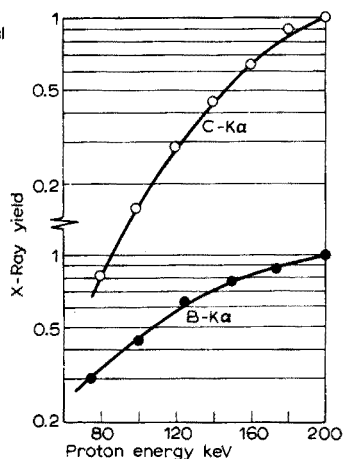
Fig. 2. The excitation efficiencies of the K X-rays of boron and carbon as a function of proton energy. The yields are normalized by the values at 200 keV.

Figure 2 shows the excitation efficiencies of the K X-rays from boron and carbon as a function of proton energy. The yields are normalized by the values at 200 keV. As the excitation efficiencies increase monotonously with energy for both elements, the higher energy excitations are preferable. Proton beams of 200 keV at 10 to 30 μA were used in the present analytical experiments.

Before the analytical measurements, $2\,\theta$ scans were performed to confirm the angular position for emitted X-rays. Figure 3 shows the boron K and molybdenum M emission spectra. About 5% molybdenum is contained in the nickel base alloy and the superposition of B-Kα line and Mo-Mζ line is observed in the spectra. There are apparent differences in the spectra between boron in boron nitride and boron in the metallic sample, reflecting the state of chemical combination.

Figure 4 shows the X-ray emission spectra from graphite and low alloy steel. Many higher-order reflections of Fe-L lines appear near the C-Kα line in the spectrum of low alloy steel containing 0.54% carbon. The carbon K emission band from graphite had a full width at half maximum of 1.6 Å with 0.5°- and 0.86°-Soller slits. The peak intensity was 6330 counts/sec for a 10-μA proton beam and the peak-to-background

ratio was 100. In addition, it was found that more intense X-rays were obtained by adopting the Soller slits of larger dispersion angle, with little reduction of peak-to-background ratio. These results indicate the superiority of this method to the electron excitation method, for which a peak intensity of 2960 counts/sec for the 7 kV–79 μA electron beam and a peak-to-background ratio of 13 have been reported.
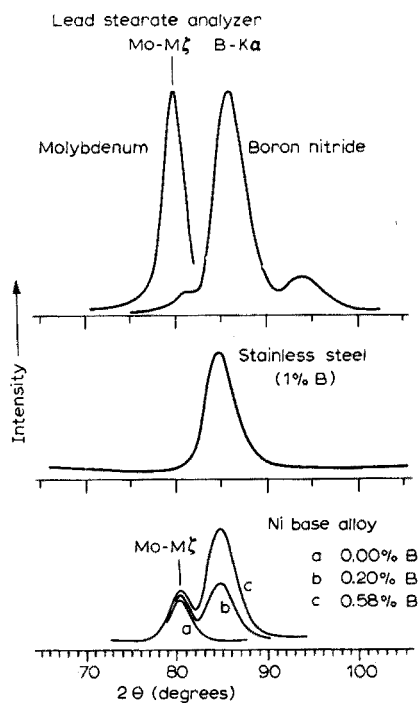

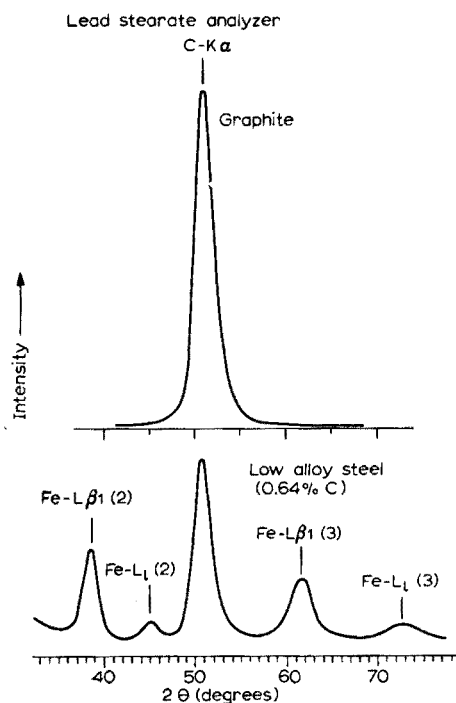Fig. 3. Boron K emission spectra (0.5° × 0.86° collimation).

Fig. 4. Carbon K emission spectra (3.0° × 0.86° collimation).

RESULTS

Figure 5 shows the calibration curve for boron in nickel base alloy. The boron concentration, wt. %, was obtained by a wet chemical method. The detection limit was calculated by the formula $S = 2\sqrt{2b}/p$ where p is the gradient of the calibration curve, and b is the background. The detection limit of boron in nickel base alloy was found to be 0.0014% for a counting time of 1 min, while the detection limit by the electron excitation method is 0.0082%[6]. The reproducibility at the concentrations of 0.05% and 0.58% of boron was 2.6% and 1.1% (relative standard deviation), respectively. Figure 6 shows the calibration curve for boron in stainless steel.

Figure 7 shows the calibration curve for carbon in low alloy steel and white iron. NBS standard samples were used. An excellent linear relationship between X-ray counts and carbon concentration was obtained for low alloy steel and white iron, which suggests that matrix effects are negligible. The detection limit was 0.0090% for a counting time of 1 min, which is considerably better than that by
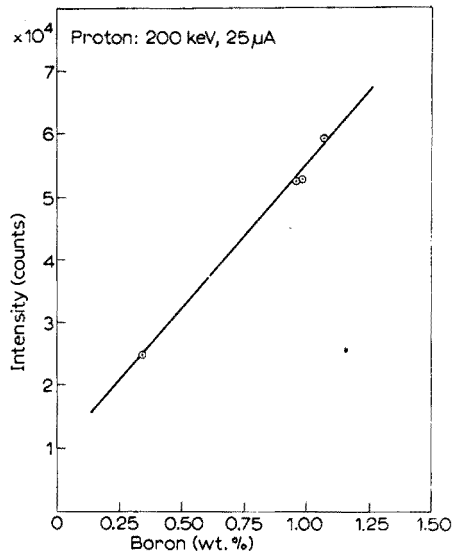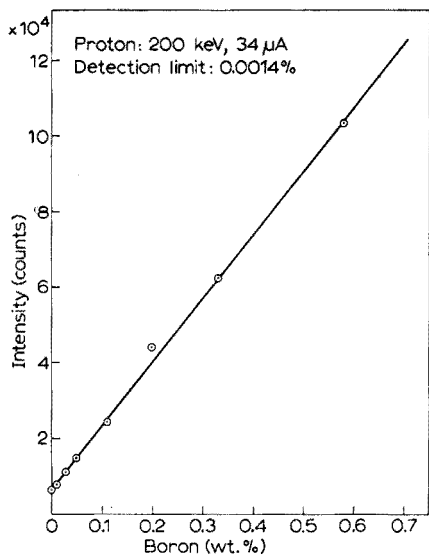
Fig. 5. Calibration curve for boron in nickel base alloy (3.0° × 0.86° collimation).

Fig. 6. Calibration curve for boron in stainless steel (3.0° × 0.86° collimation).

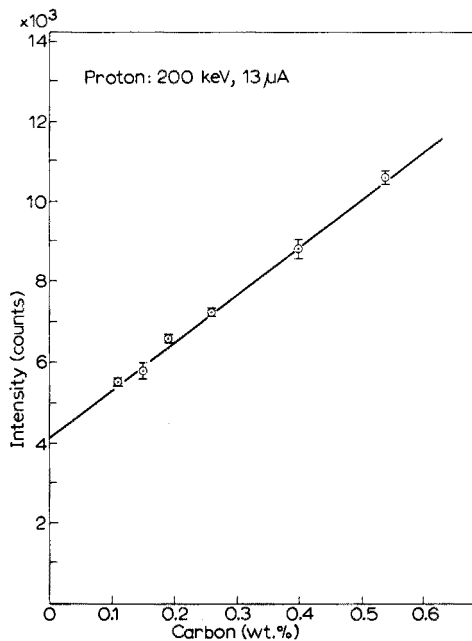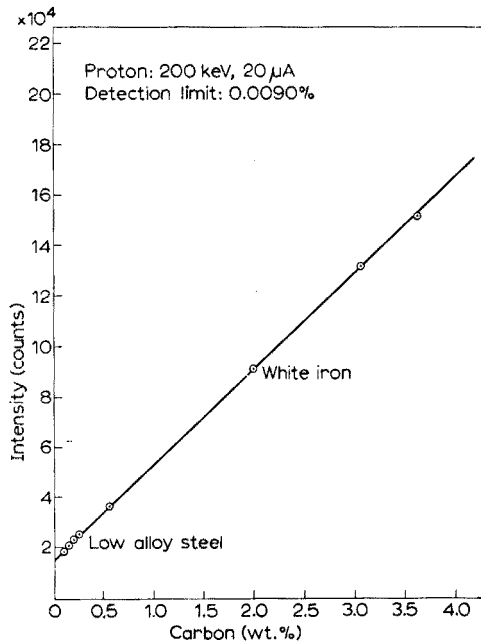

Fig. 7. Calibration curve for carbon in low alloy steel and white iron (3.0° × 0.86° collimation).

Fig. 8. Calibration curve for carbon in low alloy steel (0.5ᶜ × 5.7° collimation).

electron excitation method, 0.05%[5]. The reproducibility at the concentrations of 0.54% and 3.05% of carbon was 2.0% and 0.4% (relative standard deviation), respectively. Figure 8 shows another calibration curve for carbon in low alloy steel; the linearity of the calibration curve is excellent and the standard deviations of measurements are less than 3% relative.

DISCUSSION AND CONCLUSION

This proton excitation method makes it possible to obtain higher sensitivity for the determination of boron and carbon compared with the electron excitation method, because of the higher intensity and better peak-to-background ratio. However, there still exists some background which is larger than that expected theoretically. This background may be largely due to the low-angle specular reflection of the long wavelength X-rays from the lead stearate analyzer. Actually the peak-to-background ratio of the carbon K emission spectrum from graphite is less satisfactory, because of the high background at the low-angle side of the line. In addition, it is likely that the emission lines of base material tend to increase the background. Further investigations on dispersion and detector systems should lead to an improvement of the peak-to-background ratio and, consequently, the sensitivity.

The combination of high sensitivity and small matrix effect obtained in the present work confirms that the proton excitation method is excellent for analyses in the region of soft X-rays, especially for the determination of light elements.

SUMMARY

Proton excitation is suggested for the X-ray spectrochemical analysis of light elements; a 200-kV proton source and a flat crystal X-ray spectrometer are used. Measurements of the X-ray spectra of B-$K\alpha$ and C-$K\alpha$ show that proton excitation is promising for analyses in the soft X-ray region. For boron in nickel base alloy and carbon in low alloy steel and white iron, the calibration curves obtained showed excellent linearity. The detection limits were 0.0014% for boron and 0.0090% for carbon for counting times of 1 min.

RÉSUMÉ

On propose l'excitation protonique pour l'analyse spectrochimique aux rayons-X d'éléments légers; on utilise une source de protons 200-kV et un spectromètre à rayons-X à cristal "plat". Les mesures des spectres de rayons-X pour B-$K\alpha$ et C-$K\alpha$ sont très satisfaisantes. Pour le bore dans le nickel comme métal de base et le carbone dans les aciers faiblement alliés et dans le fer-blanc, les courbes d'étalonnage obtenues présentent une excellente linéarité. Les limites de détection sont 0.0014% pour le bore et 0.009% pour le carbone pour une durée de comptage d'une minute.

ZUSAMMENFASSUNG

Für die röntgenspektralanalytische Bestimmung leichter Elemente wird die Protonenanregung vorgeschlagen. Eine 200-kV Protonenquelle und ein Spektrometer

mit flachem Kristall werden verwendet. Messungen an den Röntgenspektren von B-Kα und C-Kα zeigen, dass die Protonenanregung für die Analyse im langwelligen Röntgenbereich vorteilhaft ist. Die Eichkurven, welche für Bor in Nickellegierungen und für Kohlenstoff in Stählen aufgestellt wurden, sind ausgezeichnet linear. Die Nachweisgrenzen betragen 0.0014% für Bor und 0.009% für Kohlenstoff bei einer Zählzeit von 1 Minute.

REFERENCES

1 B. L. HENKE, *Advances in X-Ray Analysis*, Vol. 7, Plenum Press, New York, 1963, p. 460.
2 L. S. BIRKS, *Electron Probe Microanalysis—Chemical Analysis*, Vol. 17, John Wiley, New York– London, 1963.
3 S. KIMOTO, M. SATO, H. KAMADA AND T. UI, *Advances in X-Ray Analysis*, Vol. 9, 1965, p. 508.
4 A. A. STERK, *Advances in X-Ray Analysis*, Vol. 8, 1964, p. 189.
5 H. KAMADA, T. UI, S. KIMOTO AND M. SATO, *Japan Analyst*, 16 (1967) 952.
6 H. KAMADA, T. UI AND R. INOUE, to be published.

THE DETERMINATION OF COBALT, COPPER, NICKEL AND IRON BY THIN-LAYER CHROMATOGRAPHY OF THEIR CHELATES WITH 1-(2-PYRIDYLAZO)-2-NAPHTHOL

A. GALÍK and A. VINCOUROVÁ

Lachema, N. C., Kaznějov, Pilsen North (Czechoslovakia)

In recent years an increasing number of papers has dealt with the chromatographic separation of metal chelates on thin layers of adsorbents; the greatest emphasis has been laid on studies of solvent systems and adsorbents. Thus diethyldithiocarbamates have been separated on silicagel D[1], dithizonates on silicagel G[2-4] or on cellulose MN 300[5], 1-nitroso-2-naphthoxides on silicagel G[6] or on a mixed adsorbent consisting of silicagel D and aluminium oxide D[7], and the chelates of 2-pyridine-2-aldehyde-2-quinolylhydrazone on alumina G or on prefabricated alumina sheets[8].

The application of thin-layer chromatographic separation of the metal chelates seems to be very attractive, particularly for simultaneous trace determinations of several metal ions. Apart from the convenience of the simultaneous procedure, a large concentration effect can be expected, especially when the metals are extracted as their chelates from a large volume of aqueous sample solution into a small volume of organic solvent which is then applied to the chromatoplate[8].

Quantitative evaluation of the amount of metal chelates separated on thin layers of adsorbent may be performed by various means. For routine analysis, *in situ* methods are preferable and, among these, reflectance photometry seems the most rapid[8-10] and reliable.

In the present study, 1-(2-pyridylazo)-2-naphthol (PAN) has been chosen as a quantitative scavenging agent for traces of cobalt, copper, iron and nickel. This reagent meets various requirements such as chelate stability, colour intensity, and group selectivity in slightly acidic medium[11]. In order to secure sharp separation of the group of metals named, the optimal conditions for chelate formation and extraction have been investigated, as well as the possible extraction of interferences. After preliminary experiments with loose alumina layers, the chromatographic separation of the metal chelates concerned was examined on prefabricated Silufol plates with reference to routine analyses. For quantitative evaluation of chromatograms, an automatic recording reflectance filter-photometer was used, so that additional operations with the chromatogram were eliminated.

EXPERIMENTAL

Apparatus

In investigations of the extraction of the metal chelates involved, a Unicam

SP 600 spectrophotometer was used for measurement of absorbance; a Multoscop V electronic pH meter equipped with a saturated calomel electrode and a high-resistance glass electrode were used to measure pH. Chromatographic separations were performed in large Petri dishes with loose layers and in angular glass chambers (Kavalier, Sázava) with prefabricated plates. Chromatograms were scanned by means of an "Extinktions-Registriergerät mit Integration ERI-10" (Zeiss, Jena). The instrument settings were: filter No. 2, slit width 18, sensitivity 0.3, integrator OFF.

Reagents

Redistilled water was used throughout. The titre of $5 \cdot 10^{-4}$ M PAN solution in 95% ethanol was checked absorptiometrically, as described earlier[12]. Stock solutions of metal ions were prepared by dissolving appropriate amounts of reagent-grade nickel sulphate, copper sulphate, iron(II) ammonium sulphate or cobalt nitrate in water to yield solutions containing 100 μg of the metal ion per ml. Stock solutions of iron(III) were prepared by dissolving 100 mg of iron wire (Merck zur Titerstellung) in the least necessary amount of concentrated hydrochloric acid with few drops of bromine water added; after evaporation almost to dryness, the solution was diluted to 1 l with water. On the day of use, appropriately diluted solutions were prepared.

Organic solvents used were of analytical-grade purity except for chloroform, which, after being washed with 2 N sulphuric acid, water, 2 N sodium hydroxide and with water again, was twice-distilled from an all-glass apparatus.

For calibration of the pH meter, saturated solutions of potassium hydrogen tartrate, piperazine phosphate, 0.05 M solutions of potassium hydrogen phthalate or 0.05 M sodium tetraborate were used.

All solutions of inorganic salts were prepared from reagent-grade chemicals and purified with PAN[12].

Chromatographic separations were initially tried with 1-mm loose layers of alumina, Reanal (activity II according to Brockman, 0.06–0.09 mm particle size). All quantitative work was done with fabricated Silufol plates (Kavalier, Sázava), which were activated by heating at 75° for 20 min. Some batches of Silufol plates were contaminated by trace metal impurities which reacted with free PAN. In order to make the plates uniform they were purified by elution with 5% (v/v) acetylacetone in benzene. The excess of acetylacetone together with its chelates were removed by elution with ethanol.

Procedures

Study of pH-dependence of the formation and extraction of PAN chelates. Several 20-ml portions of aqueous solutions containing 10 μg of the metal ion concerned were placed in 50-ml quartz beakers, 1 ml of ethanolic PAN was added and pH was adjusted to a definite value with 0.2 N sulphuric acid or 2 N aqueous ammonia (purified by isothermal distillation). The solutions were then set aside for 1 h. They were then transferred to 50-ml separatory funnels, and the beakers were rinsed with 5 ml of chloroform. The extraction was accomplished by shaking for 1 min. The chloroform extracts were drained into dry 1-cm cells and their absorbance was measured against pure solvent, preferably at the wavelength of maximum absorbance. After the extraction, the pH of the aqueous phase was checked again.

Dependence on salt concentration. The extraction of iron, copper and, to some

extent, cobalt was found to depend on inorganic salt concentration, hence this effect was studied. The extraction of copper was investigated earlier[12], hence attention was directed to the extraction of iron chelate. Into a series of 50-ml quartz beakers were placed x ml of inorganic salt solution, 1 ml of stock iron solution, $19-x$ ml of water, and 1 ml of ethanolic PAN (*i.e.* a substoichiometric amount). After pH adjustment (the same pH in the whole series) the above procedure was followed. After the extraction, the aqueous phase was diluted to 25 ml with acetone and the absorbance was measured at the wavelength of maximum absorbance of the unextracted chelate.

Rate of chelate formation. These tests were made similarly to the study of pH dependence, except that the time of colour development was varied, and the pH of the solutions was fixed at the optimal value.

Chromatographic methods. The solutions of the cobalt, copper, nickel and iron chelates were evaporated to dryness (separately or together) in a test tube on a water bath (*ca.* 80°) and, after the residue had been dissolved in 0.5 ml of chloroform, an aliquot of the resulting solution was pipetted on the start of the Silufol plate. The spots obtained were air-dried and the plate was positioned in chromatographic chamber lined with filter paper and containing 50 ml of the solvent system investigated. The ascending chromatography was ended when the solvent front had travelled 10 cm from the start.

In the case of loose layers of alumina, the extracts were evaporated as above, but 20 mg of alumina was added to the test tube. The alumina powder with adsorbed chelates was carefully transferred to a 4·10-mm space 1.5 cm from the lower end of the loose layer of alumina on the glass plate. The surface was then levelled with a glass slide. This prepared chromatoplate was placed at a 15° angle in a large Petri dish containing the solvent system investigated. The chromatography was ended when the solvent front had travelled 15 cm from the start.

The chromatograms obtained were scanned by reflectance photometer and R_F values were calculated from the position of the maxima of reflectance peaks.

RESULTS

Extraction

In agreement with earlier findings[11] the formation of a brownish red chelate of cobalt with PAN in aqueous solution was observed; the chelate turns completely greyish green within 20 min, but the colour transition can be speeded either by gentle heating or by addition of ethanol or ammonium chloride. The green chelate is extracted into chloroform quantitatively in the pH range 3–7.4. The extraction is facilitated by the presence of potassium bromide in the aqueous phase, but ammonium thiocyanate suppresses considerably the solubility of the green cobalt chelate in chloroform.

The extraction of copper has already been studied thoroughly[12]; the violet CuPAN$^+$ chelate produced immediately in slightly acidic medium forms an uncharged species with bromide or thiocyanate, which is then readily extracted into chloroform. An interesting effect of warming of the solution of chelate was observed; warming caused the fading of the colour, which returned on cooling again.

When an attempt was made to extract the iron(III)–PAN chelate from unbuffered aqueous solutions of pH 3–4, the chelate remained in the aqueous phase, giv-

ing it a reddish violet colour. Extraction was facilitated by adding potassium bromide, ammonium thiocyanate, sodium chloride or potassium hydrogen phthalate. Since conditions for the simultaneous extraction of iron, cobalt and copper were sought, potassium bromide was chosen for further study. It was found that the extraction of the iron(III) chelate increased with increasing concentration of potassium bromide (see Fig. 1). At pH 5.5, maximal extraction was obtained in the presence of 10^{-2}–0.5 M potassium bromide. A plot of the logarithm of the distribution coefficient *vs.* the logarithm of bromide ion concentration was linear with unity slope, suggesting that one mole of iron chelate is bound to one mole of bromide. This is in agreement with the essential electroneutrality of the extracted species, assuming that the iron chelate has the composition, Fe $(PAN)_2^+$, suggested by SHIBATA[13]. This composition was confirmed by the equilibrium shift method, where the slope of the plot was found to be 2, and by continuous variation at a $3.68 \cdot 10^{-5}M$ total concentration level of PAN and iron-(III) in 40% acetone medium. In these experiments the absorbance was measured at 480 and at 750 nm after 1 h. The same continuous variations method suggested that, within 5 min after mixing of the components, a 1:1 chelate was formed (*cf.* Fig. 2).
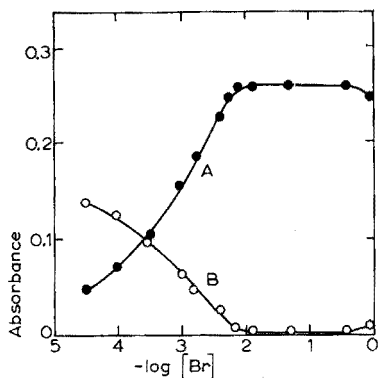
Fig. 1. Effect of the concentration of bromide on the extraction of ferric iron chelate. (A) absorbance of the extract; (B) absorbance of the aqueous phase.
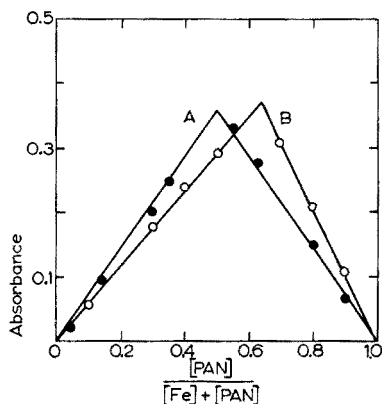
Fig. 2. Continuous variation plot for PAN and ferric iron. (A) within 5 minutes; (B) after one hour standing.
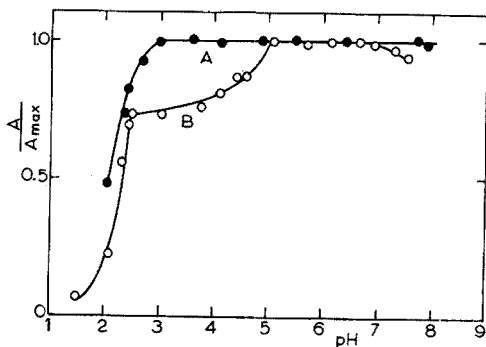
Fig. 3. Effect of pH on extraction of iron. (A) ferrous iron; (B) ferric iron.

The study of pH-dependence showed that the absorbance of the extracted iron chelate rose in 0.1 M potassium bromide from pH 1.5 to pH 2.5, and reached its maximum level only above pH 5; the shape of the curve (Fig. 3) is thus in agreement with that given by PÜSCHEL et al.[14,15]. Within the pH range 3-4, the chelate was extracted more rapidly than the excess of PAN, whereas above pH 5 the rates were reversed. Virtually complete transfer of the chelate into chloroform was achieved at any pH by shaking for 1 min.

  The iron(II)–PAN chelate was formed in the same pH range as the iron(III) chelate; colour development was complete within 10 min, when PAN was added before the pH was adjusted. The extraction of the chelate formed in 0.5% ascorbic acid medium was rapid and quantitative above pH 3 and remained so up to at least pH 8. The depression observed for the iron(III) chelate was not found (Fig. 3). Unexpectedly, the absorbance spectrum of the iron(II) chelate was essentially the same as that given by PÜSCHEL[15] and SHIBATA[13] for the iron(III) chelate. This might be explained as suggested by PÜSCHEL et al.[16]: iron(II) is oxidised by air even in the presence of ascorbic acid, if PAN is also present. If this explanation is true, then the extraction of the iron(III) chelate might be explained via formation of a $Fe(PAN)_2{}^+$– ascorbate uncharged species. The identity of the chelates formed from iron(II) and iron(III) solutions is further supported by the identical behaviour of their spots during chromatography on Silufol plates.

  Since the pH limits were set by the requirement of simultaneous extraction of the other metals investigated, the chelation of nickel with PAN was investigated only within the pH range 5-7. Chelation was virtually complete after 1 h in the cold or after 5 min of warming on a boiling water bath. The extraction of the red nickel chelate into chloroform proceeded very quickly, once the chelate was formed. No noteworthy effect of potassium bromide on the chelation or the extraction was observed.

  From the above results it may be concluded that all four metals are extracted completely at pH 5-6.7 in the presence of 0.01-0.1 M potassium bromide, when etha-nolic PAN is added to the solution of these metal ions and chelation is allowed to proceed for 1 h. The addition of a reducing or oxidizing agent is unnecessary because iron is extracted in both valency states. Under these conditions, the formation of the palladium chelate was found to be totally prevented because of masking with bromide. The extraction of zinc, cadmium, manganese(II), mercury and uranyl ions was pre-vented by the pH range chosen and the relatively small concentration of PAN[12,15,16]. The interference of the vanadyl, indium and gallium chelates is avoided by thin-layer chromatography, as indicated below.

Chromatographic separation

  Only a small volume of liquid sample can ordinarily be applied to the start of thin-layer chromatoplates, while the extraction of chelates from an aqueous phase needs a volume of solvent several orders of magnitude higher. If only a small aliquot of the extract is applied to the plate, a severe loss of sensitivity results. Evaporation of the extract to a small volume and application of a major portion of this, would be possible if the chelates were of sufficient thermal stability. Accordingly, this point was examined: $2 \mu g$ each of cobalt, copper, nickel and iron(III) were extracted under the above optimum conditions, the extracts were diluted to 10 ml with chloroform and the absorbances at the wavelengths of maximum absorbance of the chelates were

measured. The extracts were then transferred to quartz beakers and evaporated to dryness at 80° on a water bath; after the residues had been dissolved in 10 ml of chloroform, the absorbances were measured again. Essentially no decomposition occurred (Table I).

TABLE I

THERMAL STABILITY OF CHELATES

Chelate of PAN with	λ (nm)	Absorbance before evaporation	Absorbance after evaporation
Co(III)	630	0.178	0.174
Cu(II)	565	0.175	0.174
Ni(II)	570	0.510	0.516
Fe(III)	765	0.158	0.160

Because metal chelates are generally of low polarity, their separation requires solvent systems of low polarity solvent[17]. Benzene and carbon tetrachloride were therefore chosen as basic components of the solvent systems investigated. These solvents alone eluted the spots of the cobalt, copper, nickel and iron chelates with PAN too slowly, hence the polarity of the solvent systems was increased by adding solvents such as ethanol, acetone, etc.

The effect of increasing concentration of ethanol in benzene on the separation of the chelates and of excess PAN on loose alumina layers is illustrated in Fig. 4.
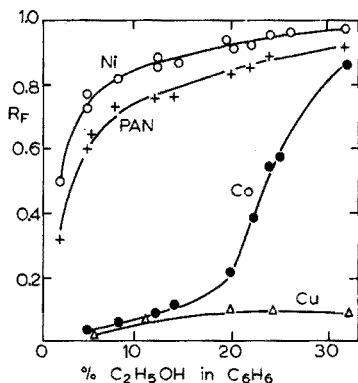
Fig. 4. Separation of PAN and of its chelates with copper, cobalt and nickel on loose alumina layers.
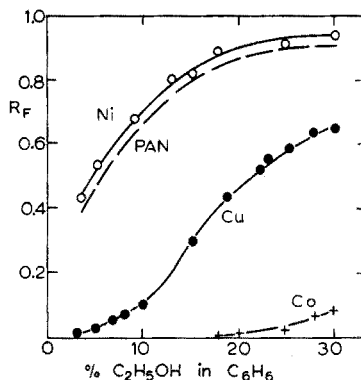
Fig. 5. Separation of PAN and of its chelates with cobalt, copper and nickel on Silufol plates.

With an increasing concentration of ethanol, the red nickel chelate starts to travel, followed by unseparated orange-yellow spot of reagent and, later, by a greyish green spot of cobalt. The violet copper chelate moves only slightly from the start. Similar behaviour was observed in ethanol–carbon tetrachloride solvent systems. The separation on loose alumina layers was not further investigated, because fabricated Silufol plates, more suitable for routine application of the method, became available.

For the separation of metal chelates on Silufol plates, the following solvent systems with various percentage compositions were investigated: ethanol–carbon tetrachloride, ethanol–benzene, ethanol–dichloroethane, acetone–carbon tetrachloride, acetone–benzene, acetone–dichloroethane, acetone–trichloroethylene, acetone–chloroform and methanol–chloroform. The behaviour of the copper and cobalt spots was different on Silufol plates from that on loose alumina layers: the copper spot travelled more quickly than the cobalt one. The most effective separation of these two spots from each other and also from the spots of nickel, iron and excess PAN was achieved with 20% (v/v) ethanol–benzene (Fig. 5). For the separation of PAN, nickel and iron, either acetone–chloroform or acetone–dichloroethane was most effective (Fig. 6); chloroform was slightly preferable to dichloroethane, because it gave a better separation between PAN and nickel(II). Successive separation of all five spots was achieved by elution first with ethanol–benzene, and after drying the chromatoplate, either with acetone–chloroform or acetone–dichloroethane. The final chromatogram is shown in Fig. 7.
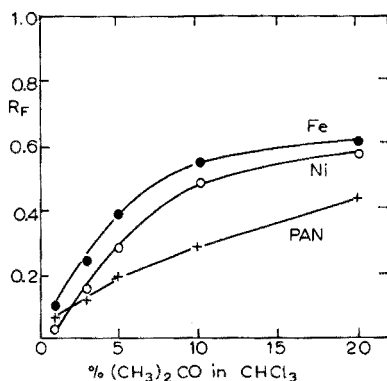
Fig. 6. Separation of PAN and of its chelates with nickel and iron on Silufol plates developed by acetone in chloroform.
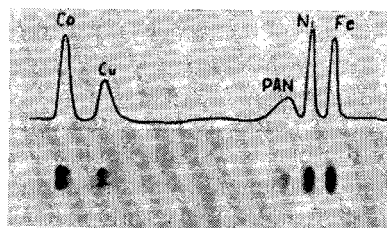
Fig. 7. Typical chromatogram obtained by development with 20% (v/v) ethanol in benzene and subsequent elution with 8% (v/v) acetone in dichloroethane.

With regard to the selectivity of the procedure, the spot of the vanadium chelate is positioned between the copper and excess reagent spot on the final chromatogram; the chelates of gallium and of indium, which might be produced partially during extraction, decompose on Silufol and travel as free PAN.

Quantitative evaluation

In order to establish the optimum range for quantitative evaluation of chromatograms, standard solutions of the metal chelates in chloroform were prepared by adding 1 ml of ethanolic $5 \cdot 10^{-4}$ M PAN to 0.1 M potassium bromide solution containing 2 μg of each of the metals investigated, extracting the chelates formed into several portions of chloroform, evaporating the combined extracts and dissolving the residue in 0.5 ml of chloroform. Various aliquots of standard solutions so obtained were pipetted on Silufol plates, the chromatographic separation was accomplished,

the chromatograms were scanned in the recording reflectance photometer, and the peak areas were manually integrated. The plot of peak area *vs.* μg of metal per spot was linear up to 0.4 μg Co, 0.7 μg Cu, 0.2 μg Ni, and 0.6 μg Fe. Above these values, the slope of the curves decreased slowly. This feature is not a great drawback, because large loadings should be avoided to preserve the sharpness of the separation.

The lower concentration limits were calculated on the arbitrary assumption that a 10-mm^2 peak is the minimum detectable. From the slopes of the calibration graphs prepared with 3% of the extract taken, it was found that 0.016 μg Co, 0.016 μg Cu, 0.007 μg Ni and 0.012 μg Fe per spot could be detected instrumentally. Visual limits of detection were about half an order lower. The real sensitivity of the whole procedure (including the extraction and the chromatography under optimum conditions for a particular type of sample) is, of course, given by the reproducibility of the blank.

The quantitative evaluation of chromatograms in routine analysis depends largely on the stability of the colour of the spots. It was found that the peak areas for chelates of cobalt, copper, nickel and iron with PAN did not change during 5 days after preparation of the chromatogram, apart from variations caused by slight variation of instrument sensitivity.

Application of the method

In order to check the suitability of this extractive chromatographic method for routine analysis, its application to the determination of cobalt, copper, nickel and iron in barium nitrate, strontium nitrate, calcium chloride, ammonium chloride and ammonium hydrogen carbonate was tested. A sample, not larger than 2 g, was placed in a 100-ml separatory funnel, and dissolved in 20 ml of water (in the case of ammonium hydrogen carbonate, the sample was dissolved in a quartz beaker and heated to a neutral reaction). To this sample solution, 1 ml of 2 N hydrochloric acid (transistor-grade) was added, followed by 1 ml of ethanolic PAN solution and 10 ml of 10% (w/v) sodium acetate solution which was also 1 M in potassium bromide. In the same run, standard iron, copper, nickel and cobalt solutions covering the range 0–3 μg were mixed and treated in the same way as the sample solution. The solutions were allowed to stand for 90 min, and then exactly 2 ml of chloroform was added to each funnel and the chelates were extracted by shaking for 1 min. The extracts were drained into test tubes and 0.05-ml aliquots of the extracts were applied on the start of Silufol plates as 8-mm long lines. (This method of application—without evaporation—was chosen for routine analysis in order to make it more rapid.) The chromatoplates were then developed with 20% (v/v) ethanol–benzene, until the solvent front reached about 6 cm from the start. Then the plates were dried in cold air and developed again, this time with 2.7% (v/v) acetone in chloroform or with 8% (v/v) acetone in dichloroethane, until clean separation of PAN, nickel and iron chelate was achieved. The plates were cut into 4 × 15-cm strips, each sample or standard being on a separate strip. The chromatograms were scanned and calibration curves were obtained as described above. The sample content may be read directly from the graphs because the calibration includes the blanks of the whole procedure.

During application of the above method to the analysis of the listed samples, many calibration graphs were prepared. Their statistical treatment[18] resulted in the conclusion that calibrations on individual Silufol plates from the same batch form a

TABLE II

ACCURACY OF THE METHOD

Sample	Cobalt		Copper		Nickel		Iron	
	μg added	% Recovery	μg added	% Recovery	μg added	% Recovery	μg added	% Recovery
CaCl₂	3.0	92	2.86	117	2.0	95	2.1	78
CaCl₂	2.0	105	1.91	94	2.0	98	2.1	89
CaCl₂	2.0	125	1.91	106	1.0	94	1.0	101
CaCl₂	4.0	136	0.95	126	2.0	105	2.1	106
Ba(NO₃)₂	2.0	105	1.91	105	2.0	94	2.1	99
Sr(NO₃)₂	2.0	110	1.91	126	1.0	95	1.0	107
NH₄Cl	1.0	120	1.91	99	2.0	85	1.0	101
NH₄HCO₃	3.0	92	1.91	98	3.0	129	3.1	98

TABLE III

DETERMINATION OF IRON IN AMMONIUM CHLORIDE

Method	No. of detns.	Average Fe found (%)	Standard deviation of single result (%)
TLC	6	$4.8 \cdot 10^{-4}$	$\pm 0.64 \cdot 10^{-4}$
Spectrophotometric (PÜSCHEL[16])	3	$5.3 \cdot 10^{-4}$	$\pm 0.22 \cdot 10^{-4}$
Spectrophotometric (ROSIN[19])	3	$4.4 \cdot 10^{-4}$	$\pm 0.35 \cdot 10^{-4}$

sufficiently homogeneous population, so that work with fixed calibration graphs is possible. This is a distinct attraction for routine analysis.

The accuracy of the method was checked by analyses of samples with known standard additions of copper, cobalt, nickel and iron, and by comparing these results with those obtained without standard addition (Table II). Most of the samples analysed had the contents of all the metals determined at very low levels; only the sample of ammonium chloride contained relatively high amounts of iron. This sample was chosen for further verification of the method—by comparing the results of the devised chromatographic method with those obtained either by the spectrophotometric method of PÜSCHEL et al.[16] or by a modified thiocyanate method[19]; all three methods gave statistically consistent results for iron (Table III).

DISCUSSION

It is interesting to note the behaviour of the chelates of copper and cobalt, which is quite different on alumina or Silufol (silicagel) plates when the chelates are eluted with ethanol–benzene mixtures. Since all the conditions are exactly the same, except for the type of adsorbent, it may be concluded that the separation mechanism is based primarily on adsorption. According to BRADLEY AND PANTONY[20], the elution order of metal chelates in adsorption chromatography is correlated to their heats of preferential adsorption. These authors found that many chelates follow the same order of heats of preferential adsorption regardless of the type of adsorbent; obviously this is not the case for the copper and cobalt chelates with PAN, and more study is needed for complete elucidation.

For the use of the data given in Fig. 6 for double elution of the spots, it must be remembered that these data were obtained with activated Silufol plates; when the plates were subjected to elution with ethanol–benzene mixture, their activity changed because of traces of water present in ethanol. This was the reason for selecting concentrations of acetone for routine work, which were lower than those indicated as optimal in Fig. 6.

The suggested procedure is rapid and economical compared with methods for the individual determination of these elements, particularly since simultaneous determinations are possible. It might be possible to separate even more chelates on the same chromatogram without the sharpness of separation being affected. There are, however, limiting conditions caused by the chelating agent, which must be capable of selectively extracting the group of metals to be determined at a single pH value. In the case of extraction of PAN chelates from slightly acidic media, the procedure might be extended, e.g., to palladium, if bromide were replaced by some anion which is capable of forming uncharged extractable species with all the chelates involved. However, the present scheme includes the determination of the most common impurities in a large variety of materials.

The sensitivity of the thin-layer procedure with reflectance photometry is very high, if expressed in terms of the absolute amount of the metal per spot. Because of the possibility of concentrating the extracts, this sensitivity might seem to be attainable even in routine analysis of practical samples. However, the data in Table II show that the real sensitivity is much lower. The main source of lack of precision in the data is obviously the contamination hazard in the extraction step, and this drawback must apply to all similar procedures. It is very important to achieve optimal purification of reagents and to maintain the conditions usual in a trace laboratory.

SUMMARY

The chelates of cobalt, copper, nickel and iron with PAN are extracted into chloroform, separated on Silufol thin-layer chromatoplates, and determined by means of scanning reflectance photometry in situ. The procedure was successfully applied to the trace analysis of various inorganic salts; the results agreed with those obtained by other methods. Experimental variables are discussed in detail.

RÉSUMÉ

On propose une méthode de dosage du cobalt, du cuivre, du nickel et du fer par chromatographie sur couches minces. Elle consiste à effectuer une extraction de ces métaux, dans le chloroforme, à l'aide de PAN (1-(2-pyridylazo-2-naphtol) et à procéder au dosage au moyen d'un photomètre à réflexion. Cette méthode a été appliquée avec succès à l'analyse de traces dans divers sels inorganiques. Les résultats concordent avec ceux obtenus par d'autres procédés.

ZUSAMMENFASSUNG

Die Chelate von Kobalt, Kupfer, Nickel und Eisen mit PAN werden mit Chloroform extrahiert, dünnschichtchromatographisch getrennt und mittels eines Reflektionsphotometers *in situ* quantitativ bestimmt. Das Verfahren wurde erfolgreich bei der Spurenanalyse verschiedener anorganischer Salze angewendet, wobei die Resultate mit denen nach anderen Methoden erhaltenen übereinstimmten.

REFERENCES

1 H.-J. SENF, *J. Chromatog.*, 21 (1966) 363.
2 M. HRANISAVLJEVIČ-JAKOVLEVIČ, in G. B. MARINI-BETTÒLO, *Thin Layer Chromatography*, Amsterdam, 1964, p. 221.
3 M. HRANISAVLJEVIČ-JAKOVLEVIČ, J. PEJKOVIČ-TADIČ AND J. MILJKOVIČ-STOJANOVIČ, *Glasnik Hemi. Drustva (Beograd)*, 29 (1964) 115; *Mikrochim. Acta*, (1965) 141.
4 T. TAKEUCHI AND Y. TSUNODA, *J. Chem. Soc. Japan, Pure Chem. Sect.*, 88 (1967) 176.
5 M. HRANISAVLJEVIČ-JAKOVLEVIČ AND J. PEJKOVIČ-TADIČ, *Mikrochim. Acta*, (1965) 936.
6 M. HRANISAVLJEVIČ-JAKOVLEVIČ AND J. PEJKOVIČ-TADIČ, *Mikrochim. Acta*, (1965) 940.
7 H.-J. SENF, *J. Chromatog.*, 27 (1967) 331.
8 R. W. FREI, D. E. RYAN AND C. A. STOCKTON, *Anal. Chim. Acta*, 42 (1968) 59.
9 R. W. FREI AND D. E. RYAN, *Anal. Chim. Acta.*, 37 (1967) 187.
10 M. M. FRODYMA, D. F. ZAYE AND V. T. LIEU, *Anal. Chim. Acta*, 40 (1968) 451.
11 W. BERGER AND H. ELVERS, *Z. Anal. Chem.*, 171 (1959) 185.
12 A. GALÍK, *Talanta*, 16 (1969) 201.
13 S. SHIBATA, *Anal. Chim. Acta*, 25 (1961) 348; 23 (1960) 367.
14 R. PÜSCHEL, E. LASSNER AND K. KATZENGRUBER, *Z. Anal. Chem.*, 223 (1966) 414.
15 R. PÜSCHEL, *Z. Anal. Chem.*, 221 (1966) 132.
16 R. PÜSCHEL, E. LASSNER AND K. KATZENGRUBER, *Chemist-Analyst*, 56 (1967) 63.
17 L. LÁBLER AND V. SCHWARZ, *Chromatografie na tenké vrstvě*, NČSAV, Praha, 1965.
18 G. GOTTSCHALK, *Statistik in der quantitativen chemischen Analyse*, F. Enke, Stuttgart, 1962, p. 451.
19 J. ROSIN, *Reagent Chemicals and Standards*, D. Van Nostrand, New York, 1955, p. 35.
20 M. P. T. BRADLEY AND D. A. PANTONY, *Anal. Chim. Acta*, 38 (1967) 113.

THE CHEMICAL SHIFT OF THE HYDROXYL PROTON OF BENZIL-DIOXIMES AND FURILDIOXIMES

M. TANAKA, T. SHONO AND K. SHINRA

Department of Chemical Technology, Faculty of Engineering, Osaka University, Osaka (Japan)

(Received February 17th, 1969)

Various *o*-diketonedioximes have been used for determination of metals. There are three possible structural isomers for the dioxime obtained from a symmetrical *o*-diketone:

$$
\begin{array}{ccc}
\text{R—C—C—R} & \text{R—C————————C—R} & \text{R—C————————C—R} \\
\text{|| ||} & \text{|| ||} & \text{|| ||} \\
\text{HO—N\ \ N—OH} & \text{N—OH\ \ \ HO—N} & \text{N—OH\ \ \ \ N—OH} \\
\text{anti-form }(\alpha) & \text{syn-form }(\beta) & \text{amphi-form }(\gamma)
\end{array}
$$
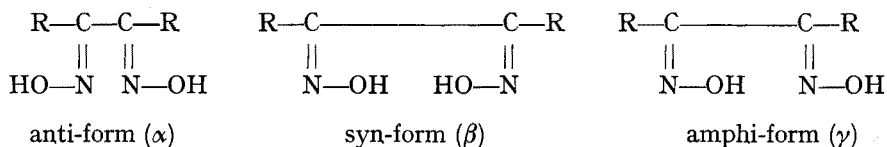
These isomers show different chemical reactions with the metal ion. It is believed that, for example, with nickel(II), the α-isomer gives a five-membered red chelate and the γ-isomer gives a six-membered green chelate but that the β-isomer cannot form a chelate because of the steric factor between the two hydroxyl groups. Differentiation of the isomers has generally been performed by electronic spectroscopy[1,2].

In this paper an investigation of the environmental difference of the hydroxyl proton of the isomers by proton magnetic resonance spectroscopy is described. It is well known that in the solvents most frequently used for PMR spectra (*i.e.*, CCl$_4$ or CDCl$_3$), the chemical shift of the hydroxyl proton of a hydroxylic compound generally exhibits a considerable concentration dependence and is therefore not readily correlated with molecular structure; moreover, the hydroxyl signal may be quite broad. KLEINSPEHN *et al.*[3] have indicated that in dimethyl sulfoxide solution most monooximes exhibit a hydroxyl proton resonance signal whose chemical-shift value is essentially independent of concentration. Similar observations have been reported in the case of alcohols[4] and phenols[5] dissolved in the same solvent. This phenomenon is presumably attributable to the tendency of the solvent to act as a strong hydrogen-bond acceptor which enables it to solvate strongly the solute monomer.

In this work benzildioxime (R = C$_6$H$_5$) and furildioxime (R = 2-C$_4$H$_3$O) were chosen as the dioxime, and dimethyl sulfoxide or hexamethyl phosphorous triamide as the solvent.

EXPERIMENTAL

The PMR spectra were obtained on a JNM-3H-60 spectrometer. Dimethyl sulfoxide (DMSO) and hexamethyl phosphorous triamide (HMPA) used as solvents

were purified by distillation. Solutions containing 1–5% (w/w) of the dioxime were used, and the chemical shifts were measured in Hz at 60 MHz to low field from internal tetramethylsilane. To prevent uptake of water, samples were prepared and sample tubes sealed in a dry-box.

Preparation of dioximes

α-Benzildioxime was prepared by heating a mixture of benzil and hydroxylamine hydrochloride in ethanol for 3 h in the presence of a few drops of concentrated hydrochloric acid[6]. The product was collected on a glass filter, washed with hot water and then with a little 50% ethanol. The crude product was recrystallized from ethanol.

β-Benzildioxime[6] was prepared by the isomerization of α-benzildioxime. A mixture containing 3 parts of ethanol to 1 part of α-benzildioxime was heated at 170–190° for 3 h in an autoclave, and then evaporated to dryness. The crude product was recrystallized from ethanol.

γ-Benzildioxime was prepared by the reaction of β-benzilmonoxime and hydroxylamine hydrochloride[7]; 1 part of β-benzilmonoxime and 4 parts of sodium hydroxide were dissolved in 20 parts of cold water, and 6 parts of hydroxylamine hydrochloride was added. After standing for 2 days at room temperature, the solution was diluted with water and filtered. The filtrate was acidified with dilute hydrochloric acid. The precipitate was collected and dissolved in cold ethanol in order to separate the γ-isomer from the α-isomer. The ethanol solution was evaporated to dryness and the product was recrystallized from ethanol.

A mixture of α- and γ-furildioximes was prepared by the reaction of furil and hydroxylamine hydrochloride[8]. These isomers were separated as follows. An aqueous solution of the mixture was added to a hot aqueous solution of nickel sulfate, which was then made weakly basic with ammonia solution, so that the red nickel chelate of α-furildioxime precipitated. This chelate was collected on a glass filter and decomposed with hot dilute hydrochloric acid. α-Furildioxime was extracted with ether and recrystallized from water. γ-Furildioxime in the filtrate was also extracted with ether and recrystallized from water.

β-Furildioxime[9] was prepared by isomerization of the α-isomer, similarly to β-benzildioxime. After the mixture had been heated for 5 h at 150–160° in an autoclave and ethanol had been removed, the product was dissolved in a little ether and reprecipitated by adding ligroin.

For identification purposes, the palladium chelates[1,2] of the dioximes were prepared: α-isomers gave orange chelates, γ-isomers yellowish chelates and β-isomers no chelates. In the absorption spectra of these chelates in chloroform, α-benzildioxime showed maxima at 260, 330 and 440 nm; γ-benzildioxime at 250 and 465 nm; α-furildioxime at 285 and 380 nm and γ-furildioxime at 265 nm. The same absorption spectra were obtained for the α-, β- and γ-isomers in ethanol. These results are consistent with those reported by YAMASAKI *et al.*[1].

RESULTS AND DISCUSSION

Table I shows the melting points and nitrogen contents of the various isomers. Figure 1 shows the PMR spectra of benzildioxime isomers in DMSO. In the α-isomer both of the hydroxyl protons are equivalent and the OH signal appears at 690 Hz as

TABLE I

DATA ON BENZILDIOXIMES AND FURILDIOXIMES

Dioxime	M.p. (°)	N %	
		Found	Calcd.
α-Benzildioxime	234–235	11.9	11.7
β-Benzildioxime	212–214	12.1	11.7
γ-Benzildioxime	163–164	11.3	11.7
α-Furildioxime	186–187	12.8	12.7
β-Furildioxime	188–190	12.9	12.7
γ-Furildioxime	184–185	12.6	12.7
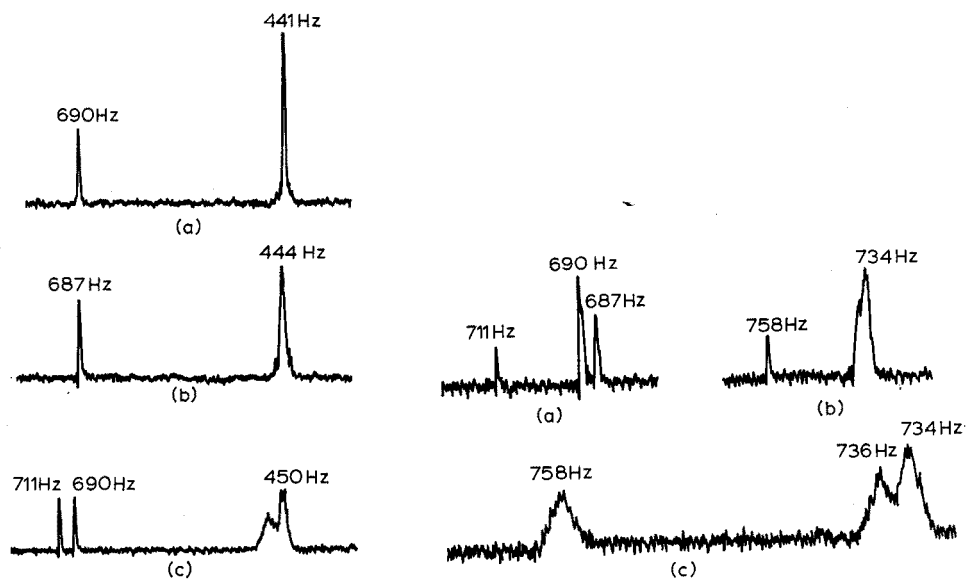
Fig. 1. PMR spectra for benzildioxime isomers in DMSO at 20° (1% w/w). (a) α-isomer, (b) β-isomer, (c) γ-isomer.

Fig. 2. PMR spectra for an equimolar mixture of α-, β- and γ-benzildioximes at 20° (1% w/w). (a) in DMSO, (b) in HMPA, (c) recorded with 1/5 sweep-width of (b).

a sharp singlet. The signal of phenyl protons appears at 441 Hz and its intensity is five times as great as that of the OH signal. In the β-isomer the OH signal appears at 687 Hz, and in the γ-isomer two signals with same intensity appear at 690 Hz and 711 Hz, since both of the hydroxyl protons are non-equivalent. The signal of the phenyl protons becomes a multiplet in the case of the β- and γ-isomers. HMPA solutions gave the same results as DMSO solutions. In the case of the furildioxime isomers, sharp signals of the hydroxyl protons were again obtained. The three signals of the furyl protons were obtained separately between 380 and 480 Hz as multiplets. The observed chemical shifts are summarized in Table II.

The three isomers gave sharp signals, hence the determination of mixtures of isomers was attempted. The hydroxyl proton chemical shifts of equimolar mixtures of the isomers were measured, and it was found that these shifts were not affected by mixing of isomers. Figure 2 shows the hydroxyl proton signals of an equimolar

TABLE II

HYDROXYL PROTON CHEMICAL SHIFTS FOR BENZILDIOXIMES AND FURILDIOXIMES AT 20° (1% w/w)

Dioxime	in DSMO (Hz)	in HMPA (Hz)
α-Benzildioxime	690	736
β-Benzildioxime	687	734
γ-Benzildioxime	690, 711	734, 758
α-Furildioxime	726	766
β-Furildioxime	702	759
γ-Furildioxime	690, 732	729, 773

mixture of α-, β- and γ-benzildioximes. In DMSO (Fig. 2a) three separate hydroxyl signals were obtained at 687, 690 and 711 Hz. Their relative intensities are in the ratio 2:3:1, respectively. The signal at 687 Hz is assigned to the two equivalent hydroxyl protons of the β-isomer, and the signal at 690 Hz to the overlapping signal of two equivalent hydroxyl protons of the α-isomer and one hydroxyl proton of the γ-isomer, while the signal at 711 Hz is assigned to the other hydroxyl proton of the γ-isomer. When HMPA is used, the three signals cannot be separated (Fig. 2b). Figure 2c shows the signal recorded with a sweep-width one-fifth of that used for Fig. 2b. Even in this case the separation of the two signals (i.e., 734 and 736 Hz) is not suitable for analytical purposes. Usually, dioximes are obtained as a mixture of the α- and γ-isomers when they are synthesized from o-diketones. The β-isomer is mainly obtained by isomerization of the α-isomer under conditions of high temperature and high pressure. Therefore the determination of α- and γ-isomers in commercial dioximes becomes important in practice. In the case of HMPA solutions, determination is possible for mixtures of the α- and γ-isomers.
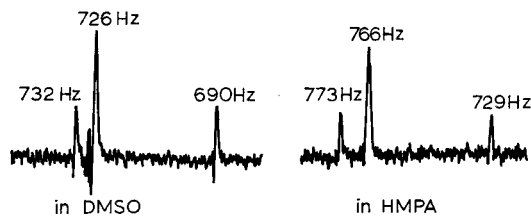
Fig. 3. PMR spectra for an equimolar mixture of α- and γ-furildioximes at 20° (1% w/w).

It can be seen from Table II that the OH signals of the isomers are better separated in the case of furildioxime than benzildioxime. Figure 3 shows the hydroxyl proton signals of an equimolar mixture of α- and γ-furildioximes. In DMSO, three signals are obtained at 690 Hz, assigned to one hydroxyl proton of the γ-isomer, 726 Hz, assigned to two equivalent hydroxyl protons of the α-isomer, and 732 Hz, assigned to the other hydroxyl proton of the γ-isomer; their relative intensities are in the ratio 1:2:1, respectively. In HMPA three signals are also obtained at 729, 766 and 773 Hz.

The temperature and concentration dependences of the hydroxyl proton chemical shifts were investigated. Furildioxime isomers did not show concentration dependence in the 1-5% (w/w) solution. Concentration dependence was not examined

TABLE III

TEMPERATURE DEPENDENCE OF THE HYDROXYL PROTON CHEMICAL SHIFT IN HMPA (1% w/w)

Temperature (°)	OH proton chemical shift (Hz)	
	α-Benzildioxime	α-Furildioxime
15	736	767
22	736	766
50	737	773
100	726	—

TABLE IV

DETERMINATION OF COMMERCIAL FURILDIOXIME (2% w/w, at 20°)

Solvent	OH proton signal (Hz)		Relative intensity	Isomer ratio (α/γ)
DMSO	726	(α-isomer)	10	
	690 and 732 (γ-isomer)		9	1.1
HMPA	766	(α-isomer)	10.5	
	729 and 773 (γ-isomer)		9.5	1.1

for benzildioxime because this compound was not very soluble in the solvents used. Table III shows the temperature dependence of the α-isomers in HMPA; with α-benzildioxime there is no effect in the range 15–50° whereas in α-furildioxime the signal is shifted 7 Hz to lower field at 50° than near room temperature.

Finally, Table IV shows the results obtained for commercial furildioxime; it can be seen that this furildioxime is a mixture of the α- and γ-isomers and that the ratio α-isomer/γ-isomer is 1:1 in both DMSO and HMPA solutions.

SUMMARY

The chemical shifts of the hydroxyl protons of benzil- and furildioxime isomers were measured in dimethyl sulfoxide or hexamethyl phosphorous triamide solvent. Each isomer gives a sharp signal at different fields and the signals are not affected by mixing of isomers, hence it is possible to determine and identify mixtures of the three isomers. The concentration and temperature dependences were investigated briefly.

RÉSUMÉ

Les transpositions chimiques des protons hydroxyle des isomères benzyl- et furyldioxime ont été mesurées en milieu diméthylsulfoxyde ou hexaméthylphospho-triamide. Chaque isomère donne un signal net aux différentes fréquences. Les signaux ne sont pas affectés par le mélange des isomères, ce qui permet de doser et d'identifier des mélanges des 3 isomères. On a examiné brièvement l'influence de la concentration et de la température.

ZUSAMMENFASSUNG

Die chemischen Verschiebungen der Hydroxylprotonen von Benzil- und Furildioxim-Isomeren werden in Dimethylsulfoxid oder Hexamethylphosphortriamid als Lösungsmittel gemessen. Jedes Isomere gibt ein scharfes Signal bei verschiedenen Frequenzen. Die Signale werden nicht durch Mischungen von Isomeren beeinflusst, so dass die Bestimmung und Identifizierung von Mischungen der drei Isomeren möglich ist. Die Konzentration und die Temperaturabhängigkeiten wurden kurz untersucht.

REFERENCES

1 K. YAMASAKI, T. MATSUMOTO AND R. ITO, *Nippon Kagaku Zasshi*, 78 (1957) 126.
2 K. SHINRA AND K. ISHIKAWA, *Nippon Kagaku Zasshi*, 74 (1953) 271.
3 G. G. KLEINSPEHN, J. A. JUNG AND S. A. STUDNIARZ, *J. Org. Chem.*, 32 (1967) 460.
4 O. L. CHAPMAN AND R. W. KING, *J. Am. Chem. Soc.*, 86 (1964) 1257.
5 R. J. OUELETTE, *Can. J. Chem.*, 43 (1965) 707.
6 V. MEYER, *Ber.*, 21 (1888) 792.
7 V. MEYER, *Ber.*, 22 (1889) 709.
8 S. E. REED, C. V. BANKS AND H. DIEHL, *J. Org. Chem.*, 12 (1947) 792.
9 K. SHINRA, K. ISHIKAWA AND H. SHIMURA, *Nippon Kagaku Zasshi*, 74 (1953) 353.

OXIDATION–REDUCTION REACTIONS IN FORMAMIDE MEDIA

RAM CHAND PAUL, K. S. SOOCH, O. C. VAIDYA AND SURAJ PRAKASH NARULA
Department of Chemistry, Panjab University, Chandigarh-14 (India)
(Received September 20th, 1968)

In continuation of the study of the solvent properties of formamide[1-3], redox reactions have been examined with a view to exploring the possibility of using formamide as a reaction medium for the determination of certain ions. Lead tetraformamide and trilead octaformamide ($Pb_3(HCONH)_8$) have been isolated as the products of solvolysis of lead dioxide and red lead in formamide and along with iodine and potassium dichromate, have been successfully employed as oxidising agents. Potentiometric methods have been used to study these redox reactions. In the case of iodine, visual titrations without any indicator have also been carried out. The results of these investigations are reported in this paper.

EXPERIMENTAL

Purification of the material

Formamide, arsenic(III) and antimony(III) chlorides were purified by the well known methods already reported[1,2]. Tin(II) chloride was placed over phosphorus-(V) oxide in a vacuum desiccator for 24 h; it was then heated in a current of dry hydrogen chloride gas with constant stirring for about 1 h. The sample was cooled in vacuum to remove the excess of hydrogen chloride gas.

Preparation of lead tetraformamide

Lead dioxide (4.0 g) was heated with formamide (100 ml), in a three-necked 250-ml flask fitted with a reflux condenser having a silica gel guard tube and with a dry nitrogen inlet tube, at 120° for 3–4 h with constant shaking. On cooling a white precipitate settled. The compound was filtered and repeatedly washed with dry acetone and finally with dry ether. (Found Pb 54.4%; $C_4H_8O_4N_4Pb$ requires Pb 54.1%. Yield 62.6%.)

Preparation of trilead octaformamide ($Pb_3(HCONH)_8$)

Formamide (100 ml) was placed in a three-necked 250-ml flask fitted as described above; pure red lead (Pb_3O_4) (3.0 g) was added in small lots of 0.4–0.5 g, and the mixture was heated at 120° and shaken. The second lot was added only when the first one had completely dissolved and a clear solution had been obtained. When all the red lead had been dissolved, and the solution had been cooled to room temperature, a white precipitate separated out. It was filtered in a dry nitrogen atmosphere,

washed with dry acetone and dried in vacuum. (Found Pb 64.2%; $C_8H_{16}O_8N_8Pb_3$ requires Pb 63.8%. Yield 83.2%.)

Preparation of chlorotin(II) formamide (SnClHCONH·2HCONH₂)

Tin(II) chloride (3.4 g) was heated with formamide (100 ml) at 120° for 3 h as described above; a light yellow solid separated out. The compound was filtered, washed with dry acetone and kept in vacuum for 24 h. (Found Sn 40.4 and Cl 71.9%; $C_3H_7O_3N_3SnCl$ requires Sn 41.2 and Cl 72.3%. Yield 67%.)

Resublimed iodine and potassium dichromate (BDH AnalaR) were used as such.

All the solids were weighed by difference and dissolved in a known volume of the solvent. Transference of the material was, as far as possible, carried out in a dry box. Potentiometric titrations were carried out with the help of a potentiometer (OSAW Vernier Potentiometer Cat. No. 30070) with an external scalamp galvanometer for end-point detection. A modified saturated calomel electrode with a capillary in the lower part which was blocked with asbestos fibre to avoid free flow of liquids was used as a reference electrode. A platinum electrode was used as the indicator electrode.

General procedure

The titration cell was flame-dried and flushed with dry nitrogen for 1 h. The cell was fitted with a micro-burette (5 ml) and the electrodes, and placed over a magnetic stirrer. The titrant and titrand (10 ml) were both prepared in formamide. After each addition of titrant, the mixture was stirred for some time and the change in e.m.f. of the solution was noted. During the titration, an atmosphere of dry nitrogen was maintained in the cell.

The strengths (moles/litre) of the various solutions used were as follows: (*a*) lead tetraformamide, 0.053 *M*; (*b*) chlorotin formamide, 0.093 *M*; (*c*) cerium(III) nitrate trihydrate, 0.05 *M*; (*d*) iodine, 0.07 *M*; (*e*) potassium dichromate, 0.052 *M*.

RESULTS AND DISCUSSION

Lead tetraformamide and trilead octaformamide are white solids which turn black on keeping in a sealed tube in the presence of light. They are sufficiently soluble in formamide to be used as oxidising agents. The solution of lead tetraformamide cannot be stored for more than 24 h, as it turns grey and loses its oxidising power. The solution of trilead octaformamide can be stored for a slightly longer time.

Lead tetraformamide as oxidising agent

When a solution of lead tetraformamide in formamide is titrated with a solution of tin(II), antimony(III) or arsenic(III) chlorides in the same solvent, there is a decrease in the e.m.f. of the solution which continues with addition of the reducing solution until a large drop in the potential appears when the molar ratio of lead tetraformamide to metal chloride reaches 1:1. Thereafter the change in e.m.f. gradually decreases and ultimately becomes constant (Fig. 1). Reverse titrations are also satisfactory. The product of solvolysis of tin(II) chloride and formamide, *i.e.* SnCl(HCONH)·2HCONH₂ is also oxidised by lead tetraformamide in formamide solution.

The curves for the titrations of tin(II) are shown in Fig. 2. These observations may be explained on the basis of the following redox reactions.

$$Pb^{4+} + Sn^{2+} \rightarrow Pb^{2+} + Sn^{4+}$$

$$Pb^{4+} + Sb^{3+} \rightarrow Pb^{2+} + Sb^{5+}$$

$$Pb^{4+} + As^{3+} \rightarrow Pb^{2+} + As^{5+}$$
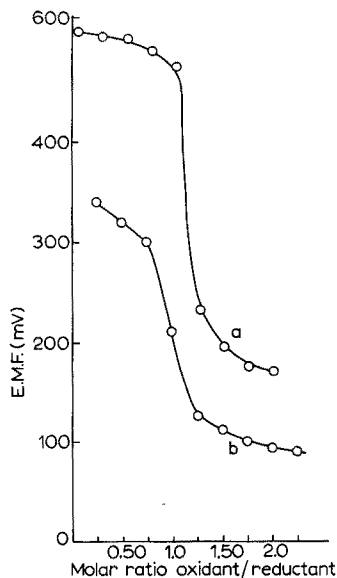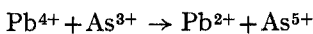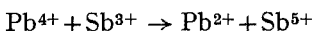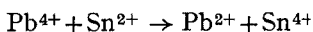
Fig. 1. Titration curves for lead tetraformamide $Pb(HCONH)_4$ (0.203 g) titrated with (a) 0.204 M $SbCl_3$, (b) 0.212 M $AsCl_3$.
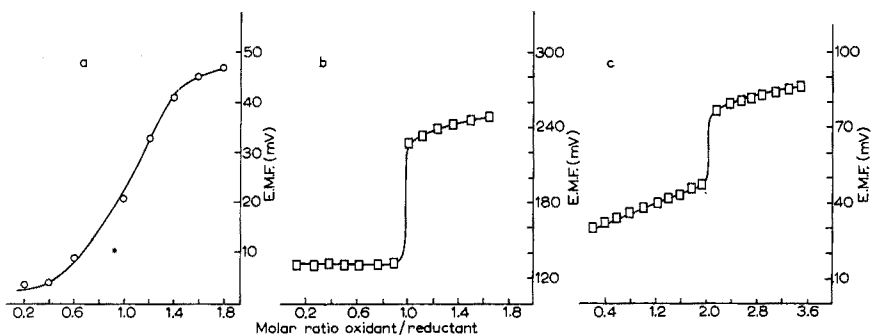

Fig. 2. Titrations with 0.053 M lead tetraformamide. (a) $SnCl_2$ (0.032 g); (b) $SnCl(HCONH)\cdot 2HCONH_2$ (0.065 g); (c) $Ce(NO_3)\cdot 3H_2O$ (0.072 g).

When a solution of lead tetraformamide in formamide is added to a solution of cerium(III) nitrate the potential shift at the end-point is again very sharp (Fig. 2c), but the end-point is observed at a cerium nitrate–lead tetraformamide molar ratio of 2:1, as would be expected by the reaction:

$$Pb^{4+} + 2Ce^{3+} \rightarrow Pb^{2+} + 2Ce^{4+}$$
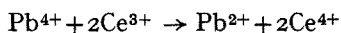
Typical potentiometric curves where trilead octaformamide acts as oxidising agent are shown in Fig. 3.

Most lead(IV) compounds are efficient oxidising agents. Lead tetraacetate, which is a solvolysed product of lead dioxide in glacial acetic acid has been used as an oxidising agent in acetic acid medium for a number of organic and inorganic compounds[4-6]. Lead tetraformamide and trilead octaformamide are the solvolysed products of lead dioxide and red lead in formamide and are soluble in it. Thus their oxidation reactions can be explained as above.
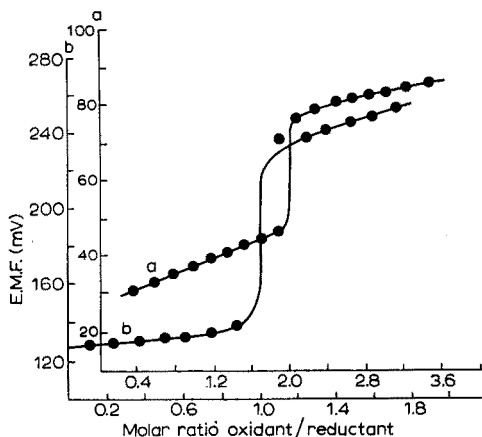
Fig. 3. Titrations with trilead octaformamide. (a) $SnCl(HCONH) \cdot 2HCONH_2$ (0.065 g) titrated with 0.093 M $Pb_3(HCONH)_8$; (b) $Ce(NO_3)_3 \cdot 3H_2O$ (0.1 g) titrated with 0.096 M $Pb_3(HCONH)_8$.

Iodine as oxidising agent

Iodine is fairly soluble in formamide. When an iodine solution in formamide is added to a solution of antimony(III) or arsenic(III) chloride in the same solvent, there is an increase in the e.m.f. of the system. The rate of change in e.m.f. is maximal at an iodine–metal chloride molar ratio of 1:2. The oxidation–reduction reactions obviously follow their normal courses, and have been found to proceed to completion in the presence of 0.5–1.0 g of dry sodium bicarbonate.

Iodine solution also oxidises tin(II) chloride and sodium thiosulphate in formamide and the end-point is indicated by a sharp change in the e.m.f. of the system at 1:2 and 1:1 molar ratios of iodine *versus* tin(II) or thiosulphate, respectively.

Typical titration curves are shown in Fig. 4.

Visual titrations with iodine. Iodine solutions in formamide have been found to be an excellent titrant in redox reactions and do not require any indicator. The end-point is detected by the appearance of a permanent faint yellow colour of iodine. Table I indicates the use of iodine solution for the titration of various reductants.

As in aqueous medium, the potentiometric as well as visual titrations with iodine as an oxidising agent in formamide require the presence of a small amount of sodium bicarbonate for the determination of arsenic and antimony.

Potassium dichromate

A solution of potassium dichromate in formamide has also been used to oxidise
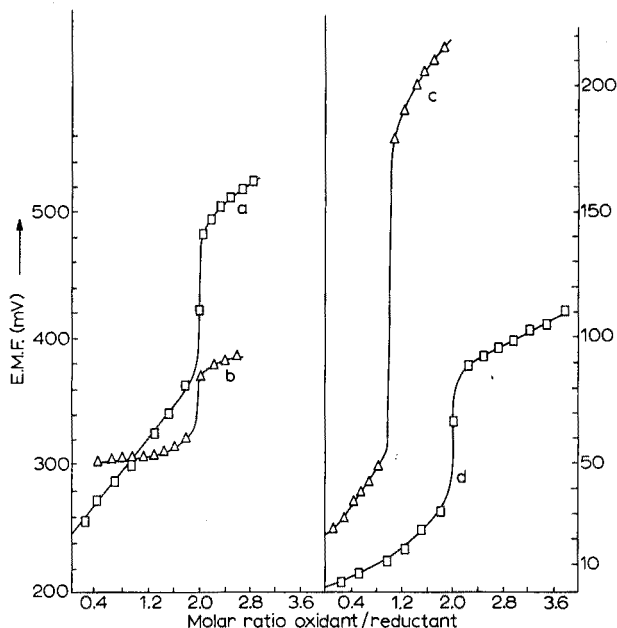
Fig. 4. Titrations with 0.07 M iodine. (a) $SnCl_2$ (0.1082 g); (b) $AsCl_3$ (0.0495 g); (c) $Na_2S_2O_3 \cdot 5H_2O$ (0.055 g); (d) $SbCl_3$ (0.055 g).

TABLE I

VISUAL TITRATIONS WITH IODINE SOLUTION IN FORMAMIDE

Compound	Wt. taken (g)	Vol. of I_2 soln. used (ml)	Vol. required (ml)	Errors
$SnCl_2$	0.084	9.02	8.96	+0.67
$AsCl_3$	0.079	5.8	5.9	−1.6
$SbCl_3$	0.025	2.0	1.98	+1
$Na_2S_2O_3$	0.04	1.4	1.4	0

arsenic(III), antimony(III) and tin(II) as chlorides. If the dichromate solution is titrated with the reductant, there is no perceptible change in e.m.f. of the solution in the beginning. On further addition, the e.m.f. of the solution begins to decrease until a big potential drop is observed as potassium dichromate/metal chloride molar ratio 1:3 is reached. Examples of such titration curves are given in Fig. 5. Examples of reverse titrations are shown in Fig. 6. The course of the reactions may be explained by the following equations:

$$2Cr^{6+} + 3Sn^{2+} \rightarrow 2Cr^{3+} + 3Sn^{4+}$$

$$2Cr^{6+} + 3As^{3+} \rightarrow 2Cr^{3+} + 3As^{5+}$$

$$2Cr^{6+} + 3Sb^{3+} \rightarrow 2Cr^{3+} + 3Sb^{5+}$$

$$Cr^{6+} + 3Fe^{2+} \rightarrow Cr^{3+} + 3Fe^{3+}$$
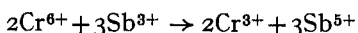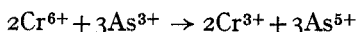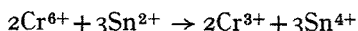
An oxidation–reduction reaction in formamide with the help of potassium
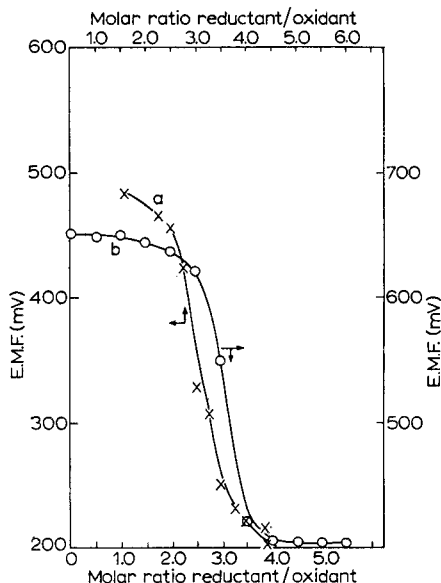
Fig. 5. Titration curves for potassium dichromate. (a) $K_2Cr_2O_7$ (0.07 g) titrated with 0.276 M $SbCl_3$; (b) $K_2Cr_2O_7$ (0.08 g) titrated with 0.281 M $AsCl_3$.
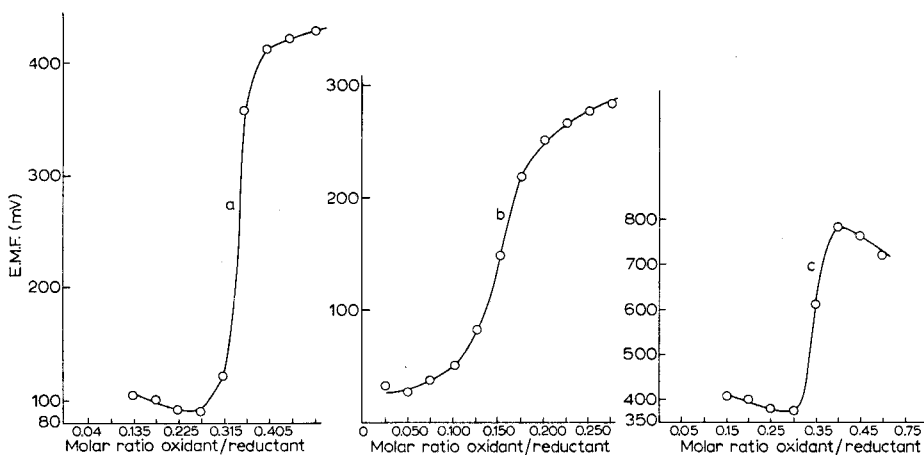
Fig. 6. Titrations with potassium dichromate. (a) $SnCl_2$ (0.5 g) with 0.275 M $K_2Cr_2O_7$; (b) $FeSO_4 \cdot$ $(NH_4)_2SO_4 \cdot 6H_2O$ (0.54 g) with 0.0918 M $K_2Cr_2O_7$; (c) $AsCl_3$ (0.5 g) with 0.218 M $K_2Cr_2O_7$.

dichromate is slightly different from the same reaction in aqueous medium as no mineral acid is required.

Potassium dichromate in formamide cannot be visually titrated with reducing agents as, unlike iodine solution, the colour change at the end-point is not sharp. Visual titrations with the help of internal indicators such as diphenylbenzidine have also not been successful.

SUMMARY

Lead tetraformamide and trilead octaformamide have been isolated and, along with iodine and potassium dichromate, have been used as oxidising agents for the determination of Sn^{2+}, As^{3+}, Sb^{3+}, Ce^{3+}, Fe^{2+} and $S_2O_3^{2-}$ ions in formamide media. The course of these oxidation–reduction reactions can be followed potentiometrically. Visual titrations without indicator are possible when iodine in formamide is used as the titrant.

RÉSUMÉ

On a pu isoler la tétraformamide et l'octaformamide de plomb. Ces deux composés peuvent être utilisés comme réactifs d'oxydation pour le dosage de Sn^{2+}, As^{3+}, Sb^{3+}, Ce^{3+}, Fe^{2+} et $S_2O_3^{2-}$ en milieu formamide. Il est possible de suivre ces réactions d'oxydo-réduction par potentiométrie. On peut aussi effectuer des titrages visuels sans indicateur lorsqu'on utilise l'iode pour le titrage en milieu formamide.

ZUSAMMENFASSUNG

Bleitetraformamid und Tribleioctaformamid wurden isoliert und zusammen mit Jod- und Kaliumdichromat als Oxidationsmittel zur Bestimmung von Sn^{3+}, As^{3+}, Sb^{3+}, Ce^{3+}, Fe^{2+} und $S_2O_3^{2-}$-Ionen in Formamid verwendet. Der Verlauf dieser Redox-Reaktionen kann potentiometrisch verfolgt werden. Visuelle Titrationen ohne Indikator sind möglich, wenn Jod als Titrationsmittel im Formamid verwendet wird.

REFERENCES

1 R. C. PAUL, K. C. MALHOTRA AND O. C. VAIDYA, *Ind. J. Chem.*, 4 (1966) 198.
2 R. C. PAUL AND O. C. VAIDYA, *Ind. J. Chem.*, 6 (1968) 151.
3 R. C. PAUL AND O. C. VAIDYA, *Ind. J. Chem.*, communicated.
4 J. R. HENERY AND L. D. ROBERT, *J. Org. Chem.*, 27 (1962) 4066.
5 G. PICCARDI, *Talanta*, 11 (1964) 1087.
6 I. M. KOLTHOFF AND R. BELCHER, *Volumetric Analysis*, Vol. 3, Interscience Publishers, New York, 1957.

SHORT COMMUNICATIONS

Reagents for the spectrophotometric determination of sulfhydryl groups over a wide wavelength range

It has recently been shown that 2,2'-dithiodipyridine and 4,4'-dithiodipyridine are excellent reagents for the determination of sulfhydryl groups, because of a shift in the ultraviolet spectrum on reaction with a thiol[1]. The reaction of these disulfides with thiols occurs as follows:
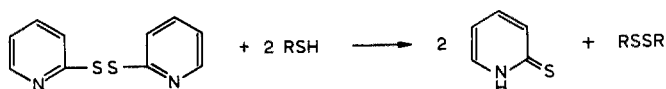
The pyridinethiol formed is virtually exclusively in the thiopyridone form; this fact has the double advantage of causing a shift in the ultraviolet spectrum and of making the reaction essentially irreversible. It has also been found that 6,6'-dithiodinicotinic acid is also suitable for the determination of sulfhydryl groups, and that it has the advantage of a higher solubility in buffers at near neutral pH than the two above-mentioned disulfides [2].

In certain cases, the sample material (*e.g.* certain complex biological materials) has its own absorption in the ultraviolet range, which may interfere with the determination of sulfhydryl by one of the reagents mentioned above. In order to expand the usable wavelength range, several additional heterocyclic disulfides capable of reacting with thiols with a shift of the absorption maxima were prepared and studied. The spectral characteristics of ten of these compounds, and those of the corresponding thiones, are reported in Table I. In addition to pyridine derivatives, Table I includes two disulfides of the pyrimidine series and one of the thiazole series; they all have the sulfur attached to a ring carbon atom, adjacent to a nitrogen. It is known that 2-mercaptopyrimidines[12] and 2-mercaptothiazoles[13] have a thionic and not a thiolic structure. Formation of the thione brings about the desired shift of absorption toward longer wavelengths.

By choosing the appropriate reagent among those listed in Table I, it is possible to carry out determinations of sulfhydryl groups at wavelengths extending from *ca.* 240 nm to *ca.* 430 nm, by following the formation of the reaction product (thione). It is also possible to follow the disappearance of the reagent in the range from 220 nm to *ca.* 340 nm.

Experimental

Determination of sulfhydryl groups. The procedure is described in detail in a previous publication[1]. A brief description follows. The material to be analyzed (0.015–0.5 μmole SH), in 1.5 ml of solvent, is mixed with 1.5 ml of a dilute solution of the disulfide (excess). The absorbance at the appropriate wavelength can be determined immediately after mixing in the case of simple thiols, or after appropriate delays in the case of proteins or other biological materials.

TABLE I

REAGENTS FOR THE DETERMINATION OF SULFHYDRYL GROUPS

Reagent	Preparation (see ref.)	Solvent[a]	Reagent		Product[b]		Useful wavelengths (nm)[c]	
			λ (nm)	ε	λ (nm)	ε	A	B
I 2,2′-Dithio-bis (pyridine-N-oxide)	4	KRP	234 (max) 290 (min) 295 (max)	$4.3 \cdot 10^4$ $5.4 \cdot 10^3$ $5.6 \cdot 10^3$	244 (max) 262 (min) 282 (max) 305 (min) 332 (max)	$2.5 \cdot 10^4$ $5.3 \cdot 10^3$ $1.2 \cdot 10^4$ $2.6 \cdot 10^3$ $4.2 \cdot 10^3$	234 (220–235) (260–265)	244 (240–255) 282 (270–295) 332 (315–350)
II 2,2′-Dithio-bis (4-carboxypyridine)	5	KRP	267 (min) 300 (max)	$4.6 \cdot 10^3$ $8.2 \cdot 10^3$	245 (min) 273 (max) 305 (min) 365 (max)	$3.9 \cdot 10^3$ $1.1 \cdot 10^4$ $1.0 \cdot 10^3$ $6.0 \cdot 10^3$	(235–245) 300 (295–315)	273 (255–290) 365 (325–420)
III 2,2′-Dithio-bis (5-amidopyridine)	6	KRP	252 (max) 272 (min) 291 (max)	$1.9 \cdot 10^4$ $1.5 \cdot 10^4$ $1.9 \cdot 10^4$	250 (min) 306 (max)	$1.1 \cdot 10^3$ $1.1 \cdot 10^4$	252 (220–270)	(285–390)
IV 2,2′-Dithio-bis (5-aminopyridine)	—[d]	KRP	225 (min) 253 (max) 290 (min) 311 (max)	$1.0 \cdot 10^4$ $2.0 \cdot 10^4$ $9.1 \cdot 10^3$ $1.0 \cdot 10^4$	230 (min) 279 (max) 309 (min) 371 (max)	$4.4 \cdot 10^3$ $1.6 \cdot 10^4$ $1.0 \cdot 10^3$ $7.1 \cdot 10^3$	253 (220–265) 311 (295–340)	279 (270–290) 371 (355–400)
V 2,2′-Dithio-bis (5-acetamidopyridine)	7	Methanol– KRP (9:1)	224 (min) 260 (max) 286 (min) 299 (max)	$9.8 \cdot 10^3$ $3.2 \cdot 10^4$ $1.4 \cdot 10^4$ $1.6 \cdot 10^4$	262 (min) 298 (max) 328 (min) 374 (max)	$2.7 \cdot 10^3$ $2.0 \cdot 10^4$ $3.1 \cdot 10^3$ $7.4 \cdot 10^3$	260 (235–275)	298 (285–420) 374
VI 2,2′-Dithio-bis (5-cyanopyridine)	—[e]	Ethanol– KRP (9:1)	225 (min) 260 (max) 276 (min) 294 (max)	$6.4 \cdot 10^3$ $1.8 \cdot 10^4$ $1.3 \cdot 10^4$ $1.7 \cdot 10^4$	248 (min) 322 (max)	$1.4 \cdot 10^3$ $1.8 \cdot 10^4$	260 (235–295)	322 (305–420)
VII 2,2′-Dithiodiquinoline	9	Methanol– KRP (9:1)	232 (min) 252 (max) 300 (min) 320 (max) 326 (min) 332 (max)	$3.2 \cdot 10^4$ $5.1 \cdot 10^4$ $7.6 \cdot 10^3$ $1.3 \cdot 10^4$ $1.2 \cdot 10^4$ $1.6 \cdot 10^4$	234 (min) 276 (max) 314 (min) 384 (max)	$3.1 \cdot 10^3$ $2.1 \cdot 10^4$ $1.3 \cdot 10^3$ $1.3 \cdot 10^4$	252 (225–260) 320 (310–335)	276 (265–300) 384 (340–430)

			Solvent	A[c]		B[c]			
VIII	2,2'-Dithiodipyrimidine	6	Methanol–KRP (9:1)	238 (max)	$1.9 \cdot 10^4$	242 (min) 277 (max)	$1.4 \cdot 10^3$ $1.6 \cdot 10^4$	238 (225–250)	277 (260–340)
IX	2,2'-Dithio-bis (6-methylpyrimidine)	6	Methanol–KRP (9:1)	239 (max)	$1.9 \cdot 10^4$	242 (min) 278 (max)	$1.6 \cdot 10^3$ $1.6 \cdot 10^4$	239 (230–250)	278 (260–350)
X	2,2'-Dithio-bis (4-methylthiazole)	10	Methanol–KRP (9:1)	240 (min) 272 (max)	$3.8 \cdot 10^3$ $8.1 \cdot 10^3$	265 (min) 316 (max)	$9.0 \cdot 10^2$ $1.1 \cdot 10^4$	272 (220–290)	316 (300–330)

[a] KRP = Krebs–Ringer phosphate buffer, pH 7.4, prepared as described in ref. 3.

[b] A solution of the thione product was obtained by adding about 50% excess of cysteine to a solution of the disulfide; this solution was used to obtain the spectral data recorded. In each case the spectrum of the pure thione was also determined separately, and found to be the same as that of the reaction product. This comparison could not be done with the thione of IV, which, owing to its ease of oxidation in air, was not obtained in a sufficiently pure form. The thiones corresponding to disulfides I, VII, VIII and IX were commercial products. The remaining thiones were prepared according to the reference given in parenthesis: II(5), III(8), V(7), VI(8), X(10).

[c] The values given in column A correspond to disappearance of the reagent and in column B to the formation of the product. The values correspond to the peaks and are followed, in parenthesis, by the range of wavelengths within which accurate determinations can be made. The limits of the range were arbitrarily set for each compound at the wavelength at which the difference in molar absorptivity between disulfide and thione was about 1,000. This was considered the minimum usable difference.

[d] See *Experimental*. This compound (IV) tends to give low SH values if the determination is carried out in air, owing to the ease of oxidation of the corresponding thione.

[e] See *Experimental*. The compound has been tested as an antibacterial by DE COURCY et al.[11].

Preparation of 2,2'-dithio-bis(5-aminopyridine) (IV). 7.0 g of 2-mercapto-5-acetylaminopyridine[7] was refluxed for 10 minutes with 24 ml of concentrated hydrochloric acid and 24 ml of water. After cooling and filtering, the filtrate was made alkaline with sodium bicarbonate. The resulting dark solid was filtered off and recrystallized from isopropanol–water (1:1). Yield: 4.0 g (76%). M.p. 175–176°. (Calcd. for $C_{10}H_{10}N_4S_2$: 47.97% C, 4.02% H; found: 48.09% C, 4.05% H.)

Preparation of 2,2'-dithio-bis(5-cyanopyridine) (VI). 0.5 g of 2-mercapto-5-cyanopyridine was dissolved in 50 ml of 0.1 N sodium hydroxide and oxidized at room temperature by slow addition of a solution of iodine in aqueous potassium iodide. The addition was continued until the color of the iodine was no longer discharged. The product precipitated and was collected by filtration. The yield was quantitative. After crystallization from 95% ethanol, the melting point was 178–180°. (Calcd. for $C_{12}H_6N_4S_2$: 53.32% C, 2.24% H; found: 53.25% C, 2.45% H.)

Arequipa Foundation,   D. R. GRASSETTI
Russ Building,   J. F. MURRAY, JR.
631 Hearst Avenue,
Berkeley, Calif. 94710 (U.S.A.)

1 D. R. GRASSETTI AND J. F. MURRAY, JR., *Arch. Biochem. Biophys.*, 119 (1967) 41.
2 D. R. GRASSETTI, J. F. MURRAY, JR. AND H. T. RUAN, *Biochem. Pharmacol.*, in press.
3 W. W. UMBREIT, R. H. BURRIS AND J. F. STAUFFER, *Manometric Techniques*, 3rd Edn., Burgess, Minneapolis, 1957, p. 149.
4 *German Patent 1,224,744*, Sept. 15, 1966 (Olin-Matheson Chem. Corp.).
5 H. H. FOX AND J. T. GIBAS, *J. Org. Chem.*, 23 (1958) 64.
6 D. R. GRASSETTI, J. F. MURRAY, JR., M. E BROKKE AND A. D. GUTMAN, *J. Med. Chem.*, 10 (1967) 1170.
7 W. T. CALDWELL AND E. C. KORNFELD, *J. Am. Chem. Soc.*, 64 (1942) 1695.
8 H. S. FORREST AND J. WALKER, *J. Chem. Soc.*, (1948) 1942.
9 T. KAMETANI, K. FUKUMOTO AND O. UMEZAWA, *Japan. J. Pharm. & Chem.*, 31 (1959) 132; *Chem. Abstr.*, 54 (1960) 11019 a.
10 E. R. BUCHMAN, A. O. REIMS AND H. SARGENT, *J. Org. Chem.*, 6 (1941) 764.
11 S. J. DE COURCY, JR., F. E. REINHART AND W. G. BATT, *J. Franklin Inst.*, 263 (1957) 557.
12 J. R. MARSHALL AND J. WALKER, *J. Chem. Soc.*, (1951) 1004.
13 Y. N. SHEINKER, I. Y. POSTOVSKII AND N. I. VORONINA, *Zh. Fiz. Khim.*, 33 (1959) 302; *Chem. Abstr.*, 54 (1960) 4147 c.

Effects of borate on absorbance of carbohydrates mixed with the phenol–sulfuric acid reagent

A recent report from these laboratories[1] described the effects of borate on the determination of a limited number of carbohydrates by the phenol–sulfuric acid method[2]. Further studies reported here indicate a relation between carbohydrate structure and borate effect and the possible use of that effect in determining the presence of certain carbohydrates in a mixture.

Experimental

Materials. Most of the carbohydrates used were analytically pure reagents from Nutritional Biochemicals Corp., Cleveland, Ohio. The more common pentoses and hexoses were from several manufacturers. Starch and pentosans were prepared from wheat flour. The starch was purified by repeated washing and centrifugation. The pentosan was isolated from an aqueous extract of flour, and purified by DEAE–cellulose column chromatography. Water-soluble starch in the pentosan-rich fraction was removed by hydrolysis with twice-recrystallized pancreatic α-amylase followed by dialysis[3].

Methods. The procedure has been described previously[1]. In all experiments reported here, 1 ml of water (or 0.125 M borate), 1 ml of a solution containing 50–300 μg of carbohydrate, 1 ml of 5% phenol, and 5 ml of concentrated sulfuric acid were used.

Results

Effects of borate on the colorimetric determination of carbohydrates are summarized in Table I. Addition of borate had no significant effect on the absorbance of any of the investigated monoketoses, on diacetone fructose, or on the fructan inulin. Decrease in absorbance in mono-, di-, and polyglucoses was essentially uniform and ranged from 9.5 to 13.9%. The effect on galactose was similar to that on glucose. Mannose was affected more than either glucose or galactose. In mannose, the hydroxyl group at the C-2 position is axially oriented in the preferred conformation, while it is equatorially oriented in galactose and glucose. It would seem that an axial hydroxyl group at C-2 enhances the borate effect. Such an effect was not noted in aldopentoses. However, the conformation analogous to mannose does not really exist in the aldopentoses. D-Lyxose would be the aldopentopyranose having an axial 2-hydroxyl group, but it appears to exist as an equilibrium between the C-1 and 1-C conformations[4].

The absorbance of the four aldopentoses (arabinose, lyxose, ribose, and xylose) was depressed significantly by borate. D-Xylose was comparable to L-xylose; and the absorbance-lowering effect on pentosans was similar to the effect on pentoses in magnitude.

The effect on oligosaccharides composed of various hexoses depended on the component monosaccharides and probably on their linkage. Thus, in disaccharides composed of the aldohexoses, galactose and glucose (lactose and melibiose), absorbance reduction was 10.3% and 12.2%, respectively. In disaccharides containing fructose and glucose (sucrose and furanose) and in commercial invert sugar, absorbance was reduced only about 5%. A similar intermediate effect was observed in the tri-

TABLE I

EFFECTS OF 0.125 M BORATE ON ABSORBANCE OF CARBOHYDRATES ASSAYED BY THE PHENOL–SULFURIC ACID METHOD

Carbohydrate	Carbohydrate level (μg per ml)	Wavelength of maximum absorbance (nm)	Absorbance reading		Absorbance decrease (%)
			without borate	with borate	
D-Fructose	50	490	0.53	0.53	—
Diacetone fructose	50	490	0.32	0.32	—
Inulin	50	490	0.56	0.56	—
L-Sorbose	50	490	0.47	0.47	—
D-Sedoheptulose hydrate	50	490	0.55	0.54	—
D-Mannoheptulose	50	490	0.55	0.54	—
D-Glucose	50	490	0.46	0.41	10.9
Maltose hydrate	50	490	0.42	0.37	11.9
Isomaltose	50	490	0.52	0.45	13.5
Cellobiose	50	490	0.46	0.41	10.9
Trehalose	50	490	0.42	0.38	9.5
Gentiobiose	50	490	0.40	0.36	10.0
Methyl-α-D-glucoside	50	490	0.40	0.35	12.5
Glucose-1-PO₄ (K salt)	125	490	0.46	0.40	13.0
α-D-Glucose pentacetate	100	490	0.26	0.26	—
2-Deoxy-D-glucose	50	490	0.54	0.53	—
Salicin	100	490	0.57	0.50	12.3
Dextrin	50	490	0.39	0.34	12.8
Glycogen	50	490	0.37	0.32	13.5
Starch	50	490	0.36	0.31	13.9
D-Galactose	50	490	0.35	0.31	11.4
L-Fucose	50	480	0.23	0.20	13.0
2-Deoxy-D-galactose	50	480	0.55	0.55	—
D-Mannose	50	490	0.37	0.30	18.9
Methyl-α-D-mannoside	50	490	0.36	0.29	19.4
L-Rhamnose	100	480	0.75	0.64	14.7
D-Arabinose	50	480	0.37	0.30	18.9
D-Lyxose	50	480	0.50	0.40	20.0
D-Ribose	50	480	0.64	0.52	18.8
2-Deoxy-D-ribose	50	500	0.44	0.45	—
D-Xylose	50	480	0.52	0.41	21.2
Methyl-β-D-xyloside	50	480	0.39	0.31	20.5
Xylan	50	480	0.36	0.29	19.4
Pentosan	50	480	0.30	0.25	16.7
Lactose hydrate	50	490	0.39	0.35	10.3
Melibiose hydrate	50	490	0.41	0.36	12.2
Sucrose	50	490	0.50	0.48	4.0
Furanose	50	490	0.54	0.51	5.6
Raffinose hydrate	50	490	0.42	0.40	4.8
Melezitose hydrate	50	490	0.51	0.47	7.8
Stachyose	50	490	0.34	0.32	5.9

saccharide, raffinose, and in the tetrasaccharide, stachyose. Absorbance of the trisaccharide melezitose was reduced by borate somewhat more than that of raffinose solutions, though they would be expected to be affected to a similar extent. The

difference is probably attributable to the difference in linkages and sequences of the component monosaccharides in the two trisaccharides.

Essentially no color developed when the phenol–sulfuric acid reagent was added (in the presence or absence of borate) to up to 300 μg per ml of straight-chain tri- to hexa-hydric alcohols (glycerol, erythritol, adonitol, arabitol, dulcitol, and sorbitol) or to the cyclic hexahydric alcohol, inositol.

Substitution of the hemiacetal group on carbon-1 in glucose [methyl glucoside, glucose-1-phosphate, or salicin (saligenin-D-glucopyranoside)], in mannose (methyl mannoside), and in xylose (methyl xyloside) did not affect the absorbance-depressing effect of borate when compared to the unsubstituted sugars.

Similarly, in deoxy-sugars in which substitution was made at position 6 (fucose and rhamnose), absorbance was significantly reduced in the presence of borate. However, if the hydroxyl group at position 2 on the carbohydrate molecule was substituted (the 2-deoxypyranoses of glucose and galactose and the 2-deoxy-furanose of ribose), the absorbance-depressing effect of borate was eliminated. Whereas borate had no effect on absorbance decrease at low concentrations of glucose pentacetate (Table I), a small though inconsistent effect was observed at higher concentrations.

Absorbance of glucosamine solutions to which the phenol–sulfuric acid reagent was added, was substantially lower than the absorbance of solutions containing glucose. However, adding borate to glucosamine solutions substantially increased the absorbance. The increase in absorbance from adding borate to solutions containing 300 μg per ml of carbohydrate, was from 0.13 to 0.66 in D-glucosamine hydrochloride, and from 0.49 to 0.63 in D-glucosamine, free base. A similar increase was observed in the trioses dihydroxyacetone (from 0.16 to 0.18) and D-glyceraldehyde (from 0.48 to 1.14).

The fact that borate has no significant effect on ketoses and lowers significantly the absorbance of solutions containing aldoses, points to the possibility of determining the presence of the sugars in a mixture. A similar procedure could also be developed for determining the presence of ribose and deoxyribose, though in this case the re-latively large difference in wavelength of maximum absorbance must be considered.

Kansas State University,   R. D. DAFTARY
Department of Grain Science and Industry   Y. POMERANZ*
and Crops Research Division,
Agricultural Research Service,
U. S. Department of Agriculture,
Manhattan, Kansas 66502 (U.S.A.)

1 F. M. LIN AND Y. POMERANZ, *Anal. Biochem.*, 24 (1968) 128.
2 M. DUBOIS, K. A. GILLES, J. K. HAMILTON, P. A. REBERS AND F. SMITH, *Anal. Chem.*, 28 (1956) 350.
3 W. KUNDIG, H. NEUKOM AND H. DEUEL, *Helv. Chim. Acta*, 44 (1961) 823.
4 D. R. LINEBACK, Private communication (11-1-1968).

* Present address: National Barley & Malt Laboratory, U.S.D.A., A.R.S., C.R.D. Madison, Wisc. 53705 (U.S.A.)

Spectrophotometric determination of iron in high-purity yttrium oxide with 1-(2-pyridylazo)-2-naphthol

The growing importance of rare-earth metals in electronics, nuclear chemistry and metallurgy has necessitated the development of methods for their rapid and sensitive determination on the microgram scale; it has also necessitated the development of very sensitive methods for trace impurities in high-purity rare-earth materials. The object of the study described in this paper was to adapt the previously described spectrophotometric method for iron in pure solution and clays with 1-(2-pyridylazo)-2-naphthol (β-PAN)[1-3] to the determination of iron in high-purity yttrium oxide. Recently, the β-PAN method has been applied to the determination of iron in molybdenum and tungsten[4] metals, and high-purity gallium[5].

Apparatus and reagents

Standard solution of iron(III). This was prepared by dissolving 1.000 g of pure metal (99.99% Johnson Matthey) in a little concentrated hydrochloric acid and diluting to 1 l with redistilled water.

Standard solution of yttrium. This was prepared by dissolving the pure oxide (99.99% Johnson Matthey) in hydrochloric acid and diluting to give a 1 mg/ml solution.

β-PAN solution. A 0.2% (w/v) solution was prepared by dissolving 200 mg of β-PAN (Dozin Kagaku, Kumamoto, Japan) in pure methanol.

Buffer solutions. Potassium chloride–hydrochloric acid and sodium acetate–acetic acid buffers were used for the pH adjustment.

Organic solvents were purified by the usual methods. All other reagents used were prepared from analytical-grade chemicals or from purified materials and the solutions were prepared with redistilled water.

All measurements were made with a Model EPS 3T Hitachi recording spectrophotometer and EPU-2A Hitachi spectrophotometer with 1-cm cells. A Yanagimoto 42A type pH meter was used.

Recommended procedure

Weigh a 0.2-g sample of well-dried yttrium oxide (which contains at least 1 μg of iron) and transfer to a 100-ml tall beaker. Add 5–10 ml of 1 + 1 hydrochloric acid, cover with a watch glass, and heat to dissolve. After evaporation of excess of hydrochloric acid, add 10 ml of water. Transfer the solution to a 60-ml separatory funnel. Finally wash the original beaker with small portions of redistilled water, and add to the funnel. The total volume of aqueous solution should be less than 20 ml. Then, add 4.0 ml of 0.2% β-PAN methanolic solution, and 10 ml of pH 4 acetate buffer, and shake vigorously for a few minutes. After 15 min, add 10.0 ml of chloroform and shake vigorously for 1 min. Drain the organic layer into a small stoppered conical flask and dry with anhydrous sodium sulfate. Measure the absorbance at 770 nm in a 1-cm cell against a reagent blank.

Results and discussion

Absorbance curve. The absorbance curve of the iron(III) complex with β-PAN in chloroform is shown in Fig. 1. The iron complex shows its absorbance maximum at a very much longer wavelength than those of other β-PAN complexes.

Effect of pH in the presence of large amounts of yttrium. A series of solutions containing 1 p.p.m. of iron, 0.5 g of yttrium oxide and 2 ml of 0.2% β-PAN solution was prepared at different pH values. An absorbance plateau was found over the pH range 3.3–5 and the optimum pH range was 3.5–4.5. It is preferable to choose a low pH value in order to ensure avoidance of the reaction between yttrium and β-PAN which occurs in basic medium (above pH 7).
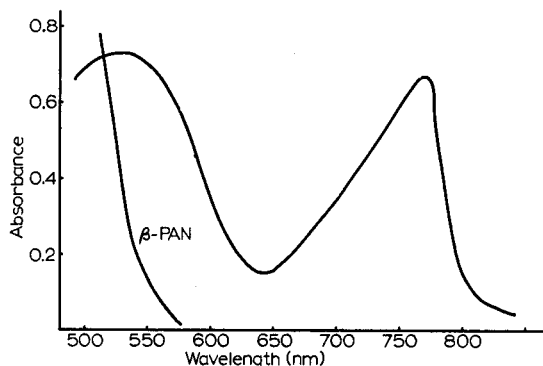
Fig. 1. Absorbance curve of iron(III)–β-PAN complex in chloroform against a reagent blank. 2 p.p.m. iron, extracted from pH 4.0 aqueous solution.

Effect of reagent concentration. Generally 2 ml of 0.2% reagent solution was satisfactory for up to 3 p.p.m. of iron. In the presence of large amounts of yttrium oxide, the addition of a large excess of reagent accelerates the reaction.

Colour development and stability. The minimum time of standing before extraction with chloroform for complete colour development of the iron complex was 10 min at room temperature (15–30°). The colour of the chloroform extract was very stable and suitable for quantitative work.

Effect of yttrium oxide. The absorbance at pH 4 of a series of solution, each containing 10 μg of iron with varying amounts of yttrium oxide, was measured in order to study any effect of the major component. The results indicated that at least 0.5 g of yttrium oxide did not interfere with the absorbance of iron complex (see Table I).

Beer's law. The absorbance of the chloroform extract of the iron–β-PAN complex conformed to Beer's law up to *ca.* 3 p.p.m. of iron.

Diverse ions. The effects of diverse ions on the reaction have already been reported in detail[1]. The amounts of calcium, magnesium, silica, lead, copper, titanium,

TABLE I

EFFECT OF YTTRIUM OXIDE

Y_2O_3 added (g)	Absorbance at 770 nm	Y_2O_3 added (g)	Absorbance at 770 nm
Nil	0.300	0.3	0.310
0.1	0.305	0.4	0.312
0.2	0.300	0.5	0.290

tantalum, nickel and rare-earth metals normally contained in high-purity yttrium oxide do not interfere. Even in the presence of other impurities which form chloroform-extractable β-PAN complexes, iron can be determined without interference because of its characteristic absorbance maximum at long wavelength.

TABLE II

DETERMINATION OF IRON IN SYNTHETIC SAMPLES

Y_2O_3 taken (g)	Iron (μg)		
	Taken	Found	Error
0.200	2.5	2.7	+ 0.2
0.200	5.0	5.2	+ 0.2
0.200	10.0	10.1	+ 0.1
0.500	2.5	2.4	− 0.1
0.500	5.0	4.8	− 0.2
0.500	10.0	9.7	− 0.3

TABLE III

DETERMINATION OF IRON IN COMMERCIAL YTTRIUM OXIDE

Commercial yttrium oxide	Iron (p.p.m.)	
A 99.9%	5.0 5.1 5.0	5.0
B 99.9%	4.3 4.5 4.2	4.3

Determination of iron in yttrium oxide. Samples of yttrium oxide which contained known amounts of iron were obtained, to assess the validity of the recommended procedure. Typical results are shown in Table II. The results are in excellent agreement over a wide range of iron contents.

Several commercial samples of high-purity yttrium oxide were also analyzed. Typical results are shown in Table III.

Government Industrial Research Institute,   SHOZO SHIBATA
Hirate-machi, Kita-ku,   KAZUO GOTO
Nagoya (Japan)   RYOZO NAKASHIMA

1 S. SHIBATA, *Anal. Chim. Acta*, 23 (1960) 434.
2 S. SHIBATA, *Anal. Chim. Acta*, 25 (1961) 348.
3 R. PÜSCHEL, *Z. Anal. Chem.*, 221 (1966) 132.
4 R. PÜSCHEL, E. LASSNER AND K. KATZENGRUBET, *Chemist-Analyst*, 56 (1967) 63.
5 V. P. SHVEDOV AND O. KLUG, *Chem. Anal. (Warsaw)*, 11 (1966) 237.

Hydrous manganese dioxide as a selective "collector" for gallium
Part I. The quantitative coprecipitation of gallium

The first use of manganese dioxide as a precipitant in analytical chemistry is ascribed to BLUMENTHAL[1] who used it in 1928 for separation of antimony. Since that time, publications have appeared sporadically, dealing with the use and the property of this collector. For example, it has been used for precipitation of bismuth[2], as a general scavenger for fission products[3], and for concentration of some trace elements from sea water[4]. TANAKA[5] found that manganese dioxide was superior to iron(III) hydroxide for the precipitation of molybdenum, and SUGAWARA et al.[6] used it for concentration and determination of molybdenum from sea water. This collector has also been used to concentrate niobium from plants in biogeochemical investigations[7] and to separate niobium from titanium, tungsten, molybdenum and chromium[8]. Radioactive isotopes have been coprecipitated with it[9], and the adsorption of strontium has been studied[10,11].

During the last few years, manganese dioxide has become more frequently applied. It has been used to concentrate radionuclides from sea water[12], to precipitate molybdenum[13], to collect antimony and tin selectively in the presence of lead[14], and to separate traces of antimony and tin from bismuth[15]. Manganese dioxide has also been utilized to concentrate cobalt[16], to collect molybdenum and tungsten from sea water[17], and to precipitate copper and zinc[18]. All these works indicate that manganese dioxide is not only an effective nonspecific adsorbent[7] but also a selective "collector" for a large number of elements.

This paper describes investigations on the coprecipitation of gallium with hydrous manganese dioxide. Gallium is a typical dispersed element which principally occurs as a substituent in minerals and rocks. A very minute quantity of gallium is contained in certain biomaterial and in some solid-state electronic devices and it is often necessary to concentrate it before determination. For industrial purposes the concentration of gallium is also of significant importance. Other problems which may be connected with coprecipitation of gallium with manganese dioxide, are related to the geochemistry of terrestrial manganese ores[19] and oceanic manganese sediments (manganese nodules)[20]. In this paper are presented the conditions under which gallium can be quantitatively precipitated on the manganese dioxide. Preliminary experiments showed that gallium may be quantitatively separated from aluminium and zinc, with which elements gallium predominantly occurs in nature.

Information about the coprecipitation of gallium is limited. Precipitation with sulphides was first described by the discoverer of gallium, LECOQ DE BOISBAUDRAN[21], and later by other workers[22-25]. Coprecipitation of gallium with aluminium and iron(III) hydroxides has been investigated[26,27], and calcium phosphate has also been used[28]. No prior use seems to have been made of manganese dioxide. The tendency for gallium compounds to hydrolyze at relatively high acidity (pH = ca. 3.0) suggested firstly examination of the behaviour of gallium in solutions of different acidity in the presence of active manganese dioxide, and secondly the possibility of separating gallium from other elements, especially from aluminium and zinc, which have a pH range of hydrolysis sufficiently different from that of gallium (Al = 5.0; Zn = 6.0). Experiments established that the precipitation of gallium with manganese dioxide was quantitative even at higher acidities than at pH 3.0, namely at pH 1.5–1.6, and preli-

minary observations showed that in this range gallium is separable from aluminium and zinc. These studies are in progress and will be reported in a later paper.

The amount of gallium used for precipitation varied from 0.5 μg to 1 mg. Of the different methods of preparation of active manganese dioxide, the reaction between manganese(II) sulphate and potassium permanganate in a hot solution was most effective and simplest and hence was used throughout.

Apparatus and reagents

Radiometer: Titrator type TTT1 for pH determination.

Unicam S.P. 600 spectrophotometer.

Standard gallium solutions were prepared in 1:1 hydrochloric acid in three concentrations: 1 ml = 100 μg Ga, 10 μg Ga, or 1 μg Ga.

Procedure

A series of solutions containing 0.5, 1.0, 10, 25, 50, 100 and 1000 μg of gallium was prepared and treated in the following way. Place 200 ml of distilled water in a 400-ml beaker and add the selected gallium amount from gallium standards; add 5 ml of 5% (w/v) manganese(II) sulphate and adjust the pH to 1.5–1.6 with 1:1 hydrochloric or sulphuric acid. If the acidity of the solution is too high, adjust with aqueous 10% sodium hydroxide. Heat the solution to boiling, add slowly *ca.* 2.5 ml of 1.25 N potassium permanganate and allow the solution to boil for 5–7 min. Allow the solution to stand for 1–2 min and then filter the precipitated manganese dioxide through an 11-cm Whatman No. 40 filter paper. Wash the precipitate with warm wash solution (water adjusted to pH 2.5 with hydrochloric or sulphuric acid) and transfer the precipitate with a stream of water into a 150-ml Vitreosil dish. Dissolve the remaining manganese dioxide on the filter paper in 10 ml of 5% hydrochloric acid containing 8–10 drops of 30% hydrogen peroxide, by allowing the warmed solution to run down the sides of the filter paper. Evaporate the contents of the dish to dryness on the water bath, add *ca.* 5 ml of concentrated hydrochloric acid and repeat the evaporation. To the dry residue add 5 ml of 6 N hydrochloric acid and after heating for 2 min on the water bath, transfer the solution to a calibrated flask and dilute to the mark with 6 N hydrochloric acid. (Use calibrated flasks of such volumes that the amount of gallium will be 0.25–5 μg per 5 ml of solution.)

Spectrophotometric determination of gallium

The method used is similar to that described by SANDELL[29]. To a 25-ml glass-stoppered test tube, add from the standard gallium solution the amount of gallium in 5 ml equal to that used for precipitation. Use as a blank 5 ml of 6 N hydrochloric acid in another test tube. To the blank, standard and test solutions (5 ml), add 0.5 ml of 15% titanium(III) chloride solution and 0.5 ml of concentrated hydrochloric acid, and allow to stand for 10 min. Add 0.4 ml of 0.5% rhodamine B solution, mix, add 5 ml of

TABLE I

PERCENTAGE ADSORPTION OF GALLIUM ON MANGANESE DIOXIDE AS A FUNCTION OF pH

pH	1.0	1.2	1.3	1.4	1.5	1.6
Gallium coprecipitation (%)	45	70	70	83	100	100

TABLE II

SPECTROPHOTOMETRIC DETERMINATION OF GALLIUM AFTER COPRECIPITATION WITH MANGANESE DIOXIDE

Ga added (µg)	Ga found[a] (µg)	Average error[b] (µg)	Ga added (µg)	Ga found (µg)	Average error (µg)
0.5	0.56	0.05	50.0	49.9	0.4
1.0	1.04	0.04	100.0	100.0	0.1
10.0	9.90	0.3	1000.0	999.0	2.0
25.0	24.6	0.2			

[a] Average of 4 determinations.
[b] Average deviation from mean.

benzene–diethyl ether solution (3:1), shake for 2 min and allow to stand for 30 min. Measure the absorbance of the organic layers at 565 nm in a 1-cm cell.

Results

The dependence of coprecipitation of gallium with manganese dioxide on the pH of the solution is shown in Table I. Quantitative coprecipitation was achieved at pH 1.5–1.6.

The results of photometric determination of gallium are given in Table II.

Geology Department,   V. S. BISKUPSKY
University of Melbourne,
Melbourne (Australia)

1 H. BLUMENTHAL, *Z. Anal. Chem.*, 74 (1928) 33; *Chem. Abstr.*, 22 (1928) 2896.
2 S. KALLMAN AND F. PRESTIRA, *Ind. Eng. Chem., Anal. Ed.*, 13 (1941) 8.
3 H. GEST AND L. E. GLENDENIN, *Natl. Nucl. Energy Ser. Div. IV*, 9; *Radiochem. Studies*, Book I (1951) 170.
4 K. B. KRAUSKOPF, *Geochim. Cosmochim. Acta*, 9 (1950) 1.
5 M. TANAKA, *Mikrochim. Acta*, (1958) 204.
6 K. SUGAWARA, M. TANAKA AND S. OKABE, *Bull. Chem. Soc. Japan*, 32 (1959) 221.
7 N. A. TYUTINA, V. B. ALESKOVSKY AND P. I. VASIL'EV, *Geochemistry International*, 6 (1959) 668.
8 V. M. DOROSH, *Sbornik Nauch. Trudov, Irkutskiĭ Nauch.-Issledovatel. Inst. Redkikh Metal.* (8) (1959) 38; *Chem. Abstr.*, 55 (1961) 26839b; *Anal. Chem.*, 23 (1951) 1813.
9 V. V. PUSHKAREV, E. V. TKACHENKO, YU. V. EGOROV AND A. S. LYUBINOV, *Radiokhimiya*, 1, 4 (1962) 49.
10 E. V. TKACHENKO, V. V. PUSHKAREV AND YU. V. EGOROV, *Izv. Vysshikh Uchebn. Zavedenii, Khim. i Khim. Tekhnol.*, 5 (1) (1962) 172.
11 YU. V. EGOROV, E. I. KRILOV AND E. V. TKACHENKO, *Kolloidn. Zh.*, 24 (1962) 159.
12 N. YAMAGATA AND K. IWASHIMA, *Nature*, 200 (1963) 52.
13 R. W. BACHMANN AND C. R. GOLDMANN, *Limnol. Oceanog.*, 9 (1964) 143.
14 G. F. REYNOLDS AND F. S. TYLOR, *Analyst*, 89 (1964) 579.
15 D. OGDEN AND G. F. REYNOLDS, *Analyst*, 89 (1964) 538.
16 R. FUKAI, L. HUYNH-NGOC AND D. VAS, *Nature*, 211 (1966) 726.
17 K. M. CHAN AND J. P. RILEY, *Anal. Chim. Acta*, 36 (1966) 220; 39 (1967) 103.
18 C. M. PYBURN AND G. F. REYNOLDS, *Analyst*, 93 (1968) 375.
19 L. YE. SHTERENBERG, I. V. BELOVA, G. V. MOTUZOVA AND YE. V. CHERKASOVA, *Dokl. Akad. Nauk SSSR*, 173 (1967) 187.
20 G. ARRHENIUS, J. MERO AND J. KORKISCH, *Science*, 144 (1964) 170.

21 P.E.LECOQ DE BOISBAUDRAN, *Ann. Chim. Phys.*, (5) 10 (1877) 100; *Chem. News*, 35 (1876) 148; *Compt. Rend.*, 83 (1876) 637, 825.
22 F. W. KRIESEL, *Chemiker Ztg. N.*, 156 (1929) 961.
23 E. M. NANOBASHVILI, E. G. DAVITASHVILI AND M. YA. GIORGOBIANI, *Tr. Inst. Khim. Akad. Nauk Azerb. SSR*, 17 (1959) 38.
24 I. S. CHAUS AND I. A. SHEKA, *Zh. Neorgan. Khim.*, 8 (1965) 480, 1270.
25 N. A. RUDNEV AND A. A. MAZUR, *Zh. Analit. Khim.*, 12 (1957) 433.
26 S. P. YATSENKO AND N. V. DEMENEV, *Zh. Neorgan. Khim.*, 5 (1960) 1618, 1626.
27 YU. V. MORACHEVSKII AND A. I. NOVIKOV, *Uch. Zap. Leningr. Gos. Univ., Ser. Khim. Nauk*, 18 (272) (1959) 130.
28 YU. V. MORACHEVSKII AND V. M. ZAITSEV, *Tr. Komis. po Analit. Khim., Akad. Nauk SSSR*, 9 (12) (1958) 135; *Uch. Zap. Leningr. Gos. Univ., Ser. Khim. Nauk*, 18 (297) (1960) 77.
29 E. B. SANDELL, *Colorimetric Determination of Traces of Metals*, 3rd Edn., Interscience, New York, 1959, p. 473.

Determination of germanium in synthetic fibers by solvent extraction and atomic absorption spectrophotometry

The atomic absorption of germanium has been described in several papers[1-3]. POPHAM AND SCHRENK[3] reported that maximum sensitivity occurred in a 50% (v/v) acetone solution in a fuel-rich nitrous oxide–acetylene flame, and that the greatest number of interferences were observed under these conditions. However, no information is available for the atomic absorption characteristics of germanium in immiscible organic solvents. This communication describes some observations on atomic absorption of germanium combined with extraction and its application to the determination of germanium in synthetic fibers.

Experimental

A Hitachi 207 atomic absorption spectrophotometer, a Hitachi recorder QPD 54 and an HTV R136 photomultiplier tube were used. The light source was a Perkin-Elmer #194R germanium hollow-cathode lamp operated with square-wave current. A Hitachi high-temperature burner (50×0.4 mm^2) was used with two light traverses through the flame. Nitrous oxide–acetylene flames were used. The 2651.18–2651.58 Å doublet was most suitable for measurement because of optimal sensitivity. An electric shaker was used for extractions.

A germanium stock solution was prepared by dissolving pure germanium dioxide in a minimum amount of sodium hydroxide solution.

Extraction and atomic absorption of germanium

Germanium tetrachloride can be extracted into methyl isobutyl ketone[4]; the percentage extraction increases from zero as the acidity increases above 5 M hydrochloric acid, but at high hydrochloric acid concentrations the solubility of methyl isobutyl ketone in the aqueous phase is increased. Some absorption was observed when an organic phase which had been extracted from 9 M hydrochloric acid solution containing no germanium, was sprayed, probably because of hydrochloric acid in the

organic phase. At lower hydrochloric acid concentrations, such absorption phenomena were not observed and subsequent work was done by extraction of germanium from 7.5 M hydrochloric acid solution.

Increased absorption occurred in fuel-rich flames, as was shown by spraying of aqueous solution. A fuel flow rate of 3.75 l/min with an oxidant flow-rate of 6.0 l/min provided a suitable compromise between sensitivity and flame noise. Figure 1 shows the effect of the flame conditions on absorption. Maximum sensitivity occurred when the hollow-cathode beam traversed the flame 0.8 cm above the burner head.

Iron, antimony, arsenic, tin and gold were extracted into methyl isobutyl ketone under the conditions used for extracting germanium. No interferences were encountered from the elements (50 μg) which were extracted into the organic phase.

The extraction method showed an approximately ten-fold absorption enhancement over that obtained in spraying the aqueous solution. The coefficient of variation for 75 μg of germanium was 4%.
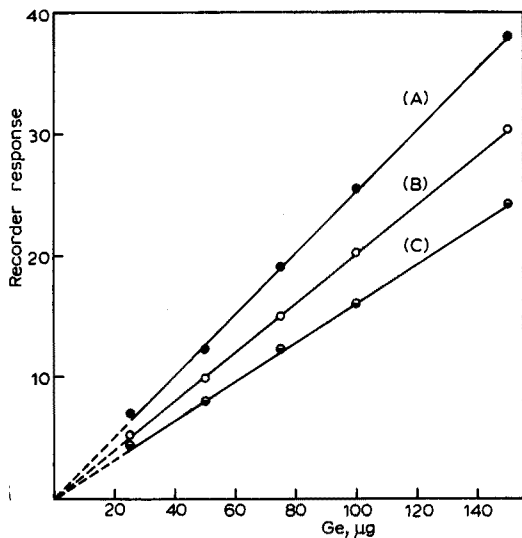
Fig. 1. Effect of flame conditions on germanium absorption. Acetylene flow-rate: (A) 4.0 l/min; (B) 3.75 l/min; (C) 3.5 l/min. Nitrous oxide flow-rate 6.0 l/min. Germanium was extracted with 5 ml of methyl isobutyl ketone.

Determination of germanium in synthetic fibers

Some synthetic fibers contain germanium derived from the polymerization catalyst. Atomic absorption could conveniently be used for determination of germanium in such fibers, which also contained titanium dioxide and other metals. The following procedure was suitable.

The sample (1 g) was ashed in a platinum crucible with 0.1 g of sodium carbonate; the sodium carbonate was added as a solution, and the ashing was done, after the contents of the crucible had been dried and melted, by heating to dull

redness for a few minutes. After cooling, the residue was cautiously treated with 7.5 M hydrochloric acid, and the solution (20 ml) was shaken for 2 min in a separatory funnel with 5 ml of methyl isobutyl ketone. The organic phase was then sprayed into the flame and the absorbance was measured. Calibration curves were obtained by treating standard germanium solutions in the same way.

The results obtained for some synthetic fibers (Table I) were in good agreement with those obtained spectrophotometrically by the phenylfluorone method.

TABLE I

DETERMINATION OF GERMANIUM IN SYNTHETIC FIBERS

Sample[a]	GeO_2 added (%)	GeO_2 found (%)	
		Atomic absorption	Spectrophotometric
No. 90	—	0.010	0.0099
No. 90	0.0076	0.018	0.018
No. 174	—	0.011	0.011
No. 237	—	0.0099	0.0092

[a] Polyethylene terephthalate.

Department of Synthetic Chemistry,   MASAAKI YANAGISAWA
Faculty of Engineering,   MASAMI SUZUKI
Nagoya University,   TSUGIO TAKEUCHI
Chikusa-ku, Nagoya (Japan)

1 W. SLAVIN, Appl. Spectry., 20 (1966) 281.
2 M. D. AMOS AND J. B. WILLIS, Spectrochim. Acta, 22 (1966) 1325.
3 R. E. POPHAM AND W. G. SCHRENK, Spectrochim. Acta, 23B (1968) 543.
4 P. SENISE AND L. SANT'AGOSTINO, Mikrochim. Acta, (1956) 1445.

(Received January 18th, 1969)

Spectrophotometric determination of thallium(III) with thiosalicylamide

  Very few organic reagents have been successfully employed for the extraction and spectrophotometric determination of thallium(III). Thallium has been extracted with diethyldithiocarbamate in chloroform[1] and with dithizone in chloroform[2]; in both cases, tartrate and cyanide are needed to mask interfering ions. Extraction with zinc dibenzyldithiocarbamate has also been used[3]. Recently, SHOME et al.[4] suggested 3-hydroxy-1,3-diphenyltriazine for the spectrophotometric determination of the metal in 70% alcohol.

  Thiosalicylamide has been employed by KRYCH AND LIPIEC[5] for the colorimetric determination of traces of iron. In the present research the analytical properties of thiosalicylamide have been investigated in detail and the reagent has been studied for the spectrophotometric determination of thallium(III).

  Thiosalicylamide forms an orange-red complex with thallium(III), which can be easily extracted with chloroform to produce an orange-red colour. Quantitative extraction is obtained from 2–3.5 N sulphuric acid solutions. The chloroform extract of the thallium–thiosalicylamide complex shows maximum absorbance at 458 nm, and Beer's law is obeyed over the range 2.8–56 μg Tl^{3+}/ml. Appreciable amounts of aluminium, gallium, indium, thorium, iron, copper, manganese, titanium, zinc, cobalt and nickel do not interfere.

  The reagent forms coloured complexes with several other metals such as copper, iron, gold, platinum, palladium, ruthenium, osmium, rhodium and vanadium. The determination and separation of these metals including the elements of the platinum group are in progress.

Apparatus

  A Carl-Zeiss spectrophotometer PMQII type with 1-cm quartz cells was used for the transmittance measurements. All the pH measurements were carried out with a Cambridge pH meter (Bench model).

Reagent and chemicals

  Preparation and properties of thiosalicylamide. Thiosalicylamide (TSA) was prepared by the following procedure[6]. Salicylamide was mixed with phosphorus pentasulphide and baked over a low flame in a porcelain basin. The mixture was dissolved in rectified spirit and filtered. The filtrate was added to a large volume of boiling water, and filtered again, and the filtrate was slowly evaporated on a water bath. Shining yellow needles separated on cooling. The compound was recrystallised from hot water (m.p. 121°).

  The compound is appreciably soluble in hot water and very soluble in alcohol, benzene, chloroform and other organic solvents. It is stable towards acid and readily decomposed by alkali.

  Thallium solution. A known quantity of thallium(III) oxide was dissolved in nitric acid and then made to volume with water. The solution was standardised by the iodimetric method. Weaker solutions were prepared by dilution with water.

  Other standard solutions of different metals used to study the effect of diverse ions were prepared by dissolving weighed amounts of their salts in distilled water or

dilute sulphuric acid. Solutions of anions were prepared from the respective alkali salts. All the chemicals used were of A.R. grade.

Procedure

Place a measured amount of thallium solution into a 100-ml separating funnel, and make the solution 2.0–3.5 N in sulphuric acid. Shake vigorously with a measured amount of alcoholic 0.01 M thiosalicylamide solution. Then shake the orange-red precipitate with three or four 5-ml portions of chloroform. Dilute the combined extracts to 25 ml with chloroform, and measure the absorbance at 460 nm against a reagent blank.

Absorbance curves

The absorbance curves of solutions of thallium–TSA chelate in chloroform obtained after extraction from 2.5 N sulphuric acid media are shown in Fig. 1.
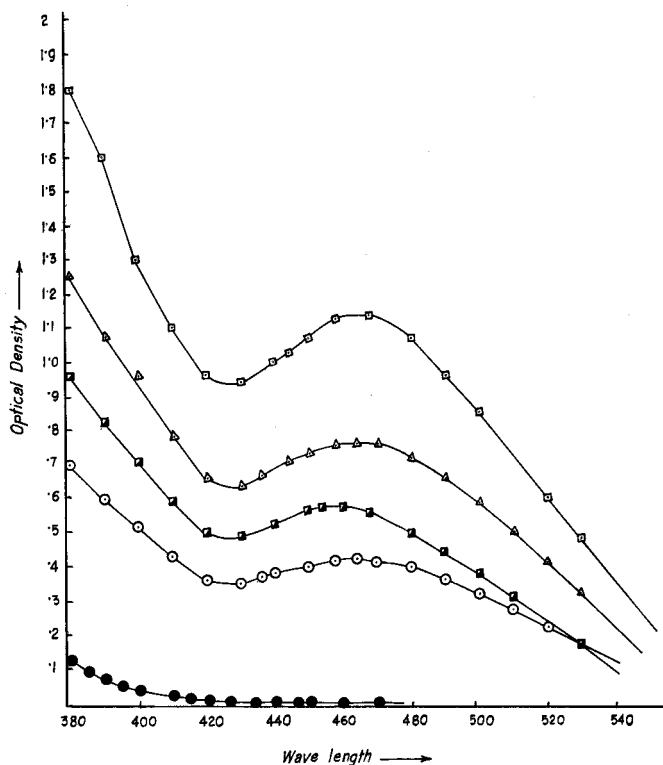
Fig. 1. Absorbance curves of thallium(III)–TSA complex in chloroform. (□) [Tl³⁺]=44.85 μg/ml; (△) [Tl³⁺]=28.03 μg/ml; (■) [Tl³⁺]=22.424 μg/ml; (○) [Tl³⁺]=16.818 μg/ml; (●) [R]=1·10⁻¹ M.

Effect of pH

The most suitable acidity for complete extraction of thallium was determined by extracting the chelate after adjustment of the pH with varying amounts of 10%

sodium acetate and dilute sulphuric acid. The transmittance of the different extracts was measured at 460 nm against the appropriate reagent blank. The acidity of the aqueous layers was measured immediately after extraction of thallium. The results indicated that the extraction of thallium starts at pH 3.25, becomes 50% at pH 1.0 and 100% in the range of acidity 1.5–3.5 N. At higher acidities the percentage extraction gradually diminishes and at 6 N sulphuric acid the reagent decomposes.

Effect of diverse ions

In the study of the effect of diverse ions, the standard thallium(III) solution containing 280.3 μg of the metal ion was mixed with a solution of the required ion, the acidity was adjusted to 2.0–2.5 N with sulphuric acid, 0.6 ml of 0.01 M reagent was added, and the mixture was extracted four times with 5-ml portions of chloroform. The combined extract was then collected in a 25-ml volumetric flask and made to volume with the solvent, and the absorbance was measured at 460 nm against the reagent blank. Table I shows the concentrations of the foreign ions that caused an error of less than ±2%.

TABLE I

EFFECT OF DIVERSE IONS

(Thallium taken = 208.3 μg)

Diverse ions added	Concentration tolerated (mg)	Diverse ions added	Concentration tolerated (mg)
Ni^{2+}	200	Ti^{4+}	80
Co^{2+}	200	V^{5+}	24
Mn^{2+}	500	Mo^{6+}	1000
Zn^{2+}	800	U^{6+}	8
Cd^{2+}	750		
Cr^{3+}	500	HPO_4^{2-}	108
Ga^{3+}	50	F^-	65
In^{3+}	60	EDTA	20
Al^{3+}	80	Tartrate	70

Nature of complex in solution

The empirical formula of the thallium–TSA complex was determined by the mole-ratio method as described by MAYER AND AYRE[7]. A series of solutions were taken which contained $4 \cdot 10^{-5}$ M thallium(III) and various concentrations of thiosalicylamide in the range $3.2 \cdot 10^{-5}–20 \cdot 10^{-5}$ M. The metal complex was extracted with chloroform as described before and the absorbance measured was plotted against the mole ratio of ligand to metal ion. The results clearly showed a stable complex containing thallium and TSA in the ratio 1:2. This ratio was verified by the conventional slope-ratio method.

Molar extinction coefficient and sensitivity

The molar extinction coefficient was found to be 5100 ± 10. The sensitivity for the thallium–TSA complex was found to be 0.04 $\mu g/cm^2$ according to Sandell's notation[8].

The authors are indebted to the Council of Scientific and Industrial Research, New Delhi, for a fellowship awarded to M.M. They thank Dr. H. R. DAS for helpful discussion.

Chemistry Department,   S. C. SHOME
Presidency College,   M. MAZUMDAR
Calcutta-12 (India)

1 D. WEISS, *Rudy (Prague)*, 9 (4-addendum) (1961).
2 J. MINCZEWSKI AND C. ROZYEKI, *Chem. Anal.*, 8 (1963) 63.
3 K. HAGIWARA, M. NAKANE, Y. OSUMI, E. ISHII AND Y. MIYAKE, *Japan Analyst*, 10 (1961) 607.
4 S. C. SHOME, H. R. DAS AND B. DAS, *Anal. Chem.*, 38 (1966) 1522.
5 Z. KRYCH AND T. LIPIEC, *Ann. Acad. Med. Lodz*, 1 (1961) 34; *Chem. Abstr.*, 60 (1964) 11367.
6 A. SPILKER, *Ber.*, 22 (1889) 2770.
7 A. S. MAYER AND G. H. AYRE, *J. Am. Chem. Soc.*, 79 (1957) 49.
8 E. B. SANDELL, *Colorimetric Determination of Traces of Metals*, Interscience, New York, 1959, p. 83.

Analytical applications of thio-, seleno- and telluroethers
Part I. Detection of palladium

LIVINGSTONE[1] has reviewed the different types of metal complexes formed by various ligands containing sulfur, selenium or tellurium as donor atoms. Among these, the properties of thioethers, selenoethers and telluroethers toward certain metals seemed particularly attractive.

It is well known that palladium chloride readily forms very well defined compounds with thioethers: $PdCl_2 \cdot 2R_2S$. These complexes are soluble in chloroform, benzene, ligroin, etc., and have been used to characterize alkyl-phenyl sulfides[1-3].

On the basis of these facts a new test for the identification of palladium was developed. This study, however, was carried out mainly to demonstrate the possibility of using a whole class of very simple organic substances to detect palladium rather than to select a single reagent for this purpose. Thio-, seleno- and telluroethers in benzene solutions were used to extract palladium chloride.

Extraction study

Series of experiments were run with aqueous solutions of palladium chloride with the pH adjusted between 1.0 and 5.0; 3% solutions of the organic reagent in benzene were used as extractant (Table I). The extraction was evaluated by the intensity of the yellow color of the extract.

TABLE I

TESTED SUBSTANCES

Methyl phenyl sulfide (I)	Methyl *p*-cresyl sulfide (V)
Ethyl phenyl sulfide (II)	Ethyl *p*-cresyl sulfide (VI)
n-Propyl phenyl sulfide (III)	*n*-Propyl *p*-cresyl sulfide (VII)
Isopropyl phenyl sulfide (IV)	Isopropyl *p*-cresyl sulfide (VIII)
Methyl *o*-cresyl sulfide (IX)	Phenyl sulfide (XIII)
Ethyl *o*-cresyl sulfide (X)	Benzyl sulfide (XIV)
n-Propyl *o*-cresyl sulfide (XI)	Methyl 2-naphthyl sulfide (XV)
Isopropyl *o*-cresyl sulfide (XII)	Isopropyl 2-naphthyl sulfide (XVI)
Phenyl selenide (XVII)	Phenyl telluride (XIX)
Benzyl selenide (XVIII)	

The compounds I, II, III, IV, VII, VIII, IX, X, XI, XII, XIV, XV and XVI were prepared by common methods, *i.e.* heating alkaline solutions of the thiols and the correspondent alkyl halide. Compounds V, VI, XIII and XVII were obtained from Eastman Kodak Co. Compound XVIII was synthesized by the method of PAINTER et al.[4], and compound XIX by the method of RHEINBOLDT AND VICENTINI[5]. Compound XV was recrystallized from petroleum ether and XVIII from ethanol. All the other compounds were purified by distillation under reduced pressure. Benzene was distilled before use.

Palladium(II) chloride solution, 0.1 M with respect to hydrochloric acid, was standardized gravimetrically with dimethylglyoxime. Solutions of most other cations were prepared from their chlorides in 0.1 M hydrochloric acid; silver was used as its sulfate and some cations, such as tin(II), tin(IV), antimony(III), arsenic(III), arsenic(V) and bismuth(III), required the addition of more concentrated acid.

Selectivity and interference study

Extractability was first studied with 1%, 2% and 3% thioether solutions in benzene; the 3% solution was the most convenient to establish a general procedure based on thioethers. The same concentration was used for selenium and tellurium compounds.

Although it has been stated[1] that "sulfur has a much lower affinity for platinum(IV) than platinum(II), and various attempts to prepare platinum(IV) complexes of thioethers have been unsuccessful", it was found that compounds I, II, III, V, VI, IX and XIX gave yellow extracts from platinum(IV) solutions which were 0.1 M in hydrochloric acid. With acetate-buffered solutions (pH 5.0) of platinum(IV), compounds I, II, V, IX and XIX yielded less intensely colored extracts.

As was expected, all the thioethers in benzene solution extracted gold(III) from either 0.1 M hydrochloric acid or acetate-buffered (pH 5.0) solutions. Under the same conditions, gold(III) solutions were decolorized by benzene solutions of benzyl selenide and phenyl telluride; this may be due to the reducing character[6] of these compounds. It was found that addition of an aqueous solution of ascorbic acid to the extraction system caused bleaching of the gold(III) extracts.

A thorough study of the influence of foreign ions was then made by testing, as described in the recommended procedure, with benzene solutions of all the compounds listed in Table I. The following ions (500 μg) were found to give colourless extracts at pH 1.0 and at pH 5.0: Rh(III), Ru(IV), Ir(IV), Os(IV), Fe(III), Ni(II), Co(II),

Mn(II), Cr(III), Zn(II), Cd(II), Hg(II), UO_2^{2+}, Sn(II), Sn(IV), Pb(II), Sb(III), Sb(V), As(III), As(V), Ti(III), WO_4^{2-} and MoO_4^{2-}. Unexpectedly, compound VI gave slightly colored extract with iridium(IV) and osmium(IV).

To complete the interference study compounds XII, XIII and XVIII were chosen as examples.

Anions such as F^-, ClO_4^-, BrO_3^-, IO_3^-, SO_4^{2-}, NO_3^-, Ac^-, HPO_4^{2-} did not interfere; SCN^-, CN^-, $S_2O_3^{2-}$, SO_3^{2-}, NO_2^-, Br^-, I^-, N_3^- and $C_2O_4^{2-}$ required previous elimination by oxidation, e.g. with aqua regia.

Special attention was given to the influence of ions of the metals that are commonly found with palladium in natural products or alloys.

Experiments were run with 2 μg of palladium(II) and 5,000 μg Pt(IV), 500 μg Ru(IV), 500 μg Cu(II), 500 μg Rh(III), 500 μg Ir(IV), 500 μg Os(IV), 500 μg Au(III), or 500 μg Ag(I). In all these cases it was always possible to detect palladium and no colour was observed in the corresponding blanks run with the same foreign ions but in the absence of palladium.

It should be mentioned that the colored organic layer can be more easily viewed if it is transferred to another microtube with the help of a capillary dropper.

Recommended procedures

Detection of palladium. Place in a microtube a drop of the test solution, 0.1 M with respect to hydrochloric acid; add 4 drops of the same 0.1 M acid or 4 drops of acetate buffer pH 5.0, and 8 drops of a 3% (v/v) benzene solution of the organic reagent*. Shake vigorously and allow the phases to separate. A yellow color appears in the organic layer if palladium is present. With all nineteen substances (Table I) it was possible to identify at least 2 μg of palladium at either pH value.

Detection of palladium in presence of gold. Run a blank in parallel containing approximately 500 μg of gold. Shake vigorously with a benzene solution of the reagent and allow the phases to separate, as described above; then add one drop of an aqueous 2% (w/v) solution of ascorbic acid and shake vigorously again. The color in the benzene layer of the blank disappears whereas the normal yellow colour remains in the sample microtube if palladium is present. It was possible to identify 2 μg of palladium(II) in presence of gold(III)**.

Discussion

This study was designed not only to develop a new test for palladium, but, particularly, to show the possibility of introducing a new analytical reagent based on the reactivity of a whole class of organic substances, inasmuch as these compounds are easily obtainable. The simplicity of the technique was also taken into account.

The extracted palladium and gold compounds will be isolated in the quantitative studies which are in progress. These types of palladium addition compounds are very well known[1].

---

* If platinum is suspected to be present, compounds I, II, III, V, VI, IX and XIX should not be used.
** Compounds XII and XIII were used as reagent. If compound XVIII or XIX is employed, the treatment with ascorbic acid is not necessary since, as mentioned, gold(III) is reduced by these compounds.

With respect to the applicability of this test to ores and alloys, the anionic interferences referred to above, may have no practical significance.

Department of Chemistry,   LUIZ R. M. PITOMBO
University of São Paulo,
São Paulo (Brazil)

1 S. E. LIVINGSTONE, *Quart. Rev.*, 19 (1965) 386.
2 V. N. IPATIEFF AND B. S. FRIEDMAN, *J. Am. Chem. Soc.*, 60 (1938) 2733, 61 (1939) 685.
3 O. KÖNIG AND W. R. CROWELL, *Mikrochem. Ver. Mikrochim. Acta*, 33 (1948) 298.
4 E. P. PAINTER, K. W. FRANKE AND R. A. GORTHER, *J. Org. Chem.*, 5 (1940) 587.
5 H. RHEINBOLDT AND G. VICENTINI, *Chem. Ber.*, 89 (1956) 624.
6 M. DE MOURA CAMPOS, E. L. SURANYI, H. DE ANDRADE JR. AND N. PETRAGNANI, *Tetrahedron*, 20 (1964) 2797.

(Received December 10th, 1968)

BOOK REVIEWS

Progress in Separation and Purification, Vol. I, edited by E. S. PERRY, Interscience Publishers–John Wiley and Sons, New York, 1968, ix + 392 pp., price 154 s.

All the nine articles in this volume are mainly concerned with preparative separations, especially those on Normal Freezing (26 pp.), Preparative Gas Chromatography (50 pp.) and Zone Refining of Chemicals (10 pp.). The theoretical description of Foam Fractionation (56 pp.) should be of some interest to analytical chemists, although no applications of the technique are described. Membrane Permeation (44 pp.), Ultrafiltration (38 pp.) and Gas and Vapor Separation by means of Membranes (38 pp.) are all techniques that should be brought to the notice of analytical chemists, and the article on a Dry Process for Separating Zirconium and Hafnium (50 pp.) includes some interesting chemistry that might have analytical implications. Finally, the paper on the Separation and Purification of Plasma Proteins (60 pp.) gives a comprehensive account of the methods used with occasional analytical applications.

This book is the first volume of a series that will appear "at regular intervals commensurate with the procurement of articles". It is well produced and has comprehensive author and subject indexes. Analytical chemists would do well to have access to the series, as it might well provide ideas for the development of new analytical separations.

A. TOWNSHEND (Birmingham)

Organometallic Chemistry Reviews, Section B, Annual Surveys, Vol. 4, No. 1, Elsevier Sequoia, Lausanne, 1968.

Annual Surveys of Organometallic Chemistry volumes 1–3 were issued as hardbacked volumes, each volume covering the whole of the subject. This year, volume 4, edited as previously by R. B. KING AND D. SEYFERTH, has been issued as a paper-back supplement to *Organometallic Reviews*; F. CALDERAZZO has been enlisted to help with the ever-increasing volume of the literature.

The first part of volume 4 covers the introduction and surveys the literature on transition metal compounds. The method of presentation remains as before: a section on lanthanides is followed by others in which the elements are taken in "vertical triads", *e.g.* titanium, zirconium and hafnium. The coverage is extensive and probably exhaustive, but not critical; particularly interesting work receives a little more attention than the rest.

The production and format are of high standard. Like its predecessors, this volume is a mine of valuable information which no worker in this field can ignore.

E. J. FORBES (Birmingham)

H. STAUDINGER, *Anleitung zur organischen qualitativen Analyse*, 7. neubearbeitete und erweiterte Auflage, von W. KERN UND K. KÄMMERER, Springer-Verlag, Berlin, 1968, x + 237 S., Geheftet DM 24,–.

Absorption Spectra in the Ultraviolet and Visible Region, Edited by L. LANG, Akademiai Kiado, Budapest, 1968, 400 pp., price 135 s.

Z. MARCZENKO, *Kolorymetryczne Oznaczanie Pierwiastkow*, Wydawnictwa Naukowo Techniczne, Warszawa, 1968, 716 pp., Cena zl. 95.–.

Progress in Nuclear Energy. Series IX. Analytical Chemistry. Vol. 8. Part 2, Edited by H. A. ELION AND D. C. STEWART, Pergamon Press, Oxford, 1968, 96 pp., price 40 s.
    This volume contains a review: Laser-induced spontaneous and stimulated Raman scattering, by C. J. SCHULER.

R. DE NEVE, *Reaction Rates from Nuclear Reactor Neutrons*, Koninklijke Vlaamse Academie, Brussel, 1968, 35 pp., 107 BF.

C. DUVAL, *Le Mercure*, ("Que sais-je?" Le Point des Connaissances Actuelles No. 1317), Presses Universitaires de France, Paris, 1968, p. 126.

The Determination of Particle Size. I. A Critical Review of Sedimentation Methods, Analytical Methods Committee, Society for Analytical Chemistry, London, 1968, iv + 42 pp., price 30 s ($4.00).

G. A. BLOKH, *Organic Accelerators in the Vulcanization of Rubber*, Translated from the Russian, Israel Program for Scientific Translations, Jerusalem, 1968, x + 424 pp., price $20.25.

Scientific Selection of Catalysts, Edited by A. A. BALANDIN, B. A. KAZANSKII, V. E. VASSERBERG, G. V. ISAGULYANTS AND G. I. LEVI, Translated from the Russian, Israel Program for Scientific Translations, Jerusalem, 1968, vii + 274 pp., price $11.50.

J. A. ALLEN, *An Outline of Polymer Chemistry*, Contemporary Science Paperbacks 25, Oliver and Boyd, Edinburgh, 1968, vii + 136 pp., price 7s.6d.

ERRATUM

F. P. IJSSELING AND E. VAN DALEN, Potentiometric titrations with ion-exchange membrane electrodes. Part IV. A further study of experimental variables, *Anal. Chim. Acta*, 45, No. 1 (1969) 121–132.

In the title the word ion-exchange should be replaced by ion-exchanging.

The word counter ion(s) should be replaced by co-ion(s) on:
p. 121, lines 9 and 16;
p. 126, lines 6, 8, 14, 15 and the first line of the legend to Figure 4; and
on p. 131, lines 16 and 25.

Journal of Mass Spectrometry and Ion Physics

SCOPE

The journal is devoted to the fundamental aspects of mass spectrometry and ion physics and to the study of the application of mass spectrometric techniques to specific problems. The following topics are considered to fall within the scope of the journal:

Theoretical and experimental studies of ion formation, ion separation and ion detection processes.

Interpretation of mass spectrometric data.

Theoretical computation; the design and performance of instruments (or their parts) and accessories.

Measurements such as natural isotope abundances, precise isotope mass measurements; ionization, appearance and excitation potentials; ionization cross sections.

Development of techniques in relation to structural determination, geological ageing, thermodynamic studies, chemical kinetics studies, surface phenomena studies, chemical analysis.

The journal publishes research papers, review articles, book reviews and short communications.

LANGUAGES

The main language of the journal is English, although papers in French or German are also published.

SUBMISSION OF PAPERS

Papers should be submitted to one of the following:

J. FRANZEN
Institut für Spektrochemie und angewandte Spektroskopie
Postfach 778, 46 DORTMUND (Germany)

A. QUAYLE
"Shell" Research Ltd., Thornton Research Centre
P.O. Box No. 1, CHESTER (England)

H.J. SVEC
Department of Chemistry, Iowa State University
AMES, Iowa 50010 (U.S.A.)

They should be submitted in three copies, in double-spaced type with adequate margins. Figures should be drawn in Indian ink on drawing or tracing paper and be in a form ready for the blockmaker. Standard symbols should be used in line drawings. Photographs should be submitted as clear black and white glossy prints. Legends to illustrations should be typed on a separate page. There are no page charges for publication. Further details are available on request.

FREQUENCY AND SUBSCRIPTION INFORMATION

Publication is monthly. One volume appeared in 1968. Volumes 2 and 3 will be published in 1969. Volumes 4 and 5 are scheduled for publication in 1970. The subscription price for 1969 is Dfl. 180.00 plus Dfl. 6.00 postage or equivalent (US$50.00 plus US$1.70; £20.19.0 plus 14s. at April 1, 1969).

A specimen copy will be sent on request.

Vol. 1 (1968); Vols. 2 and 3 (1969); Vols. 4 and 5 (1970).

OF INTEREST TO: physical, analytical, organic, inorganic and organometallic chemists; university libraries, research laboratories of the petroleum and chemical industries (e.g. pharmaceuticals, flavors, dyestuffs, polymers, carbohydrates), nuclear research centres, some of the larger geological institutes.

CONTENTS

OF

VOLUME 2

CONTENTS

OF

VOLUME 2

(continued)

International
Journal
of Mass
Spectrometry
and Ion
Physics

CONTENTS

L S Λ.U. 251